Durham E-Theses

Cross-border congestion management in the electricity market

Zhou, Qiong

How to cite:

Zhou, Qiong (2003) *Cross-border congestion management in the electricity market*, Durham theses, Durham University. Available at Durham E-Theses Online: http://etheses.dur.ac.uk/1263/

Use policy

Copy A

Cross-Border Congestion Management in the

Electricity Market

Qiong Zhou

School of Engineering

University of Durham

A thesis submitted in partial fulfilment of the requirements of the University of

Durham for the Degree of Doctor of Philosophy (Ph.D.)

December 2003

1 3 JUL 2004

Abstract

In this thesis, a congestion management method based on the merchandise surplus refund is presented, and is illustrated in a 5-bus system under the bilateral model. Furthermore, for the interconnected system consisting of several or more control areas and different transmission system operators (TSOs), the decomposition of optimal power flow (OPF) is studied, and a decomposition strategy is proposed to achieve optimum over the entire system while keeping the information exchange between neighbouring control areas at an acceptable level. Based on this decomposition strategy, an interior point method (IPM) is applied and then tested in a small system. This barrier function method complemented the previous works of several researchers, and it enables the TSOs at different control areas to calculate the OPF in parallel and coordinate through very limited information exchange. This method is compared with two existing methods, both on the algorithms and on the test system, and proved fast convergence and numerical stability. Finally, in order for researchers to study cross-border congestion management methods, a test model is created based on the UCTE (the Union for the Co-ordination of Transmission of Electricity) ultra high voltage transmission network. As it is based on public information, no commercially sensitive information is involved, and it inherits the physical characteristics of the real network in the respect of cross-border power flows. The verification of this test network is also done by comparing the calculated PTDFs (Power Transmission Distribution Factors) against the published true values.

Acknowledgements

I would like to acknowledge my appreciation to all who gave me help during my PhD course.

Many thanks to my supervisors, Professor J. Bialek and Dr. J. Bumby, who have given me lots of good advice and encouraged me to work independently at the same time.

Also thanks to the University of Durham and School of Engineering for providing me with the research studentship as well as administrative and technical supports.

Finally, I would like to thank my husband and my parents for their constant support.

Table of Contents

Glossary

AAC: the already allocated capacity

ATC: available transfer capacity

AVRs: automatic voltage regulators

BC: bottleneck capacity

CBT: cross border trade

CCR: cross-border co-ordinated re-dispatch

CRRs: congestion revenue rights

DACF: the day ahead congestion forecast

DC: direct current

EC: the European Commission

EHV: extra high voltage

ETSO: the European Transmission System Organisation

FACTS: flexible AC transmission systems

FERC: the Federal Energy Regulatory Commission

FTRs: firm transmission rights or financial transmission rights, depending on the

contexts

GIS: geographic information system

HVDC: high voltage direct current

IEM: the internal electricity market

IP: interior point

IPM: interior point method

IPPs: independent power producers

ISO: the independent system operator

ITP: independent transmission provider

LMP: locational marginal pricing

LR: Lagrange relaxation

LRAIC: long-run average incremental cost

LRMC: long-run marginal cost

LSE: load-serving entities

MB: marginal benefit

MC: marginal cost

MMU: market monitoring unit

MS: merchandise surplus

NEM: the National Electricity Market

NETA: the New Electricity Trading Arrangements

NTC: net transmission capacity

NZEM: the New Zealand Electricity Market

OASIS: the open access same time information system

OMOI: office of market oversight and investigation

OPF: optimal power flow

OTC: over-the-counter

PTDFs: power transmission distribution factors

PX: power exchange

QP: quadratic programming

RC: requested capacity

RTO: the regional transmission operator

SC: scheduling coordinators

SMD: standard market design

SO: the system operator

SPC: the State Power Corporation

SQP: sequential quadratic programming

SRMC: short-run marginal cost

T&D losses: transmission and distribution losses

TCC: transmission congestion contract

TLR: transmission load relief

TSOs: transmission system operators

UCTE: the Union for the Co-ordination of Transmission of Electricity

UKTSOA: the United Kingdom Transmission System Operators Association

List of Symbols

p_{gi} : The active generation level of ith generator in p.u. i=1,2, ... n_{ga}

n_{ga} : The number of generators in area a

$p_{gi\,min}$, $p_{gi\,max}$: The lower and upper active power bounds of ith generator, in p.u.

p_{dj} : The active demand level of jth load in p.u. j=1,2, ... n_{da}

$p_{dj\,min}$, $p_{dj\,max}$: The minimum and maximum active demand level of jth user

n_{da} : The number of loads in area a

$C(\cdot)$: Generation cost function

$B(\cdot)$: User benefit function

ρ_i : The locational price of active power at generator site

ρ_j : The locational price of active power at load site

$\rho_{gi\,min}$: The minimum price at which the ith generator is willing to produce electricity

ς_i : The sensitivity factor of ith active power generation to its locational price

ε_j : The sensitivity factor of jth active load to its locational price

δ_i : The power angle at a bus i, in radians

B_{ij} : The imaginary part of elements in the network admittance matrix in p.u.

P_{dli} : the active power loss along line l, modelled at bus i

L_{ij} : The loss coefficient of Line ij

m_a : The number of transmission lines in area a

$L_{i-j\,max}$: The transmission capacity limit of line ij, in p.u.

$V_i = |V_i| \angle \delta_i$: The voltage at bus i, in p.u.

$V_{i\,min}$, $V_{i\,max}$:The lower and upper bounds of bus voltage, in p.u.

$Y_{ij} = |Y_{ij}| \angle \theta_{ij}$: The element of the complex admittance matrix, in p.u.

θ_{ij} : The phase angle of Y_{ij}

$f(x)$: The objective function of a general mathematical model for barrier function methods to solve nonlinear constrained optimisation problems

$\mathbf{x}$: The vector of variables to be optimised

$\mathbf{x}^*$: The optimum solution

$\mathbf{g}(\cdot)$: The group of equality constraints, $\mathbf{g}(\cdot) = 0$

$\mathbf{h}(\cdot)$: The group of inequality constraints, $\mathbf{h}(\cdot) \leq \mathrm{D}$

D: The vector of right hand sides of the inequality constraints

s: The vector of nonnegative slack variables to convert inequality constraints into equality constraints

μ_j : The barrier parameter for the jth constraint. $\mu_j > 0$ and $\mu_j \rightarrow 0$ with the iteration procedure

$\boldsymbol{\mu}$: The vector of μ_j

$\boldsymbol{\lambda}$: The vector of Lagrange multipliers in association with the equality constraints

z: The vector of Lagrange multipliers in association with the inequality constraints

$L(\cdot)$: Lagrangian function

$\nabla(\cdot)$: The derivative operator

$J(\cdot)$: Jacobian vector obtained from partial derivative operation on $L(\cdot)$

$H(\cdot)$: Hessian matrix obtained from partial derivative operation on $J(\cdot)$

Δ : The increment

y: The vector of coupling variables

$M(\cdot)$: The group of coupling constraints

$\boldsymbol{\sigma}$: The vector of Lagrange multipliers in association with the coupling constraints

A_a^k: Subset of the Hessian matrix obtained at the kth iteration, corresponding to area

a

$\Delta\alpha_{ak}$:   The increment vector obtained from the kth Newton search

$\Delta\alpha_{ak} = \begin{bmatrix} \Delta x_a^T & \Delta \lambda_a^T \end{bmatrix}^T$ for area a

β_a^k: The residue vector corresponding to area a and the kth Newton iteration

q^k: The residue vector for all the coupling constraints

Γ_a: The incidence matrix for the inter-area coupling constraints corresponding to

area a

$\mathbf{P_a}$:   The active generation vector in area a

$\boldsymbol{\delta}_a$:   The bus voltage phase angle vector in area a

A: The incidence matrix indicating the starting and ending buses of the lines

$\mathbf{s_{ga}}$:   The slack variable vector corresponding to the active generation limits in area a

$\mathbf{s_{la}}$:   The slack variable vector corresponding to the line transmission limits in area a

$\mathbf{s_{\delta_a}}$:   The slack variable vector corresponding to the phase angle limits in area a

List of Figures

Introduction

For a long time, the electricity power industry had been seen as a public service and thus been structured as a vertical monopoly. The requirements for system real-time security and the economies of scale in electricity production did support such a monopoly, but the problems of low efficiency and lack of incentives has been widely criticised.

Experiences during the past twenty years have proved that the deregulation in power markets is feasible and also beneficial to the customers. However, electricity is a special commodity and thus electricity markets require special design. The major difficulties of electricity as a commodity are: (1) electricity cannot be stored on a large scale. (2) All the market participants in a market share the same transmission network, while the power flows obey physical law instead of "contract path". (3) The frequency in a synchronised system is identical everywhere, and the real-time energy balance needs to be maintained [1]. The second characteristics implies that the transmission network is a natural monopoly, and the system operator (SO) is required to provide transmission services to all the network users. Due to the first and third reasons, a balancing service must also be provided to ensure real-time system security.

Transmission congestion problems occur when the transmission facilities have scarce transmission capacities and cannot accommodate the overall power flows incurred by all the network users wishing to transfer energy from one site to another site through the network. The system operator must prevent and resolve congestion problems in order to keep the transmission grid operating properly and to avoid damaging transmission equipment [2]. If the technical transmission limits are binding, customers have to pay more to get alternative energy from other generators to meet their

demands. Thus those out-of-merit generators have to be "constrained on" while cheap generators will reduce their output to ensure system security. As congestion makes the cheaper generators reduce the output, it results in low efficiency and lost of welfare.

It is fair that the participants who caused congestions should pay for it. In this way, every participant has the correct incentive to avoid congestion. Moreover, transmission network can raise part of the fund for system expansion. However, the existence of loop flows in a grid makes it difficult to specify each party's payment. (Rather than following the pre-specified contracted paths, loop flows are the actual power flows passing through all the shunt connected circuits according to Kirchoff's current law. The distribution of power flows depends on the impedances of the shunt circuits.)

This thesis will address the congestion management in the electricity market, especially the cross-border congestion management in interconnected systems. In Chapter 1, the electricity prices are analysed and associated with the underlying mathematical model, and different types of wholesale electricity markets are outlined and compared. Congestion management methods are reviewed. The concept of transmission rights is also discussed here. Cross-border congestion management methods are listed in Chapter 2, and the current situations in Europe and the US are also briefly given. In Chapter 3, a congestion management method is proposed and illustrated on a small system example. This method is based on the analysis of merchandise surplus (MS) in electricity markets, and is designed to give correct incentives to the market participants and the system operator (SO). The optimal power flow (OPF) calculation for interconnected system is discussed in Chapter 4, especially on how to decouple the calculation among control areas. Comparison has been made between two current approaches, and study is made on how to decompose an interconnected network for the OPF calculation. Based on this study an interior point method is suggested to modify current approaches, and it is tested in Chapter 5 in

comparison with the other two methods. Chapter 5 also gives test results on experimental small systems about these decomposed OPF calculation methods. In Chapter 6 and Chapter 7, a test network is built up for methodology study in the interconnected systems. This network is based on UCTE 1st synchronised area and is similar to the real system in the sense of cross-border power flows and network structures. Verification of the model network through PTDF comparisons is also given.

Chapter 1   Electricity Market

1.1   Introduction

In an electricity power market, producers and consumers response to prices by adjusting their generation/ demand levels. If the prices can give the correct economic signals (both short-term and long-term) and if market participants can compete fairly and openly, the electricity system would be able to achieve high efficiency. As the operation of system changes from second to second, the prices will change with the operations, thus the close-to-real-time pricing (called spot pricing in economics theory [3]) is required to adapt to the changing situations in power system. A congestion fee is incurred when congestion on the bottleneck occurs, and the network users have to pay the fee for the scarce capacity if they still wish to use it. The mathematical model described in this chapter explains how the congestion fee is calculated, taking into consideration of the existence of loop flows in a grid.

The power system has special reliability requirements. As all the market participants share the same network to transfer the energy, coordination between them is necessary to ensure the real-time system security and reliability. In the long run, both over-investment and under-investment should be avoided. An ideal market mechanism is expected to encourage competition and give the correct price signals.

In the deregulated power market, congestion management involves setting up a set of rules that ensure sufficient control over generators and loads to maintain the power system security and reliability at an acceptable level, both in the short term operation and in the long term construction, and at the same time maximise market efficiency [4]. Issues like how to allocate the scarce transmission capacities, how to set the prices for

use of the capacities, and how to use the revenues collected from capacity auctioning are different forms of congestion management methods, and they vary with the form of the markets. Therefore, congestion management methods will be discussed in the following sections in association with the practical markets.

This chapter is focused on the fundamental sources of congestions, as well as congestion management methods in electricity markets. In order to avoid or reduce congestions, a congestion management mechanism must be established. In the long run, this mechanism must give incentives for network enforcements and expansions. In the short run, economic dispatch should be achieved under this mechanism [5].

In this chapter, the mathematical model of optimal power flow (OPF) is reviewed, and the components of electricity prices are interpreted from the calculation of this OPF problem. The electricity market models and financial arrangements are then discussed, and examples in several countries are given.

1.2 The optimal power flow (OPF) problem

[3] gives the underlying mathematical model for spot prices in the electricity market, and explains the price components associated with the mathematical derivations obtained from the optimal power flow (OPF) calculation. Besides, some researchers also suggested different OPF models. [6] suggested a minimum cost formulation as the objective function to solve the dispatch problem for a congested network. [7] explained the theoretical foundations of electricity pricing, and discussed how pool model and bilateral model define the transmission prices. Impact of market power was also discussed. [8] studied the models of generators, loads as well as static volt-ampere-reactive (VAR) compensators, and their impacts on optimal power flow results. For the reason of simplicity, the OPF model in [3]is used to illustrate the works done in this thesis. It's worth giving a brief description of this model in this section.

In the following discussion, the objective function and the constraints of the OPF problem are given. For simplicity the inter-temporal dependence is not considered, i.e. the generation costs and customer benefits are not affected by their behaviours in the previous or future hours. If the coupling between multiple time periods like the start-up costs and the ramp rates of generators are considered, the calculation of spot prices will be more complicated, but the basic hourly spot pricing concepts will not be changed [3].

Therefore, the simple one-hour model will be used to display a clear picture of the spot pricing components.

1.2.1 The model

The objective of this OPF problem is to minimise the social cost, which is the total generation cost minus the customer benefit from using the electricity.

Let g_j be the output of the jth generator, j=1,2, ...

d_k be the demand of the kth customer, k=1,2, ...

Then the generation cost can be expressed as: $\sum_j C(g_j)$, where the C is the cost function, And the customer benefit is: $\sum_k B(d_k)$, where the B is the benefit function.

Therefore, the objective function is:

$$\min_{d_k, g_j} \sum_j C(g_j) - \sum_k B(d_k) \qquad (1.1)$$

Unlike the traditional regulated power system where the SO knows all the cost and benefit functions, the deregulated power market requires protection of these commercial sensitive data. However generators and customers may submit their bids which should reflect their costs or benefits. Assume the generators and customers bid their true marginal costs/ benefits to the SO, then the optimal dispatch objective is still as described in equation (1.1), provided that the $C(g_j)$ and $B(d_k)$ are functions of price and quantity bids.

Let z_i be the line flow of the ith transmission line, i=1,2, ..., then the line losses can be written as: $\sum_i l(z_i)$, where the l is network loss, and the constraints can be summarised as:

System energy balance constraint: $\sum_k d_k + \sum_i l(z_i) - \sum_j g_j = 0$ (1.2)

Total generation must equal the sum of system energy losses and demands at any time.

System reserve constraint: $\sum_j g_j \leq \sum_j g_j^{max} - G_{res}$ (1.3)

where the G_{res} is the system reserve capacity, and g_j^{max} is the maximum output of the jth generator.

In the electricity system, components might go out of operation due to technical reasons, therefore the system reserve capacity should be maintained even when the demand is high.

Individual generator output limit:

$$g_j^{min} < g_j \leq g_j^{max} \quad for \quad \forall j = 1,2,\cdots \quad\quad (1.4)$$

Line flow limit:

$$- z_{ic}^{max} \leq z_i \leq z_i^{max} \quad for \quad \forall i = 1,2,\cdots \quad (1.5)$$

Where the z_{ic}^{max} and z_i^{max} are the limits of power flows at both directions of the ith line respectively. In order to obtain the standard form, this constraint can be re-written as: $z_i \leq z_i^{max}$ and $-z_i \leq z_{ic}^{max}$ (1.6)

The sources of the transmission limits include thermal limits on power lines, system stability limits[9], or other system operation limits converted approximately into line flow limits[10]. Typical limits are determined in [11] as:

- Interface power flow limits: the total power flow on a set of transmission lines between two areas does not exceed a certain value. This is related with voltage and stability limits caused by energy transfers between areas.

- Thermal limits: if the transmission line is overloaded it will overheat, causing line sag etc. The thermal limits are dependent on the ambient temperature.

- Contingency limits: due to the effect of parallel flows, if another transmission line near to the studied one is tripped off during operation, its loads will be shifted onto this line. The N-1 contingency limits require the line can remain operate even the neighbouring line is tripped off.

Here the line flow z_i are status variables determined by the control variables g_j and d_k. Additional constraints can be added here to represent the line flows:

Network representation:

$$z_i = h_{i,j}\left(g_j - d_j\right) \qquad (1.7)$$

where the g_j and d_j are generation and demand at the jth bus, respectively. $h_{i,j}$ is the contribution factor of the power flow in ith line caused by 1MW of electricity injected at the jth bus and withdrawn at the slack bus. In DC power flow calculation, $h_{i,j}$ is a constant dependent on the network parameters and structure. In AC power flow calculation, $h_{i,j}$ is also dependent on the levels of generations and demands. Generally

$$h_{i,j} = \frac{\partial z_i}{\partial g_j} = -\frac{\partial z_i}{\partial d_j} \qquad (1.8)$$

1.2.2 Solving the problem

The Lagrangian function of the above OPF problem is:

$$\Omega = \sum_j C(g_j) - \sum_k B(d_k) + \mu_e \left(\sum_k d_k + \sum_i l(z_i) - \sum_j g_j \right) +$$

$$\mu_{crit} \left(\sum_j g_j - \sum_j g_j^{max} + G_{res} \right) + \sum_j \mu_{g,j} \left(g_j - g_j^{max} \right) + \sum_i \mu_{z,i} \left(z_i - z_i^{max} \right) +$$

$$\sum_i \mu_{cz,i} \left(-z_i - z_{ic}^{max} \right) \tag{1.9}$$

Where the $\mu_e, \mu_{crit}, \mu_{g,j}, \mu_{z,i}$ and $\mu_{cz,i}$ are Lagrange multipliers for the constraints. According to Kuhn-Tucker conditions, the solution can be obtained by solving the derivative equations, and both the price and the quantity of electricity at each bus are included in the solution [12]. Here only two of the equations are listed because they are related closely to spot prices:

$$\frac{\partial \Omega}{\partial g_j} = \frac{\partial C}{\partial g_j} + \mu_e \left(\frac{\partial \sum_i l(z_i)}{\partial g_j} - 1 \right) + \mu_{crit} + \mu_{g,j} + \sum_i \left(\mu_{z,i} - \mu_{cz,i} \right) \frac{\partial z_i}{\partial g_j} = 0 \tag{1.10}$$

$$\frac{\partial \Omega}{\partial d_k} = -\frac{\partial B}{\partial d_k} + \mu_e \left(1 + \frac{\partial \sum_i l(z_i)}{\partial d_k} \right) + \sum_i \left(\mu_{z,i} - \mu_{cz,i} \right) \frac{\partial z_i}{\partial d_k} = 0 \tag{1.11}$$

1.2.3 Nodal prices and Locational Marginal Pricing (LMP)

For the swing bus s, the derivatives of line flows and losses with respect to the bus injection are 0, because the line flows are not affected by the injection in the swing bus. Therefore, equation (1.10) for the swing bus can be written as:

$$\frac{\partial \Omega}{\partial g_s} = \frac{\partial C}{\partial g_s} - \mu_e + \mu_{crit} + \mu_{g,s} = 0 ==> \mu_e = \frac{\partial C}{\partial g_s} + \mu_{crit} + \mu_{g,s} \tag{1.12}$$

Furthermore, as the designation of swing bus can be arbitrary, we can appoint the bus attached with the system marginal generator (that's the last accepted running generator) as the swing bus, and we assume that the marginal generator is not running at its full capacity, so that the system reserve constraint and the generator capacity

constraint are not binding. Thus their corresponding Lagrange multipliers are 0s, and

finally we can get: $\mu_e = \dfrac{\partial C(g_s)}{\partial g_s}$ (1.13)

Note that the item $\dfrac{\partial C(g_j)}{\partial g_j}$ is marginal cost (MC) of generation at any node j, and

it can be simply written as $MC(g_j)$. That is the cost of increasing or decreasing one

unit of generation at node j. Thus $\mu_e = MC(g_s)$ (1.14)

Customers will take the electricity at their nodal prices, as long as the price doesn't

exceed their marginal benefits. Therefore, if there is enough electricity supply in the

system, the marginal benefit should be equal to the nodal price. The item $\dfrac{\partial B(d_k)}{\partial d_k}$ is the

marginal benefit (MB) of using one unit of power at node k, written as $MB(d_k)$.

Equation (1.11) gives the nodal price:

$$\rho_k = MB(d_k) = \mu_e \left(1 + \frac{\partial \sum_i l(z_i)}{\partial d_k} \right) + \sum_i \left(\mu_{z,i} - \mu_{cz,i} \right) \frac{\partial z_i}{\partial d_k}$$ (1.15)

If a customer is connected to the swing bus, considering equation (1.14), he will

see the nodal price as: $\rho_s = \mu_e = \dfrac{\partial C}{\partial g_s}$ (1.16)

because of the insensitivity of line flows to the nodal injection at the swing bus. Thus

the marginal generator sets the nodal price as its marginal generation cost. $\dfrac{\partial C}{\partial g_s}$ is also

known as "system lambda", λ, as it reflects the marginal cost for the entire system to

maintain energy balance.

It becomes more complicated if the marginal generator is running at its full

capacity limit. In this case μ_{crit} and $\mu_{g,s}$ are both nonzero, because the demand is so

high that even the marginal generator (and also the system overall generation) is short of capacity. However, equation (1.14) still holds, and for the swing bus, we can now have:

$$\frac{\partial B}{\partial d_s} = \rho_s = \mu_e = \frac{\partial C}{\partial g_s} + \mu_{crit} + \mu_{g,s} \tag{1.17}$$

The marginal benefit of this customer is now higher than the marginal cost of the marginal generator at the swing bus. Due to the technical constraints of generator capacity and system overall generation capacity, this customer cannot take any more electricity. Should the marginal generator capacity be increased by 1MW, the customer would buy this extra 1MW and create extra social benefit by the amount of

$\left(\frac{\partial B}{\partial d_s} - \frac{\partial C}{\partial g_s} \right)$. Therefore, the marginal opportunity cost (also called shadow cost) of

these two constraints—$\left(\mu_{crit} + \mu_{g,s} \right)$—is equal to $\left(\frac{\partial B}{\partial d_s} - \frac{\partial C}{\partial g_s} \right)$, and

$$\mu_e = \frac{\partial C}{\partial g_s} + \mu_{crit} + \mu_{g,s} \tag{1.18}$$

For the buses other than the swing bus, network effects have to be taken into account. In general, the marginal benefit of customers at the kth bus sets the nodal price, as in equation (1.14).

The setting of nodal prices defined by equation (1.14) is also called locational marginal pricing (LMP). In short, the short-run (i.e., assume that the embedded cost is fixed and that there is no system expansion) nodal prices have the following three component [13]:

LMP ($/MWh)=energy component + loss component + congestion component

The energy component, also known as the system lambda, is the energy-clearing price in a non-congested lossless system, and it is identical at all locations. The loss component is the marginal cost of system losses at this location. The congestion component reflects the marginal congestion cost at this location. If there's no

congestion on a specific line, the congestion rent of this line is zero. The LMP is the basis to market operation and the transmission congestion management.

1.3 Market Models and Financial Settlements

There are two basic forms of electricity markets, the pool market and the bilateral market. Although in real life, markets with combined structures are more common [14], they are developed from these two basic types [15].

In this section, these two different market models are discussed, and the financial settlement methods under the two models are also analysed.

1.3.1 Pool model
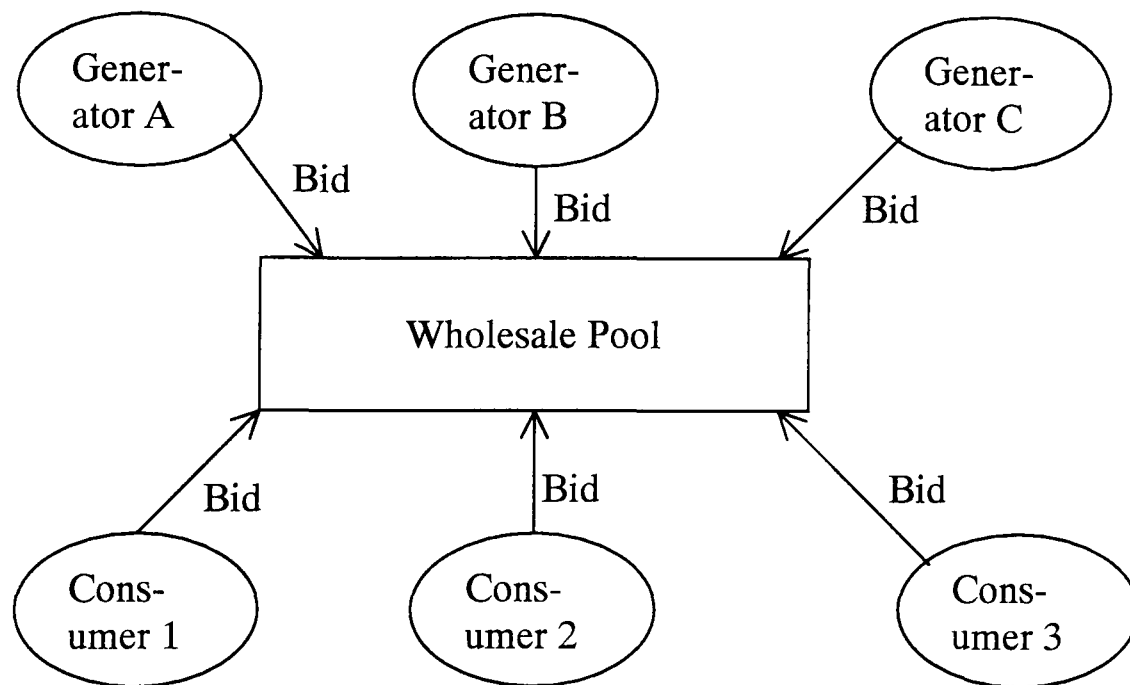
Figure 1-1   Pool Model Structure

Figure 1-1 [16] gives the structure of the pool model of the electricity wholesale market.

In the pool model, generators or other suppliers (the commercial enterprises which can inject power into the network) and customers (including distribution companies, the retail traders or large end-users) submit their price and quantity bids to the system operator (SO), and have the SO arrange the dispatch for them. The SO is responsible for selecting the optimal dispatch while keeping the constraints met, and making financial settlements for market participants[15].

In a power pool, the supply bids can be technically complex (for example, stating the start-up and non-load costs for generation units), and the system operator uses optimisation calculation to decide the dispatch[9]. Under this dispatch, the energy prices, system losses and network congestions are solved at one time [9].

1.3.2 Bilateral model

Figure 1-2 gives the structure of the bilateral model structure for electricity wholesale market. In the bilateral market, producers and consumers directly negotiate the price and quantity of energy transaction. Transaction agents submit the schedules to the SO in order to request for permission to carry out the physical energy transfer. The SO has no knowledge about energy prices in the trading, but it is responsible for determining the transmission limits, arranging the physical power deliveries, making necessary curtailment and maintaining real-time power balance in the spot market [18].

The bilateral model allows the market participants trade freely in the market place, however, due to the physical limits of the transmission network, this decentralised market often has to resort to post-trading adjustments such like curtailment or adjustment bids [19].
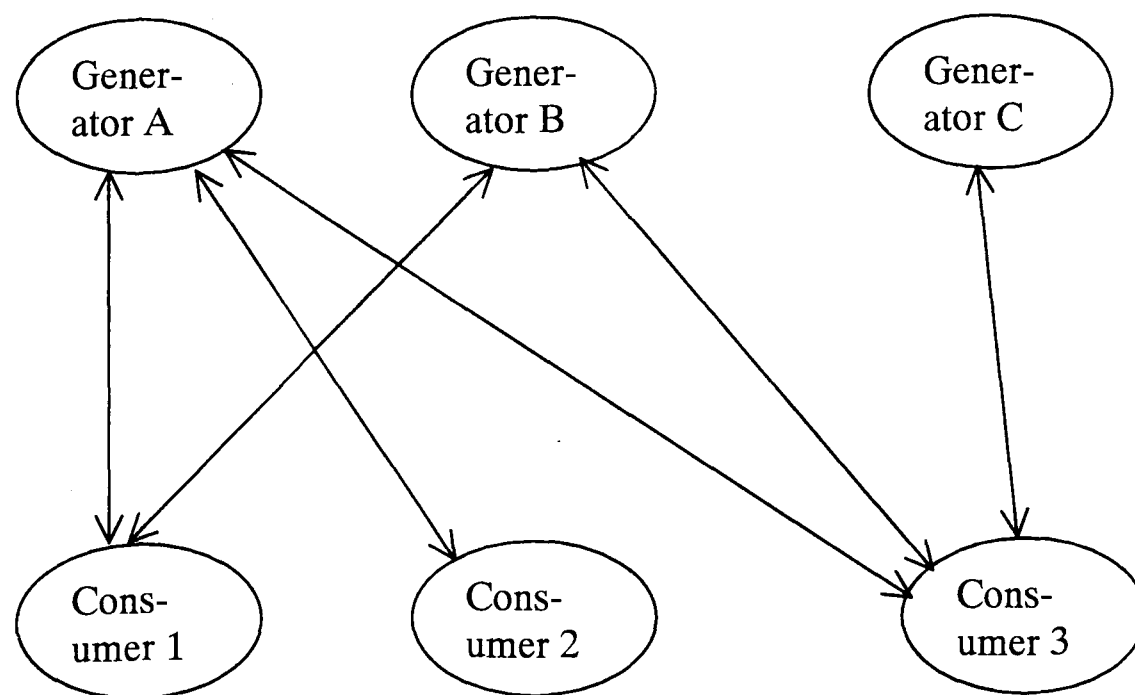
Figure 1-2   Bilateral Model Structure

A Power Exchange (PX) is a standard market place dealing with standard price and quantity bids, finding the trading counterpart for sellers and buyers [17]. A PX makes the financial arrangement and settlement, and the balancing services are left to the system operator.

1.3.3 Comparisons

It has been proved that, under perfect competition (assuming that no participants have the significant market power, and that correct price signals are available to the participants), free market competition can achieve the same perfect economic efficiency as under central dispatch [18]. Under such assumption, the bilateral model is equivalent to the pool model under perfect competition. However, the assumption of perfect competition can never hold in real world. There have been comparisons of the different market models such as [4].

In the real-time market, central coordination is required, because all the physical transactions share the same transmission network and interact with one another through loop flows. Pool model is thus desired for the real-time market. On the other hand, the forms of bids in the pool model may not give market participants enough flexibility as provided in bilateral negotiations, but it requires less trading cost and time to find the suitable counterparts and contracts [9].

In the forward markets, only financial contracts are traded, and there's no need for the central coordination. Therefore, bilateral model is favoured because of the great flexibility. The resulting energy trading in the forward markets cannot match exactly the real-time physical trading, and multi-settlement markets are organised to trade and clear contracts for different time frames. Such multi-settlement design is expected to be able to achieve both efficiency and security [9].

According to the experiences to date, markets with flexibilities for the participants to choose between bilateral contracts and the pool, have the better performance [14].

1.3.4 Transmission Pricing

Transmission pricing has been studied for a long time. [20] described a cost-based pricing based on the decomposition of power flows into transaction components and interaction components due to loop flows. [21] decomposed transmission prices into operating components and embedded cost components. [22] used a simple network to study the differences in prices and quantities under simplified models (used in many countries) and an exact model. [23] suggested a multi-period energy auction model which supports transmission congestion constraints and losses, as well as intertemporal operating constraints like start-up costs and ramp rates. [24] proposed a congestion management method to allocation the physical overload and congestion cost to individual transactions based on physical power flows. [25] gives an approach to decompose each nodal price into a set of components related with generation, transmission congestion, voltage constraints and losses, etc. [26] gives a method to compute transfer capability sensitivities. [19] propose a transmission pricing method suitable for the hybrid electricity market containing both bilateral/multilateral transactions and centralised dispatch. [27] compared several transmission loss allocation methods under the pool-based electricity market on the IEEE reliability test model. [28] proposed a multi-objective optimisation method to take into consideration both social welfare and the system security margins. This OPF method allows market operators and participants to control the system security level by controlling the weighing factors in the objective function. [29] evaluates the economic inefficiencies of a simple auction-based dispatch method.

Transmission services include operating, maintaining and expanding the transmission system [3]. Normally the long-term cost of transmission consists of four main elements:

- Transmission losses caused by the power flow in the network;
- Transmission constraints (i.e., congestion);

- Balancing services to ensure that the network is robust (e.g. reactive power support, spinning reserve);

- Returns and depreciation of the capital equipments.

The embedded cost recovery is not considered in short-term pricing. The balancing service requires central coordination of the system operator, and thus can be charged to all the network users as a flat rate [9]. Therefore the other two components are the focus in the short-run transmission prices:

(1) Shadow price (also called the opportunity price) of congestion

(2) Resistive losses cost

Long-term transmission prices should not only recover the transmission cost but also send correct financial signals to market participants [30].

The nodal prices calculated from LMP are the by-products of constrained economic dispatch, and because of the opportunity cost (shadow cost) of transmission they comprise, clear economic signals can be sent to the market participants [31]. The short-run nodal prices consist of information of the direct costs for generation and losses as well as the shadow costs for scarcity in transmission capacity. Thus the short-run transmission prices can be naturally defined as the differences between node prices, and the resulting transmission prices consist of marginal losses and congestion rents. On the other hand, given the nodal spot prices, they can be divided into a generation component and a network component [32].

Under the pool model, the market organiser (can be the power exchange—PX, or the SO) collects payments from customers at the local prices, and then distributes the payments back to generators at their local prices [33].

Under the bilateral model, the SO checks the power flows incurred by submitted transactions. If congestion is likely to occur, SO will either curtail the related

transactions or purchase congestion services from generators and customers. SO allocates losses and congestion costs to the transaction agents [15].

Marginal Transmission Pricing and congestion rents

Under LMP, the transmission network users are charged the marginal transmission cost, which is the price difference between the nodes of energy injection and extraction (the source and sink nodes). The transmission charge can be written as:

$$\rho_k - \rho_j = \mu_e \left(\frac{\partial \sum_i l(z_i)}{\partial d_k} - \frac{\partial \sum_i l(z_i)}{\partial d_j} \right) + \sum_i \left[\left(\mu_{z,i} - \mu_{cz,i} \right) \cdot \left(\frac{\partial z_i}{\partial d_k} - \frac{\partial z_i}{\partial d_j} \right) \right] \qquad (1.19)$$

The first item is the marginal social cost incurred by the marginal network losses which is caused by injecting 1MW of electricity to jth bus and extracting it at kth bus. This item is often referred as the loss component in the transmission cost.

The second item is the marginal shadow cost caused by the binding line flow limits. Moving 1 unit of electricity from bus j to bus k will give the line flow z_i an increment by $\left(\frac{\partial z_i}{\partial d_k} - \frac{\partial z_i}{\partial d_j} \right)$, and if the line flow limit is reached in either direction, this moving of electricity will incur a marginal opportunity cost of $\left(\mu_{z,i} - \mu_{cz,i} \right)$. The second item is often referred as the congestion component in marginal transmission cost.

The congestion component is the most significant component among the short-run elements. This means that the spot prices are highly volatile because of the occurring of congestions in real-time markets.

Merchandise Surplus

The total net payment from customers to the pool equals to $\sum_k \rho_k d_k$, and the pool will pay back the generators total amount of $\sum_j \rho_j g_j$. The net payment to the pool, also called merchandise surplus (MS), is equal to:

$$MS = \sum_k \rho_k d_k - \sum_j \rho_j g_j \qquad (1.20)$$

Considering that in the nodal price equation (1.14), the derivative $\frac{\partial z_i}{\partial d_k}$ and

$\dfrac{\partial \sum_i l(z_i)}{\partial d_k}$ tend to make the price higher at sink buses (where the demand is higher than

local generation level), and lower at source buses (where the demand is lower than local

generation level), the MS is normally positive [34]. Chapter 3 gives a simple 2-bus

system example to illustrate the MS>0. In fact, the congestion rents are the dominant

component in the MS [3].

Embedded Cost Recovery

It is generally recognised that because of the economies of scale in electricity

industry, the sink cost of transmission network investments cannot be fully recovered

from the short-run marginal transmission revenues discussed above [35] and [36]. One

suggestion is to use the long-run marginal cost based pricing (i.e. taking into account

capital costs and system expansion) (LRMC). In this method, the short-run operation

costs including congestion and losses can be recovered through a flat rate, or a usage-

based algorithm, but without distorting the long-term locational signals[37]. However,

the calculation of LRMC tends to be highly complicated and dependent on a number of

assumptions on costs and scenarios of expansion [30].

Alternatively, a two-part price structure can be used where the short-run marginal

cost (SRMC, i.e, capital costs and system expansion are not considered) of serving the

user is the first part of the price, and the embedded cost recovery is the second part [34].

In this method, the investment costs are usually defined as a flat rate to all the network

users to avoid distorting the short-run optimal pricing signals. Alternatively the second

part of price can be defined through a commonly accepted revenue recovery calculation

to calculate each user's share of the sunk costs [37].

There is no definite preference between these two pricing methods. Short-run marginal pricing (SRMC) may not be able to give enough incentive to the investment [38], while the effectiveness of long-run marginal cost (LRMC) depends greatly on the cost allocation method applied, as well as the relation between generation and transmission costs [39]. Even under the LRMC, transmission system expansion might still require participation of a system regulator or a pool coordinator [38]. [40] compared several embedded cost recovery methods with a special emphasis on power flow based methods. Depending on which cost is more important, SRMC or LRMC can be used, and a well-designed transmission tariff should give correct signals for both short-term economic dispatch and long-term investment incentives [37].

1.4   Transmission Rights

Due to the uncertainties in the power system, real-time spot prices are highly volatile. In a matured market, users can choose to either face the real-time prices or purchase contracts in advance to hedge the price fluctuations [41]. Transmission rights can be used to hedge the price volatility and lead to optimal dispatch [42]. In the long run, transmission rights are important to provide the right incentives for system expansions [33].

Physical transmission rights entitle the right holders to transfer energy through the network even when congestion occurs. This might give the transmission right holders opportunities to withhold the rare transmission capacities and to prevent other users from competing fairly in the market. On the other hand, financial transmission rights allow usage of the capacity from other users if they pay for it when congestion occurs. The revenue from sales of the transmission rights goes back to the transmission right holders.

Therefore, the price of transmission rights can be seen as the price signal of constraints. Furthermore, the price signals can come in either of the two forms:

conversion of the limits into nodal prices that market participants have to face, or pricing out the constraints and then calculate out the contribution to these limits from market participants [10]. With these two forms of price signals, transmission rights can also be defined in the form of explicit or implicit (bundled with energy transactions) rights. Through managing the transmission rights, the system operators can exercise congestion management and give correct signals for both short-term and long-term market efficiency.

Several forms of transmission rights have been proposed with the emphasis on the problem of loop flows. [43] suggested a method to price the congestion. [42] suggests a sequence of auctions on transmission rights in the point-to-point form and the flow gate form. Different congestion management methodologies are compared in [44].

Transmission rights can be classified into point-to-point rights, point-to-hub rights (entry/exit rights) and capacity reservation rights (link-based). Hogan [33] suggested the first two rights, while Chao and Peck [45] suggested the third form of rights. In this section, the two approaches are analysed and compared.

1.4.1 Hogan's methodology

Hogan suggested a set of implicit financial transmission rights based on LMP: [33]. In this approach, the transmission is defined as injecting power at one node and withdrawing it at another node. Such definition simplifies transmission pricing, because the complexity caused by loop flows in the network is avoided.

These financial transmission rights are priced as the marginal price difference between two locations. Using the LMP model described in Chapter 1, the differences between nodal prices determine the transmission prices:

$$\rho_k - \rho_j = \mu_e \left(\frac{\partial \sum_i l(z_i)}{\partial d_k} - \frac{\partial \sum_i l(z_i)}{\partial d_j} \right) + \sum_i \left[\left(\mu_{z,i} - \mu_{cz,i} \right) \cdot \left(\frac{\partial z_i}{\partial d_k} - \frac{\partial z_i}{\partial d_j} \right) \right] \quad (1.21)$$

Where the $\mu_{z,i}$ and $\mu_{cz,i}$ are the opportunity costs of congestion in the two directions of ith line, and z_i is the power flow on ith line. Instead of μ_e, which contains generation cost information, an average price at the balancing spot market can be used for the calculation because it is more easily available.
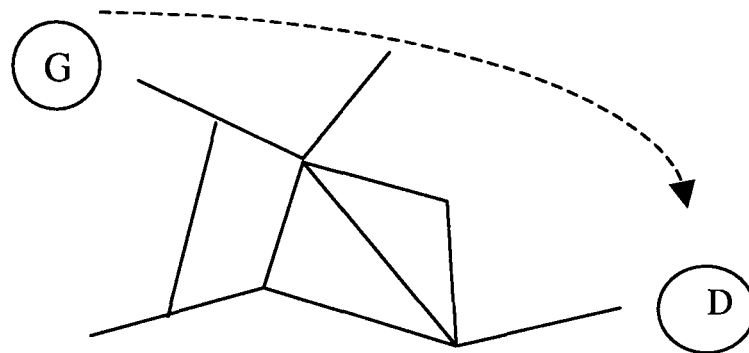
Figure 1-3   Point-to-Point Transmission Right

The definition of point-to-point transmission rights is illustrated in Figure 1-3 [31]. The bus where the generator G is attached in Figure 1-3 is also called source bus, and the bus where the user D is attached is called the sink bus.

These rights, due to the specification of source and sink buses, are not flexible for market participants. Also the calculation of the transmission right prices is not transparent. Such problems limit development of secondary transmission right markets [42]. Therefore, Hogan suggested an alternative definition of transmission rights called entry/exit rights [12]. By designating a common "hub" in the network, these point-to-point rights can be easily transformed into entry/exit rights, as shown in Figure 1-4.
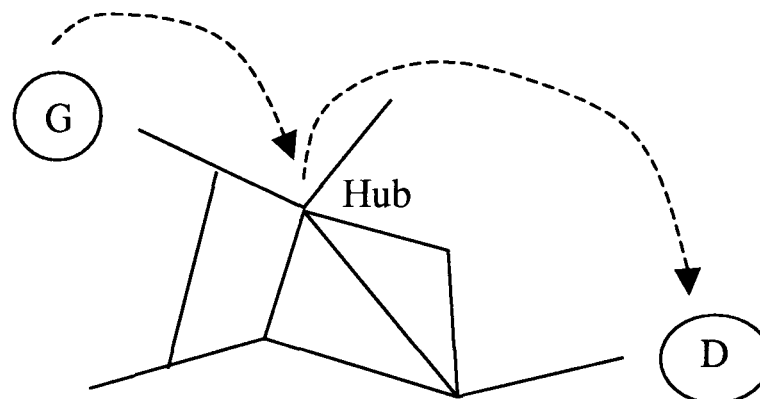
Figure 1-4   Entry/Exit Transmission Rights

In order to provide long-term hedge against price fluctuation and operation changing, Hogan also suggested the long-term transmission rights called Transmission Congestion Contract (TCC). These set of rights are long-run financially firm

transmission rights compatible with short-term locational marginal prices (LMP). The right holders are indifferent between using the physical capacity and receiving financial compensation through the congestion rents. If the right holder uses the capacity, he does not need to pay for this specific transmission. If he cannot use the capacity, he is compensated by the system operator with the real-time congestion rent. This is why the right is regarded as 'firm'. During real-time dispatch, the system operator makes decisions without consideration of the long-term TCCs. It is only at the ex-post clearing stage that right holders get their financial compensation. Therefore, these TCC rights are "firm" only in the sense of financial rights instead of physical capacity withholding.

A bidding model is suggested to allocate transmission rights. The object function in the bidding model is the auction revenue, and the auctioneer is trying to maximise the benefit from the auction[33]. This ex-ante auctioning of the transmission rights can give non-discriminatory access to those who values the capacity the most. An ex-post reconciliation process is also proposed to clears the TCCs at the real-time prices.

For example, in the network shown in Figure 1-3, the system operator runs the year-ahead auction of the TCCs. Assume the generator G obtained the TCC from G to D for a specific hour, and this TCC right allows G to transfer 50MW of electricity to D during that hour. When this hour comes, the demand D is higher than expected, and G is only allowed to transfer 20MW to D because of network capacity limitations. Therefore G is entitled to the compensation for 30MW at the congestion rent G→D. Suppose the nodal prices at G and D are £2/MW and £5/MW respectively, then under TCC, the SO compensates G for not being able to transfer the 30MW, and the price is £(5-2)=£3 (losses neglected in this simple example). Therefore, although G has to provide D with 50MW, he can buy 30MW at location D to fill the gap, for G was compensated with 30*3=£90 for not being able to fully use his transmission right. Thus G is indifferent between using the transmission capacity or receiving financial compensation.

The computation of these set of financial transmission rights is based on an optimisation, and it has been proven that with a DC approximation calculation, the revenue obtained from the TCCs is enough to cover the congestion payments, provided that the set of TCCs are compatible with a feasible power flow scenario [33]. If the AC load flow model instead of the DC model is used, there may be greater payments than that needed for the total congestion payments, so there will be some leftover congestion revenue after the clearance of the TCC rights. Hogan also suggested that this contribution as well as the contribution from losses, can be used as part of the payments of the fixed network costs [33].

There is another important point that Hogan pointed out: the "displacement" power flows from 'expensive' to 'cheap' locations [33]. The displacement power flows are the counter-flows on the congested lines. As they are in the opposite directions of the congestions, they will increase the available capacities on the lines. However, right holders will get negative congestion rent if they do not exercise the capacity in the real-time. That means they will have to pay for not being able to transfer their contracted energy along the counter-flow direction. This is fair because under this circumstance, other transactions have to be curtailed in order to maintain system security. Hogan suggested negative prices for these counter flow transmission rights in the auction, so that the right holders get payments from the grid for relieving congestions [33].

Hogan's approach is based on the centralised calculation and auctioning. It is worth noticing that a multilateral coordinated trading proposed by Wu[18] can achieve the same dispatch through decentralised trading.

The design of multilateral coordinated trade is aimed at the separation of security and economy. The system operator maintains security by calculating, publishing and charging the transmission congestions. The sensitivity factors of congestion costs to a transaction are published, so that market participants can discover the profitable

transactions which can avoid congestion charges and therefore relieve the congestions. If necessary, system operator curtails submitted schedules without consideration of economies.

If no participant has significant market power, the whole system will reach short-term economic efficiency under these multilateral trades. Under this mechanism, the security of the transmission network is public information which is open to every transmission network user, and cost-benefit information do not need to be disclosed to the system operator. Wu also suggested how to discover and arrange such trades, and how to calculate losses based on a DC flow model.

1.4.2 Chao-Peck approach

Chao and Peck suggested a definition of flow-based transmission rights in the form of capacity reservations [45]. The definition of transmission capacity right is [45]:

> A transmission capacity right entitles its owner to the right to send a unit of power through a specific transmission line in a specific direction and to collect economic rents associated with the transmission line according to the trading rule.

The idea of defining these flow-based transmission rights is to avoid the numerous point-to-point rights proposed by Hogan. As there are normally thousands of nodes in a power system, their combination of point-to-point rights will require large amount of calculation. The Chao-Peck transmission rights are called flow-based or link-based transmission rights to differentiate from Hogan's node-based rights. Unlike the point-to-point financial rights proposed by Hogan, this definition gives capacity reserve priority for each transmission line /transformer which is likely to be congested (called flow gate), and the capacity-reservation provides both financial hedge and physical scheduling priority. However, if the right holders do not schedule their energy transmissions in real-time, others can use the capacities free of charge (the use-it-or-lose-it rule for capacity reservation in electricity markets).

In this approach, the tradable transmission capacity right enables the right holder to transfer power from one node to another, and the right is composed of a set of power flow paths $P = \{P_{ij} | 1 \leq i, j \leq n\}$ across all the binding power flow constraints. . In such a market, the right to transfer 1MW from node i to j through the transmission network is unbundled into more fundamental capacity rights in different links, defined as a set of coefficients $\{\beta_{ij}^k | 1 \leq i, j, k \leq n\}$, where the value β_{ij}^k represents the quantity of transmission capacity rights on line (i,j) that a trader needs to purchase in order to transfer one unit of power from bus k to the slack bus s [45]. In addition, this transaction will probably create several capacity rights because of the counter-flows it arouses in some constrained lines due to loop flows [17]. Therefore, the prices for some transmission rights might be negative to reward the relief of congestions.

The transmission rights can be shown in Figure 1-5. The thick lines in Figure 1-5 are the so-called "flow gates", i.e. those transmission lines or transformers which are likely to get congested. For each flow gate, the transmission rights on both directions are defined.

One unit of energy transfer G→D requires:

$(\beta_{1S} - \beta_{2S})$ on P_{12} & $(\beta_{2S} - \beta_{1S})$ on P_{21}

$(\beta_{5S} - \beta_{2S})$ on P_{52} & $(\beta_{2S} - \beta_{5S})$ on P_{25}

and $(\beta_{4S} - \beta_{3S})$ on P_{43} &

$(\beta_{3S} - \beta_{4S})$ on P_{34}
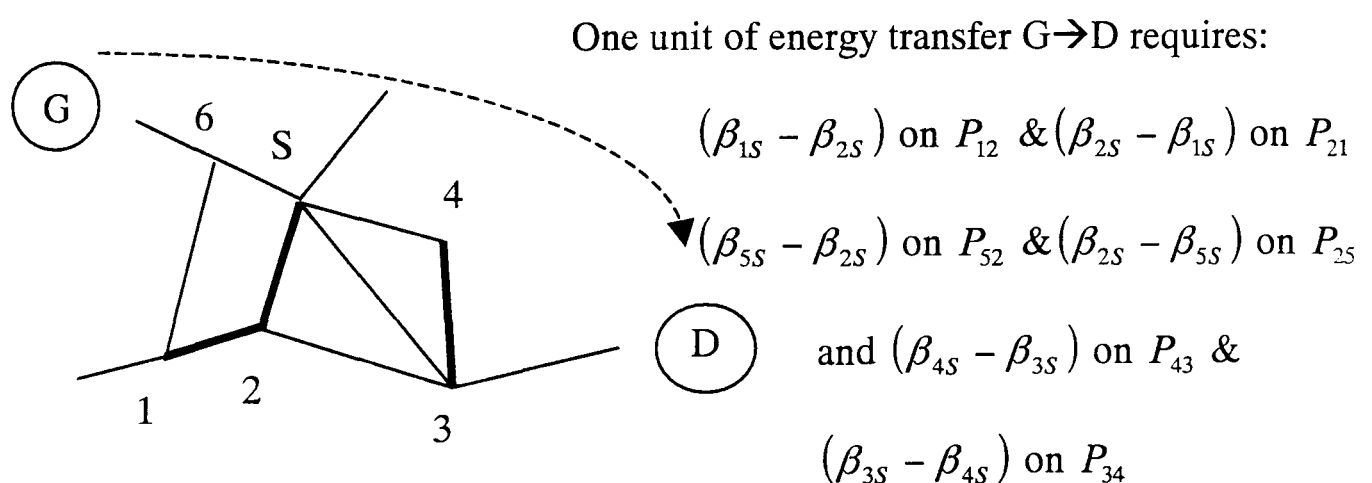
Figure 1-5   Flow-based Transmission Rights

Under this link-based transmission right system, in order to carry out a transaction, the trader must purchase the rights in all the associated links for positive and negative directional transmissions.

Losses can also be attributed to individual trades, and the marginal loss charge was suggested [45]. For the energy transfer from a node k to the slack node, λ_k is the compensation for the physical average network losses incurred by this energy transfer, and φ_{ij} is associated to each specific line (i,j), as the difference between the marginal and the average transmission losses incurred by the power flow on this line.

The system operator is in charge of defining all the transmission rights, and also organising the initial allocation well in advance of the real time. Once allocated the transmission capacity rights can be traded freely in the forward market. This forward market can be an exchange using auction or a bilateral market [17]. The right holders try to maximise their transmission rents, subjecting to each generators' willingness to pay for the rents (each generator's marginal benefit must equal to or greater than the sum of its marginal costs of generation and transmission rights). It has been proved in [45] that the final resulting congestion rents and generator dispatch are the same as those under optimal economic dispatch.

In the forward market, right holders have the schedule priority. After the forward market closes and the real-time spot market opens, all the unused transmission rights will expire and the system operator decides on dispatch to maximise social welfare while maintaining system security. This use-it-or-lose-it rule helps to mitigate market power caused by withholding the capacities in real time. However, if a trader gets all the transmission rights in a specific flowgate, it has the market power in the forward markets since all the trades in the system need him to participate in [46].

In this arrangement, only congested links require financial settlements. This is different from Point-to-point rights, in which all the nodal prices are subject to the congestions. Therefore, flow gate rights are more transparent in pricing out congestions than the point-to-point ones. Besides, it is suitable for transmission load relief (TLR)

protocols across multiple control areas by enabling a control area operator to calculate its economic impact on other control areas due to loop flows [47].

The main disadvantages of this method might be (1) the complexity of the tradable transmission rights and (2) the possibility of market power because of the ownership of a transmission line. If a trader is looking for the set of rights to support one trade, he need buy the set of associated rights on all the congested lines in the network. If a right holder owns all the rights on a transmission line, then he possesses a monopoly over all bilateral traders in the grid. Ruff [48] criticised this system, especially when under multiple contingencies. On the other hand, Oren etc. [47] claimed that direct trading of link-based physical transmission rights is needed to relief congestions. Stoft suggested an alternative congestion pricing method which can accommodate both Chao-Peck's congestion pricing and Hogan's nodal pricing [46]. This is based on the fact that under perfect competition, the same optimal quantity and prices will be revealed under both models.

1.5   Gaming and Market Power

The definition of Gaming, or strategic behaviour, is given as *a type of behaviour that aims to increase profits without achieving real efficiency gains* [49].

From the definition we can see, gaming is a kind of behaviour exploring the flaws of the market design or structure, trying to obtain more profit without making effort on efficiency improvement. Therefore, gaming should be prevented to encourage perfect competition and achieve the overall efficiency.

Gaming can be easily exercised by the market participants with market power. Market power in wholesale markets can arise from ownership concentration, scarce capacities in the transmission networks, insufficient operational reserves (including spinning reserves and supplemental reserves), and poor market designs. Even without

dominant market power, a participant can still exercise gaming if there are not enough monitoring measures and if the design or structure of the market is flawed.

Market concentration plays an important role in market power exercise. [50] analysed the fact that duopoly exists in British electricity spot market, although the phenomenon is not as serious as in theory. However, even if a market participant has small market share, he can still exercise market power if he has a dominant position (e.g. being located at a particular position, or being able to affect the system security) [51].

In the transmission product market, according to Jaskow's study [52], if a portfolio Genco in the importing region has market power, or a TransCo in exporting region has market power, holding transmission rights can enhance its market power. However, such effects depend upon the microstructure of the transmission rights market, i.e, transmission right allocation mechanisms and regulatory rules governing the market power. [53] pointed out that transmission right holding might result in reduction of available transmission capacity.

Past experiences have revealed that the power system alone cannot eliminate market power or market manipulating simply through well-defined market rules. The structures of the specific markets (e.g market concentration, network structure) will also lead to gaming. The power industry is not expected to self-regulated. Therefore, market monitoring is necessary to ensure a fair environment for suppliers and customers.

1.6   Electricity markets in the world

Many countries have opened up their electricity markets since 1980s. The common characteristics of electricity markets in the world include separation of the generation, transmission and distribution services (unbundling), and a system operator (SO) to make sure non-discrimination access to the network [15].

The characteristics of a matured deregulated market also include the extensive use of hedging contracts and a secondary contract market [15]. The contracts are used to protect market participants from the risk of electricity price fluctuations. For example, if a generator and a customer agree on a hedging contract of 50MW energy at the price of £4/MW, and in the real time, the energy price is £5/MW for this customer, then the generator will refund £(5-4)×50 to the customer. Contracts can be traded freely in the secondary market. The contracts to hedge transmission of energy in the real-time was discussed in 1.3.

Several energy market structures were compared in [54]. In this section, the market structures and transmission prices in different countries will be discussed.

UK

Before the deregulation, the UK electricity industry was formally a state-owned industry, and the problem of inefficiency has caused a heavy burden on the government. Electricity bills were high, mainly because the generator plants were required to purchase British coal at high prices [55]. Eventually under Margaret Thatcher's privatisation policies, the electricity industry was privatised in 1989 [56]. All non-nuclear state-owned power generators were privatised into four major generating companies—PowerGen and National Power in England and Wales, and ScottishPower and Hydro-Electric in Scotland [57]. The former twelve regional distribution boards in England & Wales were privatised, and customers were given the freedom to choose their suppliers. The National Grid Company (NGC) was created to own and manage the network in England & Wales. This electricity reforms in England& Wales are generally referred to as UK reforms [58].

Initially, the England & Wales market was based on the pool model, where NGC forecasts the demands and determines the dispatch of each half-hour using the supplier bids [59]. The last accepted bid sets the marginal price paid to all the online generators

[60]. Wholesale buyers and sellers must trade through the pool. NGC recovered its cost of transmission constraints through a flat uplift charge[6]. Besides, pool participants have the opportunity to hedge themselves against spot price fluctuations in the 'contracts for differences' market. According to [61], 80-90% of the generation is hedged by the contracts for differences in the day-ahead market.

This power pool has some design faults [57]. For example, as all the electricity must be traded through the pool at the uniform marginal price, portfolio bidders have the ability to set the marginal price, and submit very low prices for their base units to ensure winning the dispatch and get paid at the uniform marginal price [50]. Generally speaking, in a uniform price auction, sellers have common incentives to raise prices because they are all paid at the clearing price [9].

In 1997, British government decided to use a set of new design rules to replace the previous wholesale market design, including the Power Pool. This new market design is called the New Electricity Trading Arrangements (NETA), and it was implemented in March 2001 by Ofgem [62]. They consist of three main features [63]:

- Forwards and futures markets (i.e. the market where electricity is traded well in advance of real-time in the form of contracts)
- A Balancing mechanism
- An imbalance settlement process

The NETA are designed to promote greater competition, while maintaining a secure and reliable electricity system. The design of NETA is able to host private bilateral contracts as well as unilateral supplier/buyer bids, giving great flexibilities to market participants. Market participants can also find their counterparts through the forwards and futures markets and the three Power Exchanges (PXs) [64]. In fact, most trading is done over the counter (OTC) via direct bilateral trade between participants.

Figure 1-6 [65] illustrates the markets under NETA arranged by time horizon.
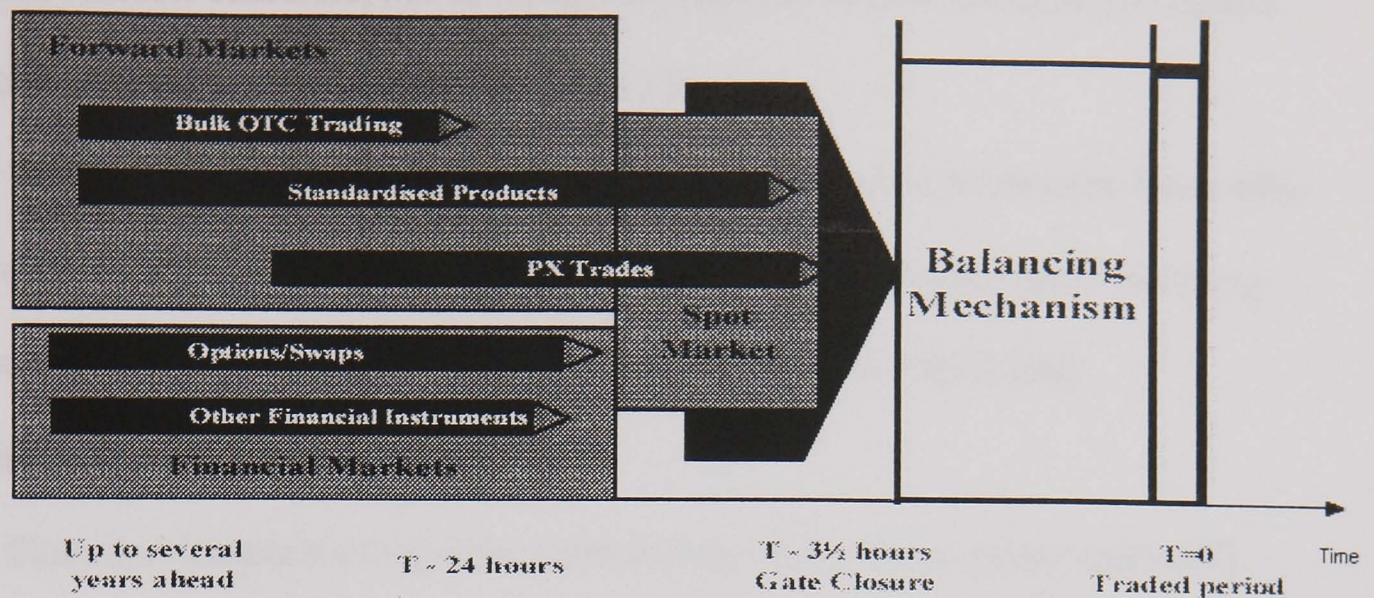
Figure 1-6 Traded Markets under NETA

Note that the gate closure time (i.e. the time between schedule notification and real-time dispatch) in Figure 1-6 has been changed from 3.5 hours to 1 hour. The reduction in the gate closure period can reduce the risks of mismatch between notified schedules and real-time dispatches.

NGC, the system operator, runs the balancing market and ensures secure operation of the system [63]. Ofgem gives the definition of balancing services in NETA [62]:

> Balancing services are technical services purchased by the SO in order to maintain the reliability and security of the transmission network, by, for example, supporting system voltage and frequency.

Generators and customers may indicate their willingness to increase/decrease the generations/ consumptions in the balancing market. NGC decides whether to accept these adjustment bids/offers to keep the system in balance in real time, or purchase balancing service from power exchanges or other short-term markets [62]. Under NETA, the prices in the balancing mechanism are determined by the accepted bids and offers (pay-as-bid). About 2 percent of electricity is bought and sold by NGC for system balancing [66].

Generators and users are described as 'out-of-balance' if they are not committed to their declared energy amounts in the spot market. This will incur additional balancing costs because NGC may have to buy or sell electricity at short notice to maintain the

31

system balance. Therefore, out-of-balance charges are applied on these participants according to the additional balancing costs [66].

The NETA is generally thought as successful. Wholesale prices have fallen 40% since 1998 when the NETA reform was proposed, due to several factors including increased competition in generation, over capacity and the NETA [66].

Asia-Pacific area

China has launched a long-term restructuring of its electric power sector[67]. Generators are being largely separated from transmission and distribution services. The State Power Corporation (SPC) divested most of its generators and was split into 11 regional transmission and distribution companies in December 2002. Electricity prices will still be regulated, but subject to major changes in tariffing.

Japan has begun a reform program to improve the efficiency of its electric utility sector. The independent power producers (IPPs) were given entry into the wholesale market, but they were only allowed to bid outside the service area they are located[15]. Large industrial and commercial consumers are allowed by law to choose their electricity suppliers, and a power exchange will be established.

The wholesale New Zealand Electricity Market (NZEM) is a voluntary pool market which can accommodate bilateral transactions as well as spot power exchanges. The spot clearing price for each half hour period is obtained from the central dispatch where losses, congestions and energy balance are taken into consideration simultaneously, and generators and demands at the same place use the same spot price [68]. A financial contracts market was created to hedge the spot price volatility, and to give incentives for grid expansion investments [69]. Decisions on network expansions and system operations are made by the system operator. The characteristics of NZEM is that customers pay for the losses at the energy exit point [70].

The National Electricity Market (NEM) consists of a wholesale pool in Australia. The system operator, NEMMCo, operates the pool and makes dispatches based on generation/demand offers/bids. Large consumers can also trade directly with suppliers through bilateral contracts. A geographically uniform spot price is applied in the pool [70]. The NEM also provide a financial contracts market to provide hedges against the spot market trading risks. The Privatisation of generation and distribution assets has attracted investments on the system expansion [67].

The United States

The 1992 Energy Policy Act and the 1996 FERC (the Federal Energy Regulatory Commission) orders [71] require non-discriminatory open access to the transmission system [72]. All transmission facilities should be accessible to the public, and non-discriminatory transmission tariffs are required. A same-time information system was developed to give all users equal access to transmission information.

The market design was left to the states. California, the Pennsylvania-New Jersey-Maryland (PJM) are two of the different examples as the former failed in 2000-2001, causing the state government to step in and purchase power [73], while the latter was regarded successful and was used as the prototype for the nationwide Standard Market Design (SMD) [13].

California: California has two market places: the day-ahead power exchange (PX), and the real-time ancillary market [73]. In the day-ahead market, bids/offers for the next day are submitted to the PX. Large electric users could also contract directly with generators using bilateral contracts. The PX then matched buyers and sellers according to their offers/bids without checking the physical constraints, and the highest accepted energy price set the "market-clearing price" in that hour. After the matching, PX as well as other scheduling coordinators (SC) sent scheduling information to the Independent

System Operator (ISO) for transmission congestion and load balancing management [74].

In the real-time balancing market, the ISO purchases ancillary services including imbalance energy, reserves and congestion relieving, from generators. The prices for ancillary services were determined from auctions conducted by the ISO. Generally the ISO has a price cap for ancillary services, but if the ISO cannot get enough qualified ancillaries at that cap, "out of market" purchases for the ancillaries have to be arranged to ensure the system security, and prices for such purchases are not capped [74].

The inconsistency on the underlying calculations between the day-ahead market and the real-time market was a design flaw. Transmission users discovered the opportunity to over schedule in the day-ahead market to cause congestions, and then 'reduce' their declared usage to get payments for relieving the artificial congestion in the real-time market [71].

The use of price cap is only applied within the state area, therefore generators in California exercised gaming by exporting their generation to other areas, and then import it back as the 'out of market' purchase [71].

The California market didn't support forward trading[75], thus the retailers cannot hedge themselves against the spot price volatility [76]. To make things worse, the retail prices were maintained low by regulations, while the wholesale prices were not regulated. [15]

Locational pricing is not used in either of the two markets. Instead, zonal pricing was applied in case of congestion [73]. The state was divided into several large transmission zones, and generators and demands at the same place use the same zonal price. The market participants can get away with such congestion charges by simply converting a spot trade into a bilateral schedule, and this lead to serious gaming behaviours [77].

The SO provides "firm transmission rights" (FTRs), which are financial rights with scheduling priority in California. The SO runs a separate congestion market to relieve congestions.

PJM: PJM operates the world's largest competitive wholesale electricity market[11]. It consists of two markets—the day-ahead market and the real-time balancing market. The day-ahead prices and the balancing (real-time) prices are all based on the concept of LMPs, which provides fundamental consistency between the energy price and the price of transmission.

The day-ahead market is a voluntary bid-based market which can accommodate both spot market bidders and self-dispatch participants [13], providing all the transmission customers with flexibilities of the bids and thus equal access to the transmission network. The hourly day-ahead clearing prices are obtained from a security-constrained unit commitment and economic dispatch, given all the bids/offers and bilateral transaction schedules submitted into the day-ahead market [11]. Bilateral transactions are broken into entry/exit bids for the power flow calculations.

The balancing market is the real-time energy market where the real-time clearing prices are calculated every 5 minutes based on the actual system operations. The underlying power flow model and operating constraints are consistent between the day-ahead market and the real-time market, therefore the resulting LMP price signals are also consistent between the two markets[11]. This fundamental consistency helps to promote economic efficiency through price signals and to avoid the gaming opportunities [11].

The financial settlement consists of two features: all the transactions in the day-ahead market are settled at the day-ahead prices, including the day-ahead congestion charges. On the other hand, all the deviations from day-ahead scheduled quantities are settled at the locational real-time prices over the hour [11].

The acronym FTR stands for the "fixed transmission rights " in PJM, but "firm transmission rights" in the California market [17]. In PJM, the FTRs are purely financial contracts and are applied to provide hedge against transmission price fluctuations and operation changes. PJM offers a monthly auction to process the residual rights. The FTRs are settled at the day-ahead LMP values [11].

South America

Chile began restructuring its power sector in the early 1980s, and is generally regarded as the first nation to reform the wholesale electricity industry structure [58]. The law was established to ensure free entry and competition in generation, and a pricing scheme based on short-run marginal costs [67]. The wholesale prices are actual pool prices, plus a regulated LRMC capacity premium, while the retail prices are regulated. Short or long-term contracts co-exist with the contract purchases [70].

The deregulation has seen positive results. There is now a competitive power generation market. From 1986 to 1998, electricity coverage rates had increased from 70% to 97% while transmission and distribution (T&D) losses decreased from 24% to 7% [78]. Privatisation also attracted private investments (especially overseas capitals) on the system expansion.

Argentina government has introduced a privatisation procedure since 1991. Access to the grid is open in order to encourage competition. The transmission prices are regulated, and the transmission companies are separated from generation service to keep their independence and thus ensure the non-discriminatory transmission access. The open electricity market has attracted foreign investments, and the domestic demand can be generally met by the generation capacity now [78]. T&D losses have been reduced from 26% in 1991 to about 7% in 1999. Service reliability has also increased mainly because of the technology newly introduced. [67]

Europe

The Electricity Directive 96/92/EC requires deregulation of the electricity industry in European Union countries. According to the directive, the electricity markets of all current 15 member countries will be fully deregulated by July 2007 [67]. The restructure processes vary among the member countries.

German market was completely liberalized in 1998, and all the end-consumers are able to choose their suppliers now. Transmission tariffs were defined by the agreements between the producers and industry consumers [15]. Customers, instead of the suppliers, bear the use-of-system charges, which depend on the voltage levels and load profile. In other words, the use-of-system charge doesn't vary with the choice of suppliers within Germany [79].

The electricity industry deregulation in Germany is thought to be successful because consumers have seen essential price reductions after the market opening.

In contrast to Germany, the power industry in France is still regulated, and the state-owned Electricité de France (EDF) dominates the market. Up to the summer 2003, only 35% of market volume was opened to competition [67]. All the customers with annual electricity consumption above 7 GWh are able to choose their suppliers. However, there are steps forward towards deregulations. The independent network operator called Reseau de Transport d'Electricité (RTE) was established in year 2000 to assure fair access to the transmission network. In late November 2001, EDF/RTE was authorised to indirectly participate in the Powernext electricity trading market through a joint venture with other European TSOs[80]. Powernext auctions standard hourly contracts for physical delivery of electricity to business customers. Powernext aims to trade 10% of the French market by 2003-2004, and also to act as a price reference for the electricity market. Powernext plans to launch French electricity futures trading, which will include

hedging products for all power-related risk (like gas, electricity futures contracts, CO_2, weather derivatives) [15].

As the grid was originally designed for centrally optimised dispatch, it might not be able to accommodate all the commercial transactions at the same time. In many occasions the network is utilised near the limits [81], making the system security service more difficult. Congestion management is one of the most challenging tasks that system operators have to face under the deregulated circumstances.

1.7 Conclusions

In this chapter, the electricity prices are analysed using an OPF model, and different types of wholesale electricity markets are outlined and compared. A more complicated topic, i.e. the cross-border congestion management, will be discussed in the next chapter. The fundamental concepts illustrated in this chapter will help to understand the following chapters.

Chapter 2   Cross-border Congestion Management

2.1 Introduction

In continent Europe, efforts are being made to achieve an internal electricity market (IEM) for competition and efficiency, and ultimately better service for consumers.

The Florence Regulatory Forum was founded to develop the framework of IEM [82]. Cross-border power trade and congestion management are among the main topics of the Florence Forum [15]. According to ETSO (European Transmission System Operation), cross-border congestion management is the main factor for the efficient performance of the European market [83].

The US is also trying to achieve the nationwide electricity market. FERC has issued a framework called SMD (standard market design) [84]. The functions of regional transmission operator (RTO) are specified, and each region is required to conform to the framework with regional flexibility [71].

There are five key characteristics of an interconnected electric transmission system[85]:

(1) The thermal limits of transmission lines

(2) The real-time frequency limits

(3) The line losses increase with the transferring distance

(4) The phenomenon of parallel path flows

(5) The siting of generators or substations should take voltage stability into consideration.

Market participants are not supposed to care about physical power flows, thus good design of market rules is necessary to lead to an efficient and secure market. Aside from providing operational service to ensure security and reliability within their own control areas ("to keep the light on"), The TSOs also provide support to enable the opening of

electricity market, including grid access, cross-border tariffication and congestion managements (" to make the market happen") [86]. It is a challenging task to maintain the system security of the electric system and implement an effective strategy for the development of the interconnected system. During the debates on the SMD framework, the problem of congestion management and transmission pricing have been deemed as critically important issues[44].

In this chapter, the proposed cross-border congestion management methods in Europe and USA are reviewed and compared.

2.2 ETSO Cross-border Congestion Management Methods Review

The European power networks were initially connected for system reliability operation, then power exchange contracts (mostly long-term ones) were developed among the member countries for mutual commercial benefits. On November 25, 2002, European Union energy ministers agreed to fully open the electricity and gas markets by July 1, 2007 [78]. Under market structure, the system operators on different control areas need to cooperate closely to ensure system security and reliability. Cross-border power trading has posed challenges to the existing congestion management methods based on the full knowledge of a control area. ETSO has summarised the general principles for the cross-border congestion management methods in the European market [82], and also gave evaluations on the several proposed mechanisms. The principles include[82]:

- Fair and non-discriminatory

- Economically efficient

- Transparent and non-ambiguous

- Applicable

- Compatible with different types of trade and contracts

The cross-border congestion management methods include non-market-based methods and market-based methods. Market-based ones are favoured because of the correct economic signals they send to market participants [82]. However, non-market-based methods (e.g. curtailment) are still necessary to maintain real-time system security because of the two demand-side flaws described by Stoft [9]: (1) Users can consume electricity from the system at real-time without warning (2) Consumers are not sensitive to spot prices.

The main non-market-based methods applied are first-come, first-serve, curtailment, etc, among which curtailment is thought to be necessary for maintaining system security [87]. This is a pure technical way based on the published NTCs (Net Transmission Capacities), and no economic incentive is given in this method. When the TSOs give approval to cross-border transactions, they can exercise this method to ensure transmission limits are not exceeded. However, there may exist conflicting curtailments when multiple congestions co-exist [87]. Moreover, the NTC values are not stable and are strongly interdependent in the meshed network [88].

In this section, several market-based cross-border congestion management methods in Europe will be reviewed and compared.

2.2.1 Available Transfer Capacity (ATC) calculation

Congestion management requires the calculation of available capacities on the transmission lines/transformers. Tabors suggested a set of cross-border capacity rights and calculation of transmission capacities [89]. [90] studied and compared several methods of available transmission capacity determination. In this section, the Available Transfer Capacity (ATC) calculation in ETSO area is summarised.

The transmission capacities are defined as NTC (net transfer capacity) and ATC (available transfer capacity). Market actors use NTC and ATC to anticipate and plan

their cross-border transactions, and TSOs use these two notions to manage these transactions[91]. The calculation procedure is given in [88]. The definition of NTC is given as [91]:

> NTC: the maximum exchange programme between two areas compatible with security standards applicable in both areas and taking into account the technical uncertainties on future network conditions. NTC=TTC-TRM

Where TTC stands for the total transfer capacity, and TRM is the transmission reliability margin. The "program" value is referred to as a commercial transaction of injecting a certain amount of energy at one place and withdrawing it at another place [91].

The calculation of TTC value has to be based on a specified power system scenario (called Base Case). This base case is generally agreed by all the related TSOs.

TRM is determined by each TSO for local system security. It is related to the real-time operation. The value of TRM may vary with the seasons or power system modification.

From the calculation of NTC we can see that NTC may also vary when TTC or TRM varies. NTC specifies the allowed transaction between two areas, and it is not a physical power flow limit. Therefore it is dependent on the choice of the base case and the security rules. During different time frames the NTC value will change. In each allocation time frame, there exist two notions—AAC (the Already Allocated Capacity) and ATC (the Available Transmission Capacity). AAC is the total amount of allocated transmission rights (can be capacity or exchange programme), and ATC is the available exchange programme after each phase of the allocation procedure. In short, ATC=NTC-AAC [91].

The definitions of transfer capacities can be summarized in Figure 2-1 [91]. From the definitions we can see that the NTC and ATC etc are directional and time dependent, i.e., they have different values in both directions of transactions, and

different values in different time horizons. In a highly meshed network like the European network, the NTC and ATC are strongly interdependent, requiring the allocation of them to be closely coordinated among the involved TSOs.

Planning
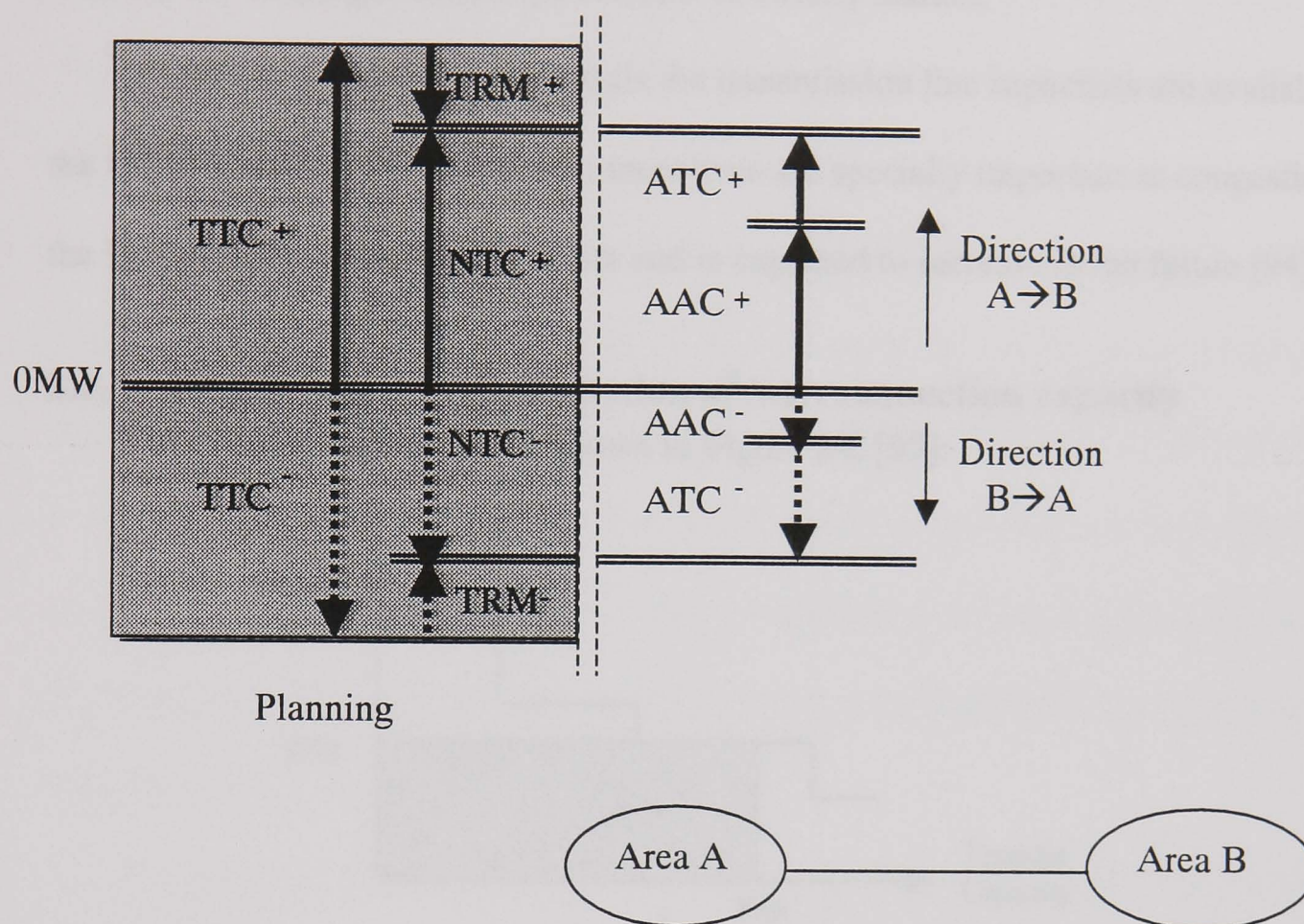
Figure 2-1   Transfer Capacity Definitions

2.2.2 Cross-border transmission pricing

Cross-border transmission pricing should be market-based, have cost-reflective transmission pricing mechanisms, and should be simple, transparent and efficient[92]. ETSO summarised the components of transmission costs[37]:

- Asset costs, including capital investment costs and the costs of operating and maintaining these transmission assets;

- System operation costs, including balancing service costs, congestion resolving costs and transmission losses recovery.

Due to the diversity of the member countries, uniform competition rules might lead to structural distortions [93]. Unlike "normal" bottlenecks within the control area of one TSO, interconnectors (equipments used to link electricity systems) involve two TSOs.

For cross-border transactions, as each involved TSO will ask for a transmission fee, the sum will be generally much greater than the local transmission fee. This "pancaking" may prohibit cross-border tradings. The problem of cross border tariffs seems the major obstacle for exchanges within the internal electricity market.

In order to provide correct signals the transmission line capacities are available on the UCTE website. The investment incentives are specially important as congestion on the European interconnections exists and is expected to increase in the future [94].

2.2.3 Cross-border explicit auction of interconnection capacity

The explicit auction can be shown in Figure 2-2 [95]:
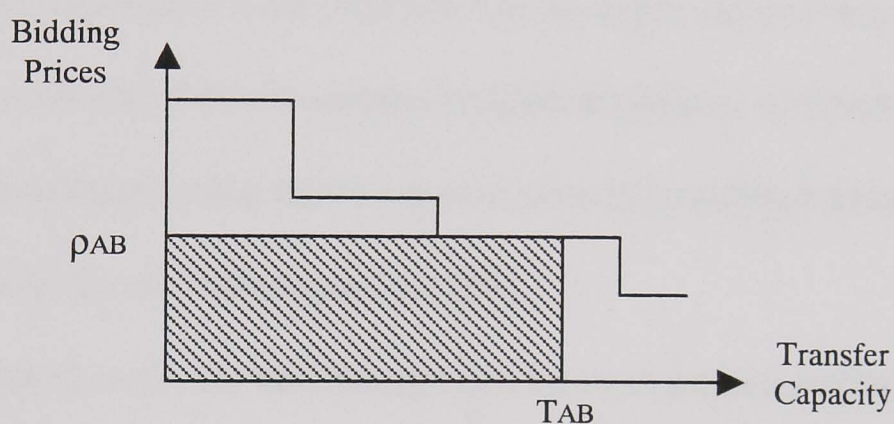
Figure 2-2   Cross-border Explicit Auctioning

In the explicit auctioning, the energy and transmission rights are unbundled. The available transfer capacity (TAB in Figure 2-2) is explicitly auctioned, and network users bid for the interconnection capacity [95]. The bids are ranked by the bidding prices from high to low, until the capacity is fully allocated. Normally buyers are charged at the marginal price instead of their bid price, because of the "no congestion no rent" principle for congestion charges—if the interconnection is not congested, network users should be free to use its capacity [96]. The marginal price is set by the lowest accepted bid (ρAB in Figure 2-2). The shadow area in Figure 2-2 shows the revenue collected from the explicit auction.

The advantage of separating the energy and transportation is that clear signals can be sent to market participants[64]. The disadvantage of it comes from the inefficiency due to the added operation complexity [95].

The co-ordinated explicit auctioning can only be organised by the TSOs who have the full information of their networks. Also it requires close coordination between TSOs and the PXs [97]. TSOs are expected to perform the system technical operation function, while power exchanges are in charge of market financial functions. Both of them are relevant to congestion management, and close coordination between them is essential for market efficiency and security [97].

The European electricity markets have great diversities from country to country. Therefore, different auction mechanisms are used in different TSO areas, bringing about difficulties in achieving overall market efficiency. If the auctions are not effectively synchronised, the results from separate regions might not converge. Besides, bad coordination among different auction systems might lead to distorted price signals [98]. If a strong interrelationship exists between several interconnections, there may exist disputes about the allocable capacities [99].

For these reasons, the auctioning must be co-ordinated and be able to accommodate both bilateral cross-border trades and power exchanges. The transmission capacity reservation must be coordinated among all the interconnected parties to allocate the scarce transmission capacities of several interdependent transmission lines between different zones. The transmission rights to be auctioned can be area-to-area transfer rights, or inject/withdraw power between one control area and a specified global hub (the entry/exit right, also called zone-to-hub rights). These two options are compatible with each other, provided that the netting rules are generally agreed (netting means that the transmission rights opposite to the direction of congested power flows are supported, so that the overall power flow can be reduced). The entry/exit model is flexible for the users, and the area-to-area rights are more stable and confidential. Thus both options are acceptable [100].

If there is no congestion, all the bids are secured, and market participants can use the capacities free of congestion charge. Otherwise marginal congestion charge applies to them. The capacity allocation procedure contains 3 steps: publishing—bidding—clearing. The TSOs publish all the security limits and PTDFs. The coordinated auctions are organised simultaneously by the TSOs. The clearing process is to maximise the overall value for the market, in other words, to minimise the transmission cost [85].

It is preferred that several auctions on transmission rights should be organised during a period (the multiple-round auction), as it is transparent in revealing the economic values of each round [85].

The co-operation between TSOs for congestion management is expected throughout all the key stages from the calculating (i.e. a commonly agreed power flow scenario as the base case load flow, and network security analysis) to the financial clearing and settlement of costs.

In order to ensure the firmness of transactions for the purpose of netting, a bottom price is set for the auction, so that the participants are really serious on their bids and attach enough values to their exchanges. Unused rights are lost during real-time (use-it-or-lose-it). At the forward right markets, reselling them is possible, but must be made through the auction office to prevent market power incurred by capacity withholding. The revenue collected from the auctions should be firstly used for the re-dispatch costs. The remaining amounts are firstly divided between the TSOs. However, as TSOs are monopoly and are not allowed to retain these revenues, they finally pass the revenue to their control areas.

Long-term contracts will reduce the available transmission capacity and thus reduce the transmission market liquidity. However, the inherent access rights should be retained for consistency, and they should also be subject to the 'use it or lose it' rule. In

the future, new long-term contract holders have to face the risk of uncertainty in transmission capacities. Hedging contracts can be used to cover this risk.

On the TSO's side, if the allocated transmission products are not available due to the real-time uncertainties (e.g. unexpected system disturbance, outage of the network components), the TSOs should arrange to buy-back the rights. However, TSOs should not be discouraged from making full use of the transmission capacities under this arrangement. Therefore, in the early allocation rounds the SO will retain some capacities at hand to leave flexibility for the power flow uncertainties. Besides, different levels of firmness on the TSOs are allowed (e.g. cost socialising, cost recovery by a portion of capacity auction revenues, or even no guarantee).

Coordinated auction has been used in the Netherlands-Belgium-Germany interfaces. The loop flows are taken into consideration in the form of interactions between minimal contract paths. However, as this approach is still based on the virtual contract paths instead of physical paths, system security problems and inaccurate price signals might occur if it is extended to the highly meshed UCTE network [101]. With good design, it is economically efficient and is compatible with existing long-term contracts and can be used for both bilateral trading and spot market exchanges.

2.2.4 Cross-border implicit auctioning/ market splitting

In the cross-border implicit auctioning, the energy is bundled with transmission rights. Figure 2-3 shows how the cross-border implicit auction works [102]:
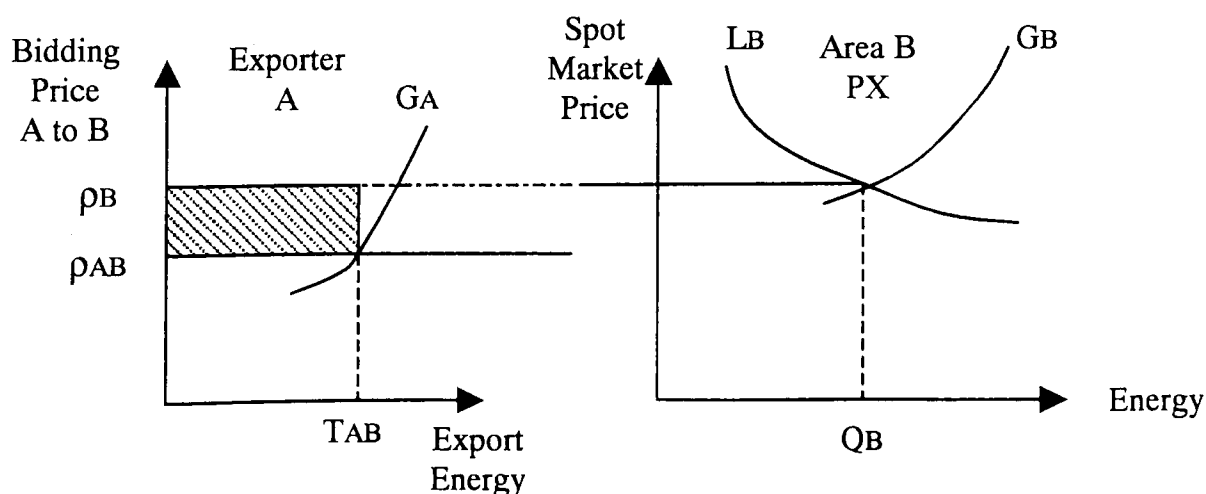
Figure 2-3   **Cross-border Implicit Auctioning**

In the implicit auction, an organised power exchange (PXs) is required in the importing area (area B in Figure 2-3) [95]. Due to the limited capacity in the interconnection from area A to B (TAB in Figure 2-3), the spot price in area B is higher than in area A. Thus generators at area A bid for exporting their outputs to area B. This bid is on energy product instead of transmission capacity. Bids in area A are ranked from lower prices to higher prices, and the lower price bids are accepted until the transmission capacity reaches its limit TAB. The highest accepted bid sets the price ρAB for energy exported from area A to B. The shadow area in Figure 2-3 shows the revenue from implicit bidding, which is $(\rho_B - \rho_{AB}) \times T_{AB}$.

Market splitting can be seen as a special form of implicit auctioning [102]. The standard market splitting can be shown in Figure 2-4 [102]. In this method, several geographical bid areas are defined by the permanently congested bottlenecks. The total demand and generation in the whole market area determine a system price without consideration of the congestions, then the TSOs compute power flows and identify the constrained lines. If congestion occurs, the bid areas on both sides of the bottlenecks apply different spot prices and form different price areas. The PXs in both areas are required to organise the energy dispatch, calculating the spot prices in their areas. In Figure 2-4, the PA and PB are calculated system prices without consideration of the energy exchanges between area A and B, while the PA' and PB' are the actual clearing prices taking the energy exchange into consideration. The revenue from market splitting is shown as the shadow area, which equals to $(P_{B'} - P_{A'}) \times T_{AB}$.

This method gives clear signals to all the participants. It is used in the NordPool area [103], where the radial network structure facilitates application of it. The radial network structure can ensure that there are no power flow interactions among interconnections across different areas. In a highly meshed network like UCTE network, the standard market splitting is not applicable because of the interdependence among the

available transmission capacities among several neighbouring control areas. However, ETSO has proved that the generalised market splitting method taking PTDFs into consideration can be developed into a general implicit auctioning[102]. In other words, the standard market splitting is a special case of implicit auctioning[104].
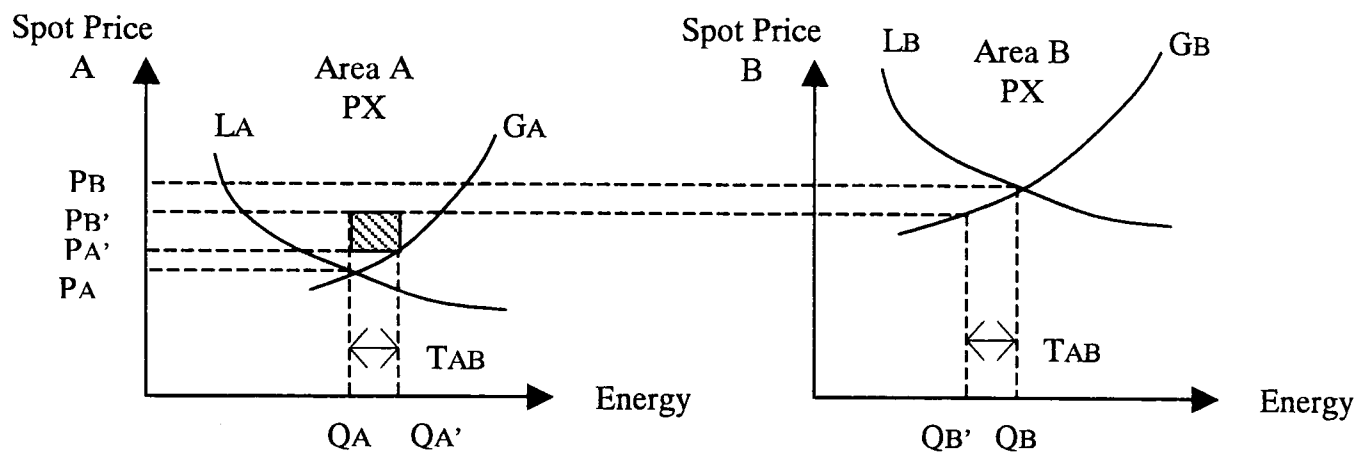
Figure 2-4   Market Splitting

The coordinated implicit auctioning should also be able to accommodate bilateral transactions across the borders, so that different market mechanisms in different control areas can be compatible. The power exchanges coordinated closely to allocate the available capacities because of their strong interdependency. Location-to-location bids are split into entry/exit bids and submitted separately to each bidding area PX. The capacity sharing between bilateral trade and implicit auction can be done through several options [85]:

- A priori allocation of transmission capacity—not market-based

- PX buy transmission capacity for use in the spot market—no level play field for PX and its customers

- Bids for transmission capacity compete with bids/offers for energy in spot markets—this is fair but requires harmonising of transmission tariffs among the markets.

In implicit auctioning/market splitting, the possible congestion revenue is retained by the TSOs as the profit made from its "brokering" activities. If the profits are not limited, TSOs will have perverse incentives to cause congestions. However, part of the

revenues can act as incentives for the TSO to make more capacities available, and to make precise forecasts of available capacity, etc [95]. In Nordic system, a regulatory cap is put on the income of TSO, so the revenue cannot become a real profit[105] .However, as the re-dispatch incurs costs, TSOs tend to "move" internal congestions to the tie-lines as they would otherwise have to pay for the congestion solution in their own control areas [106].

2.2.5 Counter trade/re-dispatch and cross-border co-ordinated re-dispatch (CCR)

Counter-trading is another market-based congestion management method. It can be illustrated in Figure 2-5 [107].

The interconnection A→B is available to all the market participants wishing to use it. However, if the total requested capacity (RC) exceeds the available capacity (AC) and A→ B will get congested, the TSO is liable to conduct counter-flow transmissions at the direction B→A. The counter flow contracts are available in the markets. The cost of these counter flow energy transactions, however, will be recovered through charges to those who requests A→B capacities [95].

Capacity Request

Area A   Area B

Counter Flow
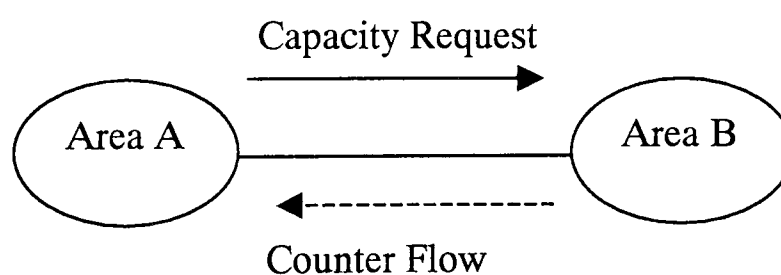
Figure 2-5   Counter Trading

The measures to relieve congestions based on changes of the generation or load pattern are called re-dispatch [100]. In the re-dispatch, a TSO modifies its generation schedule in its control area in case of congestions. Ideally the costs of dispatching the expensive generators in demand areas should be recovered through the congestion charges to those market participants responsible for the congestion. However in reality, the costs are generally charged to all the network users. For example in Nordic system,

costs are paid firstly by the TSOs at the real-time, then the TSO recover the payment through the transmission tariff to all the customers.

The co-ordinated re-dispatching (CCR) involves several TSOs to jointly act on the generators on their respective areas.

Re-dispatch and CCR are similar to counter trading, and the difference lie on two points: (1) there is a dedicated market for the re-dispatch instead of the ordinary energy markets, or generators signs long-term reserve-type contracts with their TSOs for re-dispatching. (2) The cost of re-dispatch is socialised to all the network users.

Compared with counter trading, re-dispatch and CCR are more flexible because of the dedicated market or long-term re-dispatch contracts, and they can respond to congestions in short notice [108].

Re-dispatch is specially suitable for real-time operation and require a completely independent TSO[108]. It can facilitate optimal use of the network and doesn't require all the control areas have the same market mechanisms, thus it should be widely used [109]. In reality, this method is currently only used as a preventive tool, mainly because the cost allocation requires extensive power flow calculations and is a topic of disagreement between the neighbouring TSOs [99].

2.2.6 Conclusions

The above cross-border congestion management methods were evaluated by ETSO [83]. Here the brief summaries of these methods are given:

- Explicit auctioning: this method is efficient in allocating the scarce capacities to those who value them the most, and is transparent in providing correct information. However, it cannot ensure the full utilisation of the available transmission capacities if the auctioning is not organised well. Close coordination among the TSOs is essential in the calculation, simultaneous auctioning and clearing of the capacity rights [108]. Market power may be

aroused because of the location of those generators at the congested areas. Therefore, market power monitoring must be applied. Besides, TSOs must be unbundled from energy supplying so that non-discriminatory access can be available [110]. In the mid-term, explicit auctioning is a more acceptable option for capacity allocation.

- Implicit auctioning and market splitting can send economic signals to all the market participants through the different prices on the different ends of interconnections. The technical difficulty is the definition of bid zones, because there must not be any permanent congestions within the zones, and the congestions occurring at the borders of the zones should have fixed positions. Cross-border implicit auctioning also requires close coordination among the PXs in a meshed network.

- Counter-trading or re-dispatch are suitable in meshed networks with relatively minor congestion problems, and are also appropriate for capacity allocation. This method doesn't require the interconnected systems have the same market structures. However, it requires a high degree of independence of the TSO to prevent discriminatory arrangements, and also require the congestion costs and extensive power flow calculation. In the very short term and real-time, counter-trading or re-dispatch are the most appropriate methods for congestion management. Means should be taken to prevent the market power issues posed by the few number of flexible generators [108].

- Curtailment is still necessary in the current situation to ensure system security.

2.3 Implementation of cross-border congestion methods in the European Market

European electricity markets have great diversity [110]. The market is fully opened in Germany, while the wholesale market is still absent in Belgium or France. In the Netherlands, the system operator also owns the largest generation company [79].

Congestion management might be the most important issue in European market [111]. Of the 24 interconnectors in the European Union, 12 are permanently or frequently congested, 5 are occasionally congested [99].

It is stressed that the cross-border congestion management should ensure [147]:

- Non-discriminatory access to interconnections—effective competition

- TSOs must ensure the maximum capacity usage while maintaining the network security based on a set of common criteria

- Different congestion management mechanisms in member TSOs should be coordinated and harmonised

- Transparent and simple

- The pricing and revenue distribution must give the correct short and long-term signals—economic efficiency

2.3.1 The situation of congestion management in the European electricity system

The electricity markets in Europe are at different stages of liberalisation, and a variety of transmission charging and congestion management methods are being used[112]. Therefore, the cross-border congestion management should take into consideration different market structures and the level of information exchanges. Due to the highly meshed network structure, the cross-border transmission charges should be harmonised, and the European Commission has proposed the inter TSO compensations for cross-border power exchanges[113]. The compensation payments should be based

on the long-run average incremental costs (LRAIC). Although market based congestion management will give locational signals, at present the short term congestion charges are usually not included in a harmonised tariff structure [37].

TSOs are expected to develop efficient congestion management procedures, giving appropriate economic signals, both in short-term operation action, and in long-term investment decisions. However, if a uniform cost-reflecting transmission tariff throughout UCTE network is to be applied, the technical cost calculation requires a European hub, and unified access rules as well congestion management mechanisms. Considering the diversity in the current European markets, it seems unrealistic for a single European transmission market in one step [37]. Therefore, the European Commission proposed the focus on "regional integration" for a transaction period and then convergence to an integrated pan-Europe market [101]. The co-ordination among TSOs are strongly required to ensure proper and quick convergence of regional electricity markets into a single European market (the IEM) [114].

The Day Ahead Congestion Forecast (DACF) has been adopted by members and was put in operation in 2002. This daily load-flow forecast enables the members to react in time for security of supply and a better use of system capacities. The temporary cross border trade (CBT) mechanism has also been proposed [115], because of the dispute of member TSOs on the CBT and the fact that no agreements have been achieved by all. The final internal energy market package has been adopted by the European Council and the European Parliament[114].

Currently, non-market-based capacity allocation mechanisms like first-come, first-served or pro rata rationing are still working on the major borders. They are regarded to be unfair and inefficient, but TSOs can easily manage the borders without violating the security limits.

Non-market-based congestion management methods are regarded as lacking incentives and inefficient, therefore this category was strongly objected to by all the member countries. It has been agreed that the congestion problems should be solved in a non-discriminatory way and be based on market-based mechanisms[112]. The allocation of capacity should be market-based and designed to give correct locational signals to both producers and customers[116].

As for the capacity allocation, use-it-or-lose-it principle is widely applied in member countries. Netting of opposite flows should be applied to an appropriate extent. In order to suppress market power, there should be a limit of how much capacity a market player can obtain. But currently no such limit is applied in the member countries.

Re-dispatching is applied very little on the interconnectors, mostly just as a preventive measure. The dispute is over who should pay for the re-dispatch cost. ETSO gives the definition of counter measures for congestion management including topology actions and re-dispatch [100], and also proposed several options to allocate the cost of re-dispatch[109].

2.3.2 Example: The Nordic Market and Market Splitting

The Nordic market as the world's first international spot market, is generally thought to be successful [103]. The NordPool is able to accommodate both bilateral trading and unilateral bids. In fact most of the energy trading are through bilateral transactions. Several markets are organised including forward market; one-day-ahead market and the last minute regulation market. Here only the congestion management mechanism is discussed. The congestion management is divided into different time stages as the following [117]:

1. Auctions, maintenance planning, etc

2. Capacity calculation by TSOs (36 hours ahead)

3. Bidding procedure

4. Price and capacity announced by Nordpool—price is fixed for each hour

5. Day of dispatch

6. Real-time (counter-trading in case of congesiton)

The stages (1) to (4) is planning stage, while from (5) to (6) is "in operation" stage [118].

In stage 2, the capacity calculation is based on the internal dispatches at both ends of the border. If the bids from stage 3 will cause congestions, the bidding areas are separated into different price areas. A system price will be used for all the bidding areas if no congestion occurs. Due to the calculation procedure in stage 2, those internal congestions can be "shifted" to the border by the TSO by setting a favourable internal dispatch. The main incentive is that TSOs can retain the congestion revenue from market-splitting while having to pay the congestion cost for internal re-dispatch.

Market-splitting requires at least one spot market operated in each bidding area and no permanent constraints within bidding areas. Every bid and offer is related to one and only one bidding area, and the entire system covered by bidding areas. ETSO has summarised a number of obstacles to market splitting including [104]:

- In this highly meshed network neither the locations nor the capacities of congestions are permanent

- The NTCs (Net Transmission Capacities) are interdependent.

- Cross-border bilateral transactions should also be accommodated.

- The electricity markets of member countries need harmonising.

ETSO has proposed a new methodology that can extend market splitting to meshed networks through PTDFs and BCs (bottleneck capacities). The extended method is explicit auctioning, also called "partial market splitting" in comparison with the "standard market splitting" where the limits between the bidding areas are transfer

capacities calculated ex-ante [102]. Therefore market-splitting can be treated as an implicit auctioning method. The following discussion will generally use "implicit auctioning" instead of "market splitting".

2.4 Congestion Management in the US

In the US, the standard market design (SMD) is issued by FERC [71] as guide to healthier electricity markets and cross-border transactions. Unlike the situation in the Europe where the member countries discuss on the future market rules for the internal electricity market, and the market designs and structures vary from country to country, the US FERC have the right to regulate markets in all the states and thus can give a uniform framework while allowing for regional flexibilities.

The proposal of SMD is aimed at solving the inconsistent rules across the US. SMD is expected to provide more standarisation in regional markets, better market pricing and better market safeguards. The harmonised markets can facilitate tradings throughout the US, and lower transaction costs. However, regional flexibility is also retained.

The SMD is trying to avoid the market design flaws revealed from past lessons. During 2000-2001, the California market failed as the prices rose to a very high level, and the crisis spread throughout the West. Investment in infrastructure was extremely difficult. In 2002, Enron failed because of its market manipulation, and brought about the doubt on market credibility. Under this circumstance, SMD is proposed in the hope of bringing about efficient competitions and providing stable supply to the customers.

In this section, the past lessons of market designs are studied first, so that the motivations of SMD are easily understood. Then several features of SMD are presented.

2.4.1 Past Lessons

At present, there are five ISOs (independent system operator) operating the California, PJM, New York, New England and ERCOT markets [71]. The California

market was known for the market failure in 2000-2001. It is worth taking a look at the design flaws of these present markets and compare them with the SMD.

- The day-ahead market and real-time market

The day-ahead market in California was not security-constrained. That is, the day-ahead schedules were not checked for their physical feasibility due to the constraints. In the real time market, California ISO had to pay the congestion fee to market participants for relieving congestion. Therefore, a market participant can declare a day-ahead schedule to cause congestion at no cost, and then get paid for cancelling this schedule at the real-time market.

- Seams problems

Seams are generally referred to as differences in market rules between regions, pancaking tariffs for transferring of energy from one region to another (i.e. the trader has to pay a transmission fee to each involved system operator), having to obtain congestion rights in several regions for a transaction, etc. [119]. The slight differences between markets can cause serious seams problems. The MW-laundering problem happened in California and the trading barriers in the Northeast are two examples.

A price cap is exerted in California market to prevent extremely high energy prices. However, this price worked only on the generations within this market. As a result, the local generators export electricity to outside markets and then import back the energy to evade the price cap. This is caused by the inconsistent rules in neighbouring markets. The MW-laundering was stopped after west-wide mitigation measures were applied.

The rules on ramping rate are different in PJM neighbouring markets. PJM allows ramping to accur every fifteen minutes, while in New York and New England, the ramping is limited to occur on the hour, but not within the hour. As a consequence, the seller in PJM is allowed by PJM rules to ramp up generation within the hour, while it is

rejected by the buyer in New York because it cannot ramp down the local generation at that moment.

- Zonal pricing

FERC believes that the zonal congestion system is not as effective as nodal congestion charges under LMP. The zonal method has been used in California, PJM (changed to nodal pricing later), Texas (ERCOT) and New England, to avoid the price complexity. However, market participants are more likely to game congestion in a zonal system than in a nodal pricing system [77], because it is not easy to identify who caused the congestion. For example, a customer wants to shop around for 50MW for a specific peak hour. He knows that if he bids into the PX he might have to pay for the zonal congestion fee because of the high demand in this zone. Instead, this customer managed to find a generator within its zone who promises to supply the 50MW. This bilateral transaction will not be charged for causing the inter-zonal congestion. In contrast, this customer always pays for congestion if it occurs, despite whether he choose to purchase energy from the pool or from a generator.

Another technical problem with zonal pricing is that it difficult to determine in advance the zones as power flows have been constantly changing.

2.4.2 Standard Market Design (SMD)

SMD is mainly based on the successful PJM market. It specifies the same set of rules for all the network users [120], and the system is expected to take effect by September 30, 2004. The components of a standard transmission market are shown in Figure 2-6 [2].

The major elements of SMD include the Independent Transmission Provider (ITP) to prevent discrimination by transmission owners, tradable Congestion Revenue Rights (CRRs) for flexible transmission service, transmission pricing reforms, open and

transparent energy spot markets, congestion management based on LMPs, market power

mitigation and monitoring, and resource adequacy requirement.
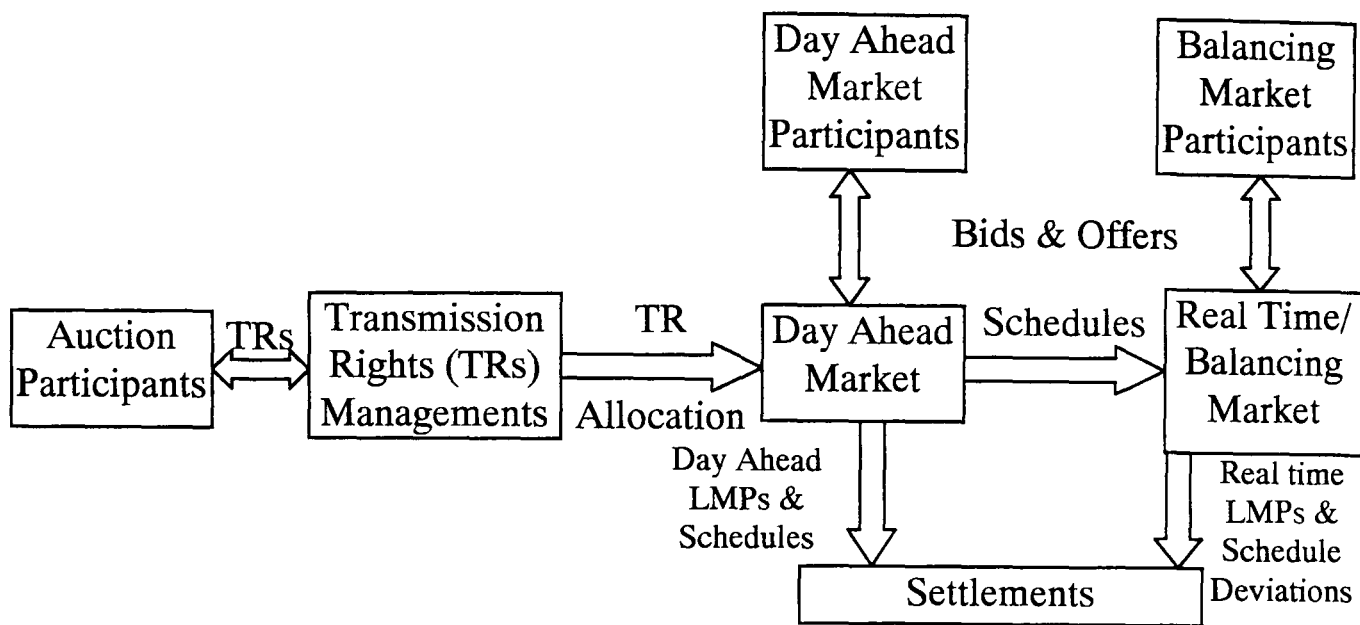
Figure 2-6   Components of Standard Transmission Market

Here several features of SMD are discussed:

- The day-ahead market and real-time market

The day-ahead market and real-time market under SMD are based on a nodal

congestion management mechanism and LMP. The day-ahead schedules must be

checked for transmission constraints in the day-ahead market, and be physically feasible

and financially binding. The introduction of the day-ahead market (some ISOs do not

organise the day-ahead market currently) is to hedge the real-time risks.

Compared with California arrangements, the congestion will be reflected in the

nodal energy prices under SMD, and there is no need for the separate congestion

relieving payment.

- Seams problems

The SMD rules will solve many seams problems caused by inconsistent market

rules in different markets. For example, a uniform bid price cap of $1000/MWh is used

to avoid the MW-laundering.

- Nodal pricing and LMP

Under SMD, the nodal pricing is used based on LMPs. Nodal pricing can send clear signals about congestion, and as the congestion rent is incorporated in the nodal prices, there is no need for a separate congestion charge. Short-term efficiency can be easily achieved under nodal pricing than under zonal pricing. The LMP is expected to signal the congestion for customers and encourage transmission and generation enhancement in the long term.

- Characteristics and functions of the RTO

The minimum characteristics and functions have been specified in the SMD platform [121]. Firstly, the RTO should be independent of any market participants to facilitate the non-discriminatory service to all. Secondly, the expansion of the RTO is encouraged to improve reliability and effectiveness, thus there are requirement on the scope and geographic structures. Finally, the RTO should have operational authority over all the transmission owners and should ensure the short-term reliability. The functions of a RTO include at least the following: (1) tariff administration and design (2) congestion management (3) solve the problems incurred by the parallel flows (4) provide ancillary services. (5) publish information on the OASIS (6) market monitoring (7) planning and expansion (8) interregional coordination.

- System balancing service

Stoft [9]has pointed out that customers normally lack price responsiveness. Besides, the system operational reserves are free-rider problem and participants have no incentives to undertake this task. Resource adequacy requirement should be met for system reliability. Under SMD, RTOs will carry out annual regional demand forecast and they are expected to make such forecast well in advance (e.g. 3 years). A minimum reserve margin of 12% is required. Penalties may be applied for overly purchase of power from spot market during shortage conditions.

- Energy uplift and congestion uplift

For the reason of energy reserves and transmission congestion, energy uplift and congestion uplift are applied to compensate the cost for out-of-merit generation. Energy uplift is used to cover part of start-up and no-load costs if the nodal price is not high enough, and it is shared by all the customers. Congestion uplift is used for transmission system security when congestion occurs, but the cost is solely borne by the congested region under SMD.

- Congestion management systems and transmission rights

The SMD specifies a congestion management system based on LMP and financial transmission rights. Market manipulation will be monitored and mitigated. The allocation of congestion revenue rights (CRRs) to market participants will be divided into two stages.

In stage I (the initial allocation), the allocation is based on the historical use, because the existing long-term contractual transmission rights have been given the priority to use the transmission network. Thus they can be converted into financial rights in this stage. These CRRs are financial hedging instrument that entitles the holder to compensation for costs associated with transmission congestion between two locations.

In stage II (within four years of adoption of SMD), the allocation should be based through auctioning. Therefore, any entity interested can acquire CRR through the auction. At this stage, the access charge will be on the load-serving entities (LSE). This seems like a price lift to the LSEs, but in fact, due to the decrease of generation costs as the result of this cost shifting, the LSEs don't necessary have to face a cost increase. Any transitional power flows will not be charged for the access fee. For inter-regional transactions, the LSEs on the net importing area will pay a load ratio share of the embedded costs to the exporting RTO. This can avoid "pancaking" of cross-border transactions across RTO borders.

Participant funding will be raised for system expansion.

- Transparency

The Internet based OASIS (open access same time information system) can publish the available transmission capacities.

- Market monitoring and manipulation mitigation.

Market manipulation monitoring and mitigation methods are to be used under the supervision of FERC Office of Market Oversight and Investigation (OMOI) and the regional independent market monitoring unit (MMU). Each of the regional markets will be evaluated, and load pockets as well as areas need reinforcements will be identified.

2.5 Conclusions

In this chapter, several cross-border congestion management methods are reviewed, and examples are given. In one word, market-based congestion management methods are favoured over non market-based ones although the latter are still necessary in the current situation to ensure system security. System operators are expected to coordinate with one another to achieve high efficiency while maintaining system security.

In the next chapter, a new congestion management method is proposed to address the merchandise surplus problem. It is illustrated in a single control area, but the methodology can be extended into multiple control areas.

Chapter 3 A Congestion Management Method Using Merchandise Surplus Allocation

3.1 Introduction

An ideal congestion management mechanism should give market participants the correct incentives to relieve congestions. That is to say, under the mechanism, those participants who caused congestions should not be encouraged, while those who helped to relieve congestions should get their rewards.

Some congestion management methods have been proposed and used in different markets, as discussed in 1.4. Due to the effect of loop flows, any transaction between two participants might in theory affect the transactions of all the other parties, and this poses challenges for specifying payment for any individual transmission network user. Hogan suggested a set of point-to-point financial contracts to hedge against price fluctuations and system uncertainties [12]. These contracts are based on LMPs [33], and the contract holders (right holders) are indifferent between using the capacity covered by their rights and receiving financial compensations. Chao and Peck [45] suggested a definition of flow-based transmission rights in the form of capacity reservations. It can be easily proved that point-to-point and flow-based rights are mathematically equivalent [46].

A new method of congestion management is proposed in this chapter. This method gives a set of rules to refund Merchandise Surplus (MS) back to the market participants. Firstly, the sources of MS are analysed, then the MS refund method is given, which is designed to punish those users who cause congestions, and to protect other users from being affected by the congestions. In this way, users who have caused congestion will pay full marginal congestion costs, while other users are compensated. This MS

allocation can be viewed as a kind of financial transmission right allocation. Under this mechanism, users have a form of financial rights-and-obligations to use the network.

In section 3.1, the philosophy of this method is illustrated on a simple 2-bus system, and the MS refund method is described. In section 3.2, a 5-node example is given to illustrate the method. Section 3.3 gives comments and conclusions.

3.2 Philosophy

The users who caused congestion should pay the marginal congestion costs, whereas other users should not be affected by the congestion on their financial payments. That's the philosophy of the congestion management method proposed in this chapter. In order to have a better understanding of the MS refund method, the simple 2-bus lossless system shown in Figure 3-1 is presented:
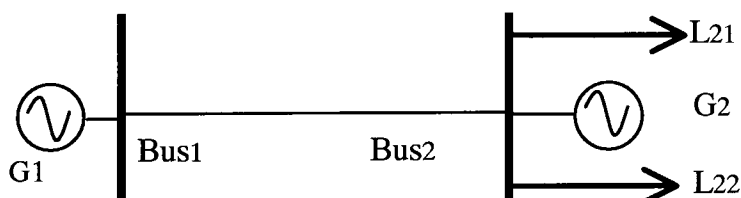
Figure 3-1   A 2-bus System

The transmission capacity of the line between bus 1 and bus 2 is 100MW. For the reason of simplicity, assume that both generators have constant marginal generation costs and sufficient capacities. G1 is the cheaper generator whose marginal cost is £5/MWh, and G2 is the expensive one whose marginal cost is £10/MWh.

3.2.1 Case 1: No congestion occurs

L21 and L22 are both 50MW. Both of them buy energy from the cheaper generator G1, so G1 produces 100MW. The transmission line is at the onset of congestion. G2 is not running at this time.

The prices at node 1 and node 2 are p1=p2= £5/ MWh for this hour, and the payments from L21 and L22 are both p2*50=£250. G1 gets its payment at p1*100= £500. There is no merchandise surplus after the payments are made.

3.2.2 Case 2: Congestion occurs

Now L22 increases from 50MW to 100MW, and L22 remains unchanged. Due to the limited transmission capacity, G1 is only allowed to generate up to 100MW, although it has enough generation capacity. In order to meet the demands, the local expensive generator G2 is running to produce 50MW of energy.

The price curve against total load at bus 2 is the thick line in Figure 3-2.
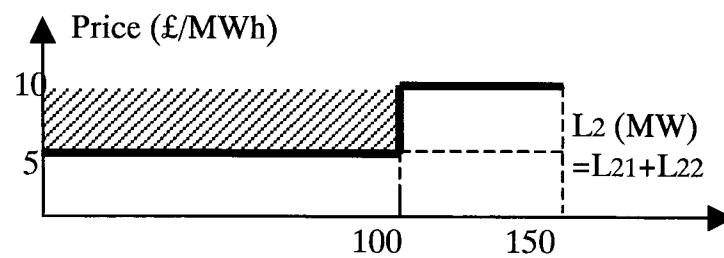
Figure 3-2   Price curve against demand

Under the locational pricing, prices at node 1 and 2 are: p_1 =£5/MWh and p_2=£10/MWh. Thus the payments from loads at bus 2 are $p_2 * L_{21}$ =£500 and $p_2 * L_{22}$= £1000 respectively. The two generators get their payments at $p_1 \cdot G_1$=£500 and $p_2 \cdot G_2$=£500.

System operator (SO) collects payments from loads and pays back to generators (under pool model), or charge traders for the transmission service at the nodal price difference (under bilateral model). Under either model the merchandise surplus is £500, which comes from the price difference between bus 1 and bus 2, i.e. the marginal congestion rent. The MS is shown as the shadow area in Figure 3-2.

3.2.3 How to allocate the MS

SO is not allowed to keep the MS, otherwise the MS will give incentives to the SO to create congestions. Comparing the nodal prices in case 1 and case 2, it is easily seen that the nodal price increase in bus 2 was caused solely by L22. However, L21 also had to pay the congestion price, although it didn't increase its usage of the line. In case 2, L21 paid extra fee (500-250=£250) compared with its payment in case 1.

Ideally, L22 should pay for the congestion costs, while L21 takes no responsibility for the congestion since its demand didn't change. Therefore, its extra payment should be refunded from MS.

During the off-peak hour (case 1), both L21 and L22 pay at the price of £5/MWh for their demands, and the transmission network can accommodate the demands without difficulties. It can be understood that the network has been structured in this way that L21 and L22 are entitled to use their share of the transmission capacity [122]. When congestion occurs, they should still have the right to use their allocated transmission capacity at no additional cost, and the increase in nodal price due to congestion should not affect their allocated share. Based on this principle, the MS allocation methodology is given as following:

The MS of £500 is refunded to transactions G1→L21 and G1→L22 according to their usage before congestion occurred (both are 50MW in this example). As L22 has increased from 50MW to 100MW, the new transaction G2→L22 should pay the expensive local generation fee at £10/MWh for the 50MW increment, for this transaction has caused congestion. After the MS refund, L21 is not affected by the congestion, while L22 pays at marginal congestion price for its increase in usage.

This MS refund method as described above was designed to discourage the increase in demands at peak time. However, it also reduces the pressure on users who maintain their demands at peak time, so that they don't have to reduce their peak time usage. Therefore, the MS refund method also reduces the incentive for efficiency.

3.2.4 How to allocate transmission rights

In order to use the MS allocation method, each trader's 'proper' usage of lines should be defined, so that no congestion fees will be charged for that set of usage. All the 'proper' usages add up to 100% use of the congested lines. Therefore, users can be seen as being given a form of transmission rights through the share calculation and MS

refund. These financial transmission rights can ensure that traders' 'proper' transactions are not affected even when congestions occur. As there are only a few lines likely to be congested in a system, the calculation of refund will not be too complicated.

The suggested method of allocating 'proper' usage must be compatible with pre-existing point-to-point or flow-based transmission rights. It can be viewed as a method of allocating left-over transmission capacity, i,e, the difference between the full capacity of congested links and the capacity already allocated to different forms of transmission rights. If the left-over capacity is not allocated, the MS associated with it is shared by all the system users [85]. Under the proposal in this chapter, the left-over MS is associated with the transactions affected by constraints, and is therefore more cost-reflective. Sharing MS among all the users will lead to a form of windfall benefit, as the user who did not contribute to congestion fees still benefit from the reallocation of use-of-system charges.

The leftover transmission capacity can be allocated in a number of ways:

(1) Scale up all the existing transmission rights on the line proportionally to get 100% total usage. For example, if L21 has the right of 10MW, and L22 has 15MW, their allocated MS refund rights are 40MW and 60MW respectively. This is simple but not necessarily fair.

(2) Allocate the leftover capacity proportionally to those whose actual usage is above their transmission rights. Again suppose the capacity rights for L21 and L22 are 10MW and 15MW, so the leftover capacity is 100-10-15=75 MW. When the real-time actual usage of both users exceed their TCC rights, for example, real-time loads L21 and L22 are 60MW and 60MW respectively, the two loads exceed their rights by (60-10)=50MW and (60-15)=45MW respectively. Therefore, the allocation of left-over capacity is 75*50/(50+45)=39.5MW to L21 and 75*45/(50+45)=35.5MW to L22. The total right for L21 is then 10+39.5=49.5MW, and the right for L22 is

15+35.5=50.5MW. After MS refund, congestion payments from the loads for this hour are:

L21: £10*60-49.5*(£10-£5)=£352.5

L22: £10*100-(15+47.2)*(£10-£5)=£347.5

and their total payment can exactly cover the total generation charge, which is 100*£5+20*£10=£700.

The downside of this approach is that the allocations of left-over rights are repeated for every trading period, resulting in some sharing of congestion costs. Assume e.g. that L22 is increasing in the next trading period from 60MW to 100MW. The full marginal cost of this increase is (100-60)*£10=£400. The allocation of left-over rights will give 75*(60-10)/[(60-10)+(100-60)]=27.8MW to L21 and 75*(100-15)/[(60-10)+(100-60)]=47.2MW to L22. Note that the allocation to L21 has decreased while the allocation to L22 has increased. Hence the payments by the loads are:

L21: £10*60-(10+27.8)*(£10-£5)=£411.1

L22: £10*100-(15+47.2)*(£10-£5)=£688.9

Compared with previous right allocation, the increase in fees for L22 is £688.9-£347.5=£341.4, which is less than the full marginal cost of £400. Clearly some of the cost of increased demand from L22 has been placed on L21 which did not increase its demand. In this method, when actual usages cause congestion on this line, the exceeding users are able to take advantage of such right allocation method, paying only a portion of the increased cost.

(3) Cut-off point of filling up the line limit. This method suggests using historical operation data to allocate the leftover transmission capacity. Those who actually filled up the capacity gap get the rights. For example, again suppose the existing rights for L21 and L22 are 10MW and 15MW. Assume that the loads change from time to time, and the full transmission capacity of the line (100MW) is reached at a cut-off point

when L21=5MW and L22=70MW, and there is an additional new load L23=25MW, which had not acquired any transmission rights. The entitled usages of the transmission capacity are 0MW for L21 (because its 10MW existing right is enough to cover its usage), 75*(70-15)/[(70-15)+(25-0)]= 51.6MW for L22, and 75*(25-0)/[(70-15)+(25-0)]=23.4 MW for L23. These allocations are fixed during the following peak-load period when the line is congested.

The advantage of this approach is that it encourages the off-peak utilisation, because the additional transmission right allocation is effectively based on off-peak usage. The disadvantage is that it may cause a rush to get in just at the instant when the line is getting congested. This problem can be solved by calculating the share based on the average use of the congested line over the whole off-peak period, rather than just at the instant when the line gets congested.

Option 3 has one additional advantage over option 2 in that the right allocations are fixed. This means any increase in the load incurs a full marginal increase in its congestion costs. Under option 2, the allocations are re-calculated for every trading period, which means that sharing of costs is the potential consequence.

3.2.5 Extended to the Meshed Network

The simple example shown above is a radial network where loop flows don't exist. In reality, meshed networks are more general, and the proposed MS refund method should be extended in the presence of loop flows. Additionally, there might be more than one line congested in the network.

For each congested line, a set of usages are allocated to all the traders. Besides the existing long-term transmission right, each user gets the additional allocation of left-over rights using one of the options 1-3 introduced above. These are line-by-line rights (like Chao-Peck's rights), but Hogan's point-to-point rights can also be accommodated

through the application of PTDFs, which can reflect the power flow influence on a line from a point-to-point trade. The allocation of MS follows the steps given below:

1. Allocate usages (%) of the first congested line to all the bilateral traders.

2. Repeat the same procedure for all the congested lines and thus get different sets of usages for different congested lines.

3. When real-time congestion occurs, collect the MS.

4. Decompose the MS into individual congestion rents in relation with individual congested lines. Refund each rent to all the loads based on their allocated usage of that line.

3.3   Illustrative Example

In this section, a 5-node network shown in Figure 3-3 is used to illustrate our MS allocation method. For the reason of simplicity we use DC power flow and consider only real power. Losses are ignored here.
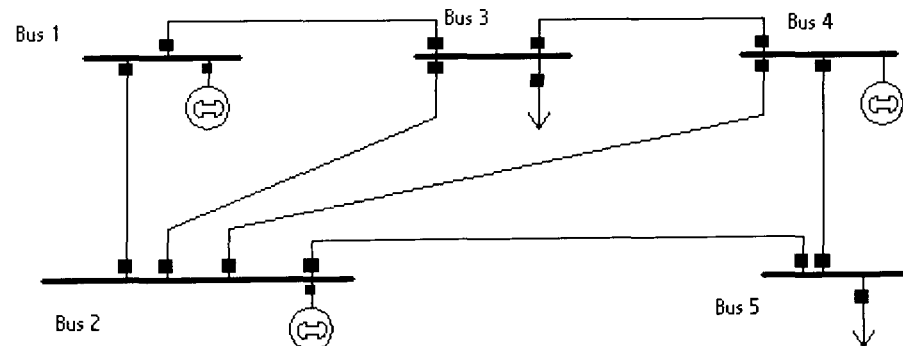
Figure 3-3   **A 5-node system**

Use p to denote the price, and q to denote the quantity, then the generation bid functions are: $p_1(q_1) = q_1 + 7.62$, $p_2(q_2) = 0.28q_2 + 7.62$ and $p_4(q_4) = 0.4q_4 + 7.74$, where the output levels of generators are given in MW.

3.3.1   Case One—only one line (5th line) is congested

The line flow limit of 5th line (bus2$\rightarrow$ bus 5) is 80MW. Assume the rights are allocated by scaling up all the long-term base load transactions (option 1). The transactions and their impact on 5th and 6th line (bus 3$\rightarrow$ bus 4) are given in Table 3-1:

Trades (MW)	PTDFs on line 5 (PTDF$_{5i}$)	PTDFs on line 6 (PTDF$_{6i}$)
Bus1→3: 40	0.11429	-0.34286
Bus 2→3: 60	0.14286	-0.42857
Bus 2→5: 40	0.72698	0.15238
Bus 4→5: 60	0.54603	-0.30476

Table 3-1   Base load transactions and their PTDFs

Allocate shares of usage on the congested line

The long-term base load transactions shown in the first column of Table 3-1 are used to determine the allocated usage of the congested line (line 5) from each trader. The total of their allocated usages should be 100% in order to make full use of transmission network while keeping it not congested.

For the 5th line, the overall influence of these long-term transactions is: Power Flow=$\sum_i \left(Transaction_i \times PTDF_{5,i}\right)$ = 74.98<80MW. Thus, under the long-term contracts, the 5th line is not fully used. Under the option 1, all the bilateral transaction quantities can be increased proportionally until the 100% overall usage is reached. This is called 'scaling up' of the trades. The scaling-up factor is 80/74.98=1.07, and the allocated usages of line 5 from the traders are 42.68MW, 64.01MW, 42.68MW, and 64.01MW.

Real-time dispatch and locational prices

Given real-time loads L3=110MW and L5=130 MW the Optimal Power Flows (OPF) and nodal prices can be obtained. The nodal prices are shown in Table 3-2:

Bus	1	2	3	4	5
Prices	30.60	22.64	62.47	73.10	225.36

Table 3-2   Real-time Nodal Prices (£/MW)

According to economics theory, bilateral or multilateral trades can achieve the same results as in the central dispatch, if each participant can compete freely [18]. Here the bilateral model is chosen, and several short-run bilateral transactions are compatible with the optimal dispatch. The SO calculate out their transmission payments based on the differences in nodal prices. The results are given in Table 3-3.

Trader	1→3	2→3	2→5	4→5	4→3
Trade (MW)	22.98	30.65	22.98	107.02	56.37
Pay (£)	732.46	1220.8	4659.2	16294	-598.8

Table 3-3   Short-term Transactions and Transmission Payments

(3) MS refund

System operator refunds the collected MS back to each trader according to its allocated usage, as shown in Table 3-4.

Note that the fifth trader from generator 4 to load 3 has got no refund, because there was no allocated transmission right for this trade.

Parties	1→3	2→3	2→5	4→5	4→3
Trade (MW)	42.68	64.01	42.68	64.01	0
Refund (£)	1360	2550	8651	9747	0

Table 3-4   Allocated Rights and MS Refunds

3.3.2 Case Two—two lines (5th and 6th lines) are congested under the real time dispatch

In the above system, the flow limit of the 6th line is reduced from 120MW to 95MW, this line will also become congested under the same real-time loads. The long-term transactions and their PTDFs stay unchanged as given in Table 1.

When both the 5th and the 6th lines are congested, the kth nodal price p_k consists of congestion rents for both 5th line and 6th line. The price difference between load k and generator j is sum of congestion rents to be paid by k and j for both 5th and 6th lines. Therefore the overall MS collected by SO is the total shadow congestion payments for 5th and 6th line.

In this example, the MS consists of two components, and they need to be dealt with separately, for they are caused by different transmission constraints. A trade has different impacts on these two line flows, and thus it should get different refunds for the two different congestions. Therefore, for each congested line, a set of allocated off-peak

usage rights, and therefore a set of refunds of the related MS congestion component, are given.

Allocated shares of usage on the congested lines

The power flows on line 5 and line 6 caused by long-term transactions are $\sum_i \left(Transaction_i \times PTDF_{5,i}\right)$ and $\sum_i \left(Transaction_i \times PTDF_{6,i}\right)$ respectively. The values are 74.98<80MW for the 5th line and |-51.62|<95MW for the 6th line. Here the negative sign in the power flow of 6th line indicates the opposite direction of actual power flow from that specified.

As discussed before, the transactions need to be scaled up to get the 100% usage. The scaling-up factors for these two lines are 80/74.98 and 95/51.62 respectively. Thus the allocated usages from all the transactions on line 5 and line 6 can be obtained, and they are shown in Table 3-5.

Trader	1→3	2→3	2→5	4→5	4→3
Use line 5 (MW)	42.68	64.01	42.68	64.01	0
Use line 6 (MW)	73.62	110.42	73.62	110.42	0

Table 3-5   Allocated Bilateral Trades for Use of the 5th and 6th lines

Real-time dispatch and locational pricing

Given real-time loads L3=110MW and L5=130MW, the real-time nodal prices can be calculated out, and the values are given in as shown in Table 3-6.

Bus	1	2	3	4	5
Nodal price	62.62	15.09	252.76	71.07	652.75
Price by 5th congestion	62.62	36.09	168.73	204.11	711.10
Price by 6th congestion	62.62	41.61	146.64	-70.41	4.27

Table 3-6   Real-time Prices in Case 2

The price difference between two nodes consists of two components, i.e. congestion rents for 5th and 6th lines. In order to refund the overall MS back to participants, the MS as well as spot prices should be decomposed according to the two congestions, i.e. two sets of nodal prices can be calculated out, each of which is caused

by one of the two congestions. Also MS is total of shadow congestion fees for 5th and 6th line.

If all participants can compete freely, their self-dispatch results will match the optimal central dispatch [18]. For example, short-term transactions can be:

1→3: 55MW, 2→3: 26.67MW, 2→5: 0MW, 4→5: 130MW, 4→3: 28.33MW.

3.3.3 MS refund

SO refunds each congestion component in the MS back to all the traders according to their allocated share of use.

	1→3	2→3	2→5	4→5	4→3
5th rent	4528.5	8491	28806	32454	0
6th rent	6185.3	11597	-2749	8247	0

Table 3-7   MS Refund under Bilateral Model

3.4 *Conclusions*

When congestion occurs, all the nodal prices will change due to loop flows. The power system operation changes frequently, causing significant fluctuations in spot prices. Long-run transmission rights are proposed to provide hedge against transmission price fluctuations. In the method proposed here, the SO uses the MS to refund transmission right holders, paying back the congestion rents for the allocated amount of capacities.

In this chapter, a new method of congestion management by using MS refund is suggested. After the MS refund, those users who were responsible for congestions pay at the expensive marginal generation prices, while the financial settlements of other users are not affected. The philosophy of this method is illustrated on a simple 2-bus system, and then the MS refund method is illustrated on a 5-node example.

Chapter 4 Decomposed Optimal Power Flow Problem

4.1 Introduction

In an interconnected transmission network, several control areas are synchronously connected through the cross-border tie lines, and each TSO is in charge of its own control area. Under power market environments, the information exchange between the neighbouring control areas is limited so that no commercially sensitive parameters are disclosed. This poses challenges to the system wide optimal power flow (OPF) calculation, which is essential in the study of cross-border congestion management methods. In order to achieve optimal use of the transmission network, the TSOs have to exchange some of their information while still keeping commercially sensitive information confidential.

The OPF calculation often involves thousands of buses and is a large-scale nonlinear optimisation problem. Efforts have been made to decompose the global OPF problem into several local OPF problems corresponding to the control areas, and to minimise the volume of information exchange among the control areas. The control areas need to coordinate with one another to start running the decomposed OPF at certain times (for example every one hour), and exchange the intermediate results, then update the OPF calculation. This loop is repeated until the results converge. Several methods have been proposed to address the interconnected or coupled OPF problem. [123] gave an approach to decompose the linear reactive power optimisation by way of grouping the buses into local and frontier ones. [124] presented an augmented Lagrangian relaxation method to decompose the generation scheduling problem. [125] suggested a decomposed OPF method based on Lagrangian relaxation, [126] applied an augmented Lagrangian relaxation method on the decomposed OPF calculation, and [127] suggested a decomposed OPF method based on interior point method. In general,

the key to a successful decomposed OPF method depends on the modelling of coupling constraints among areas, the choice of optimisation algorithms, and computational issues like the choice of starting point and upgrade of parameters.

In this chapter, a system variable decomposition method is proposed, and an improved interior point method (IPM) to solve OPF problems is applied based on the decomposition and sparse matrix technologies.

Firstly, the Lagrangian relaxation method, the penalty function method and the barrier function method are analysed and compared. Then a barrier function method which complements the existing barrier function method is proposed to address the decomposed OPF problem.

For the reason of simplicity only real power flow calculations are studied here. One can extend this decoupled DC OPF model to a full AC OPF model, but whether the DC or AC model is applied doesn't affect the basic description of the several approaches in this chapter. The following three decomposition methods are illustrated using the DC model for easy understanding. In the DC power flow model we assume, transmission lines are pure reactance, and all the bus voltages are assumed as 1.0p.u.

4.2   Lagrangian relaxation method

[125] suggested a co-ordinated OPF across multiple regions. The Lagrangian relaxation technique is used to remove those constraints involving variables in neighbour areas. After the Lagrangian relaxation, the OPF problem is decomposed into a family of regional OPF problems. Given an initial point, TSOs can upgrade the quantities and prices (Lagrange multipliers) based on the local information and the information exchanged with neighbouring areas. Both the primal variables (quantities) and the dual variables (prices) are needed in the iteration. Once the primal-dual solution converges the quantities and prices are obtained.

[129] suggested a unit commitment problem solution using Lagrangian relaxation. The step size is set to increase when the violation is large and decrease when the violation is small.

[130] gives another Lagrange relaxation approach in DC OPF. In this method, the regional OPF problem cares only for the regional cost function instead of the global cost function, and the constraints involving the neighbouring areas (including the power balance constraints and the transmission limit constraints) are converted to regional separable constraints through the introduction of power flows on the tie-lines. The iteration procedure starts from a flat base case where the power flows on the tie-lines as well as the export prices are zero, or the operational values in the real world can serve as the initial point to avoid solution oscillation. The stopping criteria is that the tie-line flows obtained from the OPF results of the two neighbouring areas agree with each other.

The Lagrangian relaxation here can be seen as 'pricing out' the cost of congestions caused by external systems for the local OPF calculations. This cost is determined by estimated shadow congestion prices and publicised PTDF factors. In this section, this approach is investigated, and an example is given in chapter 5 to compare this method with others.

The introduction of dual variables into regional decomposition is very attractive because it makes full use of market information and makes the dualised optimisation problem separable. However, this method is not perfect, as we will see in the following sections.

4.2.1 Lagrangian relaxation and regional decomposition

For a TSO, the quantity and price bids of all the participants in other areas are not available. The solution proposed by Cadwalader and Hogan is to dualise the related constraints and make a Taylor expansion on the benefit functions of other areas. The

dualised Lagrangian function then becomes separable by regions. If the starting point is well chosen and if the Lagrangian function is convex, this method can give the correct optimum without having to expose the bids to other TSOs.

Let $\max \sum_{i=1}^{A} \mathbf{B}_i(\mathbf{y}_i)$ be the total benefit of the entire network, where the $\mathbf{y}_i$ is the vector of bus net extraction in area i. It is sum of all the regional welfare functions, each is a quadratic function.

$L(\mathbf{y}_1,...\mathbf{y}_n) = 0$ is the power balance constraint (losses, generations and demands can be modelled as the yi). This is an equality constraint.

$\mathbf{K}_i(\mathbf{y}_1,......\mathbf{y}_n) \leq \mathbf{0}$ is the group of transmission constraints in ith sub-network. All the possible limitations on the power flows, including thermal, voltage, stability, or other limits, can be modelled. The net injections are explicit variables (decision variables) in this function, while others (such as voltage magnitudes and angles) are treated as intermediate variables (dependent variables). It consists of both inequality constraints and equality constraints.

Suppose λ_j is the Lagrange multiplier of jth transmission constraint (that is, the shadow price of congestion on jth line), then λ_j is either zero when the constraint is not binding or positive when the constraint is binding. According to Lagrangian relaxation, this constraint can be removed by appending an item $-\lambda_j K_j(\mathbf{y}_1,......\mathbf{y}_n)$ to the objective function. Therefore, all the transmission constraints in the areas other than ith area can be removed by way of Lagrangian relaxation. The resulting dual function provides an upper bound of the primal function, and at the optimal point the primal and dual function have the same value. Thus, once the dual problem is solved, the primal OPF problem is solved as well, and the 'duality gap' (the difference between the dual function value and the primal function value) shall be reduced to zero when the optimum is obtained.

In Cadwalader's paper, the dualised function still contains the unknown bids of other areas. The author then linearised the dual function at the starting point to obtain the first rank Taylor expansion. By upgrading the point towards the optimum, the dual function is solved. If the starting point is judiciously chosen, and if the dual function is convex, this decomposed approach can give a good result.

4.2.2 Sub-gradient approach for the dualised optimisation problem

For the loads in region i, the shadow congestion price induced by the constraints in region j can be expressed as: $\omega_{ji} = \lambda_j \nabla K_{ji}$. (4.1)

It reflects the externality of congestion in transmission systems. The Lagrange multiplier λ reflects the contribution of relaxing this constraint in the total social welfare.

This price information is the key to regional decomposition because of the close connection between a binding constraint and its shadow price [12].

The sensitivity factor ∇K_{ji} reflects the influence of nodal injection in area i on the constraint in area j. These group of sensitivity factors are normally called PTDFs (Power Transmission Distribution Factors), and they can be published among all the TSOs.

In the sub-gradient methods, one can adjust the Lagrange multipliers and primal variables interactively. The model can be described as below:

Given the estimation of Lagrange multiplier λ_k and starting point x_k, the optimal solution of the Lagrangian function at λ_k can be expressed as Δx_{k+1}, consequently the Lagrange multiplier can be upgraded as:

$$\lambda^{k+1} = \max\left(0, \lambda^k + \alpha_k C(x_{k+1})\right) \qquad (4.2)$$

Where the $C(x_{k+1})$ is the constraint function, and α_k is the step size. The step size should satisfy that when $k \to 0$, $\alpha_k \to 0$ and $\sum_{i=1}^{k} \alpha_i \to \infty$.

The choice of α_k is important for the performance of all sub-gradient methods, and thus has attracted many researchers [129].

If proper initial point and step size are chosen, the dualised model can be expected to converge at the optimal point [131], where the value of Lagrangian function equals to the value of original objective function. However, there are some limitations in using sub-gradient methods, and they will be discussed in the next section.

4.2.3 Computational problems

In order to use sub-gradient methods in solving the Lagrangian relaxed problem, the dualised objective function must be convex and differentiable with the exception of some points where the gradient method is modified. In paper [47], the author indicated that the proposed method can only work when the dualised constraints are all expressed as linear functions. If, for example, sinusoid functions of power angles are involved, the Lagrangian function is not convex and thus the sub-gradient method will fail. The same limitation applies to the method proposed in [130].

Another problem is incurred by the Taylor approximation. According to the author, it may result in large and even unbounded adjustments. In order to address this problem a set of sensitivity factors were introduced to reflect the influence of prices on net extractions. In this way, the OPF problem has a sequential quadratic programming (SQP) model because second order Taylor expansion is applied. This approach can help to speed up the convergence provided proper estimation on the parameters was made. Even if the initial starting points and sensitivity factors are carefully chosen, there still exists the problem of how to choose the step size. In fact, sub-gradient methods have been proved slow in convergence performance, especially zig-zagging near the optimum [132], or even don't converge.

4.2.4 Application issues

According to this method, the estimated shadow congestion prices should be exchanged during every iteration, and all the related PTDF factors need to be published. As PTDFs change with the operation, they need to be updated from time to time. Therefore large amount of information from other sub-systems are needed during each iteration.

It has been noticed that the Lagrange Relaxation (LR) methods are likely to have solution oscillation difficulties because of the piece-wise linearisation approach. If the linearised sub-problem is sensitive to the multipliers, the solution will oscillate between minimum and maximum values with a slight change in the Lagrange multipliers [133].

4.3 Augmented Lagrangian function method

[134] gives another decomposed approach. According to this method, PTDF factors are not needed for the system decomposition. Alternatively, a pair of 'dummy' buses are added in the middle of each tie line. Penalty functions are then used to bring the 'dummy' variables together. Considering the fact that the number of tie lines in an interconnected network should be far less than the number of PTDF factors, and that the latter will change with the operation and thus require frequent update, Kim and Baldick's approach is more attractive in terms of information exchange. Moreover, the objective functions are always convex and are irrelevant to how the transmission constraint is modelled (i.e. the popular power angle and network admittance model can be used). The augmented Lagrangian methods were used in unit commitment problems [133] and generation scheduling problems [124], and were then introduced in OPF through the design of system decomposition.

In this section, the system decomposition method suggested by Kim and Baldick is illustrated, because this innovative idea was then widely used in many papers [135], [136] and [137], etc. and finally led to the interior point method (IPM) tested in this thesis. The problem with penalty function methods is also discussed later in this section.

4.3.1 System decomposition

In an interconnected transmission network, every TSO can only have the full information (including network structure and buyer/user commitments) within its control area. However, due to the interactions among the sub-systems in the interconnected network, optimal usage of the entire system cannot be achieved only by local information. The information about other areas has to be obtained from other TSOs through information exchange.

In the market environment, the bids and bilateral transactions from market participants are confidential information and shouldn't be exposed to other parties

except the TSO in this area. Therefore, the central OPF model as described above cannot be used straightaway. Besides, such a large-scale OPF problem cannot be solved easily and quickly.

Instead of calculating the large-scale central dispatch problem, we can solve the OPF through decomposition approaches. By studying the OPF problem, we can see that the variables in different areas are coupled only through the 'frontier buses' which are at the ends of tie lines. In fact, if we can split up the interconnected network by the cross-border tie lines, the variables can be grouped into local variables and border variables.

Take this two-system network shown in Figure 4-1 as an example:
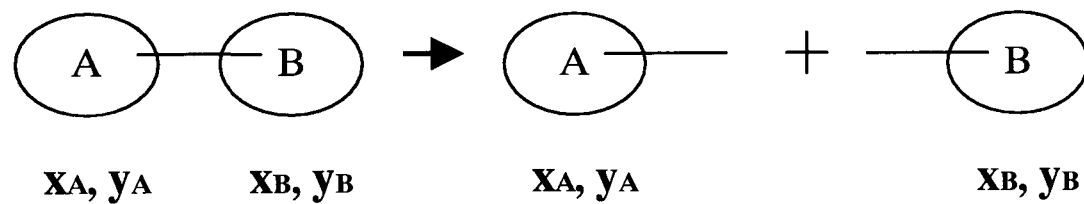
Figure 4-1   System Decomposition

The x_A and x_B are local variables while y_A and y_B are border variables.

If appropriate coupling variables are chosen, the two sub-systems as shown in Figure 4-1 can make their local OPF and then be jointed together to achieve the global OPF solution in the interconnected system. Interactive upgrading of the border variables and local variables during the calculation is needed.
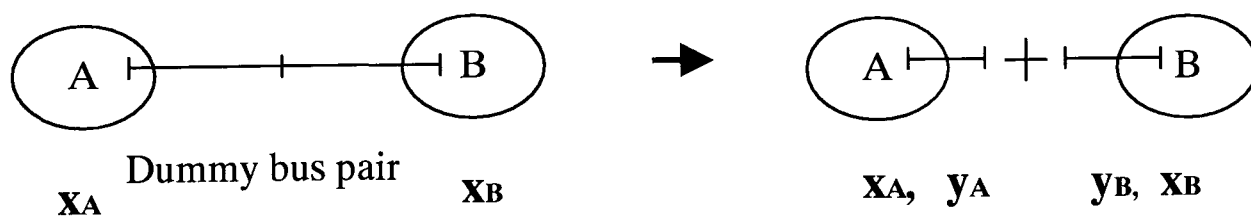
Figure 4-2   System Decomposition by Dummy Buses

Because of the introduction of the 'dummy' buses and the 'dummy' variables related with them, this approach is called augmented Lagrangian relaxation method. The decision variables now consist of both the original decision variables and the new 'dummy' variables.

Baldick and Kim [126] give a decomposition scheme based on 'dummy bus' couples at middle of the tie-lines, as shown in Figure 4-2. Each dummy bus couple must have identical real and reactive power flow variables, voltage magnitudes and the power angles. Each sub-system consists of the 'core' variables (local variables) and the 'border' variables (dummy variables) [134].

Conejo suggested another approach using two pairs of 'dummy' buses to separate each tie-line into 3 segments [135]. This is similar to Kim's method. Wang [136] proposes another decomposition scheme as shown in Figure 4-3. In this method, the dummy buses are removed, but all the coupling variables, including real and reactive power flow variables, voltage magnitudes and the power angles, are retained. In other words, the buses at both ends of the tie lines can play the same role as the 'dummy buses' in [126].
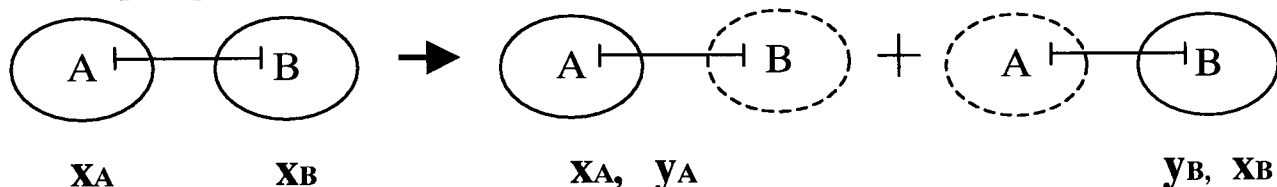
Figure 4-3   System Decomposition

Compared with Baldick's method, this method doesn't require modification of the line reactance values. However, for each tie line, the two terminal buses have to be both compared separately, while in Baldick's method, only the dummy bus pair in the middle of the tie line are to be compared.

The choice of coupling variables determines the information needs to be exchanged among the TSOs. Both the quantities and the prices of the coupling variables must be exchanged to get a global OPF solution [138].

4.3.2 Penalty function and regional decomposition

Generally, the decomposed OPF problem for a two-area system can be described as:

$$\min\ C_a(\mathbf{x_a}) + C_b(\mathbf{x_b}) \qquad (4.3)$$

a and b are the areas.

Subject to: all the local constraints discussed before, plus the coupling constraint:

$$\mathbf{y_a} = \mathbf{y_b} \qquad (4.4)$$

The coupling constraint can be dualised to obtain the Lagrangian function:

$$L(\mathbf{x_a}, \mathbf{x_b}, \mathbf{y_a}, \mathbf{y_b}, \boldsymbol{\sigma}) = C_a(\mathbf{x_a}) + C_b(\mathbf{x_b}) + \boldsymbol{\sigma}^T(\mathbf{y_a} - \mathbf{y_b}) \qquad (4.5)$$

where the σ is the vector of Lagrange multipliers for coupling constraints.

Instead of using general sub-gradient algorithms, which typically exhibit poor performance, this Lagrangian relaxed OPF can also be replaced with a sequence of quadratic sub-problems and subsequently updating of the Lagrange multiplier vector σ [139]:

$$\left(\mathbf{x}_a^{k+1}, \mathbf{x}_b^{k+1}, \mathbf{y}_a^{k+1}, \mathbf{y}_b^{k+1}\right) = \arg\min \left\{ \begin{array}{l} C_a\left(\mathbf{x}_a^{k+1}\right) + C_b\left(\mathbf{x}_b^{k+1}\right) + \boldsymbol{\sigma}^{Tk}\left(\mathbf{y}_a^{k+1} - \mathbf{y}_b^{k+1}\right) + \dfrac{\beta}{2}\left\|\mathbf{y}_a^{k+1} - \mathbf{y}_a^{k}\right\|^2 \\ + \dfrac{\beta}{2}\left\|\mathbf{y}_b^{k+1} - \mathbf{y}_b^{k}\right\|^2 + c\left(\mathbf{y}_a^{k+1} - \mathbf{y}_b^{k+1}\right)^T\left(\mathbf{y}_a^{k} - \mathbf{y}_b^{k}\right) \end{array} \right\}$$

$$(4.6)$$

and $\boldsymbol{\sigma}^{k+1} = \boldsymbol{\sigma}^k + \alpha\left(\mathbf{y}_a^k - \mathbf{y}_b^k\right) \qquad (4.7)$

where the β and c are scalar penalty constants, α is the step size during iterations, and $\|\cdot\|$ is the inner-product norm.

Noticing the fact that the series of sub-problems are regional decomposable, one can easily deduce the optimisation problems for both areas:

$$\left(\mathbf{x}_a^{k+1}, \mathbf{y}_a^{k+1}\right) = \arg\min\left\{ C_a\left(\mathbf{x}_a^{k+1}\right) + \boldsymbol{\sigma}^{Tk}\mathbf{y}_a^{k+1} + \dfrac{\beta}{2}\left\|\mathbf{y}_a^{k+1} - \mathbf{y}_a^{k}\right\|^2 + c\left(\mathbf{y}_a^{k+1}\right)^T\left(\mathbf{y}_a^k - \mathbf{y}_b^k\right) \right\} \qquad (4.8)$$

$$\left(\mathbf{x}_b^{k+1}, \mathbf{y}_b^{k+1}\right) = \arg\min\left\{ C_b\left(\mathbf{x}_b^{k+1}\right) - \boldsymbol{\sigma}^{Tk}\mathbf{y}_b^{k+1} + \dfrac{\beta}{2}\left\|\mathbf{y}_b^{k+1} - \mathbf{y}_b^{k}\right\|^2 - c\left(\mathbf{y}_b^{k+1}\right)^T\left(\mathbf{y}_a^k - \mathbf{y}_b^k\right) \right\} \qquad (4.9)$$

By introducing the second order penalty functions of the border variables into the sub-problem at each iteration, the convergence of the overall algorithm is improved.

This method can also be understood in another way: the penalty terms (the second through fourth terms in equation (4.8) and equation (4.9) are the cost function of the

dummy variables. It is dependent on the values of the Lagrange multipliers and the previous values of the iterations.

The choice of the penalty parameters is an important issue in penalty function methods. If the value is too large, ill-conditioning of the Hessian is likely to happen, causing difficulties for those optimisation algorithms relying on Hessian or a suitable approximation. On the other hand, if the penalty parameters are too small, the solution approach may not be able to converge to a solution that satisfies the coupling constraints [131]. In the next section, the choice of parameters in the series of sub-problems described in equation (4.6) will be discussed.

4.3.3 The choice of parameters

Two major approaches in decomposed OPF have been discussed in section 4.1 and 4.2 respectively, both of which are sub-gradient methods. Compared with the Lagrangian relaxation method, the Augmented Lagrangian function method in this section has better convergence performance. Moreover, it can be applied in various power flow models, because the only constraint to be relaxed is a linear equality constraint.

However, it is well known that in all kinds of sub-gradient methods, it is important to choose the starting point of the Lagrange multipliers appropriately, otherwise the convergence performance can be far worse [129].

The dummy variables are also bound in this way that at each iteration, there is no large deviation from the old values obtained from the other side of the tie line.

The choice of penalty factors is problem-dependent. [134] gives an empirical equation to help reliable convergence in the OPF problem, that is:

$$\alpha = \frac{1}{2}\beta = c \qquad (4.10)$$

For most sub-gradient problems, the step size α has to be chosen at each iteration. In this constrained optimisation problem, α must be chosen to reduce the duality gap,

while at the same time reduce the constraint violations. [129] studied extensively the adjustment of the step size in sub-gradient methods.

4.3.4 Application issues

The method discussed in this section requires less information exchange than that in section 4.1. The initial values of the Lagrange multipliers σ are obtained through co-ordination among the TSOs. The quantity information of the dummy variables is also exchanged to act as the parameters of the local sub-problems. Once these local sub-problems are solved by the local TSOs in parallel, σ can be updated according to equation (4.7). The tuning of stepsize also requires co-ordination, normally exchange of certain aggregated information. Except some special cases, the step size needs to be adjusted at each iteration [131]. The step size can be made proportional to the estimated value of the duality gap [129], the duality gap and the maximum variable increments in all the areas should be published during each iteration.

The augmented Lagrange method uses quadratic penalty terms to avoid the solution oscillation difficulties. The non-separable quadratic penalty terms are then replaced by the linear approximation around the solution obtained from the previous iteration. The quadratic terms of decision variables are added to the cost function as auxiliary functions to improve the convergence performance. In the test example presented in Chapter 5, the augmented Lagrangian relaxation method demonstrated good convergence.

4.4   A New System Decomposition Method

There have been a variety of methods of how to choose the coupling variables. One may think of using the real and reactive power flows on the tie lines as the coupling variables, which is similar to the 'market splitting' approach where the power flows on the tie lines are determined jointly by the neighbouring TSOs to make full use of the tie lines. However, a closer look at the market splitting [117] suggests that this method

only works well in radial network structures [82]. This assumption doesn't hold in a meshed network, where transition power flows travel among the sub-systems through the tie lines.

In fact, in the decomposed OPF calculation, the network structure is broken down into individual control areas, and the local TSO cannot calculate out the interactions with other control areas without the knowledge of network parameters in other control areas. The power flows, voltage magnitudes and power angles of the frontier buses are determined jointly by both of the neighbouring sub-systems, and an injection at the frontier bus or the power flow on the tie line alone cannot represent the influence from the external system. This will lead to the divergence of the decomposed OPF, or converging to a feasible but not optimal result.

In the following analysis, the power flow equations are re-written to give a better understanding of the choice of coupling variables.

The OPF problem in the interconnected system can be written as:

$$\min \sum_{a=1}^{A} C_a \qquad (4.11)$$

subject to the equality and inequality constraints:

$$\mathbf{g}(\mathbf{P}, \mathbf{Q}, \mathbf{V}, \delta) = \mathbf{0} \qquad (4.12)$$

$$\mathbf{h}(\mathbf{P}, \mathbf{Q}, \mathbf{V}, \delta) \leq \mathbf{0} \qquad (4.13)$$

for $\forall a = 1, \cdots, A$ as the area number.

The C_a is the total social cost in a control area, and it is normally expressed in a quadratic form.

The set of equations (4.12) are power balance constraints and they form the normal power flow calculation model.

The inequality constraints equation (4.13) are operating limits, including generation limits, system reserve limits, transmission limits, voltage limits, stability limits, etc.

This large-scale central dispatch problem can be decomposed into several problems within individual control areas, so that the TSOs can solve these sub-problems in parallel. In this thesis, the interconnected system is split up by the cross-border tie lines, and the variables within each control area are grouped into local variables and border variables. For example, let's study the following two-system network in Figure 4-4:
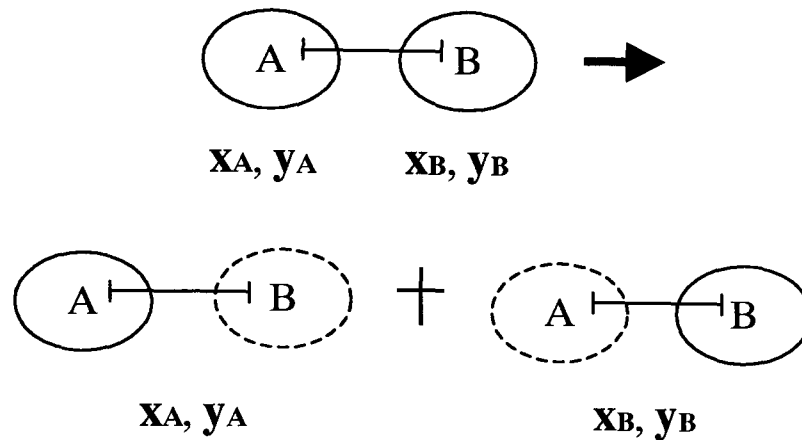
Figure 4-4   System Topology Decomposition

The x_A and x_B are local variables while y_A and y_B are border variables. Figure 4-4 gives the topology decomposition, and the next step is to choose the appropriate electrical variables to represent the neighbouring control areas.

Noticing the fact that equation (4.12) is the standard power flow equation, the system coupling variables can be easily chosen. Consider the standard power flow problem:

$$P_i = P_{Gi} - P_{Di} = U_i \sum_j U_j \left(G_{ij} \cos \delta_{ij} + B_{ij} \sin \delta_{ij} \right) \qquad (4.14)$$

$$Q_i = Q_{Gi} - Q_{Di} = U_i \sum_j U_j \left(G_{ij} \sin \delta_{ij} - B_{ij} \cos \delta_{ij} \right) \qquad (4.15)$$

As each bus has four variables (P, Q, U and δ), given two of the variables, the other two can be calculated from the power flow equations. In other words, any two of the variables can determine the bus status through the power flow equations.

In optimal power flow calculation, the real and reactive injections are decision variables which will be determined directly in the solutions, while the voltage and power angles are status variables dependent on the decision variables through the constraints. The status variables of the frontier buses are determined jointly by both of

the neighbouring sub-systems, and they also appear in the local OPF calculation. Therefore, the voltage magnitudes and power angles of the frontier buses can be chosen as the coupling variables, as shown in Figure 4-5 and Figure 4-6. The neighbouring regions can always be 'put together' without affecting any power flows as long as the coupling variables match with one another. In other words, if the coupling variables agree with one another, and all the local constraints are met, a feasible solution of the entire interconnected network is given.
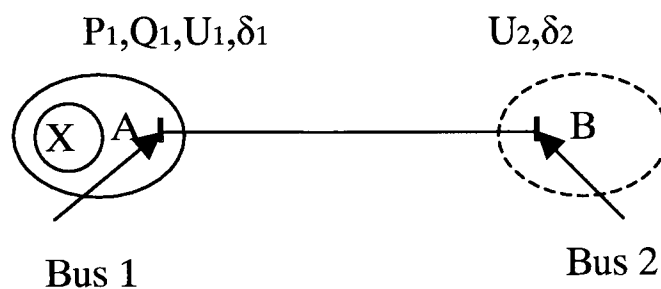
Figure 4-5   Variables available for TSO A

Figure 4-5 shows the variables appear in the local OPF problem of area A. The x_A is the vector of the internal bus variables, or the so-called "core" variables in [126] and [134], $x_A = \begin{bmatrix} P_A & Q_A & U_A & \delta_A \end{bmatrix}^T$. The vector $\begin{bmatrix} P_1 & Q_1 \end{bmatrix}$ is also part of x_A, but as it is closely connected with the frontier bus variables through the power flow equations, it is listed separately from x_A. The frontier variables are $\begin{bmatrix} U_1 & \delta_1 & U_2 & \delta_2 \end{bmatrix}$, i.e. the voltage magnitudes and power angles at the frontier buses (bus 1 and bus 2). Similarly for TSO B, the frontier variables are also $\begin{bmatrix} U_1 & \delta_1 & U_2 & \delta_2 \end{bmatrix}$, as shown in Figure 4-6, and the core variables are $\begin{bmatrix} x_B & P_2 & Q_2 \end{bmatrix}$.
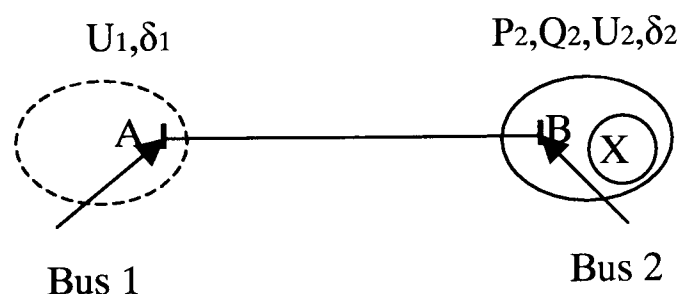
Figure 4-6   Variables available for TSO B

The aim of this decomposition approach is to separate the objective function as well as constraints. From the OPF model we can see that the objective function is regional separable. By studying the equality constraints for a "core" bus (equations (4.14) and (4.15)), we can see that the power flow equations only consist of the variables of buses directly connected to this bus. Therefore, the equality constraints in each control area are regional separable.

The inequality constraints, including voltage limits, generation limits and transmission limits are also separable.

The power flow equality constraints cannot be applied to the frontier bus on the other side of the tie-line, because the parameters of the lines connected to it are not known for the local TSO. However, a new set of equality constraints called coupling constraints can be used to replace the unknown power flow equations. For the two-system network, the coupling constraints can be expressed as:

$$U_1^A = U_1^B, \ \delta_1^A = \delta_1^B, \ U_2^A = U_2^B, \ \delta_2^A = \delta_2^B \qquad (4.16)$$

so that there is no mismatch between the two control areas.

For simplicity we can re-write the coupling constraints as:

$$y_A = y_B \qquad (4.17)$$

The equality and inequality constraints can be expressed as:

$$g_A(x_A, y_A) = 0, \ g_B(x_B, y_B) = 0 \qquad (4.18)$$

$$\text{and } h_A(x_A, y_A) = 0, h_B(x_B, y_B) = 0 \qquad (4.19)$$

These constraints apply for all the internal buses (core buses).

The method proposed in equation (4.16) doesn't require any additional virtual buses and thus avoid modification of the line reactance matrix. The neighbouring regions can always be 'put together' without affecting any power flows as long as the coupling variables match with one another. In other words, if the coupling variables agree with one another, and all the local constraints are met, a feasible solution of the

entire interconnected network is given. Therefore, by maintaining the coupling constraints, the optimal results from parallel local OPF are also the global optimum.

DC power flow calculation is widely used in network analysis. In DC power flow methods, all the bus voltages are assumed to be 1.0p.u. Therefore, the coupling variables are the power angles at the frontier buses.

This proposed system decomposition method explicitly requires the border variables in both of the neighbouring systems, and uses equality constraints instead of penalty functions to enforce the coupling relationship. It can be applied in barrier function methods as described in section 4.5.3.

If the 'dummy buses' in the middle of the tie-lines are used instead of the 'frontier buses' (as in Baldick's approach [126]), the real and reactive power flows should also be included in addition to voltages and power angles as the coupling variables. In this thesis, Wang's topology decomposition approach is used because there's no need to change the network admittance matrix.

4.5 Barrier function method (Interior Point Method)

An effective way of solving OPF problems is the interior point method (IPM). IPM has attracted great interests because of its fast convergence characteristics and numeric robustness. Past experiences have shown that the IPM is very effective in dealing with large scale ill-conditioned networks, and is not sensitive to the size of the problems [140]. For a constrained optimisation problem, the IPM can ensure that each step of search for the optimum falls within the feasible region of the solution space.

Among all the IPM methods, barrier function methods have been widely used in power system optimisation. Clements etc. [141] applied it in state estimation, [140] uses a direct IPM to find the load shedding scheme. [142] applied a predictor-corrector IPM in OPF using voltage rectangular coordinates. [143] gave a OPF method using barrier function techniques to address the dynamic OPF problem by decomposing the inter-

temporal coupling among variables. Aguado etc. applied the IPM in interconnected networks [127] and [137]. [144] gives a multiobjective OPF to evaluate voltage security costs using IPM.

A well-known figure to show the different approaches of IPM and simplex method is shown in Figure 4-7:
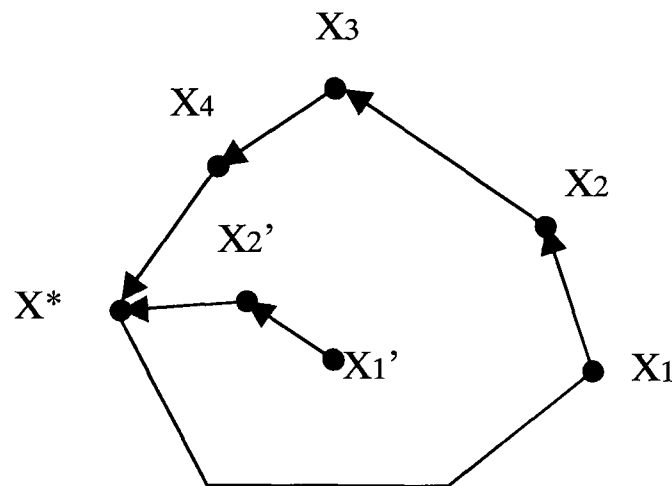
Figure 4-7   Search paths of IPM and Simplex Method

Figure 4-7 illustrates the two different approaches. The simplex method takes the path from X_1 through $X_2,...$ X_4 until X^*, jumping from one border point to the next one, therefore the search direction in the simplex method is along the borders of the feasible region. On the contrary, the IPM starts from an interior point $X_1^{'}$ and searches through $X_2^{'}$, and it can reach the optimum X^* within fewer iterations.

Barrier function method is one of the most popular IPM method, and it is used in this thesis. In this method, KKT necessary conditions are applied in conjunction with barrier functions. The Newton iteration method is used to solve a set of linear equations and approach the optimum. A group of logarithm functions are appended to the objective function as the 'barrier' terms to enforce those inequality constraints. Then the search direction is obtained with Newton search in a certain neighbourhood determined by the barrier parameters and the 'central path'[145]. The barrier parameters are forced to decrease during each Newton iteration until approaching zero, and the KKT necessary conditions are met. The IPM are used first in linear programming problems,

then extended to nonlinear optimisation problems. These path-following interior point methods have good convergence performance even in the worst case, because of the robustness of the underlying algorithm.

For a large-scale nonlinear optimisation problem, the OPF problem for example, the barrier function methods can be applied as long as the objective function and the constraint functions are all twice differentiable. For the following power flow model, this requirement is met, so the barrier function method can be applied.

As the path-following method is obtained by using Newton search, its performance is also influenced by the choice of starting point, like the ordinary Newton method. However, choosing an infeasible point as the starting point is allowed provided that the slack variables are nonnegative.

In this section, an existing decomposed OPF approach based on barrier function methods will be analysed, and then an improved method is proposed and compared with the existing ones.

4.5.1 Mathematical model of barrier function methods

Consider this optimisation problem:

$$\min \quad f(\mathbf{x}) \quad (4.20)$$

$$\text{subject to: } \mathbf{g(x)} = \mathbf{0} \quad (4.21)$$

$$\text{and } \mathbf{h(x)} \le \mathbf{D} \quad (4.22)$$

Use nonnegative slack variables to convert the inequality constraints into equality constraints: $\mathbf{h(x)} + \mathbf{s} = \mathbf{D}, \mathbf{s} \ge 0 \quad (4.23)$

After the conversion, logarithmic barrier functions are used to avoid dealing with the nonnegativeness of the slack variables s. This is done by appending the logarithm barrier terms to the objective function:

$$f_b(x) = f(x) - \sum_{j=1}^{k} \mu_j \ln s_j \quad (4.24)$$

Where the positive μ_j are constant within an iteration but upgraded during the procedure. If the inequality constraint corresponding to s_j is binding, $s_j \rightarrow 0$ and thus the barrier item makes $f_b(x) \gg f(x)$, therefore the new search direction will be prevented from going nearer to the boundary. So, the logarithm terms act as the 'barriers' and change the search direction from pure Newton direction to a new one dependent on the barrier parameters μ_j. During the iteration μ_j is forced to decrease, so that $\mu_j \rightarrow 0$ at the end of iteration procedure, thus $\mathbf{x} \rightarrow \mathbf{x}^*$ if the iteration procedure converges. Different values of the barrier parameters for different slack variable can be seen as weight factors.

Apply Lagrangian relaxation to all these equality constraints and we can get the Lagrange function:

$$L(\mu) = f - \lambda^{\mathrm{T}} \mathbf{g} - \mathbf{z}^{\mathrm{T}} (\mathbf{h} + \mathbf{s}) - \sum_{j=1}^{k} \mu_j \ln s_j \qquad (4.25)$$

where the λ and z are Lagrange multipliers associate with the constraints. During the iteration procedure $\mu \rightarrow 0$.

Kuhn-Tucker necessary conditions are used to obtain the optimal solution. According to the KKT conditions, these Lagrange multipliers z must be nonnegative, and satisfy the stationary conditions:

$$\frac{\partial L}{\partial x} = 0 \qquad (4.26)$$

$$\frac{\partial L}{\partial \lambda} = 0 \qquad (4.27)$$

$$\frac{\partial L}{\partial s} = 0 \qquad (4.28)$$

$$\frac{\partial L}{\partial z} = 0 \qquad (4.29)$$

These equations are linearised to get a symmetric positive definite Hessian matrix, and then can be solved using Newton methods or predictor-corrector methods [132]. Instead of taking several Newton steps until converging to the optimal solution to the sub-problem with fixed μ, at every iteration the μ is reduced, and the problem is re-linearised. This is the main feature different from conventional Lagrangian relaxation or augmented Lagrangian methods [132].

As the slack variables s are introduced to tackle the inequality constraints, there's no need to identify the binding inequality constraints in each iteration if the nonnegativeness of s is met. The price for this advantage is the increase in the number of variables, and the more complicated calculation of the linearised equations (4.26) through (4.29).

4.5.2 Existing approach

Barrier function methods are widely used in a variety of OPF models, for example, [142] and [146]. Aguado etc. applied the IPM in interconnected networks [127] and [137]. This idea is very appealing because of the robustness and fast speed of IPM. The decomposition is similar to Baldick's method where coupling constraints are enforced to achieve the final global optimum. [128] also gives a decomposed IPM to address the dynamic OPF problem. Both of the methods are based on Newton search direction for static point to meet the KKT conditions, and the linearisation of KKT conditions by first rank Taylor expansion is the way to decomposition. As both Aguado's and Xie's approaches finally lead to a border-blocked Newton equation set, only the former one is discussed here.

Aguado's method can be illustrated using the same two-area system as that in section 4.2:

$$\min \ C_a(\mathbf{x}_a) + C_b(\mathbf{x}_b) \qquad (4.30)$$

a and b are the areas.

Subject to: all the local constraints discussed before, plus the coupling constraint:

$$\mathbf{y}_a = \mathbf{y}_b \qquad\qquad (4.31)$$

After converting all the local inequality constraints into equality constraints and appending the barrier function terms to the objective function, the dualised Lagrangian function can be written as:

$$L(\cdot) = C_a + C_b - \mu \sum_{i=1}^{k_{a+b}} \ln s_i + \lambda^T \mathbf{g} + \mathbf{z}^T (\mathbf{h} + \mathbf{s}) + \sigma^T (\mathbf{y}_a - \mathbf{y}_b) \qquad (4.32)$$

Where the $C_a(\cdot)$ and $C_b(\cdot)$ are cost functions, g and h are equality and inequality constraints respectively. k_{a+b} is the number of inequality constraints in area a and b. The μ is a scalar whose value changes during the iterations, but keeps constant at each iteration. A single value of μ for all the s_i means no weigh difference among the inequality constraints.

By Applying KKT conditions on the Lagrangian function Aguado obtained a group of equations [137]. They are then solved using Newton iteration. The step sizes are chosen so that the s_i in each iteration are always nonnegative, therefore the new points obtained by the iterations always satisfy the inequality constraints. Furthermore, if the equality constraints are also satisfied, the new points obtained through iterations are always within the feasible region. Thus it is called an interior point method (IPM).

Note that the Lagrangian function is separable because of the introduction of Lagrangian multipliers σ on the global coupling constraints. The resulting Newton iteration can be expressed as the following border-blocked matrix:

$$\begin{bmatrix} U_1 & 0 & \Gamma_1^T \\ 0 & U_2 & \Gamma_2^T \\ \Gamma_1 & \Gamma_2 & 0 \end{bmatrix}^k \begin{bmatrix} \Delta u_1 \\ \Delta u_2 \\ \Delta \sigma \end{bmatrix} = \begin{bmatrix} r_1(\mu^k) \\ r_2(\mu^k) \\ r_\sigma(\mu^k) \end{bmatrix} \qquad (4.33)$$

Where the u is a vector consisting of decision variables, dependent variables, slack variables and the Lagrange multipliers in this area, plus the coupling variables in this

area. U is the Hessian matrix of the Lagrangian function in this area. r is residue of u or σ, and it is a function of barrier parameter μ. Γ is the incidence matrix between coupling variables and the u vector. During the iterations, the Hessian matrices are upgraded, but Γ is a constant matrix only determined by the topology. According to Aguado [137], the upgrade of σ is obtained by an elimination procedure, thus:

$$\Delta\sigma = \left(\Gamma_1 U_1^{-1}\Gamma_1^T + \Gamma_2 U_2^{-1}\Gamma_2^T\right)^{-1}\left(r_\sigma - \Gamma_1 U_1^{-1}r_1 - \Gamma_2 U_2^{-1}r_2\right) \qquad (4.34)$$

Then the Δu_1 and Δu_2 can be obtained by back-substitution of $\Delta\sigma$.

From the description we can see several disadvantages of this approach:

- Due to the inclusion of slack vector s and its Lagrangian multipliers z, the feasible conditions can be ensured, but the size of variables in the Newton equations (4.33) is greatly increased in all the areas.

- This approach requires inverting of the augmented Hessian matrix U. U is not always invertible, causing difficulties in obtaining the increments. Moreover, Γ are highly sparse matrices and thus the left item in equation (4.34) is often not available.

4.5.3 A coordinated Barrier Method for Solving Nonlinear Programming—an improved method

Based on the observation of the existing barrier method, here an improved method is proposed. It has been tested in a 3-area 7-bus system with good performance. Comparison between this method and the methods described in 4.1 and 4.2 will be given in Chapter 5.

The proposal is based on the relations between primal and dual variables in the constrained optimisation problem. Similar to Baldick's approach, the border coupling variables are used. Unlike Baldick's penalty function method which relies solely on the 'soft' enforcement of the violated coupling constraints, Aguado uses the IPM to make sure that in each iteration, the coupling constraints are strictly satisfied. In the method

proposed in this thesis, the approach Aguado suggested was also used. Unlike Aguado's method where the slack vector s appears in the Newton iteration and thus causes ill-conditioning of the Newton equations when the corresponding constraints are binding, the method proposed here doesn't require inclusion of s in the Newton equation, therefore the computation performance is improved. Secondly, least-square solutions to the Newton equation are obtained instead of explicitly inverting the matrices.

Let x be the local variables, and y be the coupling variables, equation (4.32) can be re-written as:

$$L(\mu) = \sum_{a=1}^{A} \left[f_a(x_a, y_a) - \lambda_a^T g_a(x_a, y_a) - z_a^T(h_a(x_a, y_a) + s_a) - \mu_a \ln S_a \right] - \sum_{k=1}^{K} \sigma_k^T M_k(y)$$

(4.35)

Where the A is the number of areas, and K is the number of coupling constraints.

In this global Lagrangian function, x_a, y_a, s_a are primal variables, and λ_a, z_a, σ_K are dual variables.

It must be stressed here that the number of inequality constraints must be greater than the number of independent (controlled) and dependent variables, but the number of equality constraints must not. Besides, all the objective functions and constraints should be twice differentiable to solve the KKT conditions. These requirements can be easily met in OPF problems.

Aguado etc. and some other researchers [127] apply partial derivative to both s and z, and then make modification on the derivatives with respect to s in order to avoid ill-conditioning when some of the slack variables approach 0 prematurely. However, due to this modification the Hessian matrix becomes asymmetric, causing computational difficulties when the size of the problem is large.

In this thesis, a coordinated method is proposed with its Hessian matrix having the same dimension as ordinary Newton OPF. It also requires only moderate changes on the existing Newton OPF programs, and various constraints can be easily accommodated

without many changes to the program codes. Further studies are also done to investigate the applicability on interconnected system with different OPF tools in its sub-areas.

The complementary conditions (i.e. $\mathbf{SZ} = \mu\mathbf{E}$) are used other than the Newton equations to relate s to z. Besides, as the slack variables are explicit functions of the other primal variables, they are also treated outside the Newton equations. Therefore the size of Hessian matrix is largely reduced. Even at this size the Hessian matrix is not allowed to be known to other TSOs. Thanks to the highly sparse structure of the coupling constraint matrices, only the border variables need to be published to solve the global dual variables. This small amount of information exchange can ensure the solution always be available even though the matrix is not invertible during some time in the iteration procedure.

The equality constraints are used in each iteration to relate local non-basic variables with basic ones. In the primal DC OPF problem, we can choose the nodal injections as the basic variables and power angles as the non-basic variables.

Suppose v is the basic variable vector for the OPF problem, γ is the nonbasic variable vector (slack variables and dual variables not included), then the search is to find an optimum v^* so that $J_v^* = \nabla L_v\big|_{v^*} = 0$. If Newton search is used, the iterations can be expressed as: $H_{vv}^k \Delta v^{k+1} = J_v^k$ \hspace{2cm} (4.36)

where the H is the Hessian matrix and J is the Jacobian matrix of the Lagrangian function. As the local equality constraints $\mathbf{g}(\mathbf{v}, \boldsymbol{\gamma}) = 0$ are normally nonlinear functional constraints, the nonbasic variables cannot be expressed as the explicit functions of basic variables. Thus the Hessian matrix is augmented to accommodate the nonbasic variables. Let $\Delta x = \begin{bmatrix} \Delta v & \Delta \gamma \end{bmatrix}$, the augmented Hessian matrix can be expressed as:

$$\begin{bmatrix} H_{xx} & \nabla g \\ \nabla g^T & 0 \end{bmatrix} \begin{bmatrix} \Delta x \\ \Delta \lambda \end{bmatrix} = \begin{bmatrix} -\nabla L_x \\ -g \end{bmatrix} \hspace{2cm} (4.37)$$

Where the H_{xx} is the Hessian matrix in respect with basic and nonbasic variables,

x is the vector of basic and nonbasic variables (no slack variables or dual variables), g is

the group of equality constraints, and λ is the vector of Lagrange multipliers for equality

constraints.

In order to illustrate equation (4.36) and (4.37) let's have a look at the following 3-

bus system:
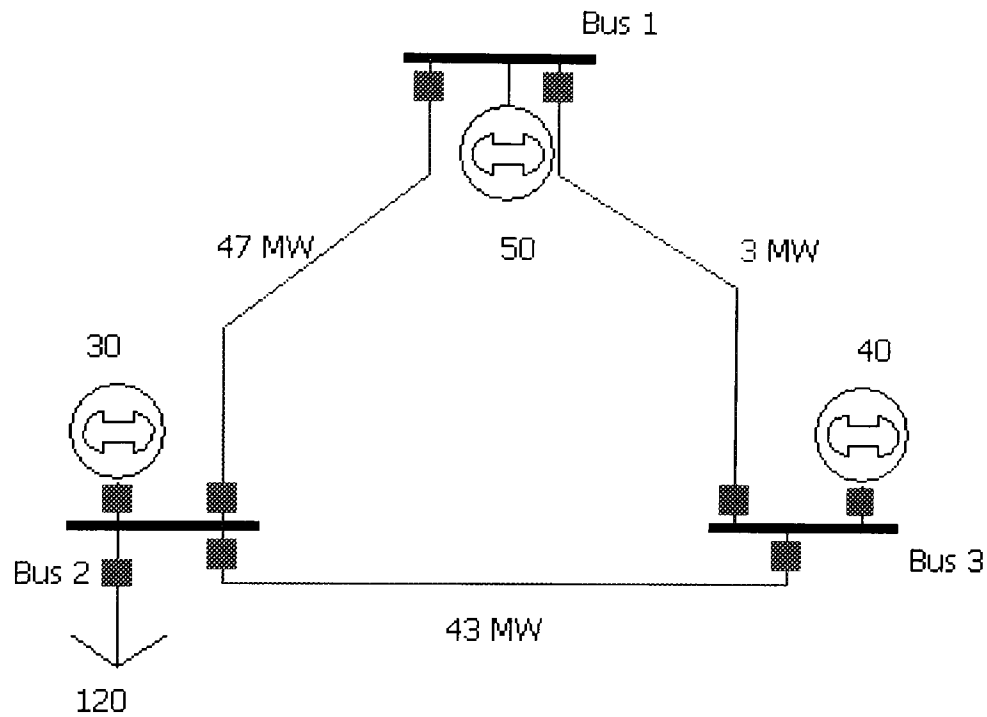
Figure 4-8   3-Bus System

Assuming DC power flow is used, the OPF problem for this specific system can be

written as:

$$\text{min. } C_1\left(p_{g1}\right) + C_2\left(p_{g2}\right) + C_3\left(p_{g3}\right) \tag{4.38}$$

subject to:

Active power balance: $p_{gi} - p_{di} - \sum_{j=1}^{n_{\delta_a}} B_{ij} \sin\left(\delta_i - \delta_j\right) = 0$ for $i = 1,2,3$ \hfill (4.39)

where p_{gi} : the generation at bus i

p_{di} : the load at bus i

B_{ij} : elements in the network admittance matrix.

δ_i : the phase angle of bus i.

Generation limits: $p_{gi\,min} \le p_{gi} \le p_{gi\,max}$ (4.40)

Transmission capacity limit: $B_{ij} \cdot \left|\sin(\delta_i - \delta_j)\right| \le L_{i-j\,max}$ for $\forall i, j = 1,2,3$ (4.41), where

the line starting from node i to j has the transmission limit $L_{i-j\,max}$.

In this example, the basic variable vector $\mathbf{v} = \begin{bmatrix} p_{g1} & p_{g2} & p_{g3} \end{bmatrix}^T$, and the nonbasic

variable vector $\gamma = \begin{bmatrix} \delta_1 & \delta_2 & \delta_3 \end{bmatrix}^T$, both are subject to the equality constraints (4.39).

Given the load at each bus, equation (4.39) can be simply written as $\mathbf{g}(\mathbf{v},\gamma)=\mathbf{0}$, and the

inequality constraints (4.40) and (4.41) can be expressed as $\mathbf{h}(\mathbf{v},\gamma) \le \mathbf{0}$. By introducing

the slack variable vector $\mathbf{s}$, the inequality constraints can be written as: $\mathbf{h}(\mathbf{v},\gamma) + \mathbf{s} = \mathbf{0}$,

and thus further written as: $\mathbf{h}(\mathbf{v},\gamma,\mathbf{s}) = \mathbf{0}$. In this way the inequality constraints were

converted into equality constraints.

The Lagrangian function of this constrained OPF problem can be written as:

$$\mathbf{L}(\cdot) = \sum_{i=1}^{3} C_i\left(p_{gi}\right) + \lambda^T \mathbf{g}(\mathbf{v},\gamma) + \mathbf{z}^T \mathbf{h}(\mathbf{v},\gamma,\mathbf{s}) - \mu \sum_{i=1}^{6} \ln s_i$$

where the λ and z are vectors of Lagrangian multipliers corresponding to the

inequality constraints and equality constraints, respectively.

According to Kuhn-Tucker conditions, the optimal values $\mathbf{v}^*$ must satisfy

$J_v^* = \nabla L_v\big|_{v^*} = 0$. Using Newton search, the direction of the searching for $\mathbf{v}^*$ can be

expressed as equation (4.36).

According to Taylor expansion of the equality constraints $\mathbf{g}(\mathbf{v},\gamma)=0$, the following

equations can be obtained: $\mathbf{g} + \begin{pmatrix} \nabla \mathbf{g}_v^T & \nabla \mathbf{g}_\gamma^T \end{pmatrix} \begin{pmatrix} \Delta \mathbf{v} \\ \Delta \gamma \end{pmatrix} = \mathbf{0}$. Therefore, the augmented

Newton search can be expressed as equation (4.37).

H_{xx} can further be written as: $H_{xx} = \begin{bmatrix} H_{vv} & H_{v\gamma} \\ H_{v\gamma}^T & H_{\gamma\gamma} \end{bmatrix}$ (4.42)

The Newton search is trying to find solution for

$$\nabla L_x = 0 \qquad (4.43)$$

$$\text{and } g(x)=0 \qquad (4.44)$$

The variables $\Delta x^k = \begin{bmatrix} \Delta P^T & \Delta Q^T & \Delta V^T & \Delta \delta^T \end{bmatrix}^T$ for AC power flow calculation, or simply

$\Delta x^{\,k} = \begin{bmatrix} \Delta P^T & \Delta \delta^T \end{bmatrix}^T$ for DC power flow calculation.

Note that during the iteration, $\nabla L_x^k = 0$ might not hold because of the Taylor

expansion (that is, ∇L_x^{k+1} is closer to 0 than ∇L_x^k is), but $g^k = 0$ is always true because it

was obtained by directly applying the equality constraints. Therefore, during the

iterations the equality constraints are always met as long as the starting point is chosen

to satisfy them. The same technique can be used on the global coupling constraints to

find the same Newton increment on the coupling variables. By choosing the same

stepsize for all the areas, we can ensure that the coupling constraints are always met. In

other words, the series of interior points (because the inequality constraints always hold

too) generated from this proposed global Newton search are always global feasible

solutions. The next question is how to decompose the global Newton search.

By applying equation (4.37) to a multi-area system as described in 4.4, the Newton

iteration can be expressed as:

$$\begin{bmatrix} A_1^k & 0 & 0 & \Gamma_1^T \\ 0 & \ddots & 0 & \vdots \\ 0 & 0 & A_A^k & \Gamma_A^T \\ \Gamma_1 & \cdots & \Gamma_A & 0 \end{bmatrix} \begin{bmatrix} \Delta \alpha_1^k \\ \vdots \\ \Delta \alpha_A^k \\ \Delta \sigma^k \end{bmatrix} = \begin{bmatrix} \beta_1^k \\ \vdots \\ \beta_A^k \\ q^k \end{bmatrix} \qquad (4.45)$$

where $\Delta \alpha_{ak} = \begin{bmatrix} \Delta x_a^T & \Delta \lambda_a^T \end{bmatrix}^T$ for any area a. The residue β_a^k is the function of α_{ak} and

σ_k and keeps constant within one iteration. q^k is the residue vector for all the coupling

constraints. A_a^k is the local part of Hessian matrix and $A_a^k = \begin{bmatrix} H_{xx} & \nabla g \\ \nabla g^T & 0 \end{bmatrix}$ (4.46)

Γ_1 through Γ_A are the incidence matrix for the K number of area coupling

constraints. They are highly sparse constant matrix with the entry values at 1 or -1.

Once the σ_k is obtained by coordination among sub-areas, the local increments can be calculated within the areas through parallel approach. The slack variables s and their corresponding Lagrangian multipliers z can also be computed within the areas.

Again lets consider the 3-bus example to illustrate the multi-area decomposition. The small system is divided into two sub-systems, as shown in Figure 4-9:
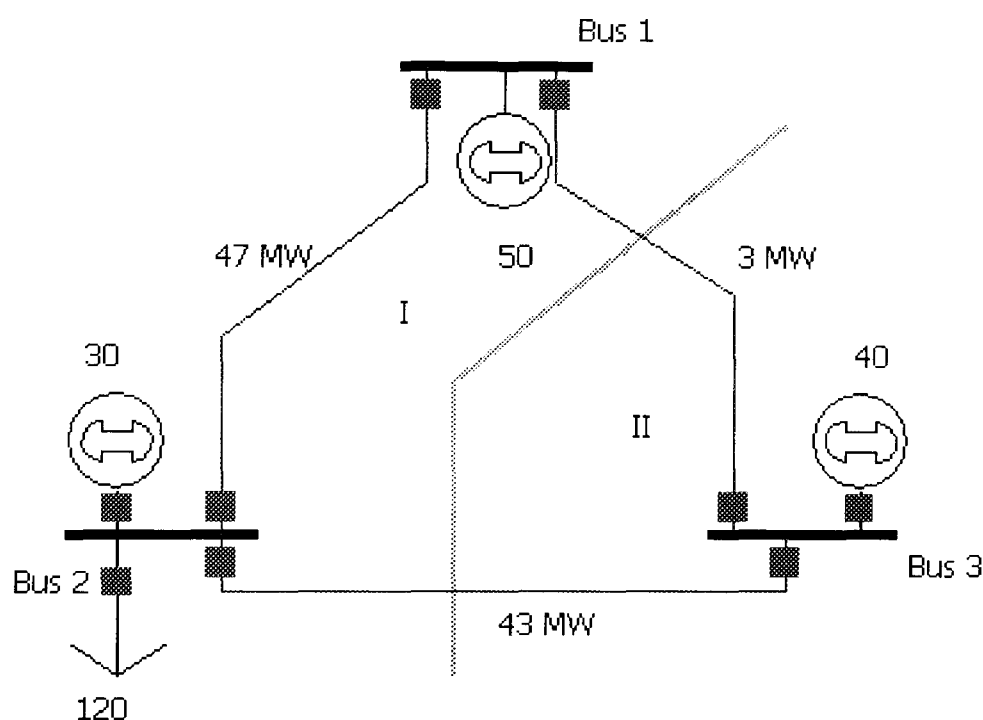
Figure 4-9   3-Bus 2-Area System

The system-wide OPF problem can be decomposed into two sub-problems corresponding to the two sub-systems. For sub-system I, the sub-problem can be written

as: min. $C_1(p_{g1}) + C_2(p_{g2})$, i.e min. $C_I(\mathbf{p_{gI}})$, where $\mathbf{p_{gI}} = \begin{bmatrix} p_{g1} & p_{g2} \end{bmatrix}^T$

subject to:

$$p_{g1} - B_{12}\sin(\delta_{1I} - \delta_{2I}) - B_{13}\sin(\delta_{1I} - \delta_{3II}) = 0$$

$$p_{g2} - p_{d2} - B_{21}\sin(\delta_{2I} - \delta_{1I}) - B_{23}\sin(\delta_{2I} - \delta_{3I}) = 0$$

$$p_{g1\min} \leq p_{g1} \leq p_{g1\max} \text{ and } p_{g2\min} \leq p_{g2} \leq p_{g2\max}$$

$$B_{12} \cdot |\sin(\delta_{1I} - \delta_{2I})| \leq L_{1-2\max} \text{ and } B_{13} \cdot |\sin(\delta_{1I} - \delta_{3I})| \leq L_{1-3\max}$$

Similarly the sub-problem for sub-system II can be written as:

as: min. $C_3(p_{g3})$ i.e min. $C_{II}(\mathbf{p_{gII}})$, where $\mathbf{p_{gII}} = [p_{g3}]$

subject to:

$$p_{g3} - B_{31}\sin(\delta_{3II} - \delta_{1II}) - B_{32}\sin(\delta_{3II} - \delta_{2II}) = 0, \quad p_{g3\min} \le p_{g3} \le p_{g3\max}$$

$$B_{32}\cdot|\sin(\delta_{3II} - \delta_{2II})| \le L_{3-2\max} \text{ and } B_{31}\cdot|\sin(\delta_{3II} - \delta_{1II})| \le L_{3-1\max}$$

A set of coupling constraints is introduced to coordinate the two sub-problems. In this example the coupling constraints are:

$$\delta_{1I} = \delta_{1II}, \quad \delta_{2I} = \delta_{2II} \text{ and } \delta_{3I} = \delta_{3II} \qquad (4.47)$$

It can be written as: $(\Gamma_I \quad \Gamma_{II})\begin{pmatrix} \gamma_I \\ \gamma_{II} \end{pmatrix} = 0$, where $\Gamma_I = \begin{bmatrix} 1 & 0 & 0 \\ 0 & 1 & 0 \\ 0 & 0 & 1 \end{bmatrix}$ and

$\Gamma_{II} = \begin{bmatrix} -1 & 0 & 0 \\ 0 & -1 & 0 \\ 0 & 0 & -1 \end{bmatrix}$, $\gamma_I = (\delta_{1I} \quad \delta_{2I} \quad \delta_{3I})^T$ and $\gamma_{II} = (\delta_{1II} \quad \delta_{2II} \quad \delta_{3II})^T$

The Lagrangian function for the overall OPF problem can be written as:

$$L(\cdot) = \sum_{k=1}^{II}\left(C_k(p_{gk}) + \lambda_k^T g_k(v_k, \gamma_k) + z_k^T h_k(v_k, \gamma_k, s_k) - \mu\sum lns_{ik}\right) + \sigma^T(\Gamma_I \quad \Gamma_{II})\begin{pmatrix}\gamma_I \\ \gamma_{II}\end{pmatrix}$$

(4.48), where σ is the Lagrangian multiplier vector corresponding to the coupling constraints.

Considering that $\dfrac{\partial L}{\partial \gamma_I} = \Gamma_I^T\sigma$, $\dfrac{\partial L}{\partial \gamma_{II}} = \Gamma_{II}^T\sigma$ and $\dfrac{\partial L}{\partial \sigma} = (\Gamma_I \quad \Gamma_{II})\begin{pmatrix}\gamma_I \\ \gamma_{II}\end{pmatrix}$, and using

A_I^k and A_{II}^k as the local part of Hessian matrix (see equation (4.46)), then equation (4.45) can be obtained. In this specific 3-bus 2-area example, equation (4.45) is:

$$\begin{bmatrix} A_I^k & 0 & \Gamma_{Iext}^T \\ 0 & A_{II}^k & \Gamma_{IIext}^T \\ \Gamma_{Iext} & \Gamma_{IIext} & 0 \end{bmatrix}\begin{bmatrix} \Delta\alpha_I^k \\ \Delta\alpha_{II}^k \\ \Delta\sigma^k \end{bmatrix} = \begin{bmatrix} \beta_I^k \\ \beta_{II}^k \\ q^k \end{bmatrix} \qquad (4.49)$$

where the $\Gamma_{Iext} = (0 \quad \Gamma_I)$ and $\Gamma_{IIext} = (0 \quad \Gamma_{II})$.

Equation (4.49) has the same border-blocked structure as in Aguado's or Xie's papers, but with greatly reduced size. Secondly, this smaller size Hessian matrix is symmetric, thus the computation time will be reduced. Moreover, instead of directly

invert the local part of Hessian matrix $\mathbf{A}_a^k$, which is not always invertible during the iteration procedure, another approach is used to obtain the global variable increments, and we will discuss it in the next section.

Compared with sub-gradient methods, this method does not generate a serious of nonlinear optimisation problems. The only iteration procedure is solving the linear Newton equations. Once the optimum is obtained it is a global optimum, which is the final result. On the contrary, in sub-gradient methods, the local optimums obtained by the TSOs are generally not compatible with one another, and the parameters of local optimisation sub-problems need to be upgraded to generate the new sub-problems.

4.5.4 Application issues
Inter-area coordination

Given the Newton equations (4.41), the first step is to solve the global Lagrangian multipliers $\mathbf{\Delta\sigma}^k$. Once they are obtained, all the areas can compute out the local variables by themselves and update all the primal and dual variables. If the iteration procedure converges, the global optimum is obtained.

The solving of $\mathbf{\Delta\sigma}^k$ does not require full knowledge of the matrix $\mathbf{A}_1$ through $\mathbf{A_A}$. One way is publishing the aggregated information in the form of $\mathbf{\Gamma A^{-1}\Gamma^T}$, like the approach proposed by [137]. However, this might cause computational difficulties as the A matrices are not always invertible. Here another approach is proposed by exploring the specific sparse structure of the Hessian matrix.

In equation (4.45), the $\mathbf{A}_a^k$ for each area a can be expressed as:

$$
\mathbf{A}_a^k = \begin{bmatrix}
\mathbf{C} & \mathbf{0} & \mathbf{E} & \mathbf{0} \\
\mathbf{0} & \mathbf{H}_{\delta_a \delta a}\big|_k & -\dfrac{\partial \mathbf{g}_{ga}}{\partial \delta_a}\Big|_k & \dfrac{\partial \mathbf{g}_{Da}}{\partial \delta_a}\Big|_k \\
\mathbf{E}^T & \left(-\dfrac{\partial \mathbf{g}_{ga}}{\partial \delta_a}\right)^T\Big|_k & \mathbf{0} & \mathbf{0} \\
\mathbf{0} & \left(\dfrac{\partial \mathbf{g}_{Da}}{\partial \delta_a}\right)^T\Big|_k & \mathbf{0} & \mathbf{0}
\end{bmatrix}
\tag{4.50}
$$

where the **C** and **E** are constant matrices and thus doesn't need to be updated during the iteration(for details please see the appendix).

Given the left-hand matrix and the right-hand vectors in equation (4.45), the increments of primal and dual variables can all be expressed as functions of the bus angles and the Lagrangian multipliers of the coupling constraints (please refer to the appendix). Therefore, in the above 2-area example, by solving the equation

$$\begin{bmatrix} N_I^k & 0 & \Gamma_I^T \\ 0 & N_{II}^k & \Gamma_{II}^T \\ \Gamma_I & \Gamma_{II} & 0 \end{bmatrix} \begin{bmatrix} \Delta\delta_I^k \\ \Delta\delta_{II}^k \\ \Delta\sigma^k \end{bmatrix} = \begin{bmatrix} r_I^k \\ r_{II}^k \\ r_\sigma^k \end{bmatrix} \qquad (4.51)$$

This equation set can be published and solved during each iteration. We can always get the least square solution with minimum norm for the equation set. It has been proved that such solution always exists and is unique as long as the left matrix in equation (4.44) is not a null matrix. More importantly, it reduces automatically to the exact solution during the iteration procedure.

Furthermore, the increments of Lagrangian multipliers of the coupling constraints, i.e. the vector $\Delta\sigma^k$, can also be expressed as functions of $\Delta\delta_I^k$ and $\Delta\delta_{II}^k$. Therefore, aggregated information on each tie-line can be exchanged to obtain the $\Delta\sigma^k$, and then update the $\Delta\delta_I^k$, $\Delta\delta_{II}^k$ and other variables. However, this approach can only be used when the search is within an approximation of the optimum, so that the solution does not diverge at the early stage.

It is also worth pointing out that in the full Hessian matrix A= $\begin{bmatrix} H_{xx} & \nabla g \\ \nabla g^T & 0 \end{bmatrix}$, H_{xx} has the size of all the P and δ in this area. Actually, the H_{xx} can be obtained by modifying the widely used Hessian matrix in Newton OPF, because the matrix is organised in the same fashion as in the Newton OPF (see appendix for details):

$$H_{xx} = H + \nabla h \cdot (S^{-1}Z) \cdot \nabla h^T \qquad (4.52)$$

Any additional constraints can be easily adapted into the A matrix without a lot changes on the program codes.

Choice of parameters

- Barrier parameters:

μ_i are set to be identical for all the s_i because there's no preference among the slack variables. The μ is made proportional to the complementary gap, which is the product of slack variables and their Lagrange multipliers. $\mu = \rho \cdot \left(z^T s\right)/k$, where the k is number of inequality constraints, and ρ is a convergence factor to force $\mu \rightarrow 0$ during the iteration procedure. $\rho_0 = 0.5$ at the beginning of the iteration, and then it is updated as $\rho^{k+1} = \max\left(0.1, 0.95\rho^k\right)$. By reducing the value of ρ we are making the cut in the complementary gap.

This choice is not problem-dependent and has been proved reliable in many papers.

- Starting points:

The choice of starting point plays an important role in finding the correct optimum through the iteration procedure. Improper starting point might even lead to divergence or to a different solution if it does exist.

It has been suggested that a load flow program can be used to obtain the starting point, and that it can speed up the procedure. In our examples a general choice is applied, and it works well in several cases. The detail of this choice is:

- Nodal injections p: a feasible solution if available, or a plain start $p_0 = p_{min} + \varepsilon$ to satisfy the inequality constraints, where the ε is a very small number. In this work, $\varepsilon = 1e-4$.

- Power angles δ: a feasible solution corresponding to p_0 if available, or $\delta_0 = 0$ for the plain start.

- Slack variables s: calculated from $h(p_0, \delta_0) + s_0 = 0$. If $s_{i0} = 0$, change the value as $s_{i0} = \varepsilon$.

- Lagrange vectors: $z_{i0} = 1 + |J_0|_1$ for every z_{i0}.

- $\lambda_0 = \varepsilon$ and $\sigma_0 = \varepsilon$.

Choice of step size

The choice of step size in IPM is very straightforward. Once the increment directions are calculated out, the stepsize is chosen so that the slack variables s and their corresponding Lagrangian multipliers z are all kept nonnegative. Here we follow Momoh's method to choose the stepsize [131]:

Let $K_1 = \min\left[\dfrac{\Delta s_i}{s_i}\right]$ and $K_2 = \min\left[\dfrac{\Delta z_i}{z_i}\right]$, i=1,2,...k. then

$\alpha_1 = \begin{cases} 1 & \text{if } K_1 \geq -1 \\ (-1/K_1) & \text{if } K_1 < -1 \end{cases}$ is the stepsize for primal variables, i.e. P, δ, s

$\alpha_2 = \begin{cases} 1 & \text{if } K_2 \geq -1 \\ (-1/K_2) & \text{if } K_2 < -1 \end{cases}$ is the stepsize for dual variables, i.e. λ, σ, z

Stopping criteria

Check the barrier parameter μ and the mismatch of the KKT, if both $\mu \leq \varepsilon_1$ and $|\nabla L|_1 \leq \varepsilon_2$, stop. Otherwise continue iteration. The ε_1 and ε_2 are normally chosen between 1e-8 to 1e-3. In the examples in Chapter 4, $\varepsilon_1 = 1e-8$ and $\varepsilon_2 = 1e-4$.

The extended Kuhn-Tucker necessary conditions are used to test the static points. If the starting point is chosen close enough, the iteration will converge to the correct result.

If the above criteria are satisfied, the iteration converges at the optimum. If numerical problems cause difficulties in achieving them, the program checks the changes in the variables and objective value, and stops as soon as the changes are negligible.

Adjustment

Considering the calculus errors, further adjustments must be made if the new point is too close to the border of the feasible region.

If both $K_1 \geq -0.995$ and $K_2 \geq -0.995$, the new point will fall reliably within the feasible region. Otherwise a conservative factor of 0.995 is used to reduce the stepsize from α_1 and α_2 to $0.995\,\alpha_1$ and $0.995\,\alpha_2$. In this way, the next point is kept within the feasible region even with the existence of calculus errors on the Newton search.

4.6 Conclusions

In this chapter, several existing decomposed OPF methods are analysed and compared. A system variable decomposition method is then proposed, and an improved interior point method (IPM) to solve OPF problems is applied based on the decomposition and sparse matrix technologies.

The contributions from this chapter are mainly on two parts: section 4.4 gives the system decomposition model, including the topology decomposition and choice of coupling variables to reflect the neighbouring areas. Based on the presented decomposition model, an improved OPF method using interior point (IP) method is suggested in section 4.5.3. This method complements [127] and [128]'s work, and it will be tested in Chapter 5.

Chapter 5   Test the Decomposed Optimal Power Flow Methods on Small Systems

5.1   Test on Cadwalader's method

In Cadwalader's method, the PTDF factors as well as nodal and congestion prices are used to couple the interconnected systems. The performance of this Lagrangian relaxation method is problem-dependent. For a symmetric network given in [125], the published results were obtained with the software. But when the code was applied to a non-symmetric network such as the test system described in this chapter, divergence was observed.

5.1.1   7-bus 2-area system
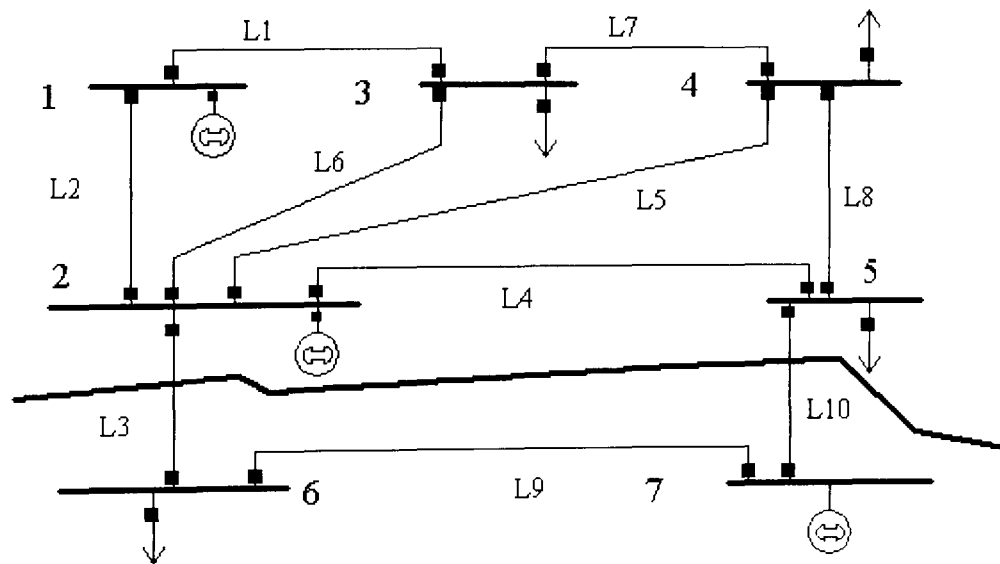
Figure 5-1   7-Bus Example

The test system is shown in Figure 5-1. This lossless system is divided into two sub-systems where the upper system is zone 1 and the lower system is zone 2. In each sub-system, the local TSO does not know the bid curves in the other sub-system. Therefore, given the initial values, each TSO makes the optimal dispatch on his own, and the results including the quantities and prices are sent to the opposite TSO to update the sub-problem of optimisation. If the dispatches obtained from the two sub-systems converge, the global optimum is obtained.

Suppose generator bid curves are linear, i.e. $\rho(q) = b + cq$, as shown below:

Supply Curve
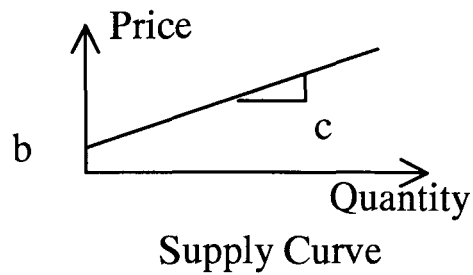
Therefore the cost function is quadratic. The bid curve factors for these generators are:

	G1	G2	G7
b	7.620	7.519	7.771
c	0.0040	0.0028	0.0038

Table 5-1   Generation cost

The users have responses to the varying spot prices. The amount of energy they take out

will decrease if the spot price is high.

Demand Curve
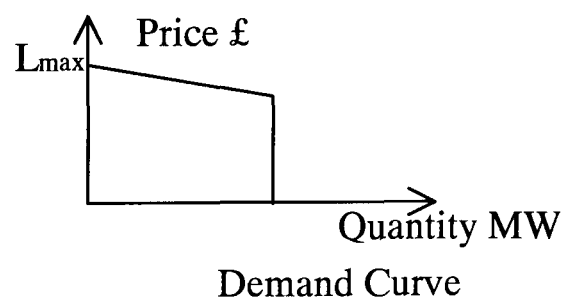
The system separation is shown in Figure 5-2:
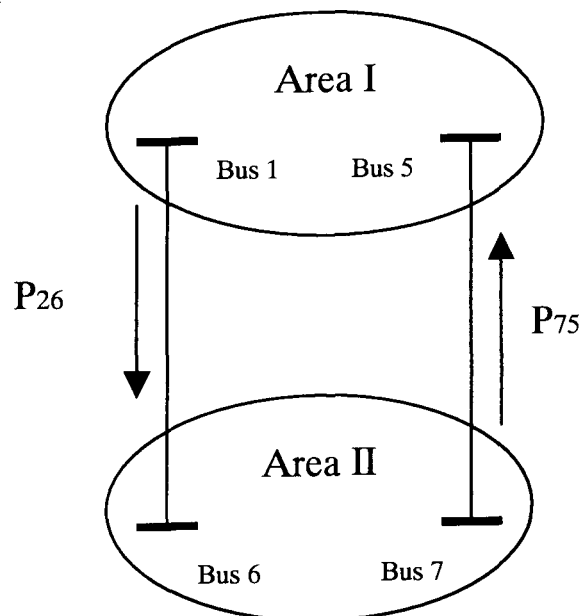
Figure 5-2   System Decomposition

For area I, re-number the nodes as shown in Figure 5-3:

113
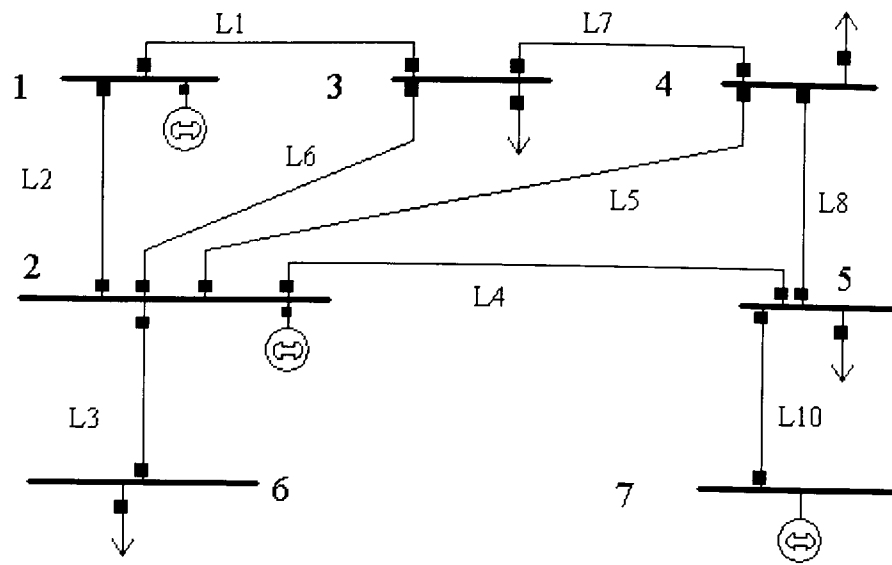
Figure 5-3   **Area I**

For area II, re-number the nodes as shown in Figure 5-4:
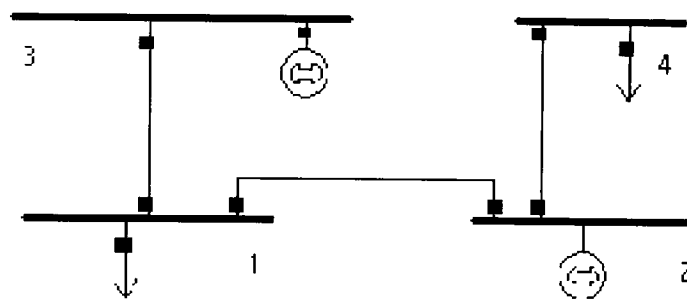
Figure 5-4   **Area II**

Test Results—Global Dispatch

Matlab software contains an optimisation toolbox which can tackle user-define, nonlinear optimisation problems. The algorithm used for medium-scale problems is a sequential quadratic programming (SQP) method. In this method, a Quadratic Programming (QP) sub-problem is solved at each iteration. A quasi-Newton method is used to estimate the Hessian of the Lagrangian.

The global OPF model is a standard SQP model with the quadratic objective function and linear constraints. Therefore, the matlab toolbox function was applied to this test system, and proved good performance. For this specific system, it took 23 iterations to converge at the precision of 1e-8, and the number of times to estimate the Lagrange function was 36 altogether. Figure 5-5 gives the value of Lagrange function at each iteration.

114
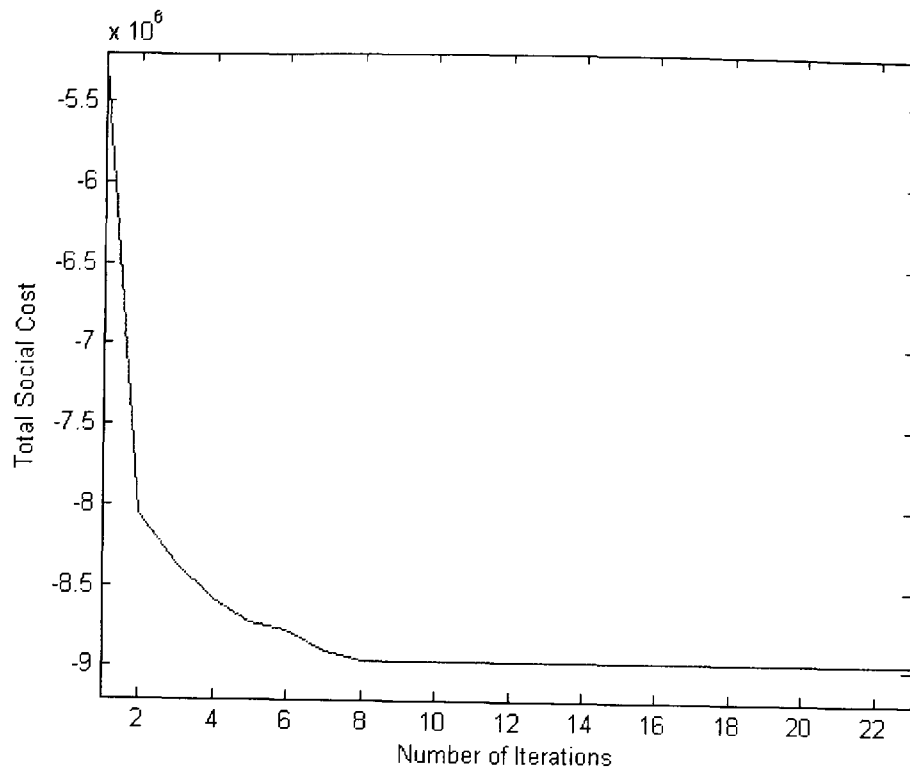
Figure 5-5   Social Cost Curve

Test Results—Decentralised Dispatch
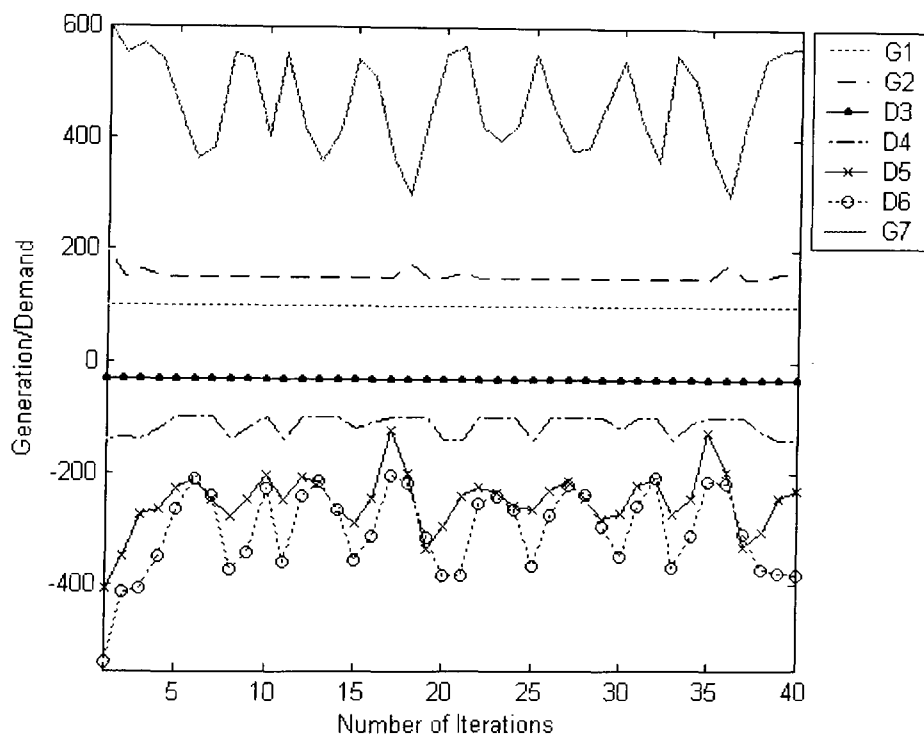
Figure 5-6   Generator/Demand level

If the two areas make parallel calculations and then upgrade the local OPF

problems with the information from the other area, this procedure is the decentralised

dispatch. Under Cadwalader's approach, this small system is tested, but the results from

the two areas cannot converge. Figure 5-6 shows how the results oscillate with the

iterations. As analysed in Chapter 3, the sub-gradient methods will normally encounter

such oscillation problem because of the high sensitivity of the results to the linearised sub-problems.

5.2 Test Kim and Baldick's approach

In this example, it took only 30 iterations to converge to the final result, so the performance is good. In each iteration, the optimums for the sub-problems are again solved using the matlab toolbox.

The total costs (negative of total welfare) at area 1, area 2 and the whole system during the iteration are shown as below. These costs contain the "shadow" cost of mismatch between coupling variables, which are soft constraints in this process.
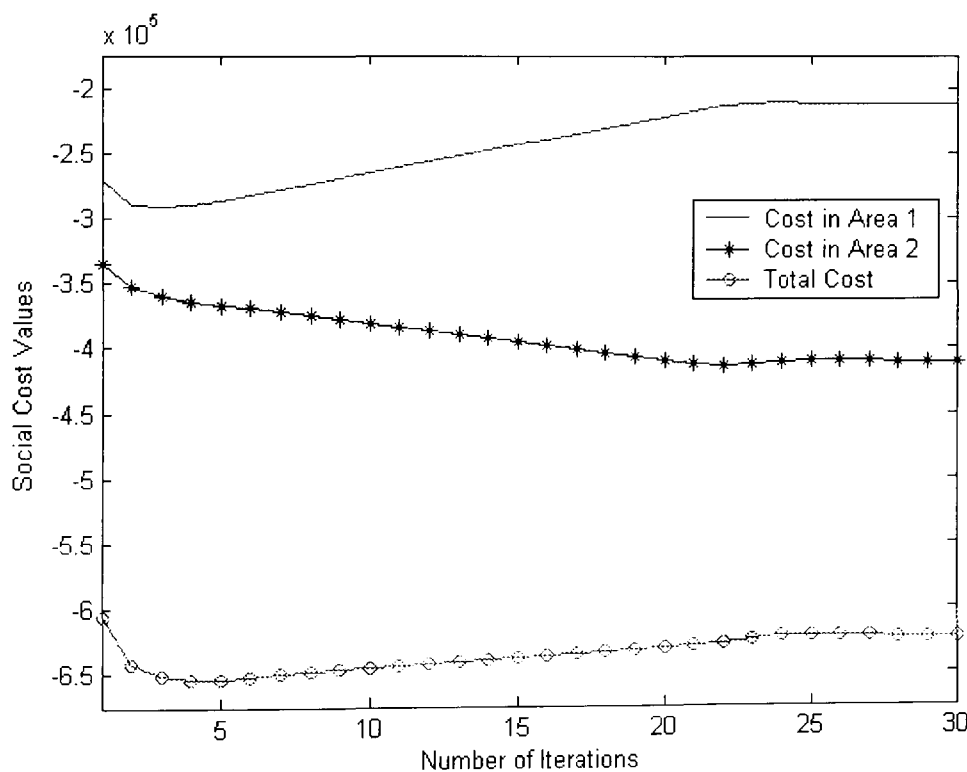
Figure 5-7   Total cost

The value of cost functions in area 1, area 2 and the entire system are presented in this figure. Notice that in area 1, the total cost firstly decrease and then increase, and finally went flat. This was caused by the drastic change of the coupling constraint cost.

The number of iterations the matlab toolbox took to obtain the optimum for sub-problems is shown below:

116
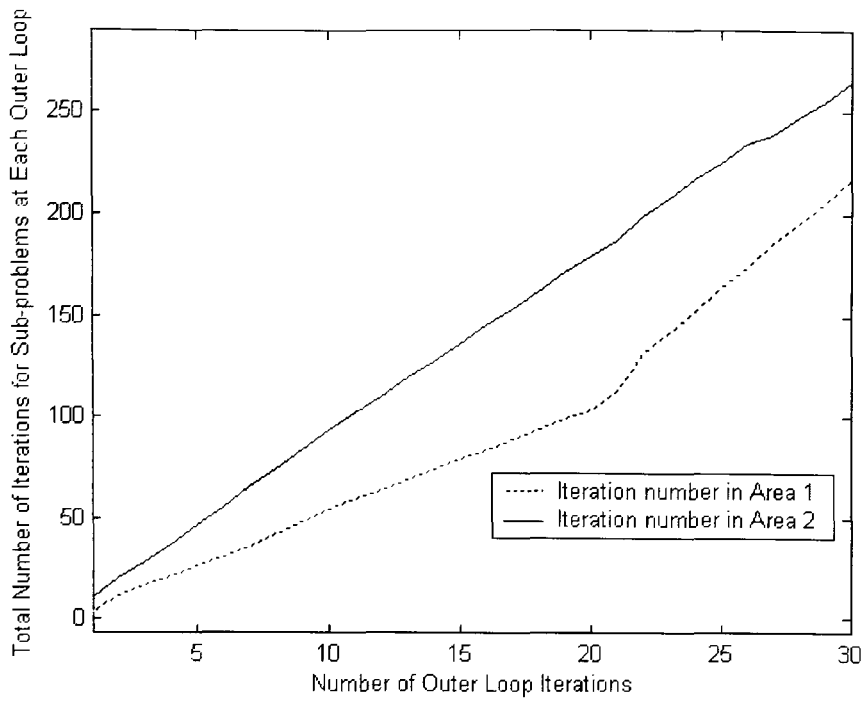
Figure 5-8   Numbers of iterations to obtain the optimums of sub-problems

From Figure 5-8 we can see, although this OPF method only involved 30 times

iterations (and thus 30 sub-problems in each area), it took several computation loops to

obtain the solutions to sub-problems each time.

The generations and demands on the buses vary with the iterations, and this can be

seen from the following figure:
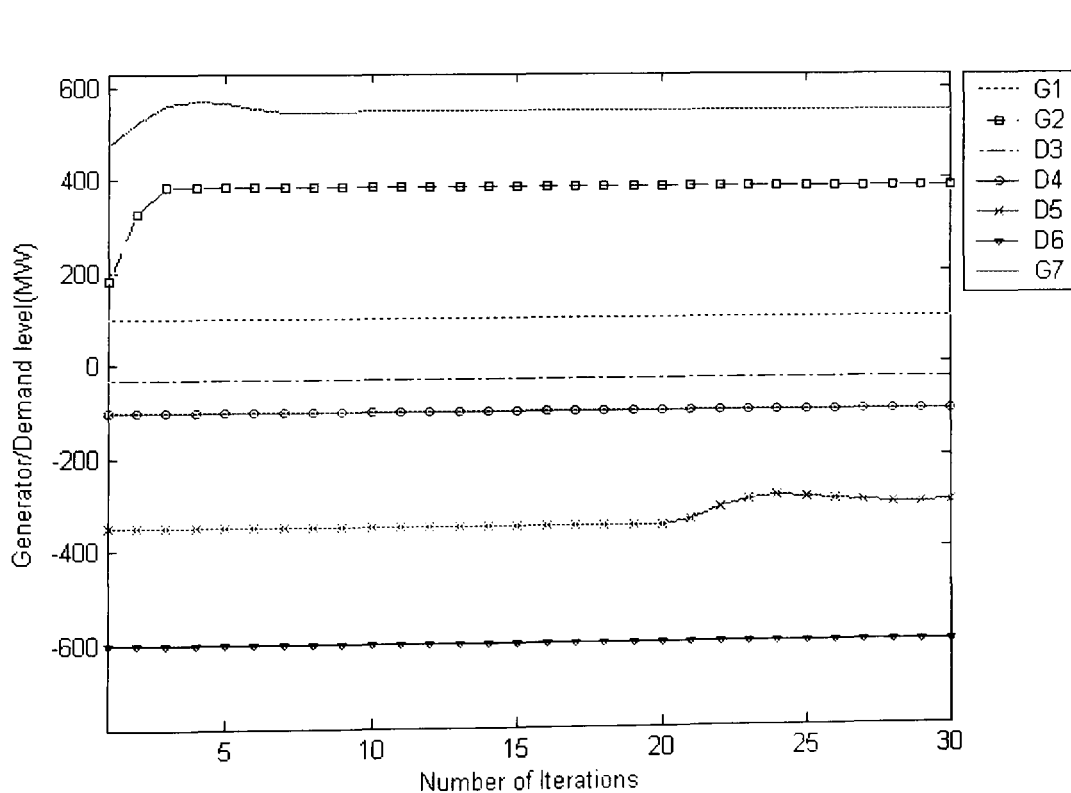
Figure 5-9   Generation/demand at each bus during the iteration

117

5.3   Test the IP method

The IPM was tested with matlab codes written by the author. A 7-bus system similar to the one in section 5.1.1 is used, and the only difference is the additional generators at bus 3 through bus 6. As the separation of the 7-bus system into 2 and 3 sub-systems will be applied, at least one generator is needed in each of the sub-system, thus those generators had to be added.

5.3.1   The 7-bus 2-area test system
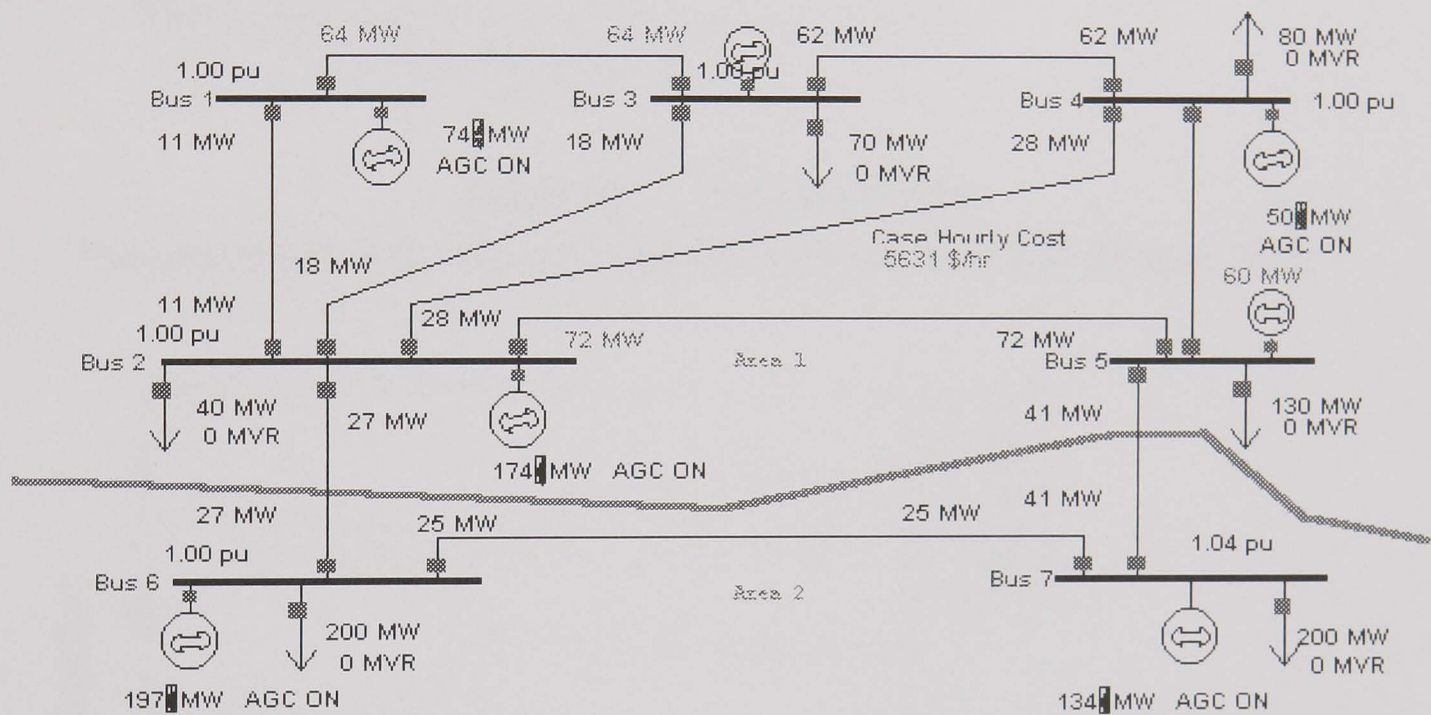
Figure 5-10   7-Bus 2-Area System

The bid curve factors for these generators are:

	G1	G2	G3	G4	G5	G6	G7
b	7.620	7.519	6.800	7.840	7.600	7.573	7.771
c	0.0040	0.0028	0.0200	0.0026	0.0200	0.0026	0.0038

Table 5-2   Generation cost

The values of the Lagrangian functions area 1, area 2 and the entire system during the iteration are shown in Figure 5-11:
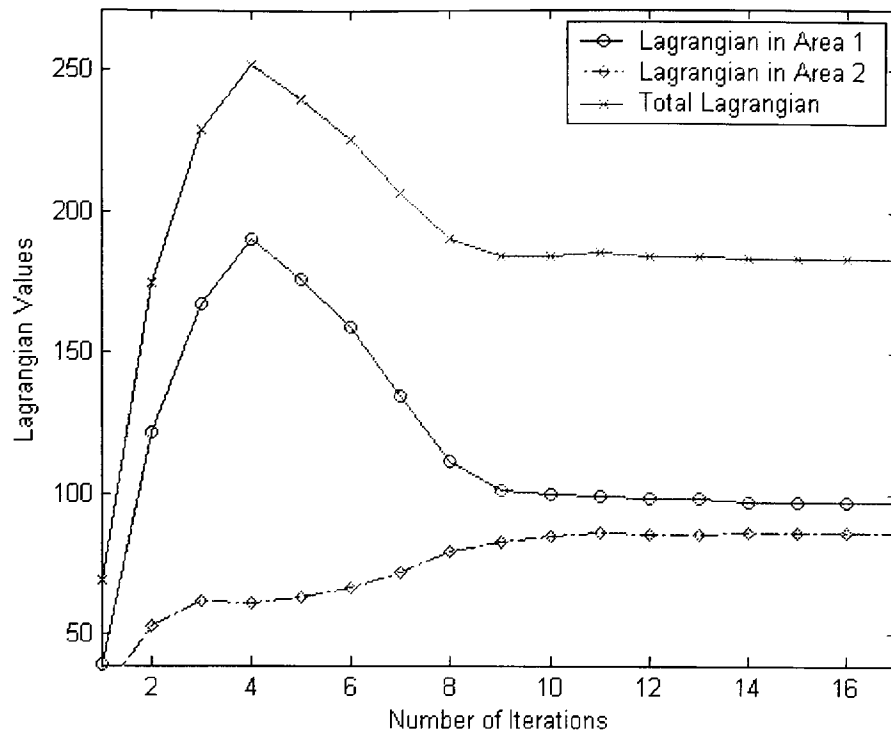
Figure 5-11   Lagrangian Values

The outputs of the Generators during the iterations are shown in Figure 5-12:
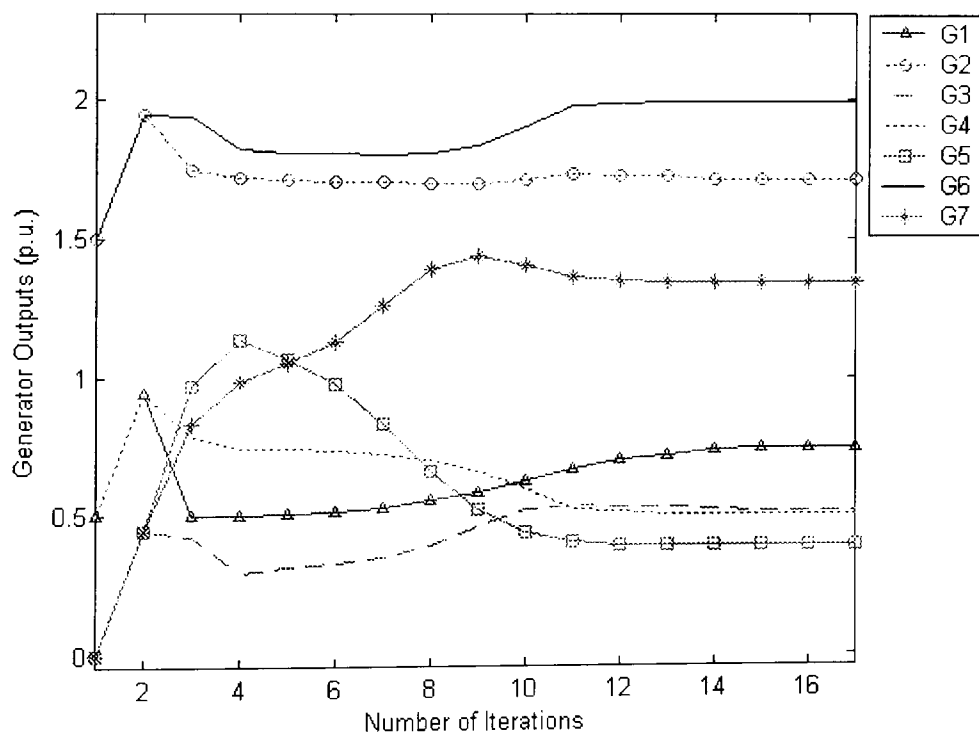
Figure 5-12   Generator Outputs

The angles are the coupling variables in this example, where DC power flow

calculation is applied. The angles at all the buses (except the slack bus—bus 7, where

the angle is set as 0) are shown in Figure 5-13:

119
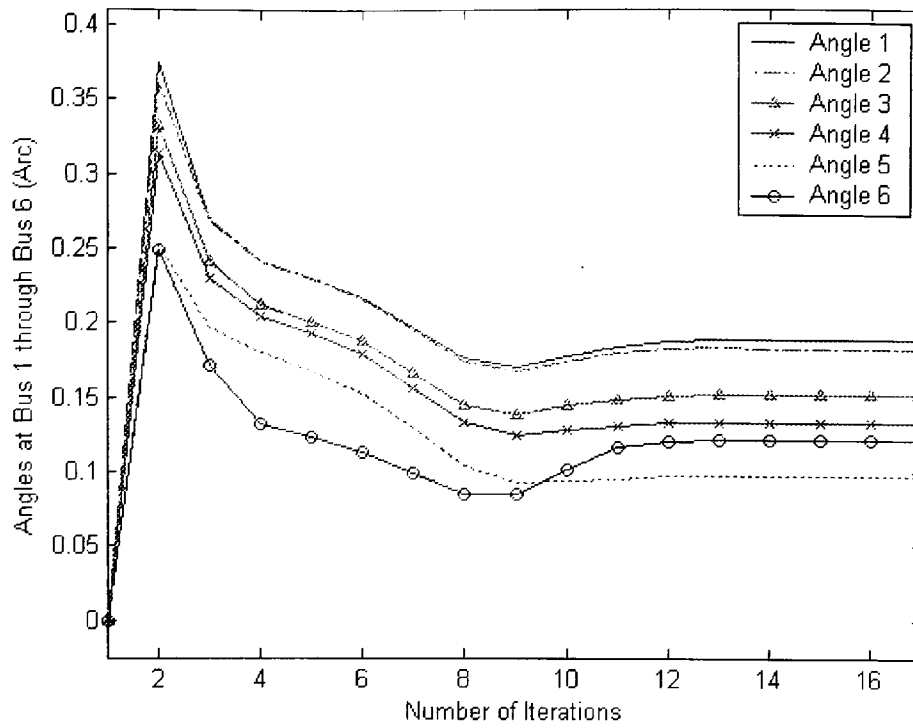
Figure 5-13   Bus Angles

The Lagrange multipliers associate with the coupling constraints (lambdas) are

shown in Figure 5-14:
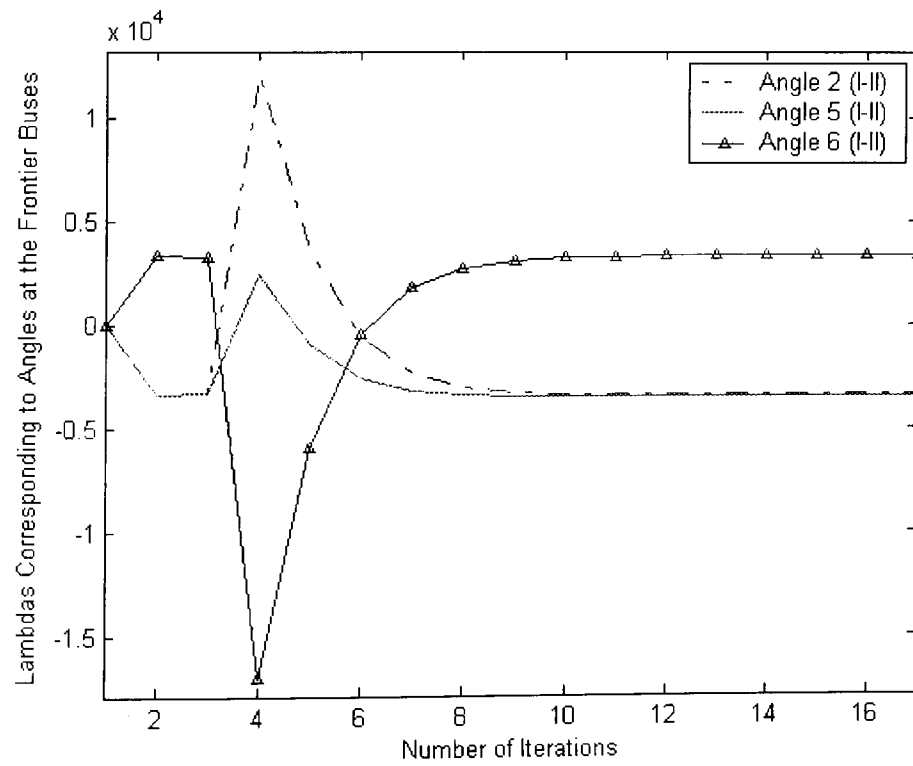
Figure 5-14   Lagrangian Multipliers

5.3.2   The 7-bus 3-area test system

To test the impact of loop flows on this OPF dispatch method, this system is

divided into 3 sub-systems.
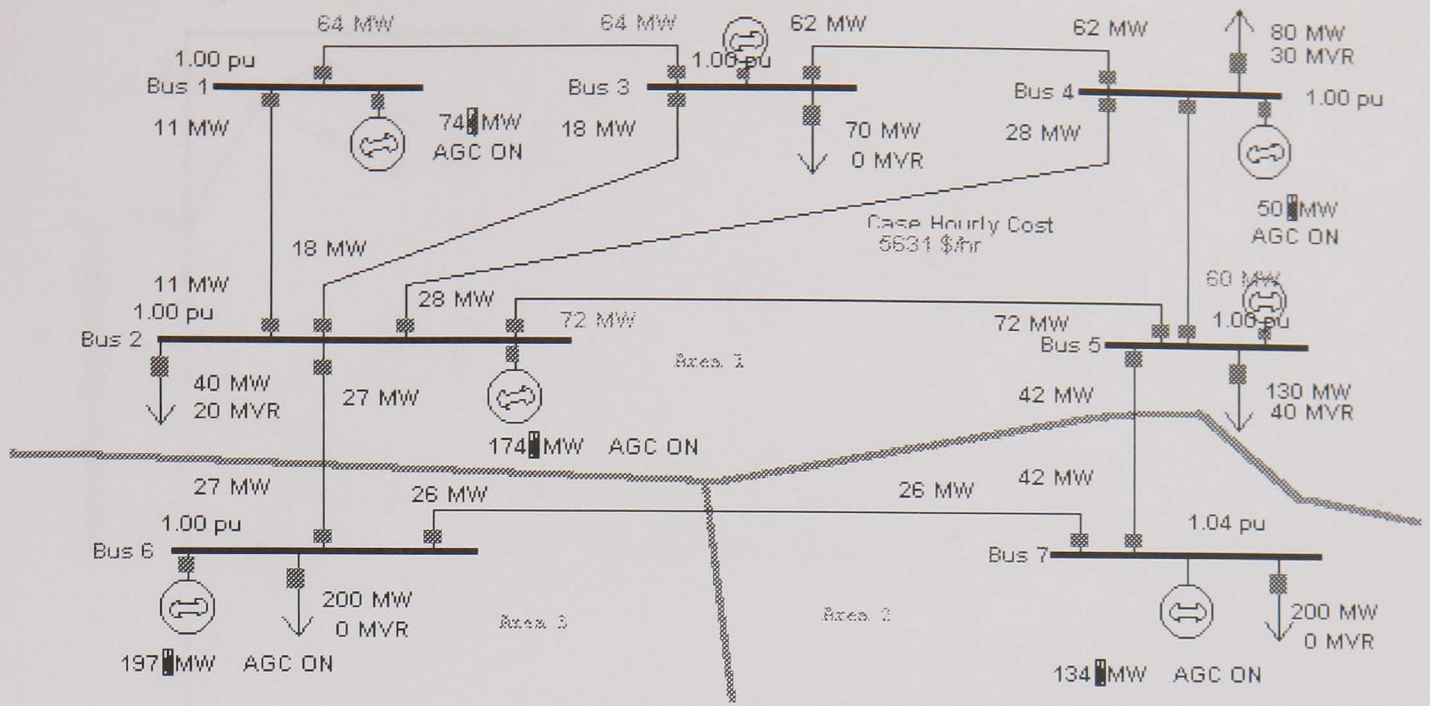
Figure 5-15   7-Bus 3-Area System

The values of the Lagrangian functions in area 1, area 2, area 3 as well as the entire system during the iteration are shown in Figure 5-16:
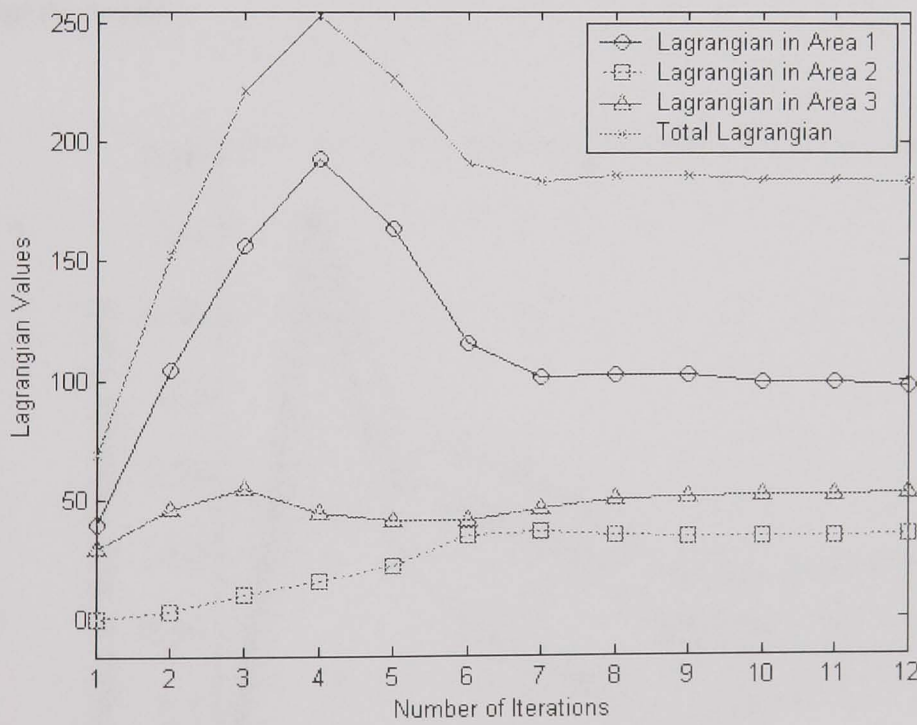
Figure 5-16   Lagrangian Values

The outputs of the Generators during the iterations are shown in Figure 5-17:
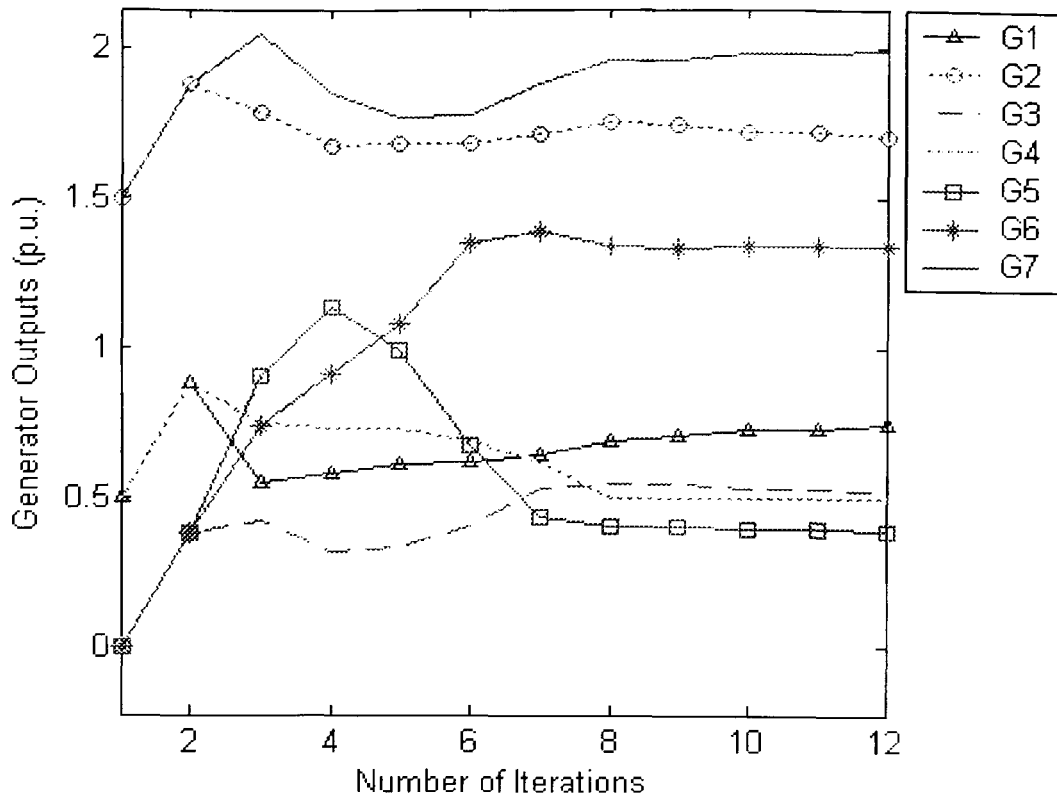
Figure 5-17   Generator Outputs

The angles at all the buses (except bus 7, which is the slack bus) are shown in

Figure 5-18:
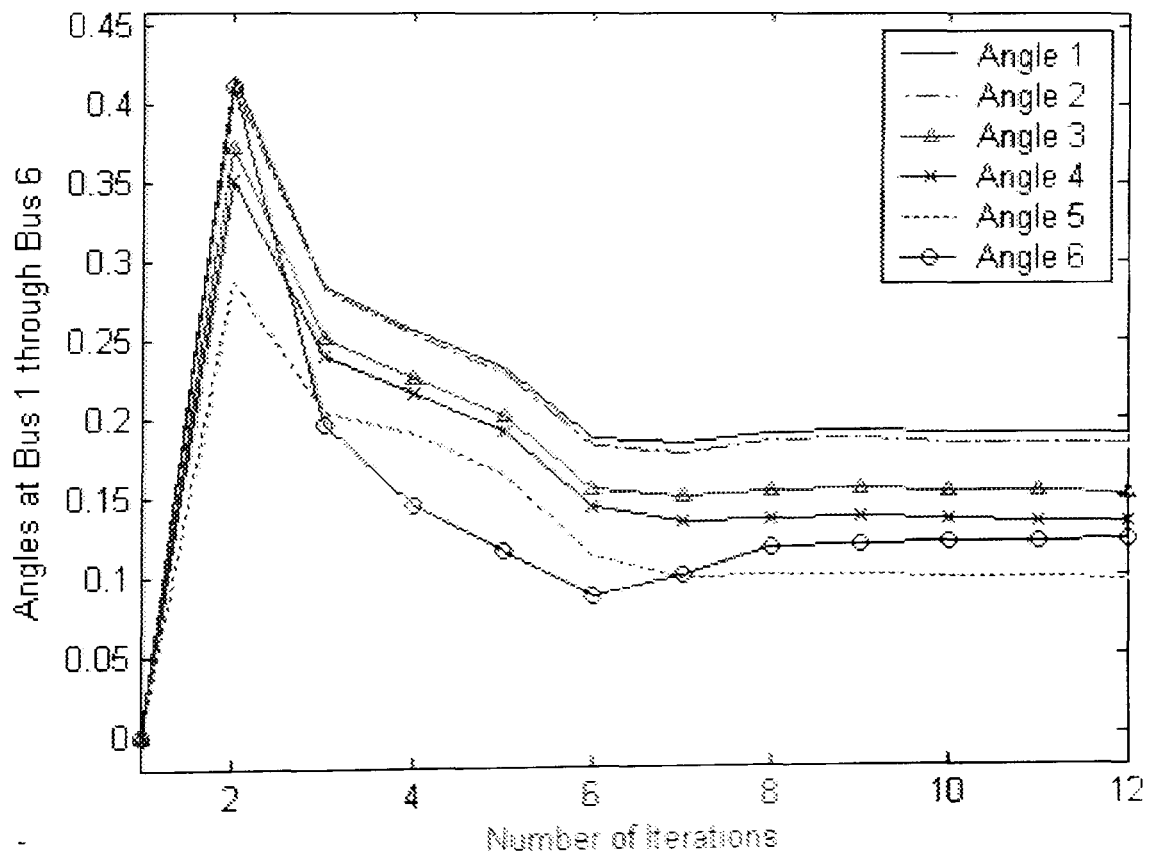
Figure 5-18   Bus Angles

The Lagrange multipliers associate with the coupling constraints (lambdas) are

shown in Figure 5-19. The equality coupling constraint of bus angle 6 works at the tie-

line between area 1 and area 2, also it works at the tie-line between area 2 and area 3.

thus there are two constraints corresponding to this power angle, and consequently two

Lagrange multipliers.
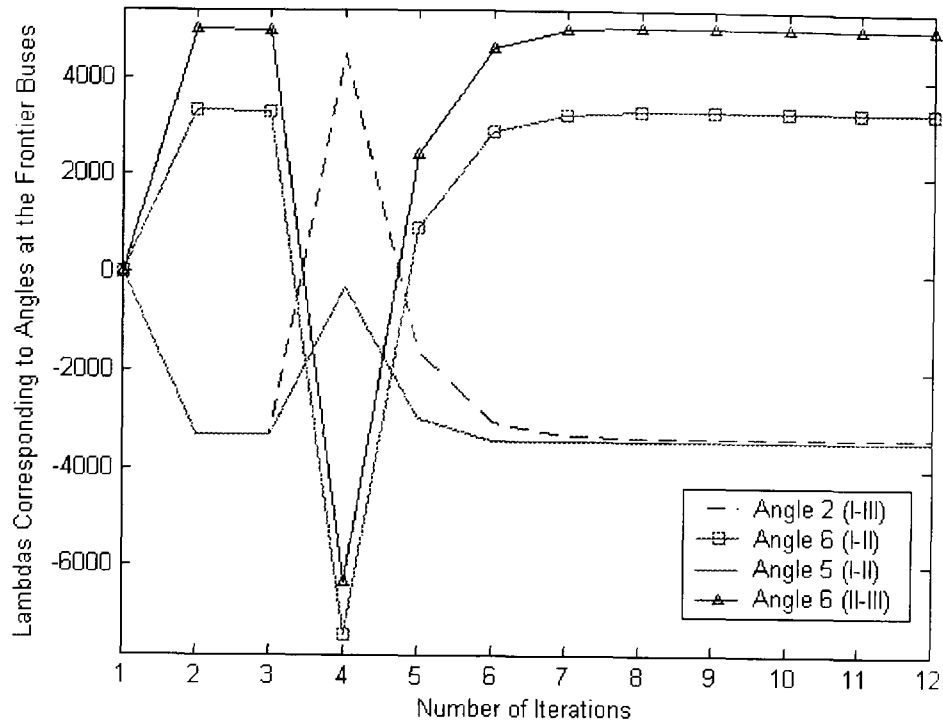
Figure 5-19   **Lagrangian Multipliers**

The Hessian matrix and barrier parameter are updated with each iteration, so there

is no more "inner loops" of iteration during the upgrade. This will greatly reduce the

computational time. By comparing the number of iterations in the 2-area and 3-area

case, we found that under the same precision requirement, the number of iterations:

7 Bus	Three-system	12
7 bus	Two-system	18

Table 5-3   **Number of Iterations**

The OPF computation can be carried in parallel in each of the sub-areas and further

reduce the computation time. In both of the case the OPF converge to the same optimal

results.

5.4   Conclusions

In this chapter, numerical tests were carried on the 7-bus system to test three cross-

border optimal power flow calculation methods: the sub-gradient methods proposed by

Cadwalader and Hogan, the augmented lagrangian function method proposed by Kim

and Baldick, and the improved barrier function method proposed in this thesis. Although the test system used here is very small, the test results are still consistent with the theoretical analysis made in Chapter 4: the sub-gradient method didn't have a successful performance in this small system, and the numerical oscillation can be observed clearly. The augmented Lagrangian method performed well, showing numerical stability and convergence. The IP method as applied in 5.3 can converge within a small number of iteration, and the search path is always within the feasible region.

The power flows on an interconnected network depend largely on the network structure because of loop flows. Therefore, any proposed cross-border congestion management method should ideally be simulated on the network before putting into practice. In the following chapter, a test network is built up using public information.

Under the three methods, the information required from neighbouring areas can be seen in Table 5-4:

Information exchange	PTDFs on the tie-lines	Nodal prices in other areas	Nodal variables at the border buses	Collective data
Cadwalader's	Yes	Yes	Yes	λ on the tie-lines
Baldick's	No	No	Yes	α, β, c
Proposed IPM	No	No	No	$N_{\delta\delta}$ and r_δ on the border buses, r_λ reflecting the coupling constraints, stepsize α

Table 5-4   **Variables exchanges among neighbouring control areas**

Chapter 6   Build Up A Test Network

6.1 Introduction

The deregulation and restructuring of a highly meshed interconnected network require a transparent and fair congestion management mechanism, which can provide incentives to improve efficiency. Apart from market structure differences in the sub-systems, the topology of such network raises extra difficulties compared with radial network. ETSO (European Transmission System Organisation) has outlined the difficulty with congestion management in a highly meshed network [104].

> Both the occurrence of congestion and the capacities of lines change significantly with nodal injections. Therefore, the values of NTCs (Net Transmission Capacities) across borders are strongly interdependent.

The connection and parameters of a network have dominant influence on the occurrence of congestions. Therefore, any congestion management method would fail if the characteristics of the network are not taken into full consideration. The best way to test any methodology is to simulate it on the actual system model.

Power market rules need to be designed carefully and tested in models before being put into practice [9]. Although a very simple model can be used to test certain market rules in terms of social cost minimisation, we still need a model network with moderate size and close-to-reality characteristics to test the congestion management methods, because such methods are dependent on the network structure and resource distributions.

UCTE transmission network, which covers the west and central continental Europe, is a highly meshed interconnected network. According to the Florence Forum, market based congestion management methods should be applied on all the interconnections among member countries by 1 January 2003 [147]. However, several

reasons have delayed this procedure, among them the technical complexity was a major reason [147]. It is believed that simulation test of the proposed methods on the system model is necessary before putting them into practice. However, we met great difficulties when trying to obtain the actual data. Information such as power plant/load description or transmission line parameters is kept confidential by some network operators, for commercial data could be deduced from the above information, and therefore they are sensitive and not publicised.

In fact, we can test methodologies on an approximate network rather than the real-world one, and such a test network doesn't have to consist of a full range of true data, although it is expected to inherit major characteristics of the original network, so that the approximate power flows can be calculated on it. In this way, no commercial confidentiality issues would be raised, for this model system will be purely based on public available information. Such a model could be used to validate and benchmark different methodologies for assessing the effects of cross-border trades and we would hope that our model could form a first step in developing such a tool.

UCTE has already stated its aiming at the information to be published in its website, including generation/load data, grid availability, and most importantly the data on the interconnections between countries[148]. However, the TSOs are given the freedom to provide or not provide the data mentioned above. At present, data collection is still a painstaking task as the availabilities and formats of them vary greatly with TSOs.

This chapter gives details of the approach to build up the testing network. In section 1, the data are classified into several groups, and the methodology of collecting them is also discussed, together with related assumptions. The processing of original data under several software environments is described in Section 2. All the original data came from public accessible information resources.

6.2 Classification of public data

As geographic structure has distinct affects on the workability of congestion management methods, one has to test methodologies on the actual or a similar network. Thus, if we are trying to give suggestion on the congestion problems in the European system, we should simulate our solutions on the actual European model, or at least a model carrying major similarities. In this section, public data are classified and useful information was extracted from them. Several assumptions were used in this procedure to simplify the daunting work of duplicating the European network, and they are discussed in this chapter.

6.2.1 Basic situation of European network

The extra high voltages (EHV) of European transmission network consists of several voltage levels: 380 kV or 400kV (standard in UCTE, GB and NORDEL—Organisation for Nordic Electric Power Co-operation) and those non-standard voltage levels varying from 220 kV or 225kV to 300 kV [149]. 750 kV is applied only in Hungary for a line [150].

UCTE (formally called UCPTE) has 21 member countries. Due to the war in the Balkans in the 90s, the UCTE area is divided into 2 synchronous areas, which were re-connected via the asynchronous DC link between Greece and Italy [99]. The so-called "1st synchronous UCTE region" is composed of 18 continental European countries, as shown in the map [151]:
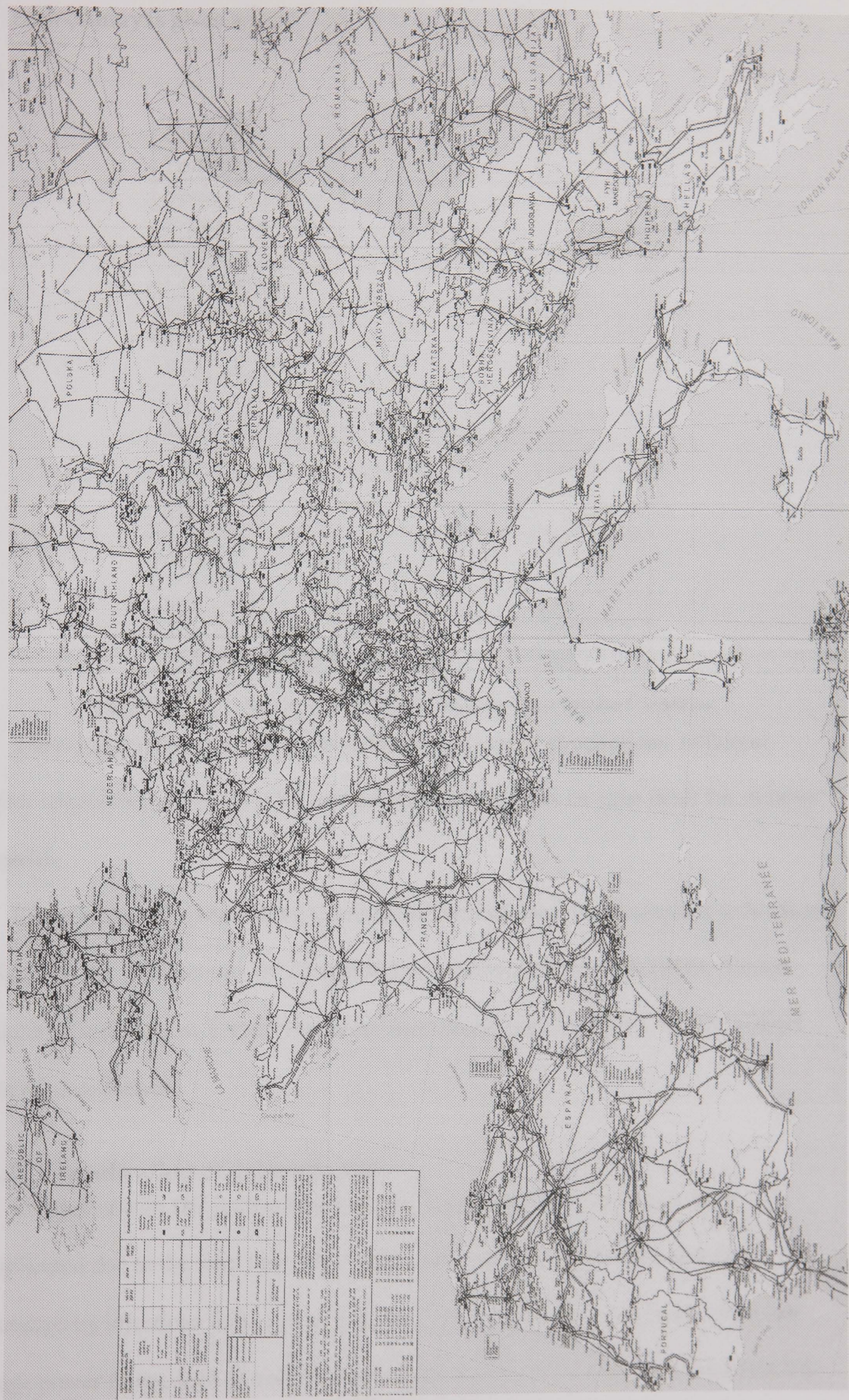
Each country is given a short term for the reason of convenience, as listed in Table 6-1.

Country	Acronym
Portugal	P
Spain	E
France	F
Belgium	B
Luxemburg	LX
Switzerland	CH
Italy	I
Netherlands	NL
Germany	D
Denmark (west, i.e. continental part)	DK
Czech	CZ
Slovakia	SK
Poland	PL
Austria	A
Hungary	H
Slovenia	SV
Croatia	CRT
Bosnia & Herzegovina (part)	BIH

Table 6-1   Acronyms of UCTE 1st Synchronous Region Countries

These acronyms were used in the database and system descriptions. Different market structures, regulatory rules and geographic structures co-exist in all the member countries.

Recently the AC (Alternating Current) connections have been extended to Northern Africa. The 1st synchronous UCTE region is also connected with UKTSOA (United Kingdom Transmission System Operators Association) and NORDEL via DC (Direct Current) connections.

6.2.2 Classification of network data

Compared with DC interconnections, AC transmission networks are more complicated due to the loop flow effect. That means the power flow in each line is influenced by injections from a large group of buses. Although some instruments can change power flows, such as voltage controllers, transformer tap changers and FACTS (Flexible AC Transmission Systems) equipments, their ability to change AC power flows are very limited so far.

As HVDC (High Voltage Direct Current) facilities are very expensive and thus are rarely implemented, the main part of the UCTE network is a highly meshed AC network. This made congestion management in this area more difficult, and also made a model network absolutely necessary. In the following sections the UCTE AC network (1st synchronised area) is studied and the model system was build upon those analyses.

For the reason of simplicity, a lossless network is chosen as the model, and the DC power flow method will be used, which will require information including reactance, voltage levels and topologies of transmission lines.

Apart from power flow information, geographic locations and the transmission limits are also important for cross-border congestion management study. Take the Nordic network as an example: it is to the credit of the radial geographic structure that market-splitting methodology as well as permanently divided pricing zones can be applied. Extending their experience into UCTE network will fail because of the highly meshed connections.

The data we need to build up the network model can be divided into the following categories:

- Transmission network data, including their electrical parameters, topologies and geographic locations.

- Power plant locations, fuel types and capacities.

- Load centre locations and capacities.

Given the above data we can create a test network. In order to double check the similarity between the model and the actual system, the following data are also needed:

- Actual power flow patterns, e.g. the total generation/demand of each member country at a specific time and the power flow on tie-lines at that time.

- PTDF values of cross-border transactions on tie-lines.

6.3 Collecting public data

We have contacted UCTE and the member TSOs (Transmission System Operators) for the above data, but the responses from them varied, and we failed to obtain any data from some key countries. Web searching also indicated that a complete system description (or even a medium-size network description of a member country) was not available.

However, there exists some public information from which we can extract useful technical data to build up a model network. Such a network, due to insufficient information, cannot duplicate the actual system in every aspects, but as it will inherit the geographic structures, connections and approximate parameters, it will be a good example for study and therefore worth building up.

The main information resources for building up the database are from:

- The publicly available generation, peak load, power flow exchange and cross-border lines information from UCTE website (www.ucte.org).

- The generation/substation description list from individual TSOs.

- The geographic information of population and industry from publicly available websites.

- Technical reports from European Commission website concerning the cross-border information.

6.3.1 Transmission network data collection

The transmission network is the backbone of the model system, and it took more effort than the nodal injection data. Although the electrical parameters of transmission lines are not directly available to the public, they can be deduced from the lengths and voltage levels of the lines, because typical reactance values per unit length for overhead lines are widely used by electrical engineers, given the voltage level and operating frequency. Transmission network maps are available from the websites of some TSOs.

therefore both the reactance and the connection were roughly given. UCTE also published its transmission network map [151], giving the voltage level, number of circuits of each EHV line, as well as its geographic location. Information like from-end and to-end locations can be extracted from this map.

Based on certain assumptions, the transmission network description can be extracted from the map. This description consists of electrical parameter list, topology connection list and transfer limits.

The transmission capacity limits among the countries were obtained from EC (European Commission) report [152], and the thermal limits of tie-lines were obtained from UCTE yearbook [153].

The following assumptions were used in building up the two lists:

(1) Only those lines with voltage levels at above 220kV (including 220kV) are taken into consideration. This assumption is generally accepted for cross-country transmission network carrying bulky energy. Among the countries there are also several tie-lines operated at 110 kV. They have relatively small capacities and play a less important role in power interactions, the test network doesn't include them.

(2) The resistance was ignored, because we only consider DC power flow method. Further assumption is that all the lines have evenly distributed electrical parameters along the full lengths. Thus the transmission line reactance was estimated by the length and number of circuits of each line, times the corresponding typical reactance value per unit length. This assumption will inevitably introduce some errors. For example, some long distance transmission lines may have series capacitors installed. The arrangement of phases and circuits also play an important role in determining reactance values. But such assumption is acceptable under general conditions.

(3) All the circuit breakers on the map are assumed to be closed under normal

operation in order to make full utilisation of the whole network. In fact, they can

be open, depending on the operation modes. For example, the 220kV line

between Belgium and Luxembourg is not energised. This makes all the power

flows deviate from the actual values due to the loop flow effect.

6.3.2 Power plant data collection

Power plant fuel types and capacities are related closely with their outputs, and

therefore influent the power flows.

This set of data has been especially sensitive ever since the privatisation, because

they can reflect the marginal generation costs. In a paper analysing the duopoly in

British electricity market, the author roughly estimated the marginal cost of fossil

thermal generators by calculating the cost of the fuel times the energy conversion

efficiency [50].

Since up-to-date information is not accessible, we had to turn to historic

information published before the deregulation of electricity industry. From a technical

aspect the historic data about capacities and fuel types have not been changed greatly in

UCTE over the past twenty years, thus the power flow calculation based on the historic

information can still reflect the present real network. A European fossil thermal power

plants database [154], published 12 years ago, is available on the internet, and it was

used in my work.

Generators in the testing network are simply classified as hydro, fossil thermal or

nuclear ones, so that no sensitive information is included. This classification

information was also obtained from the UCTE map, where the description of a certain

bus (i.e., whether it's a hydro power plant, a thermal/nuclear plant, or a transformer

substation).

6.3.3 Load data collection

Load centre locations and capacities also have important influence on the power flows. Unfortunately there is not sufficient information. An important assumption was used to help estimate the load level, details of which will be given later in this chapter. The basic idea of it is that demand levels are related closely with local population and industry.

The total demand of each UCTE member country is publicised in UCTE website (www.ucte.org). This total demand level was further distributed to all the load bus according to local population. This approach was based on the following two rules:

(1) The demand from household users in a certain area is proportional to the population in that area.

(2) The demand from industrial users in an area can be roughly reflected by the population there too, because population follows employment.

The website www.world-gazetteer.com gives population of all the administration areas (e.g. provinces) in each country, thus the total demand of a country was distributed into groups of demands by administration areas. Due to the fact that a high voltage substation can be located between two cities, further division of regional load into city loads by population was not made. Instead, within each administration area, the load buses are assumed to have equal capacities.

Comparison between this distribution method and actual demand distribution is needed to check the viability of such a load model. The example of Italy is given in table 3.1. In this table, actual area consumption list was available from the Italian TSO website (www.grtn.it), and the area population list was from www.world-gazetteer.com as year 2002 data. Column 4 and 5 are calculated by dividing the area population/consumption with national overall population/consumption, respectively. The correlation factor by comparing these two columns is also shown in the table, and it is as high as 91%. The result revealed how closely the distribution of population is

related with the electricity consumption. Although this strong correlation might not stand in all the other countries, this method can still reflect the load distribution trend.

region	population (1000)	Consumption (GWh)	Population (%)	Consumption (%)	
Abruzzo	1243.2	6105.9	2.210	2.186	
Basilicata	595.3	2351.7	1.058	0.842	
Calabria	1991.7	4582.2	3.540	1.640	
Campania	5648	14674.4	10.039	5.254	
Emilia-Romagna	3957.4	23177.2	7.034	8.298	
Friuli-Venezia Giulia	1179.4	8676.5	2.096	3.106	
Lazio	4972.2	19642.2	8.838	7.032	
Liguria	1559.5	6256	2.772	2.240	
Lombardia	8915.3	59583.9	15.846	21.332	
Marche	1462.7	6353.7	2.600	2.275	
Molise	316.3	1256	0.562	0.450	
Piemonte	4163.1	25095.1	7.400	8.984	
Puglia	3980.3	15756.2	7.075	5.641	
Sardegna	1598.2	10697.8	2.841	3.830	
Sicilia	4862.3	17392.2	8.642	6.227	
Toscana	3458.1	18594.3	6.147	6.657	
Trentino-Alto Adige	936.4	5173.3	1.664	1.852	
Umbria	814.9	5406.8	1.448	1.936	
Valle d'Aosta	119.3	819.7	0.212	0.293	
Veneto	4487	27724.5	7.975	9.926	Correlation
total	56260.6	279319.6	100	100	0.910457
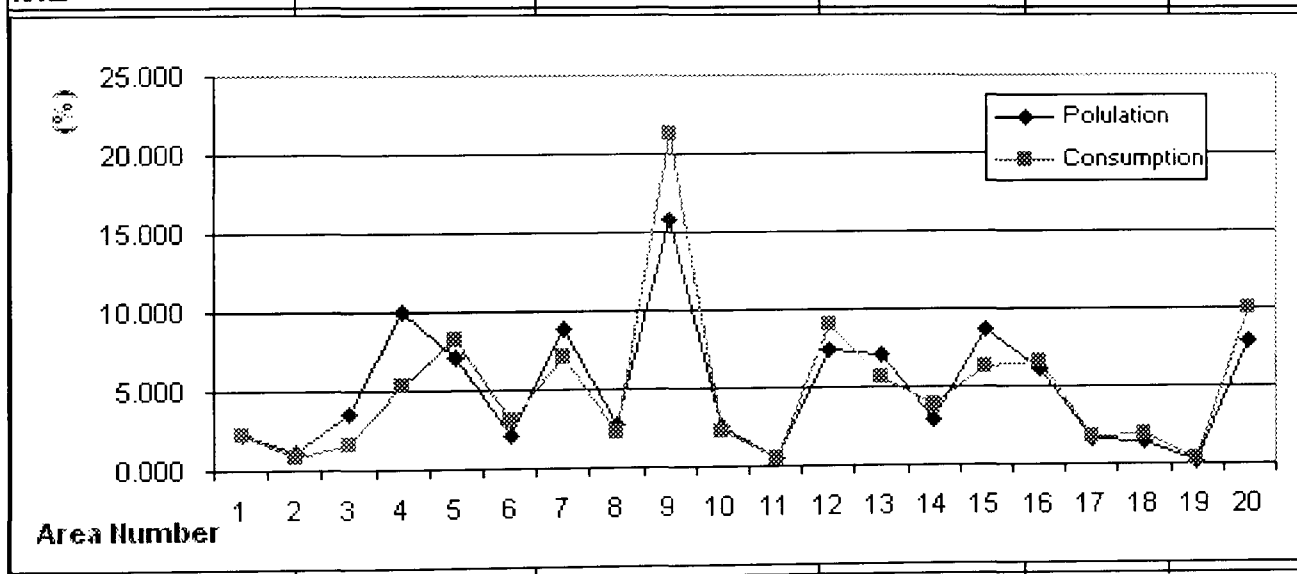
Table 6-2   **Comparison of Italian Population and Electricity Consumption**

Finally, the actual power flow patterns are needed for double checking the simulated network against the real one. In UCTE website, we can get typical power flow exchanges among the member countries, which can be used to compare the similarity between the testing network and the real one.

135

6.4 Creating the Original Transmission Network Database using GIS

One of the most time-consuming tasks is extracting out the transmission line lengths and their connections from the paper map. As the UCTE network consists of over a thousand buses, a database is needed to store and manage all the related information.

6.4.1 Digitising under ArcGis

A possible way to calculate the lengths of transmission lines from the paper map is using GIS (Geographic Information System) software. This type of software has build-in information including the longitude, latitude and altitude of every spot in a map, therefore it can store and manage any spatial information from a paper map. However, it can not automatically recognise the transmission lines on the map (although it works on radial networks, it cannot work well with a highly meshed network), thus manual digitising is needed (i.e. plot all the lines and indicate their connections. The software will automatically number these lines and nodes, calculate the lengths, and store the topology of the network). ArcGIS was used to do this work, and it can also export the GIS database it manages to a general database, facilitating our further supplementary work on the test network.

ArcGis uses the so-called 'spherical projection' to calculate the lengths of transmission lines. It calculates the integration along the line, whose location is given in spherical coordination. This method requires the actual geographic locations of the set of dots composing the line. Thus we need firstly register several points (at least 3) on the map as geographic sites defined by their longitudes and latitudes. After the registration all the points on the scanned map are related with their actual locations. Of course, the more points we register, the more accurate this coordination conversion is.

6.4.2 Format description of the original network

Besides the lengths which were automatically calculated out by ArcGis, several more characteristics for the lines and nodes (such description is called 'field' in a database) are also needed for parameter calculation.

In total, a line record consists of the following fields:

FNODE: the node number where the line starts;

TNODE: the node number where the line ends;

LENGTH: the length of the line in km.

VOLTAGE: 1 if the voltage is 220kV and 0 if the voltage is 380kV.

CIRCUIT: number of circuits for the line.

BORDER: 'Y' if this is a tie-line across multiple countries, 'N' if this line lies within a country.

COUNTRY: short form of the country in which the line is located. This field is blank for a tie-line record.

FROMCOUNTRY: only for tie-line records. The country where the tie-line starts.

TOCOUNTRY: only for tie-line records. The country where the tie-line ends.

CAPACITY: the capacity of this line. By default this value is '0', as we can see in the following example. This is obviously not true, but we ignore all the congestions within one control area and suppose the local TSO can manage them. Therefore, the only limit values we need to input are cross-border transmission limits.

The capacities of all the tie-lines were given in UCTE year book[155]. These capacities can be line thermal limit values, or limit values determined by transformers/ substations restrictions. Voltage limits or stability limits are converted into capacity limits [10]. For example, the voltage constraints can be converted to interface active power flow limits [163]: given a fixed load demand, the system operator can determine how much active power can flow through the interface lines without violating the voltage stability.

Here is an example of part of the original line records from Switzerland's internal network:

FNODE_	TNODE_	LENGTH/100	VOLTAGE	CIRCUIT	BORDER	COUNTRY	FROM COUNTR R	TO COUNTRY	CAPACITY LIMIT
24	18	0.430703	0	2	N	Swiss			0
12	3	0.264326	1	1	N	Swiss			0
26	31	0.478715	1	2	N	Swiss			0
16	22	0.574657	0	2	N	Swiss			0
14	16	0.306169	0	2	N	Swiss			0
4	11	0.464817	0	2	N	Swiss			0
2	4	0.44446	0	2	N	Swiss			0

Table 3-6-3   An Example of original line records

In this database the bus numbers are used to indicate the starting and ending points of these lines. GIS uses another table to store the bus information. The bus records have only the following four fields:

ARC: the number of the arc starting with the bus.

[COUNTRY NAME]: e.g. SWISS. This column is the identification numbers of the buses. It corresponds to the FNODE_/TNODE in Table 3-6-3.

X: the x coordination of this bus. This is the Cartesian coordination.

Y: the y coordination of this bus.

Below is part of GIS bus records of Switzerland internal network:

ARC_	SWISS_	X	Y
49	1	8.286488	47.79544
7	2	7.441521	47.68879
2	3	7.282507	47.67054
6	4	7.884427	47.65713
37	5	7.072288	47.65051
48	6	7.698944	47.58958
42	7	7.165298	47.5748

Table 6-4   GIS Bus Records

Thus we can get the geographic locations of all the buses. This information is used later in PowerWorld Simulator to create a one-line display of the whole UCTE interconnected system.

Nodal injections do not appear in this table, and they'll be addressed in the next section. We will designate the sign of injections as positive for generators and negative

for loads. The Origin of x-y coordinates is the top_left corner of the screen in ArcGis, while it is the bottom_left corner in PowerWorld. Besides, the coordinates in ArcGis are given in actual kilometres, but the "oneline screen coordinates" in PowerWorld are associated with the pixels of the display. In order to 'transplant' the network from GIS to PowerWorld, we need to establish the format conversion between these two environments. Below is the MicroSoft database query used for coordination conversion in this section.
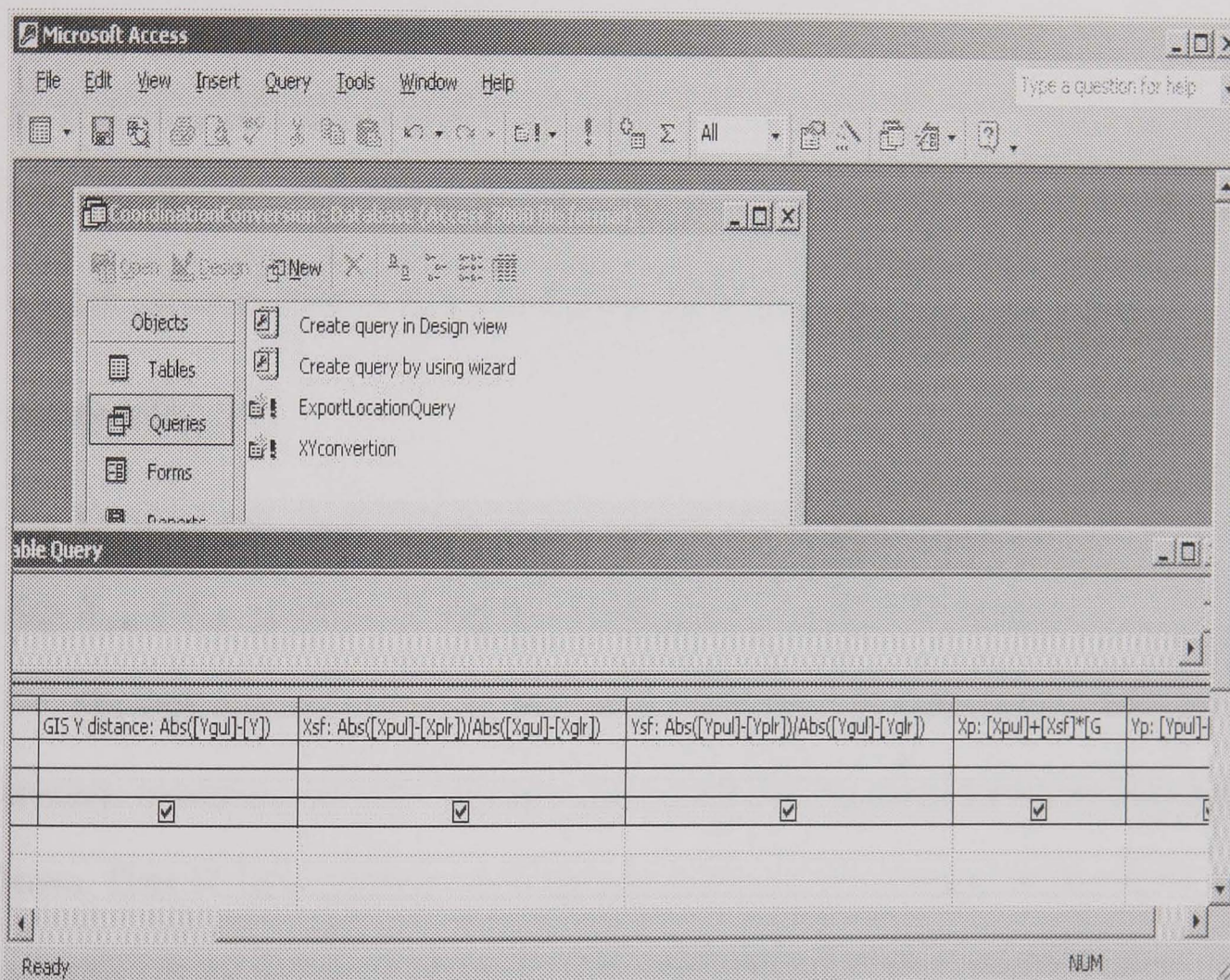
Figure 6-1   Coordination Conversion

The 'Queries' module in MicroSoft Access database enables batch processing of data and storing the results on a table. New coordinate values were calculated out using the query designed as Figure 6-1, where the constants:

Xgul, Ygul: the x, y coordinates of the top-left corner of the display window in ArcGis.

Xgul=-10.386207, Ygul=57.980912.

Xglr, Yglr: the x, y coordinates of the bottom-left corner of the display window in

ArcGis. Xglr= 25.954773, Yglr= 35.416979.

Xpul, Ypul: the x, y coordinates of the top-left corner of the display window in PowerWorld Simulator. Xpul= -500, Ypul= 1500.

Xplr, Yplr: the x, y coordinates of the bottom-right corner of the display window in PowerWorld Simulator. Xplr= 1500, Yplr= -500.

Xsf, Ysf: the converting scales of x and y from GIS coordinates to PowerWorld

coordinates. $Xsf = \dfrac{\left| X_{pul} - X_{plr} \right|}{\left| X_{gul} - X_{glr} \right|} = 55.034$, $Ysf = \dfrac{\left| Y_{pul} - Y_{plr} \right|}{\left| Y_{gul} - Y_{glr} \right|} = 88.637$.

And the variables in the query are:

X, Y: the x, y coordinates of the bus in GIS.

GIS X/Y distance: the distance between the specific bus and the origin (which is the top_left corner in GIS) in X/Y coordinates. GIS X distance= $\left| X_{gul} - X \right|$, GIS Y

distance= $\left| Y_{gul} - Y \right|$.

Xp, Yp: the x and y coordinates of the bus in PowerWorld.

$Xp = X_{pul} + X_{sf} \times (GIS\ X\ Distance)$, $Yp = Y_{pul} + Y_{sf} \times (GIS\ Y\ Distance)$.

For each country, a database was used to store the line table and bus table for a country. In addition an extra database was created for the cross-border tie-lines and their buses. Thus 18 GIS databases were built up in this section. Further work will be addressed in the coming sections on nodal power injection process and format conversion from GIS to general database, and finally to PowerWorld case file.

6.4.3 Network Simplification during digitising of the network

Some buses are connected with one another through very short transmission lines, and they can be aggregated into certain groups to simplify the network. These 'equivalent' buses are set in this way so that their power flow exchanges with outer systems are kept unchanged after the network simplification. This procedure also helps power flow computation, because too-short transmission lines in the network might

cause ill-conditioning in power flow calculation. Here is part of the bus groups being simplified in Italy:

Giugliano & Patria & Levante & Frattamaggiore & S. Maria;

Salamo & Montecorvino;

Valpelline & the four substations nearby; …

The full list is omitted here.

6.5 Electrical parameters calculation

The preliminary network database obtained from the GIS environment only consists of information about line lengths and their topology, but the electrical parameters, including reactance of lines and the power injections at buses, are not calculated yet. In this section these useful data are derived to facilitate power flow calculation in next sections.

This calculation and inputting can be done with either GIS or other general database software. We chose to general database environment (MicroSoft Access) because of its faster speed and excellent interface with other applications. Moreover, the new information inputted in this stage can also be loaded back into GIS database.

6.5.1 Transmission line reactance

The reactance of transmission lines were calculated out by MicroSoft Access Query using this equation: $X=\begin{cases} l*0.31/n_l, & V = 220kV \\ l*0.28/n_l, & V = 380kV \end{cases}$

Where l is the length of this line, and n_l is the number of circuits of this line. For the single circuit 220kV and 380kV lines at 50Hz, the typical reactance are 0.31 ohm/km and 0.28ohm/km [155] respectively.

6.5.2 Generation list

Given the network, we also need the nodal injections for power flow calculation. A 'snapshot' of the whole system (i.e. the scenario consisting of the actual energy

outputs/inputs of all the power plants/substations) is not possible to be obtained due to the commercial sensitivity under the deregulated circumstance. The only way is to make a rough estimation for the model system.

The assumption we used in this section is:

The outputs of power plants are proportional to their installed capacities.

This is not exactly the real case, but it can give a rough image of the power flow trend. The outputs of hydraulic plants are more susceptible to influence from the season in a year or the waterfall conditions. Fortunately thermal power plants (including fossil and nuclear plants) play the major role in UCTE network, and they have more stable energy outputs.

Here is the load curve of Spain in year 2001[156]:
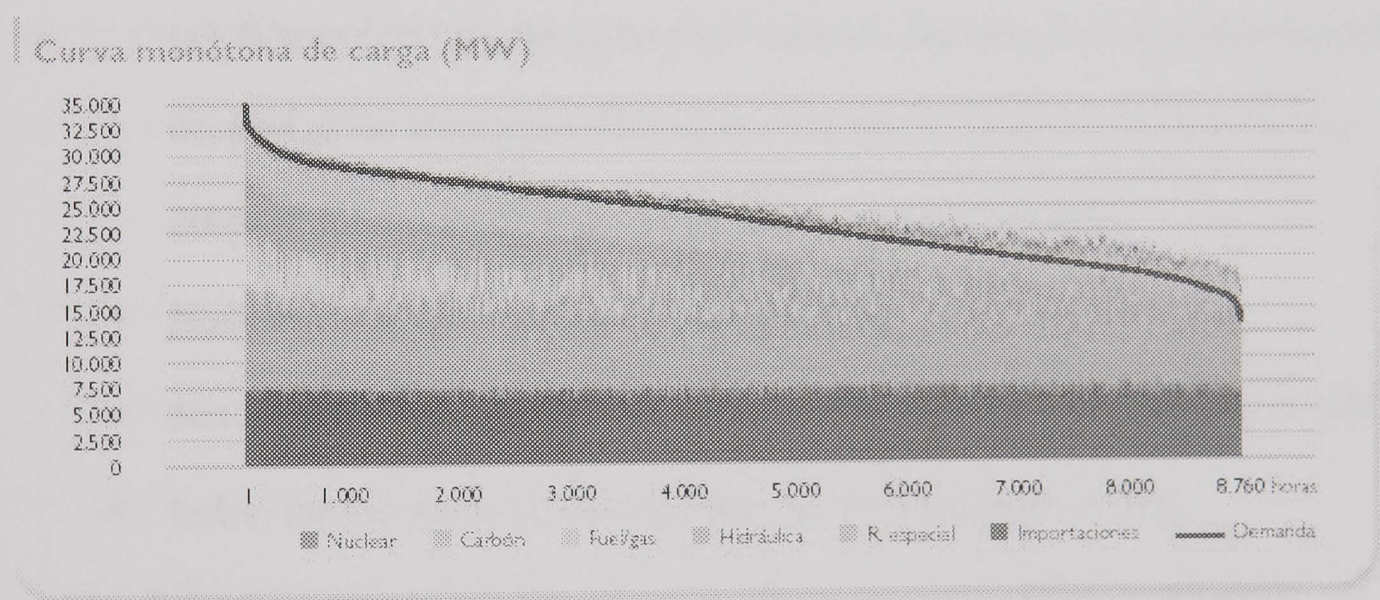
Figure 6-2   Spanish Load Curves

From this curve we can see that the nuclear and coal plants have stable generation all year round (especially nuclear plants). In this sense our assumption can reflect the true scenario to a certain extent.

Each power plant is related with a bus in the UCTE map, and the bus can be retrieved from the GIS database, where the bus record is identified by its ID number. Considering the fact that all the power plants are identified by their names (which are names of their places in most cases) in every generation list, one of the necessary tasks in this section is to relate the names of the plants with the ID of the buses. Putting the

142

names in the database enables us to check and upgrade the database easily in the future. The installed capacities of the plants can be also inputted into the database by the plant names.

The finished bus database has the following fields:

- Type: type of this bus. Possible values are 7, 8 or 9. The meanings are: 7—transformer substations, 8—nuclear/fossil thermal plant, 9—hydraulic plant.

- Capacity: the installed capacity of the power plant. For the substations, this column is left blank. The demand level will be addressed in the next section.

- Place Name: the name of place. For the equivalent bus for a merged bus group (see 6.3.3), this column consists of all the buses, joined by a plus sign (+). Some plants are not given their names in the map, so their capacities are deemed as the lowest possible values that might appear in the map (that is, 200MW for thermal plants and 50MW for hydraulic plants).

- Note: any annotation of this bus description.

- Net capacity: the capacity after merging several local buses (see also 6.3.3).

- Index: the bus name in GIS database, i.e. its ID number in GIS.

The difficulties with obtaining generation lists varied with TSOs in different countries. Data resources are:

Generator lists obtained from some TSOs.

Generator lists available on the websites of some power producers (member links of www.eurelectric.org).

If the above two resources failed in a certain country, or the generator lists are incomplete, a list of European fossil plants (including their installed capacity and type of fuel) (SEI 1990) and a list of nuclear plants [157] are used as the last resort, because these two lists are not up-to-date ones.

Here is part of the table of Spanish buses:

type	capacity	placename	note	net capacity	index
7					1
7					2
8	200			200	3
8	916	abono		916	4
8	470+563	sabon+meirama	merged with load	1033	5
7					6
8	200		merged with load	200	7
8	513	lada		513	8
8	67+254+350	soto de ribera		671	9
7					10
7					11
7					12
7					13
7					14
8	217	pasajes	merged with load	217	15
7					16
7					17
9					18
7					19

Table 6-5   Bus Record (Part)

In the Spanish bus table, the 'capacity' fields of all the type 7 and 9 buses are

blank. The transformer substations (type 7) will be dealt with in the next section. As for

hydraulic power plants (type 9), their capacity list is not available, thus the following

approximation was used for the hydraulic plants, that is: each of the hydraulic plant has

equal capacity. Thus the capacity of each of them can be calculated by:

Capacity=total installed hydro capacity/ number of hydraulic plants, where the total

installed hydro capacity can be found in UCTE year book [153].

Note: In this table only the installed capacity information was stored, instead of the

actual power outputs, which require scaling-up/down based on the total actual

generation. This is because that such original information (i.e. installed capacities) will

not change with power flow pattern. Therefore, based on the same set of original

information, different power flow scenarios can be tested on the network. If the installed

capacity of a plant is changed, we can easily update the network by changing the

corresponding figure in the table. All the scale-up/down work can be easily done by

PowerWorld Simulator.

Besides capacity information, cost curve information is also needed to run OPF

(optimal Power Flow) and get the close-to-reality power flows. Although the true cost

curves are confidential, a typical cost curve can be used for each specific type of generator.

6.5.3 Demand list

Similar to generation buses, the demand buses should also be associated with the names of their places. These names are also stored in the node table. Table 6-6 gives the data of Portugal nodes, including both the generators and the substations.

In this table, the Exceptions exist where the substation list is unavailable for some of the countries. In this case, estimation has to be made on the demand levels.

node	type	input/output
1	9	630
2	7	1306
6	7	1458
7	9	180
5	9	240
3	7	63
4	9	609
9	9	186
10	7	126
12	7	100
14	7	189
15	9	336
11	7	309
13	7	126
16	7	549
17	7	126
18	7	366
21	7	1152
20	8	584
19	7	313
22	7	656
23	7	308
24	8	900
26	8	960

Table 6-6   Demand List (Part)

Determining the demand level was more difficult than determining the generation level, because most of the countries were unable to provide either a 'snapshot' of demands or a capacity list of all the major transformer stations. In such case the assumption described in 6.2.3 has to be applied to get a rough estimation of the demand levels. To do it, the population distribution among all the administrative areas in a

country was supposed to reflect the demand distribution among all the areas. Furthermore, all the substations within a certain area are supposed as having the same demand levels. The total peak-demand of any country can be obtained from UCTE yearbook [153].

6.6 *Power flow calculation using PowerWorld Simulator*

Given the electrical parameters and the topology, PowerWorld Simulator can solve the power flow calculation with its robust and comprehensive engine [158]. In this section, focus is put on how to convert the data from database into a format that PowerWorld can recognise, and then further modifications on the testing network are to be done under PowerWorld Simulator environment.

6.6.1 Converting of Database into IEEE CF file

PowerWorld Simulator can read a variety of power system data formats, including IEEE Common format (CF), PTI Raw Data Format (*.raw) and GE PSLF Format (*.epc).

```
03/11/02JOFORAU200.02000SAUSTRA 100.0 CASE
BUS DATA FOLLOWS            34 ITEMS (HEADER)
 1  1      1 1   2 1.0   -5.0 0.0    0.0   277   0.0    380   0.0  3033.0 -3033.0  0.0    0.0    0
 3  3      1 1   2 1.0   -5.0 0.0    0.0   733   0.0    380   0.0  3033.0 -3033.0  0.0    0.0    0
 4  4      1 1   2 1.0   -5.0 0.0    0.0   200   0.0    380   0.0  3033.0 -3033.0  0.0    0.0    0
17  17     1 1   2 1.0   -5.0 0.0    0.0   137   0.0    380   0.0  3033.0 -3033.0  0.0    0.0    0
22  22     1 1   2 1.0   -5.0 0.0    0.0    0    0.0    380   0.0  3033.0 -3033.0  0.0    0.0    0
...
...
 8   8     1 1   0 1.0  -10.0 624.3636 0.0   0   0.0    380   0.0  0.0    0.0    0.0    0.0    0
10  10     1 1   0 1.0  -10.0 624.3636 0.0   0   0.0    380   0.0  0.0    0.0    0.0    0.0    0
11  11     1 1   0 1.0  -10.0 624.3636 0.0   0   0.0    380   0.0  0.0    0.0    0.0    0.0    0
12  12     1 1   0 1.0  -10.0 624.3636 0.0   0   0.0    380   0.0  0.0    0.0    0.0    0.0    0
...
...
25  25     1 1   0 1.0  -10.0 624.3636 0.0   0   0.0    380   0.0  0.0    0.0    0.0    0.0    0
-999
BRANCH DATA FOLLOWS            39 ITEMS (HEADER)
28 23  1 1 2 00.0    0.0179243 0.0    0  0  0  0  0 0.0  0.0  0.0  0.0  0.0  0.0 0.0
25 28  1 1 2 00.0    0.0050774 0.0    0  0  0  0  0 0.0  0.0  0.0  0.0  0.0  0.0 0.0
31 22  1 1 2 00.0    0.0189716 0.0    0  0  0  0  0 0.0  0.0  0.0  0.0  0.0  0.0 0.0
...
...
13 14  1 1 2 00.0    0.0201785 0.0    0  0  0  0  0 0.0  0.0  0.0  0.0  0.0  0.0 0.0
-999
LOSS ZONES FOLLOWS            1 ITEMS (HEADER)
 1 AUSTRIA
-999
INTERCHANGE DATA FOLLOWS      1 ITEMS (HEADER)            1
 1   2 2       0.0 999.99 A     A
-999
TIE LINES FOLLOW            0 ITEMS (HEADER)
-999
END  OF  DATA
```

The above is part of the *.cf file used to describe Austria network. Each country is allocated a *.cf file for its network description. The countries are interconnected with cross-border transmission lines, which were inputted into PowerWorld manually.

Among all these formats, IEEE CF (file affix *.cf) requires the simplest format descriptions, so it was chosen to input the testing network information. The complete description of IEEE CF text file can be found in [159]. As it doesn't support many of power system features like generator cost curves and multiple generators/loads in the same bus, the IEEE CF files are normally used only for inputting data instead of storing system descriptions. Further modifications on the testing network were done under PowerWorld Simulator after loading the CF file. Therefore, the final network data are stored in PowerWorld format (*.pwd).

Another advantage with PowerWorld is that it provides one-line diagram editor, which allows us edit the network graphically. PowerWorld uses *.pwb file to store the one-line diagram information. That is to say, all the geographic information (including the locations of the buses and the adjacent countries) are stored in *.pwb file.

6.6.2 DC or AC

The major problem with PowerWorld Simulator (version 8.0) is the lack of DC power flow calculation function. In the latest release version 9.0, DC approximation calculation is supported, but majority of the network-creating work was done when the version 9.0 hadn't appeared yet. Thus the AC model was used to calculate the power flows. However, as only the active power flows are to be studied, operation limits like reactive power limits and bus voltages can be relaxed during calculation.

AC calculation takes consideration of the reactive power, which is consumed on the transmission lines (pure reactance in the testing network for the reason of simplicity). The reactive power sources in this network are:

(1) Generators. All the generators are set as 'AVR=on'. That means the terminal voltages of all the generators are kept to their setpoints. Therefore the reactive power outputs will be controlled by AVRs (Automatic Voltage Regulators) instead of their inputted values. Note that by setting AVR=on, the generator is set as a PV node. In our network, all the generators are PV nodes except the only slack generator.

(2) Loads. By setting the reactive component of a load as a negative value, the load is used as a reactive power source. This scheme resembles the local reactive compensation (e.g. capacitor banks in transformer substations). A substation bus with the fixed load is deemed as a PQ node in the power flow calculation.

The basic principles of AC power flow model can be expressed as the following equations:

Suppose $\dot{U}_i = U_i \angle \delta_i$, then for any PV node (e.g. a generator whose AVR=on),

$P_i^s - U_i \sum_j U_j (G_{ij} \cos \delta_{ij} + B_{ij} \sin \delta_{ij}) = \Delta P_i = 0$, where node j is connected with node i through a line/transformer, and the corresponding entry in the Y matrix is

$Y_{ij} = G_{ij} + jB_{ij}$. The P_i^s is the given active power injection at node i.

For any PQ node (e.g. the load bus with fixed real and reactive power injection),

$Q_i^s - U_i \sum_j U_j (G_{ij} \sin \delta_{ij} - B_{ij} \cos \delta_{ij}) = \Delta Q_i = 0$

In the network we are studying, the conductance of each line is 0, thus all the G_{ij} in the Y matrix are 0s, and we can obtain the simplified equations:

$P_i^s - U_i \sum_j U_j B_{ij} \sin \delta_{ij} = 0$ and $Q_i^s + U_i \sum_j U_j B_{ij} \cos \delta_{ij} = 0$. Therefore, by changing the reactive power injection Q_i^s alone, the active power flow along the line from i to j

$P_{ij} = U_i U_j B_{ij} \sin \delta_{ij}$ can also be changed, although the real nodal injection P_i is kept constant.

We can see the influence of reactive power injection on active power flows in this simple three-node example. The parameters of the three transmission lines are:

From bus	To bus	R	X	C
1	2	0	0.2	0
1	3	0	0.4	0
2	3	0	0.4	0

Table 6-7   Transmission Line Parameters

In Figure 6-3 the active power injections at the three buses are set as 200MW, -100MW and -100MW, respectively, and the reactive power at bus 2 and bus 3 are both zero. The resulting active power flows on the network are also shown in this figure.
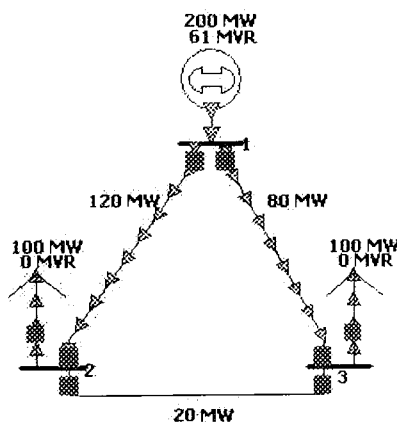
Figure 6-3   3-Bus System (Scenario 1)

Number	PU Volt	Angle (Deg)
1	1	0
2	0.96061	-14.51
3	0.94937	-19.62

Table 6-8   Bus Status (Scenario 1)

The voltage magnitude (in p.u) and power angle in each bus is shown in the above Table 6-8.

Now we change the reactive power injection at bus 3 from 0 to -50MW (local reactive power compensation), and the resulting active power distribution is shown in Figure 6-4:
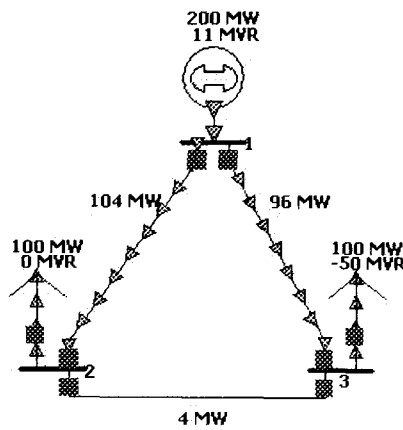
Figure 6-4   3-Bus System (Scenario 2)

The corresponding bus voltages and power angles are:

Number	PU Volt	Angle (Deg)
1	1	0
2	1.00368	-13.68
3	1.07042	-17.68

Table 6-9   Bus Status (Scenario 2)

Thus in AC power flow solution, active power flows are affected by both real and reactive nodal injections. However, as in high-voltage network the power angle difference between both ends of a transmission line is normally small, and the influence of reactive power on active power flows is generally not significant.

6.6.3 Simulation Cases and Results

The test network has 17 areas (each area stands for a country except for BiH and Croatia which were treated as one area) and 28 cross-border interfaces. For the countries outside the UCTE 1st synchronised area while having power exchanges with the member countries, generator/load buses are put at the borders to emulate the power injections/extractions.

The finished testing network needs to be compared with real network on their cross-border power flows in the hope to get similar results. Modifications on the model network can be done only when the differences between the model and real network are discovered and analysed.

The following three real scenarios were used to compare with the model network:

(1)   UCTE 16 January 11am—winter peak load [160]

(2)   UCTE 16 January 3am—winter valley load [160]

150

(3)　　　UCTE 21 August 11am—summer peak load [161]

These three cases give the total demand and generation of each country at the specific time, and power flows on interfaces of neighbouring countries are also given. For each case, the testing network was set to have the same total demand/generation of each country as the real case, and the power flow calculation was carried out on the testing network. The resulting inter-area power flows on all the interfaces were compared with the real ones using the correlation factor. Among all the three scenarios, the 2002 winter peak load scenario was the most important one, because it has the highest demand and thus is related closely with the congestion management study. Generation and demands together with total cross-border power exchanges for the winter peak load 2002 are shown in Figure 6-5. For example 9491/9407 for Switzerland (CH) means that internal generation of Switzerland was 9491MW while internal demand was 9407. The number next to links between any two countries refers to the actual and calculated cross-border flows. For example 2086(-65) for the D-NL link means that the actual cross-border exchange was 2086 MW but the load flow result using the approximate network representation 2086 (-65) for the D-NL link means that the actual cross-border exchange was 2086 MW but the load flow result using the approximate network representation was 2086-65=2021MW. After modifications made on the model network, the correlation factor between real power flow data and the calculated data had satisfactory improvement from 83.7% to 99.28%. The 2002 winter night and summer cases were then used, in order to check whether the model network has the flexibility for different scenarios. The correlation factors for these two comparisons are also as high as 97.34% and 94.72% respectively, and their cross-border power flows were obtained simply by scaling up/down the generation/demand values at all the countries from the values in case 1 to those in case 2 and 3. Thus the model

network is suitable for analysing UCTE network performance in the sense of cross-border power flows.

It should be noted that UCTE data show only total cross-border exchanges between countries without breaking down into individual tie-lines. Hence a link between any two countries, which is shown as a single connection in Figure 6-5, in fact may consist of a number of tie-lines. Sometimes power may even flow in opposite directions in different tie-lines linking the neighbouring countries.

6.6.4 Network modification

Before modification, the power flow results obtained from the model network were already close to the real data in case 1, with the correlation factor between these two sets of data close to 90%. Considering the assumption that all nodal injections are proportional to their installed capacities, which is far from the reality, further modifications can be made to bring the testing network closer to the real system. Possible changes on the model can be:

- Increasing/ decreasing the generation within its generation limit.

- Increasing/ decreasing the load at certain place to make it fit the local population more precisely.

Basically these increase and decrease on the nodal injections were done manually to make the cross-border power flows closer to the real values. When making modifications, care has to be taken to recognise the influence from transit power flows to avoid unnecessary adjustments. In order to illustrate the transit power flows let's have a look at the cross-border power flows in Figure 6-5 (the correlation factor between the real power flows and the calculated values in Figure 6-5 is 90%):

NL
10998/13138
54 (+64.9)
2086 (-65)
90 (+99.1)
PL
22105/20462
335 (-299.1)

162 (-162)
L
739/800
223 (-162)
D
67618/69500
1097 (+156.2)
SK
4583/4025

B
10847/11773
F
76693/69552
1642 (+219.7)

2159 (-609.4)
200 (-635.1)

818 (+226.3)
936 (+426.1)
CZ
9819/9086
368 (+97.3)

CH
9491/9407
1551 (-960.2)
A
8655/8335
892 (-15.8)
1387 (-238.7)

494 (+85.1)
H
5178/5697
50 (+31.2)

2665 (-49.8)
2293 (+38.8)
I
43670/49641
352 (+37.3)
801 (-269.9)

216 (+528)
SV
1795/1690
CR
2068/2572

597 (-236.4)
140 (-273.7)

Figure 6-5   Cross-Border Power Flow

The transit power flows can be easily detected in Figure 6-5. For example, Croatia (CR, on the bottom right of the map) is connected with both Hungary (H) and Slovenia (SV), and the power flow deviations on the interfaces (H→CR and CR→SV) should be –66.1MW and –69.9MW, respectively. From the map we can see that this is mainly caused by the transit power from Hungary to Slovenia. Thus, instead of adjusting the nodal injections within Croatia, we should adjust the injections in Hungary or Slovenia if we want to reduce the power flow deviations from real case.

The adjustment on Slovenia can be done in the following procedure:

(1) Find all the interfaces and their power flow deviations. Slovenia has three interfaces, they are: A→SV (48.2MW), SV→I (-21.9MW) and CRT→SV (-69.9MW).

(2) Find the border buses (Slovenia side) of the interfaces, and change their injections to reduce the power flow deviations.

(3) In order to keep the total generation/demand within Slovenia unchanged, after the adjustments in step 2, the unbalanced generation/demand should be balanced by the other generators or loads in this country.

153

Similar adjustment work can be done for the other countries. As the UCTE network is a highly meshed network, the existence of loop flows make it impossible to achieve 100% similarity by simply adjusting the nodal injections. However, the final correlation factor of 99.28% is sufficient for the cross-border congestion management analysis. Final results and the comparison with real case (case 1, winter peak 2002) are shown in Figure 6-6:
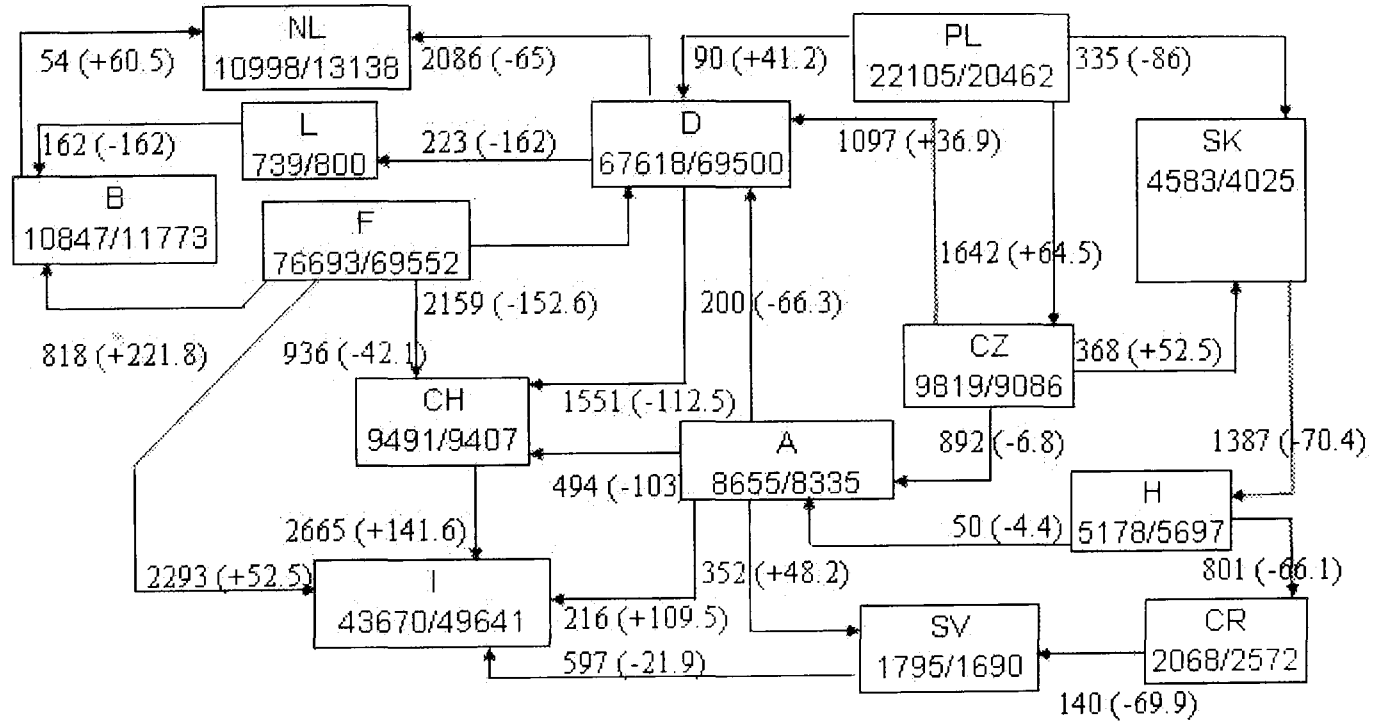
Figure 6-6 Cross-Border Power Flow (Modified)

The "correlation coefficient" is used to check how strong the relationship between the expected power flow values and the calculated power flow values. The correlation coefficient between these two sets of data can be expressed as:

$$\rho_{X,Y} = \frac{Cov(X,Y)}{\sigma_X \cdot \sigma_Y}$$

where $\sigma_X^2 = \frac{1}{n}\sum_i (x_i - \mu_X)^2$ and $\sigma_Y^2 = \frac{1}{n}\sum_i (y_i - \mu_Y)^2$ are average square deviations of the vectors, respectively.

$Cov(X,Y) = \frac{1}{n}\sum_i (x_i - \mu_X) \cdot (y_i - \mu_Y)$ is the covariance of X and Y.

Therefore, $-1 \le \rho_{X,Y} \le 1$, and if $\rho_{X,Y}$ is close to 1, the two sets of data have strong relationship (that is, large values of one set are associated with large values of the other). In the case shown in Figure 6-6, the correlation factor is 99.28%.

The comparison between calculated cross-border power flows and real ones are shown in Figure 6-7:
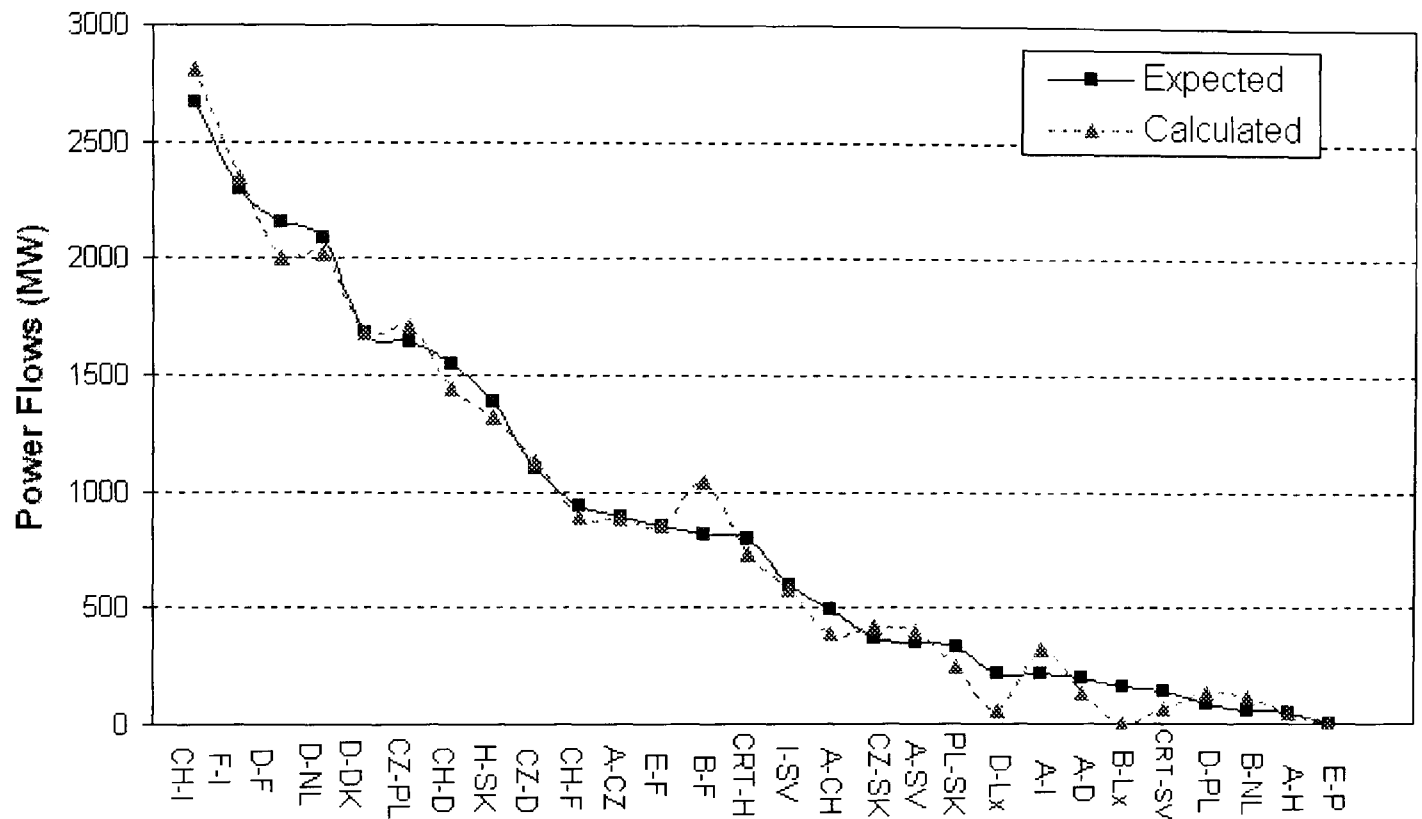
Figure 6-7   **Power Flows on the interfaces**

In order to see how the high correlation factor is obtained, the power flows were listed in the order of magnitudes, and they can be split into two groups as shown in Figure 6-8 and Figure 6-9. Although the calculated values in Figure 6-9 have noticeable discrepancy with the expected value, the values in Figure 6-8 agree with the expected power flows approximately. As the power flows on the interfaces CH-I through B-F are much larger than those on the interfaces CRT-H through A-H, the overall correlation factor is as high as 99.28%.
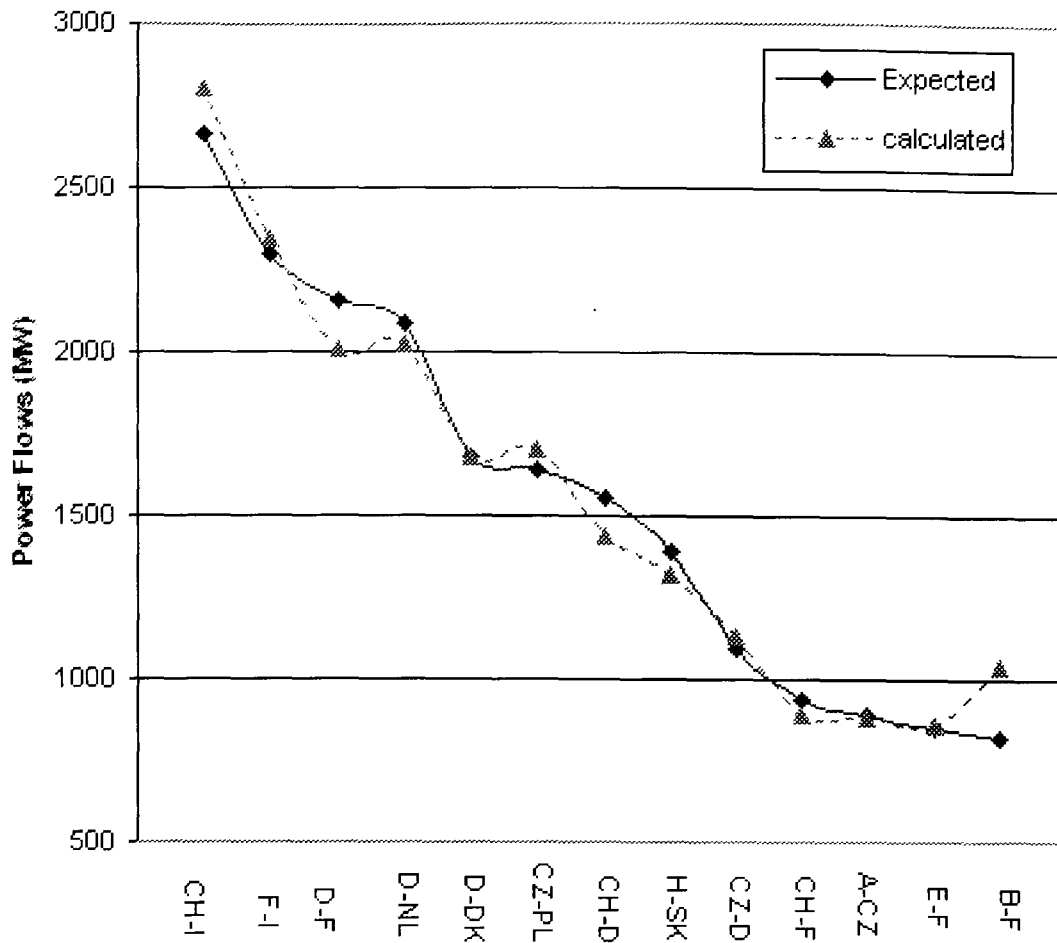
Figure 6-8   **Power Flows on the interfaces CH-I through B-F**
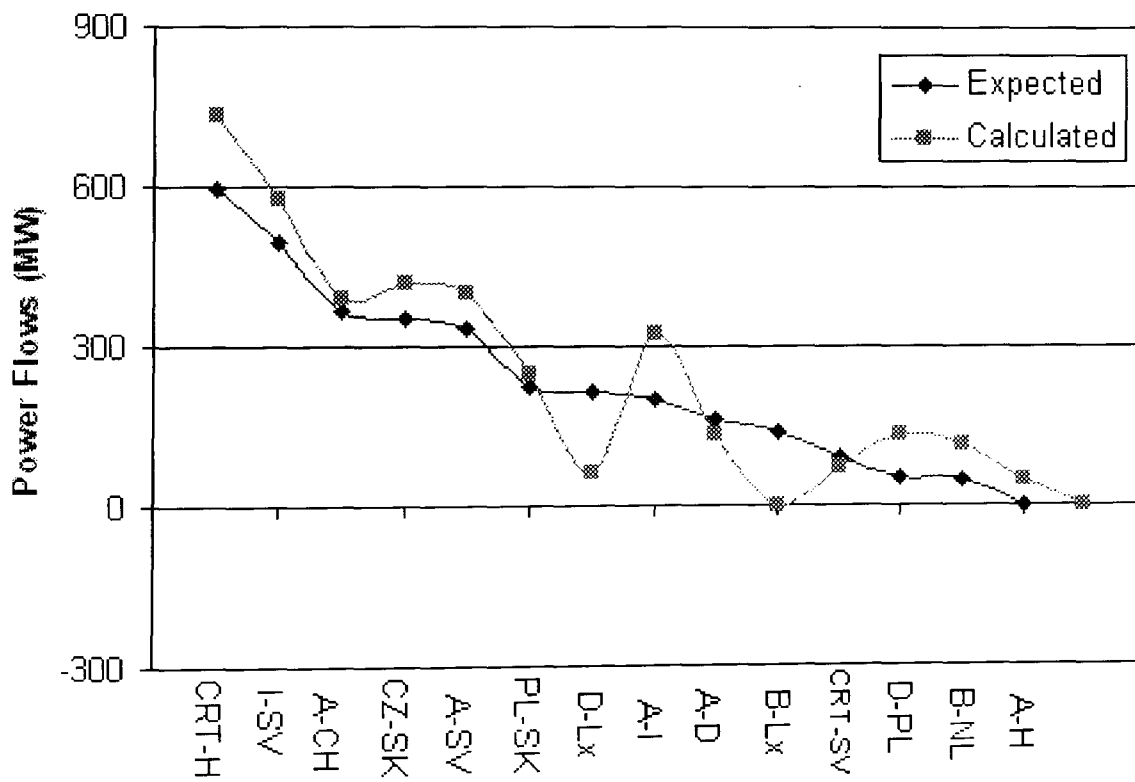
Figure 6-9   **Power Flows on the interfaces CRT-H through A-H**

6.7 Conclusions

The details of how to build up the testing network are given in this chapter. Several

assumptions are used to simplify the approach, while keeping the similarity with the real

network. The format of data in every procedure is given to facilitate further work. All the original data came from public accessible information resources.

In Chapter 7, further validations are done on the testing network to check the similarity with the real UCTE network in the respect of cross-border power flows and PTDFs.

Chapter 7 PTDF Check and TLR Test

7.1 Introduction

In order to test further the applicability of the model network under various dispatch conditions, PTDF (Power Transfer Distribution Factor) check on the cross-border interfaces were done, and the results were compared with the data from real system. Again the comparison was presented in the form of correlation factor, and it is 94.48%. In this chapter the procedure of PTDF check is given, and the results are presented in the form of diagrams. Furthermore, TLR (Transmission Load Relief) tests are done to study the curtailment schemes in case of congestion.

7.2 PTDF check

PTDF factors are used to measure the impacts of a commercial transaction on the physical power flows on the studied transmission lines/interfaces. In congestion management, PTDF factors are very important because their values, together with the amounts of transactions, will determine whether a line will be overload. Due to the phenomenon of loop flows in a meshed network, PTDF factor calculation requires the full network information and thus can only be carried out by the TSOs.

The power flow calculation in Chapter 6 was done by PowerWorld Simulator and was based on the following conditions:

- DC power flow, i.e. only active power flows are studied.

- The OPF (Optimal Power Flow) controls of all the areas were set as 'Off OPF'. That is to say, the nodal power injections were all fixed at the given levels.

These two conditions were used to ensure the simulation of a specific scenario, with the focus on the real power flows on the cross-border tie-lines.

7.2.1 Modification on the model to facilitate PTDF calculation

PowerWorld is able to calculate PTDF factors of transactions between areas, zones and buses. Given the Seller and the Buyer areas/zones, PowerWorld can compute the PTDFs by scaling up/down the output of all generators on AGC in the source/ sink areas in proportion to their relative participation factors [158].

From the user manual we can see two points about PTDF computation by PowerWorld Simulator:

(1) The software obtains PTDF factors by calculating the unit increment scenario and comparing it with the present one. This is computational approximation and might introduce errors. Therefore, even under DC power flows where the PTDFs should be unchanged with the power flows, PowerWorld can still give slightly different values with the operating points.

(2) PowerWorld cannot calculate PTDF factors if the participation factors of all the generators are set as 0 (by default). For PTDFs of transactions between areas or zones, the 'AGC Status' of the related areas/zones should also be set active.

The participation factor is the sensitivity factor of how the real power output of a generator changes with the demand. Only when the generator is available for AGC and the area is on participation factor control can the participation factors take effect.

In this model system, all the participation factors were defined in this way such that they are proportional to the capacities of these units (this is the default setting).

After the above changes were made on the model network, the PowerWorld Simulator is now ready to compute PTDF factors. These values are to be compared with the published ones in the real system, to see their similarity.

The published PTDF values of UCTE network were obtained from European Commission reports [152] and [162]. In order to get the PTDF values, a user can either specify the buyer, seller and the interface through the dialog box provided by PowerWorld, or input commands in the form of script language— a text-based

command line interface to facilitate batch processing in PowerWorld. Script is especially useful when processing large number of similar calculations.

PTDFs in PowerWorld were calculated and exported with the following two commands:

```
CalculatePTDF([AREA i], [AREA j], DC);
SaveData("ThePTDi j.aux", AUX,Interface,
[IntNum,FGPTDF,FGMW,FGLim,IntHasCTG,IntMonDir,FGLimA,FGLimB,FGLimC
], [interfaceelement],);
```

Where the i and j are selling area and buy area, respectively. The command 'SaveData' was used to export the case description in the format of PowerWorld auxiliary file. If the file already exists, PowerWorld will append the new data.

7.2.2 PTDF factors comparison with the real ones

Table 7-1 gives the published[152] and calculated PTDFs of several transmission lines.

	published	calculated	
albertville-piossasco	13	12.51	
Mettlen-lavorgo	10	4.6	
chippis-airolo	5.7	3.49	correlation
lavorgo-roncovalgrande	15	5.41	0.515213

Table 7-1   PTDFs Comparison of Several Lines

Comparison on PTDF factors didn't appear satisfactory, as the correlation coefficient is only 51.52%. This is due to the scarcity of samples. PTDF factors of individual transmission lines are difficult to obtain from public resources, and the above 4 values are all we can get from [152]. As all the 4 values are small (no greater than 15%), any small deviations from them will result in a much lower correlation coefficient.

Extensive searching for additional PTDF factors from public resources is not advisable, because it is time-consuming and not necessary. As our study is focused on the cross-border congestions instead of internal congestions, we can focus on the cross-country interface PTDF factors instead of individual line PTDF factors. It should be

noted that the model network built up in the last chapter is not a replica of the UCTE network in all aspects. Emphasis has been always put on the similarity of cross-border power flows.

The inter-area PTDF factors indicate the incremental distribution factors associated with power transfers between two different areas [158]. These values provide a linearised approximation of how the flows on the interfaces change in response to transaction between the Seller area (source) and the Buyer area (sink). The transaction for which the PTDFs are calculated is modelled by scaling the output of all generators on AGC (Automatic Generation Control) in the source and sink areas in proportion to their relative participation factors. Generators in the source area increase their output, while generators in the sink area decrease their output [158].

Figure 7-1, Figure 7-2 and Figure 7-3 give the PTDF factors (in %) on the cross-border interfaces by the transactions from Belgium to Italy [88], North France to Netherlands and North France to Italy [162], respectively. The published PTDF data are listed on the interconnections followed by the calculated PTDF values in the braces. The correlation factor of the real PTDFs and the calculated PTDFs in Figure 7-1 is 97.20%.
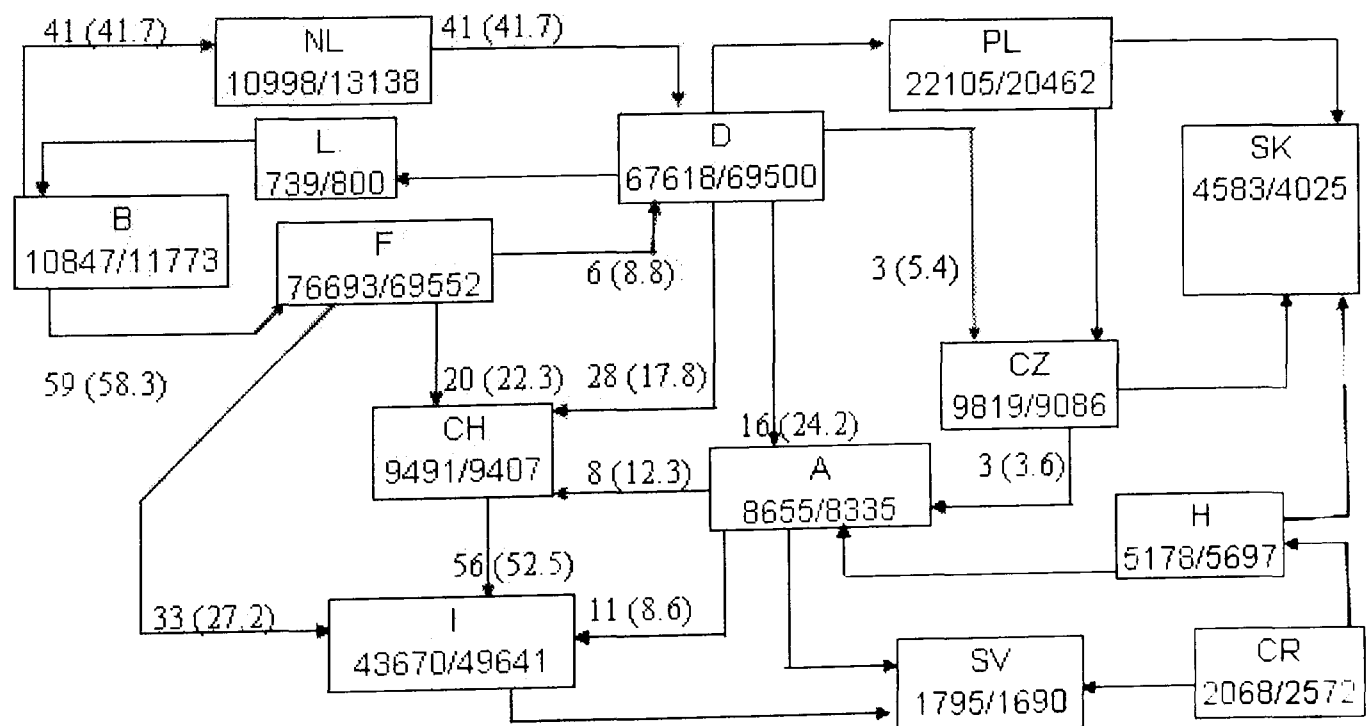
Figure 7-1   PTDFs (%) Comparison for B→I Transaction

The correlation factor in Figure 7-2 (on the next page) is 90.96%.
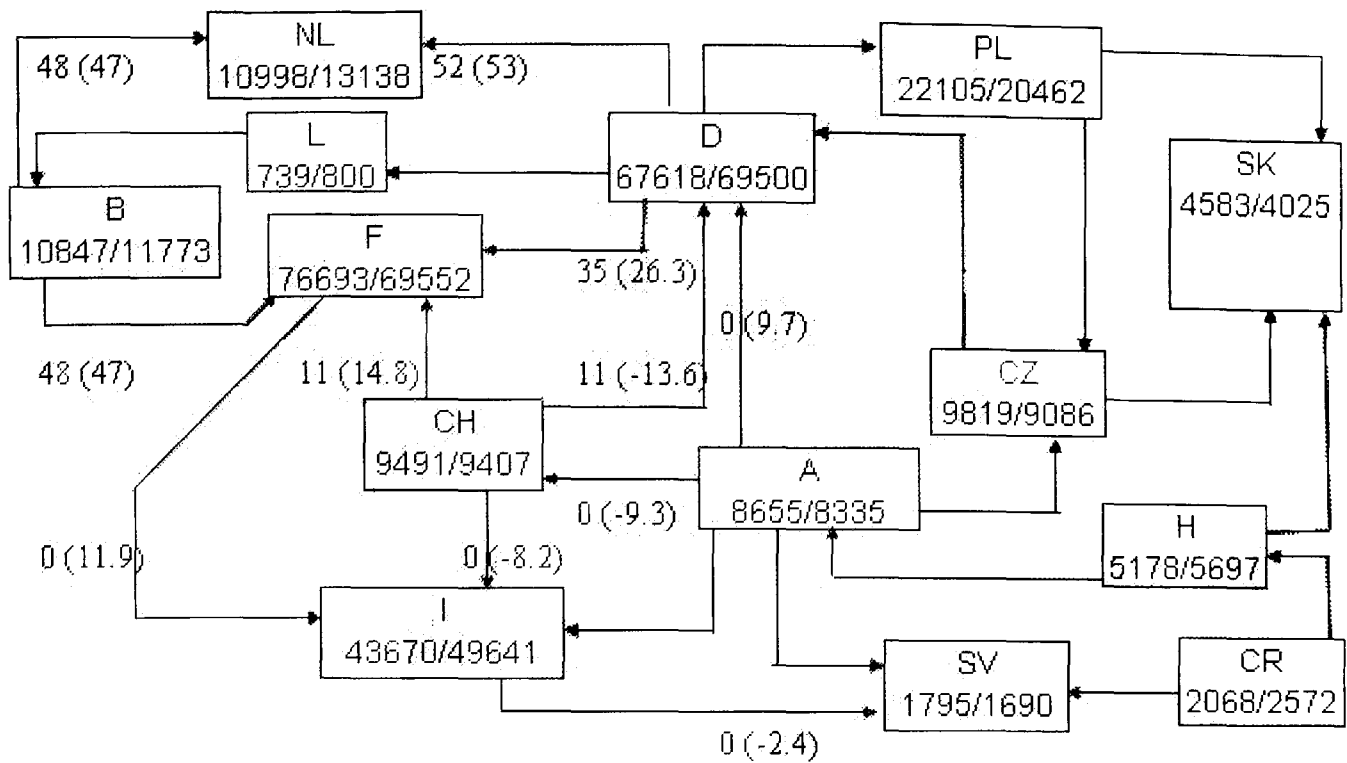
Figure 7-2   **PTDFs (%) Comparison for North France→NL Transaction**

The correlation factor in Figure 7-3 is 94.93%.
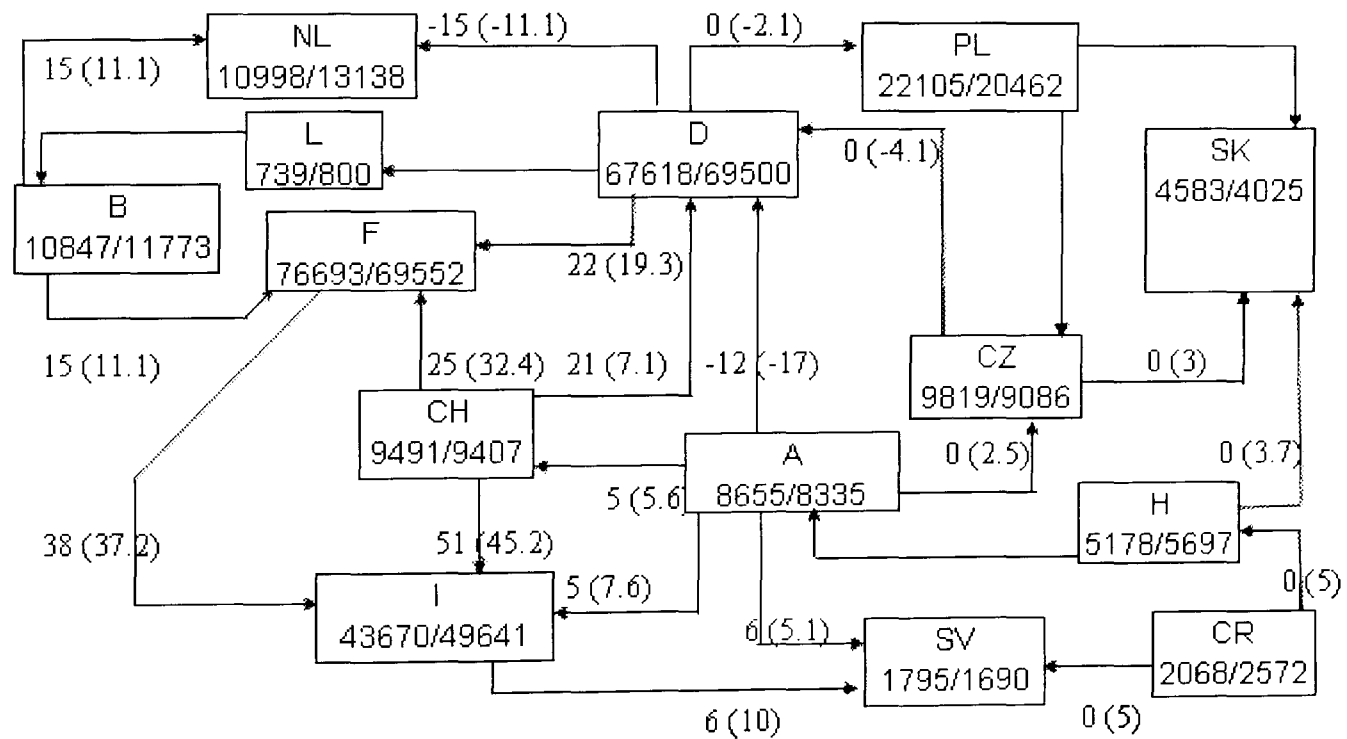
Figure 7-3   **PTDFs (%) Comparison for North France→I Transaction**

From the above three tables we can see that the model network is very similar to real network in the sense of their PTDF values on the cross-border interfaces.

7.3   TLR Test

An interesting test on the model is the TLR test. TLR is used by FERC (the Federal Energy Regulatory Commission) to curtail submitted bilateral transactions if the transmission lines will get congested. Although it is widely criticised as a non market-

based method, FERC insists that it is a necessary method to maintain system security [87]. TLR doesn't require any cost or price information, therefore it is the easiest method to be tested on the model network, which also lacks cost information. The TLR test validates the model network, as the results shows the power flows after TLR curtailments are similar to those in the real world.

7.3.1 TLR algorithm

Suppose two transactions have influence on the congested line, and their PTDF factors (PTDFs) are $\lambda 1$ and $\lambda 2$ respectively (none is greater than 1). We suppose both $\lambda 1$ and $\lambda 2$ are positive. Therefore, in the case of congestion both transactions are to be curtailed. We denote the submitted amounts of transactions as x01+Δx1 and x02+Δx2 respectively, where the Δx1 and Δx2 are the amount to be curtailed, and the x01 and x02 are the transactions after curtailment. Now the TLR problem becomes:

Given the total amounts (x01+Δx1) and (x02+Δx2), given PTDFs $\lambda 1$ and $\lambda 2$, we need to find Δx_1 and Δx_2 to satisfy:

$\lambda_1 \Delta x_1 + \lambda_2 \Delta x_2 = \Delta F$, where the ΔF is overflow on the congested line. And

$\lambda_1 x_{01} + \lambda_2 x_{02} = F_0$, where the F0 is the transmission limit of the line.

We assume $\lambda 1 > \lambda 2$ to facilitate our analysis.

As the two equations are not linear independent, there exists more than one solutions. The question is: how to allocate the overflow to each user, so that fair and economic (small overall curtailment) allocation is achieved?

NERC's TLR rule is one of the answers. Obviously PTDF factors should be taken into consideration in the relief procedure to avoid unnecessary curtailments. Besides, the submitted transaction amounts (i.e. (x0i+Δxi), i=1,...,n where n is the number of transactions to be curtailed) should also be considered in the effort to avoid

opportunistic behaviours from users. Therefore, the share of overflow should be proportional to both the PTDF factor and the transaction amount of the user, that is, $\Delta x_i * \lambda_i = \Delta F (\lambda_i F_i / \sum (\lambda_i F_i))$, where $F_i = (x_{0i} + \Delta x_i) * \lambda_i$ is the share of physical power flow on the flowgate from ith submitted transaction.

7.3.2 TLR curtailment calculation

The TLR scheme is based on commercial transactions, while in the model network, only physical nodal injections were given. Therefore in order to execute the TLR curtailments, transactions should be calculated out first to fit with the physical power flows, then curtailments can be put on the transactions, and the resulting physical power flows can be obtained to check the congestion status on the flowgate.

This procedure consists of the following modules in Figure 7-4:
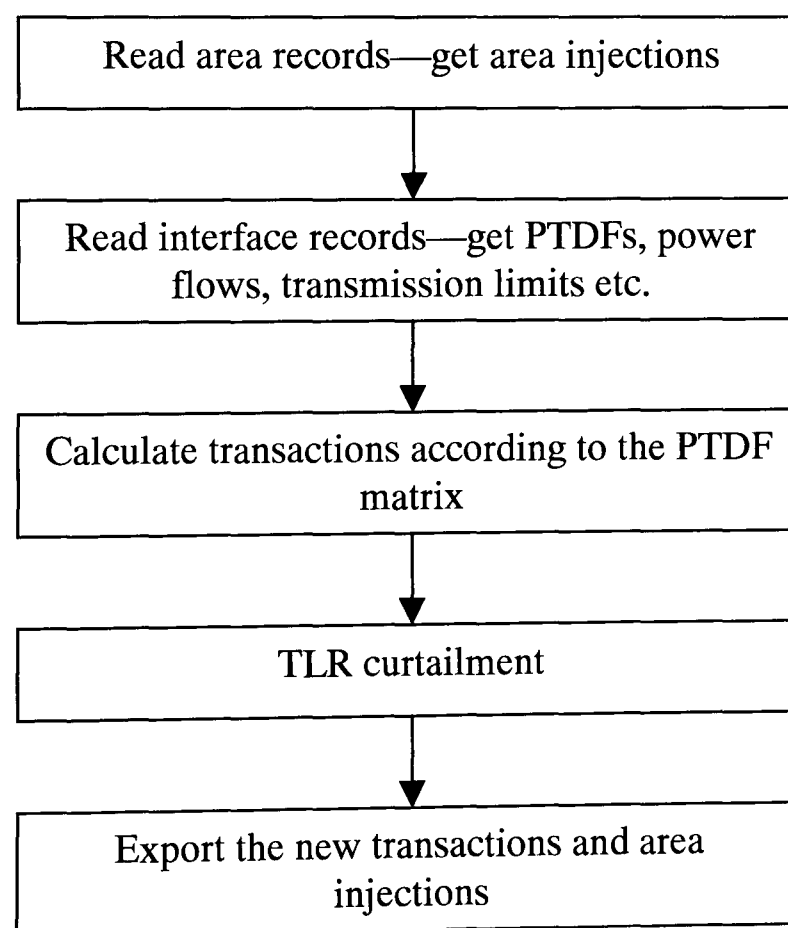
Figure 7-4   TLR Curtailment

The interface being studied in this section is interface 8, that is the one between Switzerland and Italy. According to the EC report [152], this interface is often congested.

7.3.3 Obtain Bilateral Transactions from Physical Power Flows

In the model network, the physical power flows, net area injections and PTDFs were already obtained, but the energy transactions agreed among market participants are unknown to us. In this circumstance we need to make assumption on energy transaction based on the actual power flow information, so that TLR can be carried out.

Suppose the numbers of areas and interfaces in a network are n and m, respectively. The interfaces are physical connections between neighbouring areas. The number m could be either greater/ less than n, or equal to n.
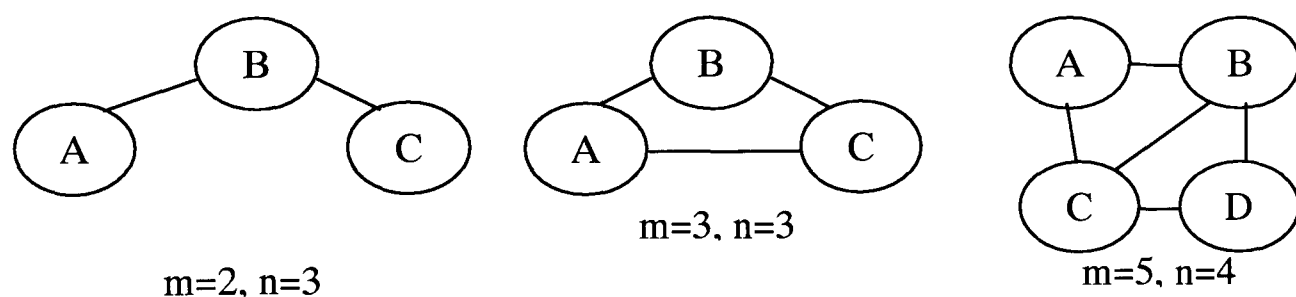
Figure 7-5 **Examples of the Number of Areas and Interfaces**

A network with n nodes/areas can theoretically consist of $C_2^n = \dfrac{n(n-1)}{2!}$ number of transactions. However, this number is unnecessarily large when the number of nodes/areas in a system increases. Suppose the total number of transactions is T, and the task in this section is to find a set of transactions, so that all the physical constraints are met.

Generally the direction of an energy transaction is always from the lower price area to the higher price area. However, considering the high volatility of spot prices, we can arbitrarily specify the directions of transactions, and use positive or negative signs to indicate whether the real directions comply with their designated ones.

The set of transactions in a network should be subject to the following two types of constraints:

- All the transactions starting/ending at a certain area should add up to the net injection of this area. (Losses are ignored. Positive injection stands for generation.)

- The impacts from all the transactions on a specific interface should result in the physical power flow on that interface.

The first set of constraints can be expressed as the following equation:

$$A'_{T,n-1}\mathbf{t}_T = \mathbf{b}_{n-1} \qquad (7.1)$$

Where $A_{T,n-1}$ is the incidence matrix indicating the relations between areas and

transactions. If the lth transaction starts at area i and ends at area j, the elements a_{li} and

a_{lj} in A matrix are 1 and -1 respectively. In this way we can create a $T \times n$ incidence

matrix which is singular. By removing any column in this singular matrix we can obtain

the $A_{T,n-1}$ in equation (7.1).

$\mathbf{t}_T = [t_1\ t_2\ \dots\ t_T]'$ is the column vector indicating the amount of each transaction.

$\mathbf{b}_{n-1} = [b_1\ b_2\ \dots\ b_{n-1}]'$ is the column vector indicating the injection of each area.

T must be no less than (n-1) to satisfy this set of constraints. The minimum number (n-

1) occurs when there is a 'chain' of transactions from the first area to the nth area, i.e.,

T_{12}, T_{23}, T_{34},..., $T_{(n-1,n)}$.

The second set of constraints can be expressed as the following equation:

$$\mathbf{PTDF}'_{T,m}\mathbf{t}_T = \mathbf{l}_m \qquad (7.2)$$

Where $\mathbf{PTDF}_{T,m} = \begin{bmatrix} \mathbf{ptdf}_{1,1:m} \\ \mathbf{ptdf}_{2,1:m} \\ \vdots \\ \mathbf{ptdf}_{T,1:m} \end{bmatrix}$, and $\mathbf{ptdf}_{1,1:m}$ stands for the PTDF factors on all the m

interfaces on by the first transaction, T is the total number of transactions. Therefore, T

must be no less than m in order to get a full expression of interface power flows.

$\mathbf{I}_m = [l_1\ l_2\ ...\ l_m]'$ is the column vector indicating the physical power flows on all the interfaces.

The number of independent equations among all the two sets determines the smallest possible value of T.

A transaction between distant areas can be split into a set of transactions between neighbouring areas. Take the first network in Figure 1 as an example, the energy transaction from area A to area C (T_{AC}) can be accomplished with a transaction from area A to B, and then one from area B to area C, both at the same amount as specified in T_{AC}, i.e. $T_{AC}=T_{AB}=T_{BC}$. In our study, both the distant transactions and the neighbouring transactions were studied.

Interface Code	Interface Name	Interface Limit (MW)	Power Flow Before TLR (MW)	Power Flow Before TLR (%)	Power Flow After TLR (MW)	Power Flow After TLR (%)
1	E-P	2275	0.4	0.02	0.4	0.02
2	E-F	2954	-856.7	-29	-856.7	-29
3	F-I	3413	2347.3	68.78	2255.6	66.09
4	B-F	2828	-1057.1	-37.38	-1136.2	-40.18
5	B-Lx	716	0	0	0	0
6	B-NL	5429	131.8	2.43	211	3.89
7	CH-F	7126	-876.2	-12.3	-837.4	-11.75
8	CH-I	2572	2800.5	108.88	2565.2	99.74
9	CH-D	1580	-1438.5	-91.05	-1342.5	-84.97
10	I-SV	2042	-579.2	-28.36	-521.7	-25.55
11	D-F	3436	-2004.5	-58.34	-2078.7	-60.5
12	D-Lx	2676	61	2.28	61	2.28
13	D-NL	12892	2008.1	15.58	1929	14.96
14	D-DK	3620	-1681.9	-46.46	-1250.2	-34.54
15	D-PL	6324	-129.9	-2.05	-148.8	-2.35
16	A-CH	6362	402.5	6.33	323.9	5.09
17	A-I	257	325.6	93.04	278.1	79.44
18	A-D	11215	118.9	1.06	248.6	2.22
19	A-CZ	2462	-884.2	-35.91	-854.9	-34.72
20	A-H	4448	-22.8	-0.51	-27.9	-0.63
21	A-SV	2151	379.6	17.65	346.1	16.09
22	CZ-D	6576	1134.3	17.25	1168.3	17.77
23	CZ-PL	2760	-1709.8	-61.95	-1688.8	-61.19
24	CZ-SK	4190	424.4	10.13	398.6	9.51
25	PL-SK	5736	247	4.31	237.7	4.14
26	H-SK	1660	-1318.5	-79.43	-1283.4	-77.32
27	CRT-H	1246	-759.6	-60.96	-719.9	-57.78
28	CRT-SV	7191	94.8	1.32	65.5	0.91

Table 7-2   **Effect of TLR—Interface Power Flows (in MW and in %) before and after TLR Curtailments**

All the independent equity constraints must be satisfied by the transaction vector $\mathbf{t}_T$, Therefore we can obtain the minimum value of T, T$\geq$max (m,n-1).

PowerWorld uses an approximation to calculate out the PTDF factors. Thus we might get very small PTDF factors in some entries instead of the actual 0 values. This results in ill-conditioning when calculating the commercial transactions.

In order to avoid this ill-conditioning, filters were used for the PTDF factors with the value of 0.5% and 5%, respectively. If the value of a certain entry is lower than the filter value (0.5% or 5% as the filter being used), it is set to 0 when calculating the transactions.

The TLR curtailment is seen as a non market-based method to prevent congestions. In this case, 39 transactions are used, and the effect of TLR curtailments can be seen in Table 7-2.

From Table 7-2 we can see, the TLR methodology was tested successfully on the testing network. Assuming there are 39 inter-country transactions altogether, without TLR the power flows on the interfaces will probably exceed the limit, as we can see on the 8th interface (Switzerland to Italy) in the fourth and fifth columns in Table 7-2. After the TLR curtailment, the resulting power flows are shown in the sixth and seventh columns, and the interface between Switzerland and Italy is now operating within its limit.

Chapter 8 Conclusions and Further Work

As power systems have special reliability requirements and power flows follow Kirchoff's laws, the use of a transmission network must be administrated by the system operator. The system operator might have to exert limits on the power flows passing through some network components to ensure the system operation security. In the case that power flows are limited by the scarce transmission capacities of those components, the components are said to be congested. As congestions reduce overall efficiency by restraining electricity from cheap generators going to the demand areas, congestion management is an important topic to study.

In electricity markets, the electricity prices are expected to direct producers and customers into short-term efficient operation as well as long-run investments. The electricity prices can be deduced from a constrained optimal dispatch model, as described in Chapter 1. The resulting nodal marginal price contains price elements in association with the network losses, electricity generations and transmission congestions. Therefore, the short-term marginal transmission price is the price difference between the source and destination nodes, as explained in section 1.3.4. In a power system, the congestion rent often plays an important role in the overall transmission charge.

Due to system uncertainties, real-time spot prices are highly volatile. Transmission rights can be used to hedge the price volatility and lead to optimal dispatch, and provide the incentives for system expansion in the long run (section 1.4). Transmission rights entitle the right holders to transfer electricity through the network even when congestion occurs. There are two major forms of transmission rights: the nodal-price-based rights proposed by Hogan [12], and the link-based rights proposed by Chao and Peck [17]. Each of them has its advantages and downsides, but they both conform to optimal economic pricing, and thus lead to the same optimal results if under perfect competition.

The congestion management across several different control areas under different system operators, namely the cross-border congestion management, gives rise to more challenges because close coordination among the system operators is required to achieve the overall efficiency while the data sharing should be restricted at the same time to ensure fair commercial operation.

The European interconnected network has to accommodate various market mechanisms in different countries, and cross-border power trade and congestion management are among the main topics under discussions (section 2.1). Market-based congestion management methods are favoured over non market-based ones although the latter are still necessary in the current situation to ensure system security. In Chapter 2, several major market-based cross-border congestion management methods, including implicit auctioning, explicit auctioning/market splitting, counter-trade and re-dispatch were studied. Close coordination among the neighbouring system operators and markets are required for all the methods. Due to the diversity of member countries, a uniform method is unlikely to be adopted widely throughout the system because it might lead to distortions under different circumstances. For example, one of the reasons that the Nord Pool can apply the market-splitting is that because PXs (power exchanges) covers all the related areas. This is unlikely to be applied throughout European area.

In contrast to Europe, the US is likely to follow a set of guidelines towards the standard market design (SMD) across all the states, although regional flexibilities are allowed. This uniform framework is mainly based on the successful PJM market rules, and it is aimed at solving the inconsistent rules in different states to facilitate cross-border trade and lead to a healthier nationwide electricity market.

The locational marginal pricing (LMP) requires that every trader must pay for the congestion, even it didn't cause the congestion. Under the merchandise surplus (MS) allocation suggested in Chapter 3, initial payments from traders are identical to those

under the LMP method, but the way the system operator (SO) deals with the MS is different. The SO refunds MS to all the traders according to their allocated share of usage of the congested lines. A trader is able to use its allocated share without paying for the related congestion fee —the congestion rent it paid to the SO will be fully refunded.

This MS allocation method gives pure financial rights to users without capacity scheduling, therefore users cannot withhold such rights in the attempt to prevent other participants' use of the transmission grid. In order to increasing market liquidity, the rights may be tradable in a secondary market once allocated by the SO.

Under Hogan's or Chao-Peck's transmission right mechanism, market participants must purchase in advance the transmission rights on the likely to be congested lines. Information inadequacy and the system operation uncertainties make it difficult to achieve the most effective allocation of rights in advance, so there is usually MS leftover. The method suggested in Chapter 3 can supplement the existing transmission rights and allocate 100% of transmission capacities to users, ensuring that the leftover MS be totally refunded to the users. Moreover, such allocation is based on congestion data which reflect the influences on the power flows (use of transmission network) from transmission users. The leftover MS is therefore shared by those who contributed to it. Thus the sharing is fair, and no windfall benefits are gained by other users who did not contribute towards congestion fees.

Under the MS allocation method, the calculation of congested line usages is not too complicated. Besides, by setting correct capacity shares, users can be correctly signalled to use the power grid in the most efficient way. Users will pay a full marginal congestion costs for their increase in use of the congested line, and off-peak utilisation of the network is encouraged.

For cross-border congestion management, the decomposed optimal power flow (OPF) calculation is a challenging topic. Cadwalader and Hogan's method [125] takes the close relation between constraints and their shadow prices into consideration, and PTDF factors are used to help 'pricing out' the exterior congestions. A sub-gradient algorithm is used to solve the primal-dual problem. This method is easy to understand, but it does not have good convergence performance if appropriate estimation of the parameters is not given. Besides, it requires large amount of information exchange if used in nodal pricing model. It works fine in some examples [125] but require that the dualised constraints are convex [47]. Kim and Baldick [126] gave an innovative idea to decompose the interconnected system by putting a pair of 'dummy buses' in the middle of each tie line. This gives a good start for a number of later proposals, including the method suggested in this thesis. This method uses a series of sub-problems, and the parameters need to be tuned depending on the problems [137]. Aguado [127] suggested a barrier function method in which the enlarged KKT conditions are used. This makes the size of the unknown variables much bigger than an ordinary Newton OPF problem. Xie [128] proposed a barrier function method to solve the dynamic OPF problem, where the intertemporary coupling constraints are decomposed in the Newton search. However, the coordination among the decomposed problems is still a problem as the Hessian matrix contains full information of the sub-systems.

To overcome some of these problems, a decomposition method was proposed in section 4.4. This method is based on the analysis of minimum number of variables to determine the influence from neighbouring areas, and it is applied on an improved barrier function method proposed in section 4.5.3. Unlike sub-gradient methods, this method doesn't require a series of OPF problems whose parameters are obtained from the result of the last OPF. Once the result converges it is the final global solution. Therefore the inter-area OPF calculation is much faster than those sub-gradient

methods. Besides, interior point methods are well known for their fast convergence performance and mathematical robustness.

A simple 7-bus system is used in Chapter 5 to test the above three methods. The test results proved the theoretical analysis in Chapter 4 and suggested that the proposed method is quick in convergence.

A model network of decent size and appropriate connection structure is necessary for simulation of congestion management methods. As true networks are not available to the public due to the commercial significance of the technical data, an approximate network is build up in Chapter 6 basing on public-accessible information. This model inherits the major characteristics of the original UCTE 1st synchronous area network, and the cross-border power flows were compared against the real ones. The comparison proved the similarities between the model and the real networks, and therefore the cross-border congestion management methods can be tested on the model to see the resulting power flows and financial settlements.

The model network obtained in Chapter 6 bears similarities with the UCTE network, and the generation and demand levels are based on a typical UCTE network scenario. As the operations of a network always change, and the power injections and extractions can be very different from this specific scenario, so the model network needs further validations to see its applicability under various dispatch conditions. In Chapter 7 the cross-border PTDF factors are calculated and compared with the real data. Good comparison was obtained with the correlation factor between these two sets of PTDFs being over 90%. This means that cross-border power flows calculated from the model will be similar to the real power flows even when the dispatch changes.

Further work

The proposed barrier function method requires that the objective function and constraints are second differentiable. How to apply this algorithm on OPF problems

with discrete constraints, like tap-changing limits and unit-commitment model, needs future research.

Due to the mechanism of IPM methods, the speed of converge is fast at the early stage but slower near optimal solution, because the changes in the values of the variables are small. Therefore, in order to reduce the computational effort, partial re-linearisation of the KKT conditions may be applied in the later stage of the search, as suggested in [132]. However, how to choose the part of variables for re-linearisation needs further study.

The proposed congestion management method as well as the OPF calculation method worked well on the examples in this thesis. However, further study is needed to extend them onto more complicated network, like the testing model network built in Chapter 6.

This thesis was mainly focused on cross-border power flow calculation, congestion management methods and testing model. Although a benchmark model can help to check proposed methods, it is not enough to validate a method theoretically. In the future, a general mathematical model is needed which can quantify the influences on market performances from market rule designs. This model should ideally be able to be compatible with various market mechanisms as cross-border congestion management generally involves various mechanisms.

Appendix Barrier Function Method Applied in the Decomposed OPF

1 The objective function

The objective function can be total fuel cost or system active power losses. In a pool model, the total social welfare/cost can be obtained from the market participants' bids and act as the objective function.

The Objective functions are normally expressed in a quadratic form. If the 'minimum social cost' objective is used, it can be expressed as:

$$\min \sum_{a=1}^{A} \left(\sum_{i=1}^{n_{ga}} C_i(p_{gi}) - \sum_{j=1}^{n_{da}} B(p_{dj}) \right) \qquad \text{(A.1) for } \forall a = 1, \cdots, A \text{ as the area number.}$$

where n_{ga} and n_{da} are the numbers of generators and demands in area a, respectively. p_{gi} is the output of ith generator, and it is subject to the supply-price elasticity constraints:

$$p_{gi} = \varsigma_i (\rho_i - \rho_{gi\,\min}) \qquad \text{(A.2)}$$

Similarly, the demand level of p_{dj} is subject to the demand-price elasticity constraint:

$$p_{dj} = p_{dj\,\max} - \varepsilon_j \rho_j \text{ for } \forall i = a_1, \cdots, a_{n_a} \qquad \text{(A.3)}$$

Here the ρ_i and ρ_j are the nodal prices, ς_i and ε_j are the supply and demand price elasticity factors. $\rho_{gi\,\min}$ is the minimum price at which the ith generator produce electricity, and $p_{dj\,\max}$ is the maximum demand of jth user.

Generally the production bids curves are not continuous [9]. One way to treat this discontinuity is replacing these vertical edges with very steep but continuous slopes[9]. The total bid curve is obtained by putting together all the bid curves from market participants, and this will also help the continuity.

In the real world, the short-term demand-price elasticity is normally small, i.e. users are not very sensitive to the price changes. Therefore in a simplified model, the demands

can be treated as constant. However, taking customer response into consideration can reduce the effect of those discontinuities and help determine market clearing price[9].

2 Equality constraints

In a constrained optimisation problem, the equality constraints, together with the binding inequality constraints (when the inequality constraints are binding they become equality constraints too), constitute the border of the feasible region for the solution set. The constraints can contain variables that appear in the cost function (decision variables) and variables only appear in the constraints (dependent variables). In the DC OPF problem, the most common equality constraints are the power balance constraints for all the buses. Considering the assumptions in DC power flow, the power balance constraints can be expressed as:

For those buses with generators attached,

$$p_{gi} - p_{di} - \sum_{j=1}^{n_{\delta_a}} B_{ij} \sin(\delta_i - \delta_j) = 0 \text{ for } \forall i = a_1, \cdots, a_{n_{ga}} \qquad (A.4)$$

where p_{gi}: the generation at bus i

p_{di}: the load at bus i

B_{ij}: elements in the network admittance matrix.

The sinusoid item cannot be further simplified to $\delta_i - \delta_j$, because in modern transmission systems this value can be even greater than $\dfrac{\pi}{2}$ if proper voltage support is given in the middle of the transmission line. Nonlinearity of $\sin(\delta_i - \delta_j)$ has to be retained.

For those buses without generators attached,

$$p_{di} + \sum_{j=1}^{n_{\delta_a}} B_{ij} \sin(\delta_i - \delta_j) = 0 \text{ for } \forall i = a_1, \cdots, a_{n_{Da}} \qquad (A.5)$$

176

If line losses are taken into consideration, they can be modelled as the additional loads at both ends of a line:

$P_{dli} = L_{ij}\left(1 - \cos\left(\delta_i - \delta_j\right)\right)$, where the L_{ij} is called loss coefficient of Line ij,

$$L_{ij} = \frac{r_{ij}}{r_{ij}^2 + x_{ij}^2}$$

In the full AC OPF problem, the real and reactive power balance can be expressed as:

$$p_{gi} - p_{di} - V_i \sum_{j=1}^{n_{\delta_a}} V_j \left|Y_{ij}\right| \cos\left(\delta_i - \delta_j - \theta_{ij}\right) \qquad (A.6)$$

and $q_{gi} - q_{di} - V_i \sum_{j=1}^{n_{\delta_a}} V_j \left|Y_{ij}\right| \sin\left(\delta_i - \delta_j - \theta_{ij}\right) \qquad (A.7)$

where V_i, V_j: the voltage magnitudes at bus i and j, respectively

$\left|Y_{ij}\right|$: magnitude of the complex admittance matrix element.

θ_{ij}: the phase angle of the complex admittance matrix element.

p_{di} and q_{di}: the active and reactive load at bus i. They are subject to power factor constraint.

3 Inequality constraints

Generation limit: $p_{gi\,min} \le p_{gi} \le p_{gi\,max}$ for $\forall i = a_1, \cdots, a_{n_a}$ (A.8)

Load curtailment limit: $p_{dim\,in} \le p_{di} \le p_{dim\,ax}$ for $\forall i = a_1, \cdots, a_{n_a}$ (A.9)

Transmission capacity limit: $B_{ij} \cdot \left|\sin(\delta_i - \delta_j)\right| \le L_{i-j\,max}$ for $\forall i, j = a_1, \cdots a_{n_\delta}$, and the

line starting from node i to j is numbered as k, $\forall k = 1, \cdots, m_a$ (A.10)

The m_a is the number of transmission lines in system a.

For AC power flow problem, several more constraints are normally used [142]:

Reactive power limit: $q_{i\,min} \le q_i \le q_{i\,max}$ for $\forall i = a_1, \cdots, a_{n\delta_a}$ (A.11)

Bus voltage limit: $V_{i\,min} \le V_i \le V_{i\,max}$ for $\forall i = a_1, \cdots, a_{n\delta_a}$ (A.12)

Some other technique constraints can be approximately converted to line flow

constraints [10]. For example, the voltage constraints can be converted to interface

active power flow limits [163], that is to determine under a fixed load demand, how

much active power can flow through the interface lines without violating the voltage

stability.

The decision variables are the active generator outputs and loads. Because of the

inclusion of customer response to prices under market environment, the loads become

an important control on OPF [3].

4 Mathematical model of the barrier function method

Given the problem described in section 4.5.1, and given the following notations:

$$\nabla L = \left(\frac{\partial L}{\partial x}\right)^T = \left[\frac{\partial L}{\partial x_j}\right]^T \qquad (A.13)$$

$$\nabla g = \left(\frac{\partial g}{\partial x}\right)^T = \left[\frac{\partial g_i}{\partial x_j}\right]^T \qquad (A.14)$$

$$\nabla h = \left(\frac{\partial h}{\partial x}\right)^T = \left[\frac{\partial h_i}{\partial x_j}\right]^T \qquad (A.15)$$

$$\nabla^2 f = \left[\frac{\partial^2 f}{\partial x_i \partial x_j}\right], \ \nabla^2 g_k = \left[\frac{\partial^2 g_k}{\partial x_i \partial x_j}\right] \ \text{and} \ \nabla^2 h_k = \left[\frac{\partial^2 h_k}{\partial x_i \partial x_j}\right] \qquad (A.16)$$

$$\nabla L = \nabla f + (\nabla g)\lambda + (\nabla h)z = L(x, \lambda, z) = 0 \qquad (A.17)$$

let S and Z be the diagonal matrices that contain the elements of the vectors s and z,

respectively. The optimality conditions with respect to s are:

$$-S^{-1}u + Z = 0 \qquad (A.18)$$

5 Reduced-size Newton function

In order to avoid ill-conditioning when some of the slack variables approach 0 because

of the binding constraints, re-write the condition (A.18) as:

$$SZ = u \qquad (A.19)$$

And its increment equations are:

$$(S + \Delta S)(Z + \Delta Z) = u \quad \text{u is the penalty vector} \qquad \text{(A.20)}$$

By neglecting the terms $\Delta S \Delta Z$ we obtain the increment of the dual variables:

$$\Delta z = S^{-1}u - z - S^{-1}\Delta S z \qquad \text{(A.21)}$$

Noticing the fact that $\Delta S z = Z \Delta s \qquad \text{(A.22)}$

$$\Delta z = S^{-1}u - z - S^{-1}Z\Delta s \qquad \text{(A.23)}$$

Taylor expansion of h(x)+s=D:

$$\nabla h^T \Delta x + \Delta s = D - h - s = d_1 \rightarrow \Delta s = d_1 - \nabla h^T \Delta x \qquad \text{(A.24)}$$

$$\Delta z = S^{-1}(u - Zd_1) - z + S^{-1}Z\nabla h^T \Delta x \qquad \text{(A.25)}$$

The increment equation of ∇L : $(\nabla^2 L)_{aug} = \nabla L + H\Delta x + \nabla g \Delta \lambda + \nabla h \Delta z \qquad \text{(A.26)}$

where $H = \nabla^2 f + \sum_{k=1}^{p} \lambda_k \nabla^2 g_k + \sum_{j=1}^{m} z_j \nabla^2 h_j \qquad \text{(A.27)}$

We can simply write: $(\nabla^2 L)_{aug} = A\Delta x + \nabla g \nabla \lambda + b = 0 \qquad \text{(A.28)}$

where $A = H + \nabla h(S^{-1}Z)\nabla h^T$ is a block diagonal matrix. $\qquad \text{(A.29)}$

and $b = \nabla L + \nabla h(S^{-1}(u - Zd_1) - z) \qquad \text{(A.30)}$

The linearised equations of the equality constraints are:

$$g + \nabla g^T \Delta x = 0 \qquad \text{(A.31)}$$

Combination of the two equations makes:

$$\begin{bmatrix} A & \nabla g \\ \nabla g^T & 0 \end{bmatrix} \begin{bmatrix} \Delta x \\ \Delta \lambda \end{bmatrix} = -\begin{bmatrix} b \\ g \end{bmatrix} \qquad \text{(A.32)}$$

the (n+p) symmetric square matrix on the left can be easily inverted even for large n+p, where the numbers of primal variables and the dual variables for the equality constraints are n and p, respectively.

Each component of u may be chosen differently to achieve the discriminative penalty. If there is no preference, one may choose the uniform penalty scheme.

6 Inter-area coordination

Suppose the coupling constraints among the sub-areas are expressed as:

$$\mathbf{M}\mathbf{y} = 0 \qquad\qquad\qquad\text{(A.33)}$$

where $\mathbf{y}$ is a vector containing variables in other systems. Also suppose the Lagrangian multipliers corresponding to the constraints can be expressed as a vector $\boldsymbol{\sigma}$, then these constraints also appear in the Hessian matrices. Re-arrange Hessian matrices so that the coupling constraints are the last part of the Newton variables, we can get:

$$
\begin{bmatrix}
A_1^k & 0 & 0 & \Gamma_1 \\
0 & \ddots & 0 & \vdots \\
0 & 0 & A_A^k & \Gamma_A \\
\Gamma_1^T & \cdots & \Gamma_A^T & 0
\end{bmatrix}
\begin{bmatrix}
\Delta\alpha_1^k \\
\vdots \\
\Delta\alpha_A^k \\
\Delta\sigma^k
\end{bmatrix}
=
\begin{bmatrix}
\beta_1^k \\
\vdots \\
\beta_A^k \\
q^k
\end{bmatrix}
\qquad\text{(A.34)}
$$

Where the Γ_1 through Γ_A are highly sparse constant matrices. For the 1st control area, the following equations hold:

$$A_1^k \Delta\alpha_1^k + \Gamma_1 \Delta\sigma^k = \beta_1^k \qquad\qquad\text{(A.35)}$$

This set of equations can be written as the block matrices like:

$$
\begin{bmatrix}
X & 0 & X \\
0 & X & X \\
X & X & 0
\end{bmatrix}
\cdot
\begin{bmatrix}
\Delta P^k \\
\Delta\delta^k \\
\Delta\gamma^k
\end{bmatrix}
+
\begin{bmatrix}
0 \\
X \\
0
\end{bmatrix}
\Delta\sigma
=
\begin{bmatrix}
\beta_P^k \\
\beta_\delta^k \\
\beta_\gamma^k
\end{bmatrix}
\qquad\text{(A.36)}
$$

Where the Xs are non-empty matrices.

Therefore, the ΔP and $\Delta\gamma$ can be expressed as functions of $\Delta\delta$. Furthermore, $\Delta\delta$ can be expressed as the function of $\Delta\sigma$.

In addition, the last set of equations $\sum \Gamma_a^T \Delta a_a^k = q_k$ can be written as:

$$
\sum \left(\begin{bmatrix} 0 & X & 0 \end{bmatrix} \cdot \begin{bmatrix} \Delta P^k \\ \Delta\delta^k \\ \Delta\gamma^k \end{bmatrix} \right) = q_k \qquad\qquad\text{(A.37)}
$$

As discussed above, $\Delta\delta$ can be expressed as the function of $\Delta\sigma$. By substituting the $\Delta\delta$ in equation (A.37) with functions of $\Delta\sigma$, $\Delta\sigma$ can be obtained from the above equation. By back-substitution we can obtain $\Delta\delta$, ΔP and $\Delta\gamma$.

7 The specific OPF problem and its sparse structure

For the DC OPF problem described in Chapter 1, the inequality constraints can be converted into equalities ones using slack variables:

$$\mathbf{s}_{ga} + \mathbf{Kp}_a - \mathbf{b}_a = 0 \text{, where } \mathbf{s}_{ga} \text{ is a } 2*n_{ga} \text{ slack vector.} \qquad (A.38)$$

$\mathbf{K} = \begin{bmatrix} \mathbf{E} \\ -\mathbf{E} \end{bmatrix}$ is a constant matrix, and E is a $n_{ga}*n_{ga}$ diagonal unity matrix.

$\mathbf{b}_a = \begin{bmatrix} \mathbf{P}_{amax} \\ -\mathbf{P}_{amin} \end{bmatrix}$ is a constant $2*n_{ga}$ vector storing the generator limits in area a.

$$\mathbf{s}_{\delta a} + \mathbf{N}\boldsymbol{\delta}_a - \mathbf{d}_a = 0 \text{, where } \mathbf{s}_{\delta a} \text{ is a } 2*n_{\delta a} \text{ slack vector.} \qquad (A.39)$$

$\mathbf{N} = \begin{bmatrix} \mathbf{E} \\ -\mathbf{E} \end{bmatrix}$ is a constant matrix, and E is a $n_{\delta a}*n_{\delta a}$ diagonal unity matrix.

$\mathbf{d}_a = \begin{bmatrix} \boldsymbol{\delta}_{amax} \\ -\boldsymbol{\delta}_{amin} \end{bmatrix}$ is a constant $2*n_{\delta a}$ vector storing the power angle limits in area a.

$\left| b_{ij}\sin(\delta_i - \delta_j) \right| \le L_{i-j\max}$ can also be expressed as $\left[b_{ij}\sin(\delta_i - \delta_j) \right]^2 \le L_{i-j\max}^2$ for any

transmission line. Noticing that $\sin^2\theta = \frac{1}{2}(1 - \cos 2\theta)$, then

$$\mathbf{s}_{la} + \|\mathbf{b}_1\|_2 - \|\mathbf{b}_1\|_2 \cdot \mathbf{cos2A}_{Full}\boldsymbol{\delta}_{aFull} - 2\cdot\mathbf{L}_{amax}^2 = 0 \qquad (A.40)$$

where the $\mathbf{s}_{la}$ is a slack vector whose dimension is m_a, $\mathbf{b}_1$ is a diagonal matrix whose diagonal entry is the branch inductance b_{ij}, A is the incidence matrix of system a indicating the starting and ending nodes of each transmission line, and $\mathbf{L}_{amax}^2$ is the modified transfer limit vector whose elements are $(L_{i-j\max})^2$ for $\forall L_{i-j}$.

The slack variables must be nonnegative, i.e. $\mathbf{s}_{ga} \ge 0$ and $\mathbf{s}_{la} \ge 0$

Re-write the equality constraints as:

Power balance constraints: $\mathbf{p_a} - \mathbf{g}_a(\mathbf{B_a}, \boldsymbol{\delta_a}) - \mathbf{p_{La}} = 0$ (A.41)

Coupling constraints: $\mathbf{M}\delta = 0$ (A.42)

where $\delta = [\boldsymbol{\delta}_1^T \cdots \boldsymbol{\delta}_A^T]^T$ is a vector containing variables in other systems.

In order to make sure that the slack variables are nonnegative, the logarithm barrier function is added to the cost function:

$$\sum_{a=1}^{A}(\mathbf{p_a^T Q_a p_a} + \mathbf{b_a^T p_a}) - \mu \sum_{a=1}^{A}\sum_{i=1}^{k_a} \ln s_i \qquad (A.43)$$

In this OPF problem, the objective function (A.43) and the constraints equation (A.38) through equation (A.41) are all separable, but constraint equation (A.42) is a global coupling constraint. Suppose the Lagrangian for constraint equation (A.42) is $\boldsymbol{\sigma}$, and the Lagrangian for constraints (A.41), (A.39), (A.38) and (A.40) are λ_{ga}, $z_{\delta a}$, $\mathbf{z}_{ga}$, $\mathbf{z}_{la}$, respectively, and using convex dualisation, we can obtain the Lagrangian function for this OPF problem:

$$L(\cdot) = \sum_{a=1}^{A}[(\mathbf{p_a^T Q_a p_a} + \mathbf{b_a^T p_a}) - \mu \sum_{i=1}^{k_a} \ln s_i + \mathbf{z}_{ga}^T(\mathbf{s_{ga}} + \mathbf{Kp_a} - \mathbf{b_a})$$

$$+ \mathbf{z}_{la}^T(\mathbf{s_{la}} + \|\mathbf{b}_1\|_2 - \|\mathbf{b}_1\|_2 \times \cos 2A\delta_a - 2 \times \mathbf{L}_{amax}^2) + \lambda_{ga}^T(\mathbf{p_a} - \mathbf{g}_{ga}(\mathbf{B_a},\boldsymbol{\delta_a}) - \mathbf{p_{La}})$$

$$+ \lambda_{Da}^T(\mathbf{g}_{Da}(\mathbf{B_a},\boldsymbol{\delta_a}) + \mathbf{p_{La}}) + \mathbf{z}_{\delta a}^T(\mathbf{s_{\delta a}} + \mathbf{N}\delta_a - \mathbf{d_a})] + \boldsymbol{\sigma}^T\mathbf{M}\delta$$

    (A.44)

$$\text{here } \boldsymbol{\sigma}^T\mathbf{M}\delta = \boldsymbol{\sigma}^T\begin{bmatrix} \mathbf{M}_1 & \cdots & \mathbf{M}_A \end{bmatrix}\begin{bmatrix} \boldsymbol{\delta}_1 \\ \vdots \\ \boldsymbol{\delta}_A \end{bmatrix} = \boldsymbol{\sigma}^T\sum_{a=1}^{A}\mathbf{M}_a\boldsymbol{\delta}_a \qquad (A.45)$$

Thus, given the global Lagrangian $\boldsymbol{\sigma}$, the $L(.)$ is a separable function. Therefore, by updating σ we can obtain the optimum through parallel dispatches in all the sub-systems.

The KKT condition for the primal-dual problem can be expressed as: $\mathbf{J(u)} = \partial L/\partial \mathbf{u} = 0$

and $\mathbf{J}(\sigma) = \partial L/\partial \sigma = 0$, where $\mathbf{u} = \begin{bmatrix} \mathbf{u}_1 \\ \mathbf{u}_2 \\ \vdots \\ \mathbf{u}_A \end{bmatrix}$ is the set of local variables, and the local

variable vector $\mathbf{u}_a = [\lambda_{Da}^T \lambda_{ga}^T z_{\delta a}^T z_{ga}^T z_{la}^T s_{la}^T s_{ga}^T s_{\delta a}^T p_a^T \delta_a^T]^T = \begin{bmatrix} \eta & x \end{bmatrix}$, where

$\eta = \begin{bmatrix} \lambda_{Da}^T \lambda_{ga}^T z_{\delta a}^T z_{ga}^T z_{la}^T \end{bmatrix}^T$ is the Lagrange multiplier vector (dual variables), and

$x = \begin{bmatrix} s_{la}^T s_{ga}^T s_{\delta a}^T p_a^T \delta_a^T \end{bmatrix}^T$ is the vector of control variables and state variables (primal

variables).

If we can find $(\mathbf{u}^*, \sigma^*)$ to make $\mathbf{J(u)} = 0$ and $\mathbf{J}(\sigma) = 0$, then the optimum is found.

Newton method can be used to solve the KKT conditions.

For each area a, given $(\mathbf{u}^k, \sigma^k)$, the Newton method can be expressed as:

$$\begin{bmatrix} H_{uu}^k & H_{u\sigma}^k \\ H_{\sigma u}^k & H_{\sigma\sigma}^k \end{bmatrix} \cdot \begin{bmatrix} \Delta u^{k+1} \\ \Delta \sigma^{k+1} \end{bmatrix} = \begin{bmatrix} -J_u^k \\ -J_\sigma^k \end{bmatrix} \qquad (A.46)$$

where the H and J are Hessian and Jacobian matrices with respect to the Lagrangian

function of the OPF problem. .

And the update procedure is $\begin{bmatrix} u^{k+1} \\ \sigma^{k+1} \end{bmatrix} = \begin{bmatrix} \eta^k \\ x^k \\ \sigma^k \end{bmatrix} + \begin{bmatrix} \alpha_D^k \Delta \eta^k \\ \alpha_P^k \Delta x^k \\ \alpha_D^k \Delta \sigma^k \end{bmatrix}$ (A.47)

where the α_D^k and α_P^k are the step sizes for the dual and primal variables respectively.

In primal-dual interior point methods, the step size is chosen so that the new point is

still within the μ neighbourhood, so the choice does not depend on the specific OPF

problem or experience. By enforcing $\mu^k \to 0$, the optimum can finally be found.

By expanding $\mathbf{u}$ into $\mathbf{u} = \begin{bmatrix} \eta & x \end{bmatrix} = [\lambda_{Da}^T \lambda_{ga}^T z_{\delta a}^T z_{ga}^T z_{la}^T s_{la}^T s_{ga}^T s_{\delta a}^T p_a^T \delta_a^T]^T$, the H_{uu}^k can be

written as:

$$
\begin{bmatrix}
H^k_{\lambda_D\lambda_D} & H^k_{\lambda_D\lambda_g} & H^k_{\lambda_D z_\delta} & H^k_{\lambda_D z_g} & H^k_{\lambda_D z_l} & H^k_{\lambda_D s_l} & H^k_{\lambda_D s_g} & H^k_{\lambda_D s_\delta} & H^k_{\lambda_D P_a} & H^k_{\lambda_D \delta_a} \\
\left(H^k_{\lambda_D\lambda_D}\right)^T & H^k_{\lambda_g\lambda_g} & H^k_{\lambda_g z_\delta} & H^k_{\lambda_g z_g} & H^k_{\lambda_g z_l} & H^k_{\lambda_g s_l} & H^k_{\lambda_g s_g} & H^k_{\lambda_g s_\delta} & H^k_{\lambda_g P_a} & H^k_{\lambda_g \delta_a} \\
 & & H^k_{z_\delta z_\delta} & H^k_{z_\delta z_g} & H^k_{z_\delta z_l} & H^k_{z_\delta s_l} & H^k_{z_\delta s_g} & H^k_{z_\delta s_\delta} & H^k_{z_\delta P_a} & H^k_{z_\delta \delta_a} \\
 & & & H^k_{z_g z_g} & H^k_{z_g z_l} & H^k_{z_g s_l} & H^k_{z_g s_g} & H^k_{z_g s_\delta} & H^k_{z_g P_a} & H^k_{z_g \delta_a} \\
 & & & & H^k_{z_l z_l} & H^k_{z_l s_l} & H^k_{z_l s_g} & H^k_{z_l s_\delta} & H^k_{z_l P_a} & H^k_{z_l \delta_a} \\
\vdots & & & \ddots & & H^k_{s_l s_l} & H^k_{s_l s_g} & H^k_{s_l s_\delta} & H^k_{s_l P_a} & H^k_{s_l \delta_a} \\
 & & & & & & H^k_{s_g s_g} & H^k_{s_g s_\delta} & H^k_{s_g P_a} & H^k_{s_g \delta_a} \\
\vdots & & & & & & & H^k_{s_\delta s_\delta} & H^k_{s_\delta P_a} & H^k_{s_\delta \delta_a} \\
 & & & & & & & & H^k_{P_a P_a} & H^k_{p_a \delta_a} \\
\cdots & & \cdots & & & & \cdots & & & H^k_{\delta_a \delta_a}
\end{bmatrix}
$$

(A.48)

The lower triangle is the transposition of the upper triangle and is thus omitted.

Both the Hessian and the Jacobian are sparse matrices as many of the entries are zero due to the relations between variables. The following equations give the nonzero entries in the Jacobian and Hessian according to the specific OPF problem we are studying:

$$
\frac{\partial L}{\partial s_{la}} = -\mu \begin{bmatrix} \dfrac{1}{s_{la}} \end{bmatrix}^T + z_{la}^T = 0_{(1\times m_a)} \qquad (A.49)
$$

$$
\frac{\partial L}{\partial s_{ga}} = -\mu \begin{bmatrix} \dfrac{1}{s_{ga}} \end{bmatrix}^T + z_{ga}^T = 0_{(1\times 2n_a)} \qquad (A.50)
$$

$$
\frac{\partial L}{\partial s_{\delta a}} = -\mu \begin{bmatrix} \dfrac{1}{s_{\delta a}} \end{bmatrix}^T + z_{\delta a}^T = 0_{(1\times 2n_{\delta a})} \qquad (A.51)
$$

$$
\frac{\partial L}{\partial P_a} = 2p_a^T Q_a + b_a^T + z_{ga}^T K + \lambda_{ga}^T = 0_{(1\times n_{ga})} \qquad (A.52)
$$

$$
\frac{\partial L}{\partial \delta_a} = \frac{\partial}{\partial \delta_a}\left[z_{la}^T \|\mathbf{b}_1\|_2^2 \cdot \left(-\cos 2A_{Full}\delta_{Full}\right) + z_{\delta a}^{\mathrm{T}}(N\delta_a) - \lambda_{ga}^T \cdot g_{ga}(B_a,\delta_a) + \lambda_{Da}^T \cdot g_{Da}(B_a,\delta_a) + \sigma^T M \right.
$$

$$
= \frac{\partial}{\partial \delta_a}\left[f_a(\cdot) + h_a(\cdot) + l_a(\cdot) \right] + z_{\delta a}^T N + \delta^T M_a = 0_{(1\times n_\delta)} \qquad (A.53)
$$

where $\dfrac{\partial f_a}{\partial \delta_a} = z_{la}^T \|\mathbf{b}_1\|_2 \cdot \left[\dfrac{\partial}{\partial \delta_a}\left(-\cos 2A_{Full}\delta_{Full}\right) \right] =$

184

$$2z_{la}^T \|\mathbf{b}_1\|_2 \begin{bmatrix} \sin(2\vec{a}_1\delta_{Full}) & \cdots & 0 \\ \vdots & \ddots & \vdots \\ 0 & \cdots & \sin(2\vec{a}_m\delta_{Full}) \end{bmatrix} * A \to 1\times n_{\delta_a} \text{ vector} \quad \text{(A.54)}$$

and $\vec{a}_1 \ldots \vec{a}_m$ are the 1st...mth row vector in matrix A_{Full}. A is the incidence matrix obtained by cutting off the sth column in matrix A_{Full}, where s is the slack bus number.

$$\frac{\partial h_a}{\partial \delta_a} = -\frac{\partial}{\partial \delta_a}\left(\sum_{k=1}^{n_{ga}}\left(\lambda_{gk}\sum_{j=1}^{n_a} b_{kj}\sin(\delta_k - \delta_j)\right)\right)$$

$$= -\frac{\partial}{\partial \delta_a}\left(\sum_{k=g_1,k\neq s}^{g_a}\left(\lambda_k \sum_{j=1}^{n_{\delta a}} b_{kj}\sin(\delta_k - \delta_j) + \lambda_k b_{ks}\sin(\delta_k - \delta_s)\right) + \lambda_s \sum_{j=1}^{n_{\delta a}} b_{sj}\sin(\delta_s - \delta_j)\right) =$$

$$-\lambda_{ga}^T \begin{bmatrix} \vec{b}_{g1}diag\left(\cos\left(\left[\vec{I}\vec{e}_{g1}^T - E\right]\delta_a\right)\right)*\left[\vec{I}\vec{e}_{g1}^T - E_{n_{\delta_a}}\right] + b_{g1s}\cos(\delta_{g1} - \delta_s) \\ \vdots \\ \vec{b}_{g_a}diag\left(\cos\left(\left[\vec{I}\vec{e}_{g_a}^T - E\right]\delta_a\right)\right)*\left[\vec{I}\vec{e}_{g_a}^T - E_{n\delta_a}\right] + b_{g_as}\cos(\delta_{g_a} - \delta_s) \end{bmatrix}$$

$$+ \lambda_s \begin{bmatrix} b_{s1}\cos(\delta_s - \delta_{g1}) \\ \vdots \\ b_{s\delta_a}\cos(\delta_s - \delta_{ng_a}) \end{bmatrix}^T = \left[\sum \lambda_{gi}o_i\right] \text{(A.55)}$$

where $o_i =$

$$\begin{cases} \left[b_{i1}\cos(\delta_i - \delta_1) \quad \cdots \quad b_{is}\cos(\delta_i - \delta_s) \quad \cdots \quad b_{in_{\delta_a}}\cos(\delta_i - \delta_{n_{\delta_a}})\right] & i = g_1\ldots g_a, i \neq s \\ -\left[b_{s1}\cos(\delta_s - \delta_1) \quad \cdots \quad b_{sn_{\delta_a}}\cos(\delta_s - \delta_{n_{\delta_a}})\right], & i = s \end{cases}$$

is a $1\times n_{\delta a}$ vector. (A.56)

Note that only when the slack bus has generators attached does the multiplier λ_s exist.

The λ_{ga} is the vector storing the multipliers for all the generators within area a except the slack generator.

Similarly, $\dfrac{\partial l_a}{\partial \delta_a} = \dfrac{\partial}{\partial \delta_a}\left(\sum_{k=1}^{n_D}\left(\lambda_{Dk}\sum_{j=1}^{n_a} b_{kj}\sin(\delta_k - \delta_j)\right)\right) = \left[-\sum \lambda_{Di}o_i\right]$ (A.57)

$$\frac{\partial L}{\partial \gamma_{ga}} = \left[\mathbf{p}_a - \mathbf{g}_{ga}(\mathbf{B}_{ga},\delta_a) - \mathbf{p}_{Lg}\right]^T = \mathbf{0}_{(1\times n_{ga})} \quad \text{(A.58)}$$

$$\frac{\partial L}{\partial \gamma_{Da}} = \left[\mathbf{g}_{Da}(\mathbf{B}_{Da},\delta_a) + \mathbf{p}_{LD}\right]^T = \mathbf{0}_{(1\times n_{Da})} \quad \text{(A.59)}$$

$$\frac{\partial L}{\partial z_{ga}} = \left[\mathbf{s}_{ga} + \mathbf{K}\mathbf{p}_a - \mathbf{b}_a \right]^T = \mathbf{0}_{(1\times 2n_{ga})} \qquad (A.60)$$

$$\frac{\partial L}{\partial z_{\delta a}} = \left[\mathbf{s}_{\delta a} + N\delta_a - d_a \right]^T = \mathbf{0}_{(1\times 2n_{\delta a})} \qquad (A.61)$$

$$\frac{\partial L}{\partial z_{la}} = \left[\mathbf{s}_{la} + \|\mathbf{b}_1\|_2 - \|\mathbf{b}_1\|_2 \cdot \cos 2\mathbf{A}_{Full}\delta_{aFull} - 2 \cdot \mathbf{L}_{amax}^2 \right]^T = \mathbf{0}_{(1\times m_a)} \qquad (A.62)$$

$$\frac{\partial L}{\partial \sigma} = \delta^T \mathbf{M}^T = \sum \delta_a^T M_a^T = \mathbf{0}_{(1\times n_T)}, \text{ where } n_T \text{ is the number of coupling variables.}$$

(A.63)

Plus $\mathbf{s}_{ga} \geq 0$, $\mathbf{s}_{\delta a} \geq 0$, $\mathbf{s}_{la} \geq 0$ and $\mathbf{z}_{ga} \geq 0, z_{\delta a} \geq 0, \mathbf{z}_{la} \geq 0$.

8 List of derivatives

In this OPF problem,

$$\mathbf{x}_a = \begin{bmatrix} \mathbf{P}_a & \delta_a \end{bmatrix}, \quad \lambda^T = \begin{bmatrix} \lambda_{ga}^T & \lambda_{Da}^T & \sigma^T \end{bmatrix}^T, \quad \mathbf{z}^T = \begin{bmatrix} \mathbf{z}_{ga}^T & \mathbf{z}_{\delta a}^T & \mathbf{z}_{la}^T \end{bmatrix}^T,$$

$$\mathbf{f}(\cdot) = \sum_{a=1}^A [(\mathbf{p}_a^T \mathbf{Q}_a \mathbf{p}_a + \mathbf{b}_a^T \mathbf{p}_a) \qquad (A.64)$$

$$\lambda^T \mathbf{g}(\cdot) = \lambda_{ga}^T (\mathbf{p}_a - \mathbf{g}_{ga}(\mathbf{B}_a, \delta_a) - \mathbf{p}_{La}) + \lambda_{Da}^T (\mathbf{g}_{Da}(\mathbf{B}_a, \delta_a) + \mathbf{p}_{La}) + \sigma^T \mathbf{M}\delta$$

(A.65)

$$\mathbf{z}^T (\mathbf{h}(\cdot) + \mathbf{s} - \mathbf{D}) = \mathbf{z}_{ga}^T (\mathbf{s}_{ga} + \mathbf{K}\mathbf{p}_a - \mathbf{b}_a) + \mathbf{z}_{\delta a}^T (\mathbf{s}_{\delta a} + N\delta_a - d_a)$$
$$+ \mathbf{z}_{la}^T (\mathbf{s}_{la} + \|\mathbf{b}_1\|_2 - \|\mathbf{b}_1\|_2 \times \cos 2\mathbf{A}\delta_a - 2\times \mathbf{L}_{amax}^2) \qquad (A.66)$$

and the computation is as the following procedure:

(1) Given $\mathbf{x}_a^0$, and thus $\mathbf{s}_0 = \mathbf{D} - \mathbf{h}(\mathbf{x}_a^0)$. $\mathbf{z}_0$ and λ_0 are functions of both μ and $\mathbf{x}_a^0$.

(2) $\nabla \mathbf{g}^k = \begin{bmatrix} \mathbf{E} & 0 & 0 \\ -\dfrac{\partial \mathbf{g}_{ga}}{\partial \delta}\bigg|_k & \dfrac{\partial \mathbf{g}_{Da}}{\partial \delta}\bigg|_k & \mathbf{M}^T \end{bmatrix}$ and $\nabla \mathbf{h}^k = \begin{bmatrix} \mathbf{K} & 0 & 0 \\ 0 & N & \dfrac{\partial \mathbf{h}_1}{\partial \delta}\bigg|_k \end{bmatrix}$

(3) $\nabla \mathbf{L}^k = \begin{bmatrix} \dfrac{\partial L}{\partial \mathbf{P}_a}\bigg|_k \\ \dfrac{\partial L}{\partial \delta_a}\bigg|_k \end{bmatrix}$ and $\mathbf{H}^k = \begin{bmatrix} \mathbf{H}_{P_a P_a}\big|_k & 0 \\ 0 & \mathbf{H}_{\delta_a \delta_a}\big|_k \end{bmatrix}$

(4) $\mathbf{d}_1^k = \mathbf{D}^k - \mathbf{h}^k - \mathbf{s}^k$

(5) $\mathbf{A}^k = \mathbf{H}^k + \nabla\mathbf{h}^k\left(\mathbf{S}_k^{-1}\mathbf{Z}^k\right)\nabla\mathbf{h}_k^{\mathrm{T}} = \begin{bmatrix} \mathbf{A}_{P_aP_a} & \mathbf{0} \\ \mathbf{0} & \mathbf{A}_{\delta_a\delta_a}^k \end{bmatrix}$, thanks to the sparse structure

of $\nabla\mathbf{h}^k$ and $\mathbf{H}^k$

(6) Equation (A.34) thus becomes

$$\begin{bmatrix} \mathbf{T}_1 & \mathbf{0} & \mathbf{0} & \mathbf{M}_1 \\ \mathbf{0} & \mathbf{T}_2 & \mathbf{0} & \mathbf{M}_2 \\ \mathbf{0} & \mathbf{0} & \ddots & \cdots \\ \mathbf{M}_1^{\mathrm{T}} & \mathbf{M}_2^{\mathrm{T}} & \cdots & \mathbf{0} \end{bmatrix}\begin{bmatrix} \Delta\mathbf{v}_1 \\ \Delta\mathbf{v}_2 \\ \cdots \\ \Delta\boldsymbol{\sigma} \end{bmatrix} = \begin{bmatrix} \mathbf{r}_1 \\ \mathbf{r}_2 \\ \cdots \\ \mathbf{r}_\sigma \end{bmatrix} \qquad \text{(A.67)}$$

where the

$$\mathbf{T}_a = \begin{bmatrix} \mathbf{A}_{P_aP_a} & \mathbf{0} & \nabla\mathbf{g}_P \\ \mathbf{0} & \mathbf{A}_{\delta_a\delta_a}^k & \nabla\mathbf{g}_\delta^k \\ \nabla\mathbf{g}_P^{\mathrm{T}} & \nabla\mathbf{g}_\delta^{\mathrm{T}}\big|_k & \mathbf{0} \end{bmatrix} = \begin{bmatrix} \mathbf{C} & \mathbf{0} & \mathbf{E} & \mathbf{0} \\ \mathbf{0} & \mathbf{H}_{\delta_a\delta a}\big|_k & -\dfrac{\partial\mathbf{g}_{ga}}{\partial\boldsymbol{\delta}_a}\Big|_k & \dfrac{\partial\mathbf{g}_{Da}}{\partial\boldsymbol{\delta}_a}\Big|_k \\ \mathbf{E}^{\mathrm{T}} & \left(-\dfrac{\partial\mathbf{g}_{ga}}{\partial\boldsymbol{\delta}_a}\right)^{\mathrm{T}}\Big|_k & \mathbf{0} & \mathbf{0} \\ \mathbf{0} & \left(\dfrac{\partial\mathbf{g}_{Da}}{\partial\boldsymbol{\delta}_a}\right)^{\mathrm{T}}\Big|_k & \mathbf{0} & \mathbf{0} \end{bmatrix} \qquad \text{(A.68),}$$

$$\Delta\mathbf{v}_a = \begin{bmatrix} \Delta\mathbf{P}_a^k \\ \Delta\boldsymbol{\delta}_a^k \\ \Delta\boldsymbol{\lambda}^k \end{bmatrix} = \begin{bmatrix} \Delta\mathbf{P}_a^k \\ \Delta\boldsymbol{\delta}_a^k \\ \Delta\lambda_{ga}^k \\ \Delta\lambda_{Da}^k \end{bmatrix} \quad \text{and} \quad \mathbf{r}_a = -\begin{bmatrix} \mathbf{b}_{P_a}^k \\ \mathbf{b}_{\delta_a}^k \\ \mathbf{g}_\lambda^k \end{bmatrix} = \begin{bmatrix} \mathbf{r}_{P_a}^k \\ \mathbf{r}_{\delta_a}^k \\ \mathbf{r}_{\lambda_{ga}}^k \\ \mathbf{r}_{\lambda_{Da}}^k \end{bmatrix}, \ a=1,2,\ldots$$

Only those matrices labelled with 'k' need to be updated at each iteration, and the others are constant.

(7) The above matrix can be written as a set of equations:

$$\mathbf{C}\Delta P_a^k + \mathbf{E}\Delta\lambda_{ga}^k = \mathbf{r}_{P_a}^k \qquad \text{(A.69)}$$

$$\mathbf{H}_{\delta_a\delta_a}\big|_k\Delta\boldsymbol{\delta}_a^k + \left(-\dfrac{\partial\mathbf{g}_{ga}}{\partial\boldsymbol{\delta}_a}\Big|_k\right)\Delta\lambda_{ga}^k + \left(\dfrac{\partial\mathbf{g}_{Da}}{\partial\boldsymbol{\delta}_a}\Big|_k\right)\Delta\lambda_{Da}^k + \mathbf{M}_a\Delta\boldsymbol{\sigma}^k = \mathbf{r}_{\delta_a}^k \qquad \text{(A.70)}$$

$$\mathbf{E}\Delta\mathbf{P}_a^k + \left(-\dfrac{\partial\mathbf{g}_{ga}}{\partial\boldsymbol{\delta}_a}\right)^{\mathrm{T}}\big|_k\Delta\boldsymbol{\delta}_a^k = \mathbf{r}_{\lambda_{ga}}^k \qquad \text{(A.71)}$$

$$\left(\frac{\partial \mathbf{g}_{Da}}{\partial \boldsymbol{\delta}_a}\right)^{\mathbf{T}}\Big|_k \Delta \boldsymbol{\delta}_a^{\ k} = \mathbf{r}_{\lambda_{Da}}^k \qquad (A.72)$$

$$\sum_a \mathbf{M}_a^{\mathbf{T}} \Delta \boldsymbol{\sigma} = \mathbf{r}_\sigma^k \qquad (A.73)$$

From equation (A.69) we can get: $\Delta \lambda_{ga}^k = r_{Pa}^k - C\Delta P_a^k \quad$ (A.74)

From equation (A.71) we can get: $\Delta P_a^k = r_{\lambda_{ga}}^k - \left(-\dfrac{\partial \mathbf{g}_{ga}}{\partial \boldsymbol{\delta}_a}\right)^{\mathbf{T}}\Big|_k \Delta \boldsymbol{\delta}_a^{\ k} \qquad$ (A.75)

Substitute (A.75) into (A.74) we can get:

$$\Delta \lambda_{ga}^k = r_{Pa}^k - Cr_{\lambda_{ga}}^k - C\left(-\frac{\partial \mathbf{g}_{ga}}{\partial \boldsymbol{\delta}_a}\right)^{\mathbf{T}}\Big|_k \Delta \boldsymbol{\delta}_a^{\ k} \qquad (A.76)$$

By substituting (A.76) into (A.70), we get:

$$\mathbf{H}_{\delta_a \delta a}\big|_k \Delta \boldsymbol{\delta}_a^{\ k} + \left(\frac{\partial \mathbf{g}_{ga}}{\partial \boldsymbol{\delta}_a}\Big|_k\right)\mathbf{C}\left(-\frac{\partial \mathbf{g}_{ga}}{\partial \boldsymbol{\delta}_a}\right)^{\mathbf{T}}\Big|_k \Delta \boldsymbol{\delta}_a^{\ k} + \left(\frac{\partial \mathbf{g}_{Da}}{\partial \boldsymbol{\delta}_a}\Big|_k\right)\Delta \lambda_{Da}$$
$$+ \mathbf{M}_a \Delta \boldsymbol{\sigma} = \mathbf{r}_{\delta_a}^k + \left(\frac{\partial \mathbf{g}_{ga}}{\partial \boldsymbol{\delta}_a}\Big|_k\right)\left(\mathbf{r}_{Pa}^k - C\mathbf{r}_{\lambda_{ga}}^k\right) \qquad (A.77)$$

Let $\mathbf{A}_A^k = \mathbf{H}_{\delta_a \delta a}\big|_k + \left(\dfrac{\partial \mathbf{g}_{ga}}{\partial \boldsymbol{\delta}_a}\Big|_k\right)\mathbf{C}\left(-\dfrac{\partial \mathbf{g}_{ga}}{\partial \boldsymbol{\delta}_a}\right)^{\mathbf{T}}\Big|_k \qquad$ (A.78)

And $\mathbf{r}_A^k = \mathbf{r}_{\delta_a}^k + \left(\dfrac{\partial \mathbf{g}_{ga}}{\partial \boldsymbol{\delta}_a}\Big|_k\right)\left(\mathbf{r}_{Pa}^k - C\mathbf{r}_{\lambda_{ga}}^k\right) \qquad$ (A.79)

Then (A.68) can be simplified as:

$$\begin{bmatrix} A_A^k & \dfrac{\partial \mathbf{g}_{Da}}{\partial \boldsymbol{\delta}_a}\Big|_k & \mathbf{M}_a \\ \left(\dfrac{\partial \mathbf{g}_{Da}}{\partial \boldsymbol{\delta}_a}\right)^{\mathbf{T}}\Big|_k & 0 & 0 \end{bmatrix}\begin{bmatrix} \Delta \boldsymbol{\delta}_a^{\ k} \\ \Delta \lambda_{Da}^k \\ \Delta \boldsymbol{\sigma} \end{bmatrix} = \begin{bmatrix} \mathbf{r}_A^k \\ \mathbf{r}_{\lambda_{Da}}^k \\ \mathbf{r}_\sigma \end{bmatrix} \qquad (A.80)$$

Also from (A.77) through (A.79) we can get:

$$\Delta \boldsymbol{\delta}_a^{\ k} = \left(\mathbf{A}_A^k\right)^{-1}\left(\mathbf{r}_A^k - \left(\frac{\partial \mathbf{g}_{Da}}{\partial \boldsymbol{\delta}_a}\Big|_k\right)\Delta \lambda_{Da} - \mathbf{M}_a \Delta \boldsymbol{\sigma}\right) \qquad (A.81)$$

$$\left(\frac{\partial \mathbf{g}_{Da}}{\partial \boldsymbol{\delta}_a}\right)^{\mathbf{T}}\Big|_k \Delta \boldsymbol{\delta}_a^{\ k} = \mathbf{r}_{\lambda_{Da}}^k \qquad (A.82)$$

$$\text{and } \sum_a \mathbf{M}_a^T \Delta \delta_a = \mathbf{r}_\sigma^k \qquad (A.83)$$

By substituting (A.81) into (A.82) we get:

$$\left(\frac{\partial \mathbf{g}_{Da}}{\partial \delta_a}\right)^T \bigg|_k \left(\mathbf{A}_A^k\right)^{-1} \left(\frac{\partial \mathbf{g}_{Da}}{\partial \delta_a}\bigg|_k\right) \Delta \lambda_{Da} + \left(\frac{\partial \mathbf{g}_{Da}}{\partial \delta_a}\right)^T \bigg|_k \left(\mathbf{A}_A^k\right)^{-1} \mathbf{M}_a \Delta \sigma$$

$$= -\mathbf{r}_{\lambda_{Da}}^k + \left(\frac{\partial \mathbf{g}_{Da}}{\partial \delta_a}\right)^T \bigg|_k \left(\mathbf{A}_A^k\right)^{-1} \mathbf{r}_A^k \qquad\qquad (A.84)$$

Similarly by substituting (A.81) into (A.83) we get:

$$\sum_a \left\{ \mathbf{M}_a^T \left(\mathbf{A}_A^k\right)^{-1} \left(\mathbf{r}_A^k - \left(\frac{\partial \mathbf{g}_{Da}}{\partial \delta_a}\bigg|_k\right) \Delta \lambda_{Da} - \mathbf{M}_a \Delta \sigma \right) \right\} = \mathbf{r}_\sigma^k$$

and thus

$$\sum_a \mathbf{M}_a^T \left(\mathbf{A}_A^k\right)^{-1} \left(\frac{\partial \mathbf{g}_{Da}}{\partial \delta_a}\bigg|_k\right) \Delta \lambda_{Da} + \sum_a \mathbf{M}_a^T \left(\mathbf{A}_A^k\right)^{-1} \mathbf{M}_a \Delta \sigma = -\mathbf{r}_\sigma^k + \sum_a \mathbf{M}_a^T \left(\mathbf{A}_A^k\right)^{-1} \mathbf{r}_A^k$$

Let $\mathbf{D}_A^k = \left(\frac{\partial \mathbf{g}_{Da}}{\partial \delta_a}\right)^T \bigg|_k \left(\mathbf{A}_A^k\right)^{-1} \left(\frac{\partial \mathbf{g}_{Da}}{\partial \delta_a}\bigg|_k\right)$, $\mathbf{B}_{D_a\sigma}^k = \left(\frac{\partial \mathbf{g}_{Da}}{\partial \delta_a}\right)^T \bigg|_k \left(\mathbf{A}_A^k\right)^{-1} \mathbf{M}_a$

$$\mathbf{B}^k = \sum_a \mathbf{M}_a^T \left(\mathbf{A}_A^k\right)^{-1} \left(\frac{\partial \mathbf{g}_{Da}}{\partial \delta_a}\bigg|_k\right) = \sum_a \mathbf{B}_a^k \qquad \text{(considering that } \left(\mathbf{A}_A^k\right)^{-1} \text{ is symmetric)}$$

$$\mathbf{\Gamma}^k = \sum_a \mathbf{M}_a^T \left(\mathbf{A}_A^k\right)^{-1} \mathbf{M}_a \text{ and } \mathbf{t}_A^k = -\mathbf{r}_{\lambda_{Da}}^k + \left(\frac{\partial \mathbf{g}_{Da}}{\partial \delta_a}\right)^T \bigg|_k \left(\mathbf{A}_A^k\right)^{-1} \mathbf{r}_A^k$$

$$\mathbf{t}_\sigma^k = -\mathbf{r}_\sigma^k + \sum_a \mathbf{M}_a^T \left(\mathbf{A}_A^k\right)^{-1} \mathbf{r}_A^k$$

then
$$\begin{bmatrix} \mathbf{D}_1^k & 0 & 0 & \mathbf{B}_{D_1\sigma}|_k \\ 0 & \mathbf{D}_2^k & 0 & \mathbf{B}_{D_2\sigma}|_k \\ 0 & 0 & \ddots & \cdots \\ \mathbf{B}_1^k & & \cdots & \mathbf{\Gamma}^k \end{bmatrix} \begin{bmatrix} \Delta \lambda_{D1}^k \\ \Delta \lambda_{D2}^k \\ \cdots \\ \Delta \sigma^k \end{bmatrix} = \begin{bmatrix} \mathbf{t}_1^k \\ \mathbf{t}_2^k \\ \cdots \\ \mathbf{t}_\sigma^k \end{bmatrix} \qquad (A.85)$$

9 Newton directions

$$H_{s_{la}s_{la}} = \mu \cdot diag(\frac{1}{s_{la}^2}) \rightarrow (m_a \times m_a) \text{ matrix} \qquad (A.86)$$

$$H_{s_{la}z_{la}} = E = H_{z_{la}s_{la}}^T \rightarrow (m_a \times m_a) \text{ matrix} \qquad (A.87)$$

$$H_{s_{ga}s_{ga}} = \mu \cdot diag(\frac{1}{s_{ga}^2}) \rightarrow (2n_a \times 2n_a) \text{ matrix (A.88)}$$

$$H_{s_{ga}z_{ga}} = E = H_{z_{ga}s_{ga}}^T \rightarrow (2n_a \times 2n_a) \text{ matrix} \quad \text{(A.89)}$$

$$H_{s_{\delta a}s_{\delta a}} = \mu \cdot diag(\frac{1}{s_{\delta a}^2}) \rightarrow (2n_{\delta a} \times 2n_{\delta a}) \text{ matrix} \quad \text{(A.90)}$$

$$H_{s_{\delta a}z_{\delta a}} = E = H_{z_{\delta a}s_{\delta a}}^T \rightarrow (2n_{\delta a} \times 2n_{\delta a}) \text{ matrix} \quad \text{(A.91)}$$

$$H_{\delta_a \delta_a} = \frac{\partial^2 f_a}{\partial \delta_a^2} + \frac{\partial^2 h_a}{\partial \delta_a^2} + \frac{\partial^2 l_a}{\partial \delta_a^2} \quad \text{(A.92)}$$

where $\dfrac{\partial^2 f_a}{\partial \delta_a^2} = \dfrac{\partial}{\partial \delta_a}\left(2z_{la}^T \|\mathbf{b}_1\|_2 \begin{bmatrix} \sin(2\vec{a}_1\delta_{Full}) & \cdots & 0 \\ \vdots & \ddots & \vdots \\ 0 & \cdots & \sin(2\vec{a}_m\delta_{Full}) \end{bmatrix} * A \right)$

$$= \frac{\partial}{\partial \delta_a}\left(\begin{bmatrix} z_{la1}b_{l1}^2 \sin(2\vec{a}_1\delta_{Ful}) & \cdots & 0 \\ \vdots & \ddots & \vdots \\ 0 & \cdots & z_{lam}b_{lm}^2 \sin(2\vec{a}_m\delta_{Full}) \end{bmatrix} * 2A \right) =$$

$$\frac{\partial}{\partial \delta_a}\left(\begin{bmatrix} \sin(2\vec{a}_1\delta_{Full}) \\ \vdots \\ \sin(2\vec{a}_m\delta_{Full}) \end{bmatrix}^T \cdot diag(z_{la}) \cdot diag(\|b_l\|_2^2) \cdot 2A \right)$$

$$= 2A^T \begin{bmatrix} \cos(2\vec{a}_1\delta) & \cdots & 0 \\ \vdots & \ddots & \vdots \\ 0 & \cdots & \cos(2\vec{a}_m\delta) \end{bmatrix} diag(z_{la}) \cdot diag(\|b_l\|_2^2) \cdot 2A \quad \text{(A.93) is a}$$

$n_{\delta_a} \times n_{\delta_a}$ matrix

$$\text{and } \frac{\partial^2 h_a}{\partial \delta_a^2} = \frac{\partial}{\partial \delta_a} \left[\begin{array}{l} -\lambda_{ga}^T \begin{bmatrix} \vec{b}_{g1} diag\left(\cos\left(\left[I\vec{e}_{g1}^T - E\right]\delta_a\right)\right) \cdot \left[I\vec{e}_{g1}^T - E_{n_{\delta_a}}\right] \\ \vdots \\ \vec{b}_{g_a} diag\left(\cos\left(\left[I\vec{e}_{g_a}^T - E\right]\delta_a\right)\right) \cdot \left[I\vec{e}_{g_a}^T - E_{n\delta_a}\right] \end{bmatrix} \\[20pt] -\lambda_{ga}^T \begin{bmatrix} b_{g1s}\cos(\delta_{g1} - \delta_s) & & \\ & \ddots & \\ & & b_{g_as}\cos(\delta_{g_a} - \delta_s) \end{bmatrix} \\[20pt] +\lambda_s \begin{bmatrix} b_{s1}\cos(\delta_s - \delta_1) & & \\ & \ddots & \\ & & b_{sn_{\delta_a}}\cos(\delta_s - \delta_{n_{\delta_a}}) \end{bmatrix} \end{array} \right] =$$

$$\sum_{k=g_1, k \ne s}^{g_a} \lambda_{gak} \left[\left[I\vec{e}_k^T - E\right]^T \begin{bmatrix} b_{k1}\sin(\delta_k - \delta_1) & \cdots & 0 \\ \vdots & \ddots & \vdots \\ 0 & \cdots & b_{kn_{\delta a}}\sin(\delta_k - \delta_{n\delta a}) \end{bmatrix} \left[I\vec{e}_k^T - E\right] + b_{ks}\sin(\delta_k - \delta_s)\vec{e}_k^T \right]$$

$$+\lambda_s \cdot \begin{bmatrix} b_{s1}\sin(\delta_s - \delta_1) & & \\ & \ddots & \\ & & b_{sn_{\delta a}}\sin(\delta_s - \delta_{n\delta a}) \end{bmatrix} \qquad (A.94)$$

$$\text{and } \frac{\partial^2 l_a}{\partial \delta_a^2} =$$

$$-\sum_{k=1}^{n_{Dg}} \lambda_{Dak} \left[\left[I\vec{e}_1^T - E\right]^T \begin{bmatrix} b_{k1}\sin(\delta_k - \delta_1) & \cdots & 0 \\ \vdots & \ddots & \vdots \\ 0 & \cdots & b_{kn_{\delta a}}\sin(\delta_k - \delta_{n\delta a}) \end{bmatrix} \left[I\vec{e}_1^T - E\right] + b_{ks}\sin(\delta_k - \delta_s)\vec{e}_k^T \right]$$

$$(A.95)$$

$$H_{\delta_a z_{la}} = 2A^T \begin{bmatrix} \sin(2\vec{a}_1\delta_{Full}) & \cdots & 0 \\ \vdots & \ddots & \vdots \\ 0 & \cdots & \sin(2\vec{a}_m\delta_{Full}) \end{bmatrix} \cdot \|b_l\|_2^2 = H_{z_{la}\delta_a}^T \qquad (A.96)$$

is a $n_{\delta_a} \times m_a$ matrix. (A.97)

$$H_{\delta_a \gamma_{ga}} = \begin{bmatrix} \vec{o}_1 \\ \vdots \\ \vec{o}_{na} \end{bmatrix}^T = H_{\gamma_{ga}\delta_a}^T \rightarrow n_{\delta_a} \times n_{ga} \text{ matrix.} \qquad (A.98)$$

$$H_{\delta_a \gamma_{Da}} = -\begin{bmatrix} \vec{o}_1 \\ \vdots \\ \vec{o}_{na} \end{bmatrix}^T = H_{\lambda_{Da}\delta_a}^T \rightarrow n_{\delta_a} \times n_{Da} \text{ matrix.} \qquad (A.99)$$

$$H_{\delta_a z_{\delta a}} = N^T = H_{z_{\delta a} \delta_a}^T \rightarrow n_{\delta_a} \times 2n_{\delta a} \text{ vector.} \qquad (A.100)$$

$$H_{\delta_a \lambda} = M_a^T = H_{\lambda \delta_a}^T \rightarrow n_{\delta_a} \times T \text{ matrix.} \qquad (A.101)$$

$$H_{p_a p_a} = 2Q_a^T \rightarrow (n_a \times n_a) \text{ matrix} \qquad (A.102)$$

$$H_{p_a z_{ga}} = K^T = H_{z_{ga} p_a}^T \rightarrow (n_a \times 2n_a) \text{ matrix} \qquad (A.103)$$

$$H_{p_a \gamma_{ga}} = E = H_{\gamma_{ga} p_a}^T \rightarrow (n_{ga} \times n_{ga}) \text{ matrix} \qquad (A.104)$$

$$H_{\sigma\sigma} = 0_{n_T \times n_T} \qquad (A.105)$$

Thus for each system a, the Newton method can be expressed as:

$$\begin{bmatrix} H_{u_a u_a} & H_{u_a \sigma} \\ H_{\sigma u_a} & H_{\sigma\sigma} \end{bmatrix} \begin{bmatrix} \Delta u_a \\ \Delta\sigma \end{bmatrix} = - \begin{bmatrix} J_{u_a} \\ J_\sigma \end{bmatrix} \qquad (A.106)$$

$$\text{where } H_{u_a \sigma} = \frac{\partial}{\partial \lambda} J_{u_a} = \frac{\partial}{\partial \sigma} \begin{bmatrix} J_{s_{la}} \\ \vdots \\ J_{\delta_a} \\ \vdots \\ J_{z_{la}} \end{bmatrix} = \begin{bmatrix} 0 \\ \vdots \\ H_{\delta_a \sigma} \\ \vdots \\ 0 \end{bmatrix} = H_{\sigma u_a}^T \qquad (A.107)$$

and $H_{\sigma\sigma} = 0$ \qquad (A.108)

$H_{u_a u_a}$ is a highly sparse symmetric matrix,

$$\text{and } H_{u_a u_a} = \begin{bmatrix} H_{\eta\eta} & H_{\eta x} \\ H_{x\eta} & H_{xx} \end{bmatrix} = \begin{bmatrix} 0 & L^T \\ L & D \end{bmatrix} \qquad (A.109)$$

$$\text{where } D = \begin{bmatrix} H_{s_l s_l} & & & & 0 & 0 \\ & H_{s_g s_g} & & & & \\ & & H_{s_\delta s_\delta} & & & \\ & & & H_{p_a p_a} & & \\ 0 & & & & H_{\delta a \delta a} \end{bmatrix} \qquad (A.110)$$

is a $((m_a + 3n_a + n_{\delta a}) \times (m_a + 3n_a + n_{\delta a}))$ matrix,

$$L^T = \begin{bmatrix} 0 & 0 & 0 & 0 & H^k_{\lambda_D \delta_a} \\ 0 & 0 & 0 & H^k_{\lambda_g P_a} & H^k_{\lambda_g \delta_a} \\ 0 & 0 & H^k_{z_\delta s_\delta} & 0 & H^k_{z_\delta \delta_a} \\ 0 & H^k_{z_g s_g} & 0 & H^k_{z_g P_a} & 0 \\ H^k_{z_l s_l} & 0 & 0 & 0 & H^k_{z_l \delta_a} \end{bmatrix} \qquad \text{(A.111)}$$

is a $\left((m_a + 3n_a + 1) \times (m_a + 3n_a + n_{\delta a})\right)$ matrix.

Substituting the constant entries into this matrix, we get:

$$L^T = \begin{bmatrix} 0 & 0 & 0 & 0 & H^k_{\lambda_D \delta_a} \\ 0 & 0 & 0 & E & H^k_{\lambda_g \delta_a} \\ 0 & 0 & E & 0 & H^k_{z_\delta \delta_a} \\ 0 & E & 0 & K & 0 \\ E & 0 & 0 & 0 & H^k_{z_l \delta_a} \end{bmatrix} \qquad \text{(A.112)}$$

and the Hessian matrix can be written as:

$$\begin{bmatrix} & & & & & 0 & 0 & 0 & 0 & H^k_{\lambda_D \delta_a} \\ & & & & & 0 & 0 & 0 & E & H^k_{\lambda_g \delta_a} \\ & & 0 & & & 0 & 0 & E & 0 & N^T \\ & & & & & 0 & E & 0 & K & 0 \\ & & & & & E & 0 & 0 & 0 & H^k_{z_l \delta_a} \\ 0 & 0 & 0 & 0 & E & H^k_{s_l s_l} & 0 & 0 & 0 & 0 \\ 0 & 0 & 0 & E & 0 & & H^k_{s_g s_g} & 0 & 0 & 0 \\ 0 & 0 & E & 0 & 0 & & & H^k_{s_\delta s_\delta} & 0 & 0 \\ 0 & E & 0 & K^T & 0 & & 0 & & H^k_{P_a P_a} & 0 \\ \left(H^k_{\lambda_D \delta_a}\right)^T & \left(H^k_{\lambda_g \delta_a}\right)^T & N & 0 & \left(H^k_{z_l \delta_a}\right)^T & & \cdots & & & H^k_{\delta_a \delta_a} \end{bmatrix}$$

The full system Newton method can be expressed as:

$$\begin{bmatrix} H_{u_1 u_1} & 0 & 0 & H_{u_1 \sigma} \\ 0 & \ddots & 0 & \vdots \\ 0 & 0 & H_{u_A u_A} & H_{u_1 \sigma} \\ H^T_{u_1 \sigma} & \cdots & H^T_{u_a \sigma} & 0 \end{bmatrix} \begin{bmatrix} \Delta u_1 \\ \vdots \\ \Delta u_A \\ \Delta \sigma \end{bmatrix} = - \begin{bmatrix} J_{u_1} \\ \vdots \\ J_{u_A} \\ J_\sigma \end{bmatrix} \qquad \text{(A.113)}$$

through back-substituting $\Delta u_i = H^{-1}_{u_i u_i}\left(-J_{u_i} - H_{u_i \sigma}\Delta\sigma\right)$ into the last equation, we get:

$$-J_\sigma = \sum_{i=1}^{A}\left(-H^T_{u_1 \sigma} H^{-1}_{u_i u_i} J_{u_i}\right) + \sum_{i=1}^{A}\left(-H^T_{u_1 \sigma} H^{-1}_{u_i u_i} H_{u_i \sigma}\right)\Delta\sigma \qquad \text{(A.114)}$$

Therefore, the global variables

$$\Delta\sigma = \left[\sum_{i=1}^{A}\left(H_{u_1\sigma}^T H_{u_iu_i}^{-1} H_{u_i\sigma}\right)\right]^{-1}\left(J_\sigma - \sum_{i=1}^{A}\left(H_{u_1\sigma}^T H_{u_iu_i}^{-1} J_{u_i}\right)\right) \qquad (A.115)$$

is obtained from the information of all the sub-systems.

the inverse $H_{u_au_a}^{-1} = \begin{bmatrix} D & L \\ L^T & 0 \end{bmatrix}^{-1} = \begin{bmatrix} 0 & L^{-T} \\ L^{-1} & -L^{-1}DL^{-T} \end{bmatrix}$ \qquad (A.116)

$$H_{u_1\lambda}^T H_{u_iu_i}^{-1} H_{u_i\lambda} = \begin{bmatrix} 0 & \cdots & H_{\delta_a\lambda}^T & \cdots & 0 \end{bmatrix}\begin{bmatrix} D & L \\ L^T & 0 \end{bmatrix}^{-1}\begin{bmatrix} 0 \\ \vdots \\ H_{\delta_a\sigma} \\ \vdots \\ 0 \end{bmatrix} \qquad (A.117)$$

Where $\begin{bmatrix} 0 & 0 & 0 & H_{\delta_a\sigma}^T \end{bmatrix}D\begin{bmatrix} 0 \\ 0 \\ 0 \\ H_{\delta_a\sigma} \end{bmatrix} = H_{\delta_a\sigma}^T H_{\delta a\delta a} H_{\delta_a\sigma}.$ \qquad (A.118)

$$\sum_{i=1}^{A}\left(H_{u_1\sigma}^T H_{u_iu_i}^{-1} H_{u_i\sigma}\right) = \sum_{i=1}^{A}\left(H_{\delta_a\sigma}^T H_{\delta a\delta a} H_{\delta_a\sigma}\right) = \begin{bmatrix} H_{\delta_1\sigma}^T & \cdots & H_{\delta_a\sigma}^T \end{bmatrix}\begin{bmatrix} H_{\delta_1\delta_1} & & 0 \\ & \ddots & \\ 0 & & H_{\delta_A\delta_A} \end{bmatrix}\begin{bmatrix} H_{\delta_1\sigma} \\ \vdots \\ H_{\delta_A\sigma} \end{bmatrix}$$

$$= \begin{bmatrix} M_1 & \cdots & M_A \end{bmatrix}\begin{bmatrix} H_{\delta_1\delta_1} & & 0 \\ & \ddots & \\ 0 & & H_{\delta_A\delta_A} \end{bmatrix}\begin{bmatrix} M_1^T \\ \vdots \\ M_A^T \end{bmatrix} = M\begin{bmatrix} H_{\delta_1\delta_1} & & 0 \\ & \ddots & \\ 0 & & H_{\delta_A\delta_A} \end{bmatrix}M^T \qquad (A.119)$$

References

1. Weber, J.D., *Implementation of a Newton-based Optimal Power Flow into a Power System Simulation Environment.* 1997. Available on www.powerworld.com

2. Irisarri, G.D., et al., *The Future of Electronic Scheduling and Congestion Management in North America.* IEEE Trans. on Power Systems, 2003. **18**(2): p. 444-451.

3. Schweppe, F.C., et al., *Spot Pricing of Electricity.* 1988, Kluwer: Boston.

4. Christle, R.D., Wollenberg B.F., and Wangensteen,I. , *Transmission Management in the Deregulated Environment.* Proceedings of the IEEE, 2000. **88**(2): p. 170-195.

5. Pérez-Arriaga, I., Camacho, L.O. and Odériz, F.J.R., *Report on Cost components of cross border exchanges of electricity.* 2002, European Commission.

6. Singh, H., Hao, S., and Papalexopoulos, A. *Transmission congestion management in competitive electricity markets.* IEEE Transactions on Power Systems, 1998. **13**(2): p. 672-80.

7. Green, R., *Competition in Generation: The Economic Foundations.* Proceedings of the IEEE, 2000. **88**(2): p. 128-139.

8. Rosehart, W.D., Canizares, and Quintana, V.H., *Effect of Detailed Power System Models in Traditional and Voltage-Stability-Constrained Optimal Power-Flow Problems.* IEEE Trans. on Power Systems, 2003. **18**(1): p. 27-35.

9. Stoft, S., *Power System Economics.* 2002: John Wiley & Sons, Inc.

10. Alvarado, F.L., *Converting System Limits to Market Signals.* IEEE Trans. on Power Systems, 2003. **18**(2): p. 422-427.

11. Ott, A.L., *Experience with PJM Market Operation, System Design, and Implementation.* IEEE Trans. on Power Systems, 2003. **18**(2).

12. Hogan, W.W., *Competitive electricity market design: a wholesale primer.* 1998, Harvard University: Cambridge, Massachusetts. Available on http://ksghome.harvard.edu/~.whogan.cbg.Ksg/

13. ISO New England Inc., *Congestion Management Under Standard Market Design.* 2003. Available on http://www.iso-ne.com/

14. Galiana, F.D., Kockar, I., and Franco, P.C., *Combined Pool/Bilateral Dispatch--Part I: Performance of Trading Strategies.* IEEE Trans. on Power Systems, 2002. **17**(1): p. 92-99.

15. Bower, J., and Bunn, D.W., *A Model-based Comparison of Pool and Bilateral Market Mechanisms for Electricity Trading.* 2000. Available on http://www.caiso.com/docs/2000/11/22/2000112212555313344.pdf

16. The Government of South Australia, *Electricity reform in South Australia: some audit observations.* 1997. Available on http://www.audit.sa.gov.au/97-98/a4/electreform.html.

17. Chao, H.-p., et al., *Flow-Based Transmission Rights and Congestion Management.* The Electricity Journal, 2000(Oct. 2000): p. 38-58.

18. Wu, F.F. and Varaiya, P., *Coordinated multilateral trades for electric power networks: theory and implementation.* Electrical Power and Energy Systems, 1999. **21**(2): p. 75–102.

19. Ilic, M., Hsieh, E. and Ramanan, P., *Transmission Pricing of Distributed Multilateral Energy Transactions to Ensure System Security and Guide Economic Dispatch.* IEEE Transactions on Power Systems, 2003. **18**(2): p. 428-434.

20. Zobian, A. and Ilic, M.D., *Unbundling of Transmission and Ancillary Services.. Part I: Technical Issues. Part II: Cost-Based Pricing Framework.* IEEE Trans. Power Systems, 1997. **12**(2): p. 539-558.

21. Yu, C.W. and David, A.K., *Pricing transmission services in the context of industry deregulation.* IEEE Transactions on Power Systems, 1997. **12**(1): p. 503-10.

22. Green, R., *Electricity Transmission Pricing: How much does it cost to get it wrong?* 1998, University of California Energy Institute. Available on http://www.sal.hut.fi/Teaching/Mat-2.142/elmarket/Saariselka/Green.pdf

23. Motto, A.L., et al., *Network-Constrained Multiperiod Auction for a Pool-Based Electricity Market.* IEEE Trans. on Power Systems, 2002. **17**(3): p. 646-653.

24. Tao, S. and Gross, G., *A Congestion-Management Allocation Mechanism for Multiple Transaction Network.* IEEE Trans. on Power Systems, 2002. **17**(3): p. 826-833.

25. Chen, L., et al., *Components of Nodal Prices for Electric Power Systems.* IEEE Trans. on Power Systems, 2002. **17**(1): p. 41-49.

26. Greene, S., Dobson, I. and Alvarado, F.L., *Sensitivity of Transfer Capability Margins With a Fast Formula.* IEEE Trans. on Power Systems, 2002. **17**(1): p. 34-40.

27. Conejo, A.J., et al., *Transmission Loss Allocation: A Comparison of Different Practical Algorithms.* IEEE Trans. on Power Systems, 2002. **17**(3): p. 571-576.

28. Milano, F., Canizares, C.A. and Invernizzi, M., *Multiobjective Optimization for Pricing System Security in Electricity Markets.* IEEE Transactions on Power Systems, 2003. **18**(2): p. 596-604.

29. Conejo, A.J., et al., *Economic Inefficiencies and Cross-Subsidies in an Auction-Based Electricity Pool.* IEEE Trans. on Power Systems, 2003. **18**(1): p. 221-228.

30. Shirmohammadi, D., et al., *Some fundamental technical concepts about cost based transmission pricing.* IEEE Trans. on Power Systems, 1996. **11**: p. 1002-1008.

31.   Harvey, S.M., Hogan, W.W. and Pope, S.L., *Transmission capacity Reservations Implemented Through a Spot Market with Transmission Congestion contracts.* The Electricity Journal, 1996: p. 42-55.

32.   Rivier, M. and Perez-Arraga, I.J., *Computation and decomposition of spot prices for transmission pricing.* in *Proc. 11th PSCC.* 1993. Avignon, France.

33.   Hogan, W.W., *Contract Networks for Electric Power Transmission: Technical Reference.* 1992.

34.   Bialek, J. and Kattuman, P., *Real and Reactive Power Tracking: Proof of Concept and Feasibility Study.* 1999, EPRI: Palo Alto.

35.   Perez-Arriaga, I.J., et al., *Marginal Pricing of Transmission Services: An Analysis of Cost Recovery.* IEEE Trans. on Power Systems, 1995. **10**(1): p. 546-553.

36.   Oren, S., et al., *Nodal prices and transmission rights: a critical appraisal.* 1994, University of Berkeley,report.

37.   ETSO, *ETSO Position Paper on Locational Signals and European Transmission Charging.* 2002. www.etso-net.org

38.   Marangon Lima, J.W. and Oliveira, E.J.d., *Long-term impact of transmission pricing.* IEEE Transactions on Power Systems, 1998. **13**(4): p. 1514-1520.

39.   Calviou, M.C., Dunnet, R.M. and Plumptree, P.H., *Charging for use of a Transmission System by Marginal Cost Method.* Proc. Power System Computation Conference. 1993. Avignon.

40.   Marangon Lima, J.W., *Allocation of transmission fixed charges: an overview.* IEEE Trans. on Power Systems, 1996. **11**: p. 1409-1418.

41.   Vries, L.J. *Capacity allocation in a restructured electricity market: technical and economic evaluation of congestion management methods on*

interconnectors. Proceeding of the 2001 IEEE Porto Power Tech Conference. 2001.

42.   O'Neill, R.P., et al., *A Joint Energy and Transmission Rights Auction: Proposal and Properties.* IEEE Trans. on Power Systems, 2002. **17**(4): p. 1058-1067.

43.   Hao, S. and Shirmohammadi, D. *Congestion Management With Ex Ante Pricing for Decentralized Electricity Markets.* IEEE Trans. on Power Systems, 2002. **17**(4): p. 1030-1036.

44.   Bompard, E., et al., *Congestion-Management Schemes: A Comparative Analysis Under a Unified Framework.* IEEE Trans. on Power Systems, 2003. **18**(1): p. 346-352.

45.   Chao, H.-p., *A Market Mechanism For Electric Power Transmission.* Journal of Regulatory Economics, 1996(10,1996): p. 25-59.

46.   Stoft, S., *Congestion Pricing with Fewer Prices Than Zones.* The Electricity Journal, 1998: p. 23-31.

47.   Oren, S.S. and Ross, A.M., *Economic congestion relief across multiple regions requires tradable physical flow-gate rights.* 2000.

48.   Ruff, L.E., *Flowgates,Contingency-Constrained Dispatch, and Transmission Rights.* The Electricity Journal, 2001(January/February 2001): p. 34-55.

49.   Jamasb, T., Nillesen, P. and Pollitt, M., *Strategic Behaviour under Regulation Benchmarking,* in *CMI working paper 19.* 2003, CMI.

50.   Wolfram, C.D., *Measuring Duopoly power in the British Electricity Spot Market.* The American Economy Review, 1999.

51.   Macatangay, R.E.A., *Market definition and dominant position abuse under the new electricity trading arrangements in England and Wales.* Energy Policy, 2001. **29**(29,2001): p. 337-340.

52.   Joskow, P.L. and J. Tirole, *Transmission rights and market power on electric power networks.* Journal of Economics, 2000. **31**(3, Autumn 2000): p. 450-487.

53.   Bushnell, J., *Transmission Rights and Market Power.* The Electricity Journal, 1999(October 1999): p. 77-85.

54.   Allen, E., M. Ilic, and Z. Younes, *Providing for transmission in times of scarcity: an ISO cannot do it all.* Electrical Power and Energy Systems, 1999. **21**(21 1999): p. 147-163.

55.   Northup, M.E. and J.A. Rasmussen, *Electricity reform abroad and U.S. investment.* 1997.

56.   Weber, J.D., *Individual Welfare Maximization in Electricity Markets including Consumer and Full Transmission System Modeling.* 1999. Available on www.powerworld.com

57.   Sweeting, A., *The Wholesale Market for Electricity in England and Wales: Recent Developments and Future Reforms.* 2000, Cambridge MIT.

58.   EIA, *International Energy Outlook 2003.* 2003. Available on http://www.eia.doe.gov/oiaf/archive/ieo03/index.html

59.   NGT, *Company Background,* on http://www.nationalgrid.com/uk/.

60.   Electricity Association, *Introduction to the UK Electricity Market.* 2002. Available on www.electricity.org.uk/media/documents/pdf/ Intro_UK_Elec_Market.pdf

61.   Green, R., *England and Wales: A Competitive Electricity Market?* 1998, University of California Energy Institute.

62.   Ofgem, *The New Electricity Trading Arrangements--A review of the first three months.* 2001. Available on www.ofgem.gov.uk

63.   ELEXON website, *ELEXON – The Balancing and Settlement Code Company.* 2002. Available on http://www.elexon.co.uk/

64. Ofgem, *Transmission Access and Losses under NETA --A Consultation Document*. 2001. Available on www.ofgem.gov.uk

65. Ofgem, *The review of the first year of NETA*. 2002. Available on www.ofgem.gov.uk

66. Ofgem, *NETA at a Glance*. 2002. Available on www.ofgem.gov.uk

67. EIA, *World Country Analysis Brief*. 2003. Available on http://www.eia.doe.gov/

68. Green, R., *Electricity Transmission Pricing: an International Comparison*. Utilities Policy, 1997. **6**(3): p. 172-184.

69. *Electricity Market Design & Creation in Asia Pacific*. 2003. Available on http://www.worldenergy.org/wec-geis/publications/default/launches/market/market.asp

70. Asia Pacific Energy Research Centre, *Electricity Sector Deregulation in the APEC Region*. 2000. Available on www.ieej.or.jp/aperc/final/deregulation.pdf.

71. FERC, *Docket No. RM01-12-000*. 2002. Available on ftp://ftp.nerc.com/pub/sys/all_updl/docs/ferc/NOPR/FERC-NOPR-RM-01-12-000.pdf

72. EIA, *The Restructuring of the Electric Power Industry: A Capsule of Issues and Events*. 2000. Available on http://www.eia.doe.gov/cneaf/electricity/page/restructure.html

73. Puller, S.L., *Pricing and Firm Conduct in California's Deregulated Electricity Market*. 2001, University of California Energy Institute.

74. Joskow, Paul L., *California's Electricity Crisis*. September, 2001. Available on http://www.ksg.harvard.edu/hepg/Papers/

75. Borenstein, S., *The Trouble With Electricity Markets (and some solutions)*. 2001, PWP. Available on http://www.ucei.berkeley.edu/PDF/pwp081.pdf

76. Newbery, D.M., *European deregulation: Problems of liberalising the electricity industry.* European Economic Review, 2002(46).

77. Hogan, W.W., *Getting the Prices Right in PJM: What the Data Teaches Us.* The Electricity Journal, 1998: p. 61-67.

78. Gülen, G. and M.M. Foss, *Commercial Frameworks for Electricity.* Privitization Watch, 2003.

79. VDN, *Facts and Figures--Electricity networks in Germany 2002.* Available on www.vdn-berlin.de/facts_figures.asp

80. SYSTINT, W., *European Interconnection: State of the Art 2002.* Available on www.ucte.org/pdf/Publications/ 2002/SYSTINT_Report_2002.pdf

81. UCTE, *Interim Report of the Investigation Committee on the 28 September 2003 Blackout in Italy.* 2003. Available on www.ucte.org/

82. ETSO, *Evaluation of congestion management methods for cross-border transmission.* 1999, ETSO. Available on www.etso-net.org/

83. ETSO, *ETSO Comments on the European Commission's discussion document "Congestion Management".* 2003. Available on www.etso-net.org/

84. FERC, *Working Paper on Standardized Transmission Service and Wholesale Electric Market Design.* Available on http://www.ferc.gov/industries/electric/indus-act/smd/nopr/work-pap.PDF

85. ETSO, *Design Options For Implementation of a Coordinated Transmission Auction.* 2002, ETSO. Available on www.etso-net.org/

86. UCTE, *Transforming UCTE Rules and Recommendations into binding Security and Reliability Standards.* 2002. Available on www.ucte.org

87. Bialek, J., A. Germond, and R. Cherkaoui, *Improving NERC Transmission Loading Relief Procedures.* Electricity Journal, 2000(June, 2000): p. 11-19.

88.   ETSO, *Net Transfer Capacities (NTC) and Available Transfer Capacities (ATC) in the Internal Market of Electricity in Europe (IEM) --Information for User.* 2000. Available on www.etso-net.org/

89.   Tabors, R.D., *Auctionable Capacity Rights and Market-Based Pricing.* 1999. Available on http://www.tca-us.com/Publications/Auction_Paper_working_paper_version.pdf

90.   Ou, Y. and Singh, C., *Assessment of Available Transfer Capability and Margins.* IEEE Trans. on Power Systems, 2002. **17**(2): p. 463-468.

91.   ETSO, *Definitions of transfer capacities in liberalised electricity markets.* 2001. Available on www.etso-net.org/

92.   ETSO. *ETSO Comments on the European Commission's Discussion document "Inter TSO Compensations".* 10th Florence Forum. 2003. Available on www.etso-net.org/

93.   European Commission, *Second Report to the Council and the European Parliament on Harmonisation Requirements.* 1999, EUROPA. Available on europa.eu.int/comm/energy/electricity/ publications/doc/cb_harmo2_en.pdf

94.   CEER, *First Survey on Security of Supply in the CEER Member Countries.* 2002. Available on europa.eu.int/

95.   EURELECTRIC, *Congestion Management and Allocation of Interconnection Capacity--Annexes.* 2000, Eurelectric. Available on www.eurelectric.org

96.   Florence Forum. *Conclusions in Ninth Meeting of the European Electricity Regulatory Forum.* 2002. Rome. Available on europa.eu.int/comm/energy/electricity/ florence/index_en.htm

97.   ETSO, *Co-operation with Power Exchanges.* 2002, ETSO. Available on www.etso-net.org/

98. ETSO, *Co-ordinated auctioning A market-based method for transmission capacity allocation in meshed networks.* 2001. Available on www.etso-net.org/

99. ETSO, *Congestion Management in the EU electricity Transmission Network--Status Report.* 2002. Available on www.etso-net.org/

100. ETSO. *Counter Measures for Congestion Management Definitions and Basic Concepts.* in *10th Florence Forum.* 2003. Available on www.etso-net.org/

101. EURELECTRIC. *Union of the Electricity Industry-EURELECTRIC Comments on the Commission's Stategy paper "medium term vision for the internal electricity market".* 10th Florence Forum. 2003.

102. ETSO, *Reconciliation of Market Splitting with Coordinated auction concepts--technical issues.* 2002, ETSO. Available on www.etso-net.org/

103. NordPool, *The Nordic Spot Market--The world's first international spot power exchange.* 2003, Nord Pool ASA. Available on www.nordpool.com/

104. ETSO, *Co-ordinated use of Power Exchanges for Congestion Management in Continental Europe: Market Design and Role of Power Exchanges.* 2002. Available on www.etso-net.org/

105. Flatabo, N., et al., *Experience with the Nord Pool Design and Implementation.* IEEE Trans. on Power Systems, 2003. **18**(2): p. 541-547.

106. Glanchant, J.M. and V. Pignon, *Nordic Electricity Congestion's Arrangement as a Model For Europe: Physical Constraints or Operators' Opportunity*, in *DAE Working Paper WP 0313.* 2002, DAE.

107. Andersson, G., *Liberalisation of the Scandinavian Electricity Markets Experiences since 1991.* 2001, ETH: Zurich. Available on http://www.eeh.ee.ethz.ch/downloads/news/events/eth-sem-000627.pdf

108. EURELECTRIC working group, M.R.S.T., *EURELECTRIC position paper on congestion management.* 2000. Available on www.eurelectric.org

109. ETSO. *General Guidelines for Joint Cross-border Redispatch*. 10th Florence Forum. 2003. Available on www.etso-net.org/

110. ETSO Task Force, *Benchmarking on transmission pricing in Europe : synthesis (February 2003)*. 2003, ETSO. Available on www.etso-net.org/

111. ETSO. *Congestion Management--more than ever a key issue*. in *10th Florence Forum*. 2003. Available on www.etso-net.org/

112. EURELECTRIC. *Union of the Electricity Industry-EURELECTRIC Position Paper Contribution to the 10th Electricity REgulatory Forum*. 10th Florence Forum. 2003. Available on www.eurelectric.org

113. European Commission. *Inter TSO Compensations--Discussion Document*. 10th Florence Forum. 2003. Available on europa.eu.int/comm/energy/electricity/florence/index_en.htm

114. Florence Forum. *Conclusions*. in *Tenth Meeting of the European Electricity Regulatory Forum*. 2003. Rome. Available on europa.eu.int/comm/energy/electricity/ florence/index_en.htm

115. ETSO. *ETSO proposal for 2003 CBT Mechanism*. Ninth Florence Forum. 2002. Available on www.etso-net.org/

116. European Commission. *Stratety Paper--Medium Term Vision for the Internal Electricity Market*. 10th Florence Forum. 2003. Available on europa.eu.int/comm/energy/electricity/ florence/index_en.htm

117. Nord Pool, *The Nordic Power Market--Electricity Power Exchanges across National Borders*. 2003, Nord Pool ASA. Available on www.nordpool.com/

118. Nord Pool, *Derivatives Trade at Nord Pool's Financial Market*. 2002, Nord Pool ASA. Available on www.nordpool.com/

119. Rau, N.S., *Issues in the Path Toward an RTO and Standard Markets*. IEEE Trans. on Power Systems, 2003. **18**(2): p. 435-443.

120.   Fernandez, A., *An Overview of FERC's Standard Market Design NOPR*. 2002.

121.   ISO New England Inc., *RTO Characteristics and Functions GRIDORG/ Modified ISO Model*. 2000. Available on www.iso-ne.com/

122.   Fink, L.H., M.D. Ilic, and F.D. Galiana, *Transmission access rights and tariffs*. 1997, Electric Power Systems Research. p. 197-206.

123.   Deeb, N. and S.M. Shahidehpour, *Linear Reactive Power Optimization in a Large Power Network Using the Decomposition Approach*. IEEE Trans. on Power Systems, 1990. **5**(2): p. 428-438.

124.   Wang, S.J., S.M. Shahidehpour, and D.S. Kirschen, *Short-term Generation Scheduling with Transmission and Environmental Constraints using an Augmented Lagrangian Relaxation*. IEEE Trans. on Power Systems, 1995. **10**(3): p. 1294-1301.

125.   Cadwalader, M.D., et al., *Market coordination of transmission loading relief across multiple regions*. 1998. Available on http://ksghome.harvard.edu/~.whogan.cbg.Ksg/extr1298.pdf

126.   Baldick, R., et al., *A Fast Distributed Implementation of Optimal Power Flow*. IEEE Trans. on Power Systems, 1999. **14**(3): p. 858-864.

127.   Aguado, J.A. and Quintana, V.H., *Inter-Utilities Power Exchange Coordination: A Market-Oriented Approach*. IEEE Trans. on Power Systems, 2001. **16**(3): p. 513-519.

128.   Xie, K. and Song, Y.H., *Dynamic optimal power flow by interior point methods*. Iee Proceedings-Generation Transmission and Distribution, 2001. **148**(1): p. 76-84.

129.   Zhai, Q., Guan, X., and Cui, J., *Unit Commitment with Identical Units: Successive Subproblem Solving Method Based on Lagrangian Relaxation*. IEEE Trans. on Power Systems, 2002. **17**(4): p. 1250-1257.

130.	Bakirtzis, A.G. and Biskas, P.N., *A Decentralized Solution to the DC-OPF of Interconnected Power Systems.* IEEE Transactions on Power Systems, 2003. **18**(3): p. 1007-1013.

131.	Momoh, J.A., *Electric Power System Applications of Optimization*, ed. H.L. Willis. 2001: Marcel Dekker, Inc.

132.	Wu, Y.-C., Debs, A.S. and Marsten, R.E., *A Direct Nonlinear Predictor-Corrector Primal-Dual Interior Point Algorithm for Optimal Power Flows.* IEEE Trans. on Power Systems, 1994. **9**(2): p. 876-882.

133.	Zhang, L., Luh, P.B. and Guan, X., *Optimization-based Inter-utility Power Purchases.* IEEE Trans. on Power Systems, 1994. **9**(2): p. 891-897.

134.	Kim, B.H. and Baldick, R., *Coarse-grained distributed optimal power flow.* IEEE Trans. on Power Systems, 1997. **12**(2): p. 932-939.

135.	Conejo, A.J. and Aguado, J.A., *Multi-area Coordinated Decentralized DC Optimal Power Flow.* IEEE Trans. on Power Systems, 1998. **13**(4): p. 1272-1278.

136.	Wang, X., Song, Y.H. and Lu, Q., *Lagrangian Decomposition Approach to Active Power Congestion Management across Interconnected Regions.* IEE Proc. Gener. Transm. Distrib., 2001. **148**(5): p. 497-503.

137.	Aguado, J.A., et al. *Coordinated Congestion Management of Cross-Border Electricity Markets.* 14th PSCC. 2002. Sevilla.

138.	Smeers, Y. *International Congestion Management.* 2003. Available on http://www.econ.cam.ac.uk/electricity/news/transmission/smeerscongestion.pdf

139.	Baldick, R., *The Generalized Unit Commitment Problem.* IEEE Trans. on Power Systems, 1995. **10**(1): p. 465-475.

140. Granville, S., J.C.O. Mello, and Melo, A.C.G., *Application of Interior Point Methods to Power Flow Unsolvability*. IEEE Trans. on Power Systems, 1996. **11**(2): p. 1096-1103.

141. Clements, K.A., Davis, P.W. and Frey, K.D., *Treatment of Inequality Constraints in Power System State Estimation*. IEEE Trans. on Power Systems, 1995. **10**(2): p. 567-573.

142. Torres, G.L. and Quintana, V.H., *An Interior-Point Method for Nonlinear Optimal Power Flow Using Voltage Rectangular Coordinates*. IEEE Trans. on Power Systems, 1998. **13**(4): p. 1211-1218.

143. Xie, K. and Song, Y.H., *Power Market Oriented Optimal Power Flow via an Interior Point Method*. IEE Proc. Gener. Transm. Distrib., 2001. **148**(6): p. 549-556.

144. Rosehart, W.D., Canizares, C.A. and Quintana, V.H., *Multiobjective Optimal Power Flows to Evaluate Voltage Security Costs in Power Networks*. IEEE Trans. on Power Systems, 2003. **18**(2): p. 578-587.

145. Wright, S.J., *Primal-Dual Interior-Point Methods*. 1997: SIAM-the Society for Industrial and Applied Mathematics.

146. Castronuovo, E.D., Campagnolo, J.M. and Salgado, R., *On the Application of High Performance Computation Techniques to Nonlinear Interior Point Methods*. IEEE Trans. on Power Systems, 2001. **16**(3): p. 325-331.

147. ETSO. *Guidelines on Congestion Management--conclusions of the ETSO 6th Florence Forum*. 2000. Available on www.etso-net.org/

148. ETSO, *Transparency and Data Publication Role of ETSO*. 2002. Available on www.etso-net.org/

149. ICF Consulting Ltd, *Unit Costs of constructing new transmission assets at 380kV within the European Union, Norway and Switzerland.* 2002. Available on http://www.icfconsulting.com/Publications/energy.asp

150. UCTE, *UCTE Operation Handbook: Transforming UCTE Rules and Recommendations into binding Security and Reliability Standards.* 2003, UCTE. Available on www.ucte.org.

151. UCTE, *UCTE interconnected network.* 2001. Available on www.ucte.org.

152. European Commission, *Analysis of Electricity Network Capacities and Identification of Congestion, Final Report.* 2001: Archan.

153. UCTE, *UCTE Statistical Yearbook 2001: Transmission lines and inventory of power stations.* 2001.

154. SEI, *The European Fossil-fueled Power Station Database Used in the SEI CASM Model.* 1990, Stockholm Environment Institute at York. Available on http://www.sei.se/dload/1996/TEFFPSDUITSCM.pdf

155. Say, M.G., *Electrical engineer's reference book.* 13 ed. 1973.

156. REE (Spanish TSO) Annual Report, *"EL Sistema Electronico Espanol Informe 2001".* 2001. Available on www.ree.es

157. Comedition.Com, *World List of Nuclear Power Plants.* 1995. Available on http://www.comedition.com

158. PowerWorld, *Pw80userguide.pdf*, PowerWorld Corporation.

159. IEEE Working Group, *Common Data Format for the Exchange of Solved Load Flow Data.* IEEE Transactions on Power Apparatus and Systems, 1973. **PAS-92**(6): p. 1916-1925.

160. UCTE, *Half-yearly Report I/2002.* 2002. Available on www.ucte.org/

161. UCTE, *Half-yearly Report II/2002.* 2002. Available on www.ucte.org/

162. Haubrich, H.-J. and W. Fritz, *Study on Cross-Border Electricity Transmission Tariffs*. 1999, European Commission: Aachen. Available on europa.eu.int/comm/energy/electricity/ publications/index_en.htm

163. Lee, B., H. Song, and S.-H. Kwon, *A Study on Determination of Interface Flow Limits in the KEPCO System Using Modified Continuation Power Flow (MCPF)*. IEEE Trans. on Power Systems, 2002. **17**(3): p. 557-564.